# CYTOSKELETAL DEFECTS LEAD TO CYTOKINESIS FAILURE AND GENOMIC INSTABILITY IN CANCER CELLS

by

**Qian Wu**

B.S., Beijing Normal University, China, 2003

Submitted to the Graduate Faculty of

Arts and Sciences in partial fulfillment

of the requirements for the degree of

Doctor of Philosophy

University of Pittsburgh

2008

UNIVERSITY OF PITTSBURGH

ARTS AND SCIENCES

This dissertation was presented

by

Qian Wu

It was defended on

April 17, 2008

and approved by

Jeffrey L. Brodsky, PhD, Professor

Jeffrey D. Hildebrand, PhD, Associate Professor

Anthony Schwacha, PhD, Assistant Professor

Simon C. Watkins, PhD, Professor

Dissertation Advisor: William S. Saunders, PhD, Associate Professor

**CYTOSKELETAL DEFECTS LEAD TO CYTOKINESIS FAILURE AND GENOMIC INSTABILITY IN CANCER CELLS**

Qian Wu, PhD

University of Pittsburgh, 2008

Cancer cells typically have unstable genomes and ploidy, and these changes play an important part of malignant transformation in most tumorigenesis models. I observe that cancer cells can increase ploidy by failure of cell division producing a single daughter with a doubled genome. Cytokinesis failure usually is followed by the formation of multipolar spindles in the tested cell lines. Some of these cells are still capable of dividing and the daughters of multipolar division have an even greater chance of being multinucleated and multicentrosomal due to failure of cytokinesis and thus likely enter another round of multipolar division. However, some of the daughters inherit a single nucleus and centrosome, suggesting that they may escape a cycle of multipolarity and give rise to centrosomally-stable clones.

I also show here that failure of cytokinesis in cancer cells is associated with cytoskeleton abnormalities. One type of defect is caused by decreased phosphorylation of the myosin regulatory light chain, a key regulatory element of cortical contraction during cell division. Reduced phosphorylation is often associated with high expression of myosin phosphatase and/or reduced myosin light chain kinase (MLCK) levels in a variety of cancer cell lines. When myosin light chain phosphorylation is restored to normal levels by phosphatase knockdown, the mitotic defects of malignant cells, including cytokinesis failure, multinucleation, and multipolar mitosis are all markedly reduced. Both overexpression of myosin phosphatase and inhibition of the

MLCK can recapitulate the multinucleation in nonmalignant cells. These results show that ploidy defects in tumor cells can be caused by deficiencies in myosin light chain phosphorylation resulting from high expression of myosin phosphatase and low activity of MLCK.

GpIbα, a membrane glycoprotein, which is widely upregulated in cancer cells, has been shown here for the first time to play a role in cytokinesis, possibly also through regulating cytoskeleton remodeling. The overexpression of GpIbα in p53-knockdown primary cells induces cytokinesis failure, tetraploidization, genomic instability and tumorigenesis. In addition, knockdown of GpIbα reduces chromosome segregation defects in cancer cells. Together, these observations support a model that cytoskeleton-defect-mediated cytokinesis failure plays a major role influencing the chromosomal instability of cancer cells.

## TABLE OF CONTENTS

## LIST OF TABLES

## LIST OF FIGURES

## PREFACE

First and foremost, I would like to thank my dissertation advisor, Dr. William S. Saunders, for giving me such a great project to work on. He has guided me through tough times with many helpful suggestions and endless discussions. I appreciate all the insights he has given me in science and his advice on my academic career.

I would like to thank my thesis committee members, Dr. Jeffrey D. Hildebrand, Dr. Anthony Schwacha, Dr. Susan P. Gilbert, Dr. Jeffrey L. Brodsky and Dr. Simon C. Watkins for their time and great comments on my project.

I am thankful to all Saunders lab members for creating a scientific, friendly and enjoyable working environment. I thank Dr. Li Luo for mentoring me when I joined the lab and working together on the multipolarity project. I also thank Ruta Sahasrabudhe to collaborate in the MLCK study. I appreciate Dr. Nicholas Quintyne and Dr. Alec Vaezi's suggestions on my research. In addition, I have to thank Dr. Ceyda Acilan and Kristen Bartoli, not only for their insightful discussions and help with experiments, but also for their wonderful friendship. I thank Abigale Lade and Fengfeng Xu for their efforts in making a joyful working area. I am indebted to my collaborator Dr. Youjun Li and Dr. Edward Prochownik for providing cell lines and antibodies in GpIbα project, Dale Lewis and Dr. Susanne Gollin for sharing cell lines and FISH assays, and

Youssef Rbaibi and Dr. Kirill Kiselyov for reagents and electron microscopy analysis. Lastly, I would like to thank some scientists around the world for their generous offers, including Dr. David J. Hartshorne (University of Arizona) for kindly providing HEK293 with MYPT1 expression cell line, Dr. Jeffrey D. Hildebrand (University of Pittsburgh), Dr. Adam D Linstedt (Carnegie Mellon University), Dr. Anne R. Bresnick (Albert Einstein College of Medicine), Dr. Kathleen Kelly (National Cancer Institute), Dr. David J. Hartshorne (University of Arizona) and Dr. James T. Stull (University of Texas Southwestern Medical Center) for plasmids and antibodies. I also thank Dr. Xiaojing Wang (University of Pittsburgh) for statistical analysis discussion.

I have gratitude toward the entire Biological Sciences department for the facilities and the supportive environment. Everybody in this department has been very generous in sparing their time and also sharing reagents. I particularly would like to thank the Brodsky lab, the Arndt lab, the Hildebrand lab and the Martens lab for letting me use their equipment. I owe a lot to Dr. Lydia B. Daniels for her guidance in my teaching experience. I am also grateful to Ms. Cathy Barr for managing to register classes and kind caring to me. I also thank my fellow classmates, for helping me through core courses and accompanying me on the stress of completing the graduate school, especially Shruthi Vembar and Julia van Kessel.

I cannot thank enough my dear friends in the United States and China. I would like particularly thank Chen Li for taking care of me in the first two years in the US and listening to my stories all the time. I should also note Jing Yang and Dr. Xiaoqun Wang for always being there for scientific, as well as friendly, conversations. I can not list all the names here; however,

all the kind companionship and happy moments with these friends are in my memories forever. I do appreciate everything they have done for me.

I dedicate this work to my beloved family. I can't express my appreciations to my mom and dad for thousands of minutes of phone calls to take care of my life and encourage me to complete my Ph.D. Although they are on the other side of the earth for most of time, I still can feel their love and care all the time. I love you too. I also want to give this dissertation to my great-grandma and grandfather. They passed away during these last five years. Although I could not make the funerals for them due to my busy schedule, I know they are always blessing me in heaven. Furthermore, I am grateful to my parents-in-law for their visiting and taking care of my life in Pittsburgh.

Lastly but most importantly, I would like to thank my husband, Pu Li, for always being supportive and thoughtful to me whenever I am happy or I am sad for these years. I really appreciate every great moment he has brought to me and every single thing he has done for me from the deep bottom of my heart. I can not forget all of his sacrifices for me during my pursuit of this Ph.D. and he always means more than what I can say.

# 1.0 CHAPTER I: INTRODUCTION

## 1.1 CYTOKINESIS IN ANIMAL CELLS

### 1.1.1 Cytokinesis regulation in mammalian cells

Cytokinesis, the last step in mitosis, is the process in which the cytoplasm of a cell is physically divided into two after nuclear division to ensure that the chromosome number is maintained from one generation of cells to the next. This complicated event requires coordinated actions of the cytoskeleton, tubulin and membrane system as well as protein kinases and signaling networks. Understanding the mechanism and regulation of cytokinesis is important because defective cytokinesis, resulting in tetraploid cells, is considered to be associated with chromosomal instability and tumorigenesis (see section 1.1.2 for details) (Fujiwara et al., 2005; Li et al., 2007a).

#### 1.1.1.1 Temporal regulation of cytokinesis

Animal cell cytokinesis initiates shortly after the onset of sister chromatid separation in anaphase of mitosis (Figure 1C). Recent reports have demonstrated that the inhibition of cyclin-dependent kinase 1 (Cdk1) activity by drugs is sufficient to induce cytokinesis without chromosome segregation in HeLa cells (Niiya et al., 2005). It indicates that Cdk1 activity must

be retained high to prevent cytokinesis until chromosome separation. Consistently, the Cdk1/cyclinB1 activity drops at the onset of anaphase in all organisms in mitosis by anaphase-promoting complex (APC)-dependent proteolysis. APC is the E3 ligase that regulates cell cycle by ubiquitination of cyclin B (King et al., 1996).

Although it is still not clear, some evidences suggest that APC is also involved in cytokinesis exit via ubiquitin-mediated proteolysis. It has been shown that polo-like kinase 1 (Plk1) proteolysis contributes to the inactivation of Plk1 in telophase, which is required for the proper control of mitotic exit and cytokinesis (Lindon and Pines, 2004). Additionally, an *in vitro* screen in mammalian cells has found that anillin, an actin-binding protein, and Aurora B kinase, which are essential for cytokinesis, are substrates of APC proteolysis in late M to G1 transition. It is very likely that appropriate timing of cytokinesis in animal cells is regulated by the APC-directed proteolysis system (Stewart and Fang, 2005; Zhao and Fang, 2005).

#### 1.1.1.2 Astral and central spindles

Cytokinesis is strongly associated with chromosome segregation. To specify the future division site is one of the first steps in cytokinesis (Figure 1C). This is very important because the correct positioning relative to the segregated chromatids ensures that each daughter will inherent a single copy of the genome. Based on the early studies from Rappaport over forty years ago (Rappaport, 1961), it has been accepted that spindle microtubules play a key role in

Figure 1

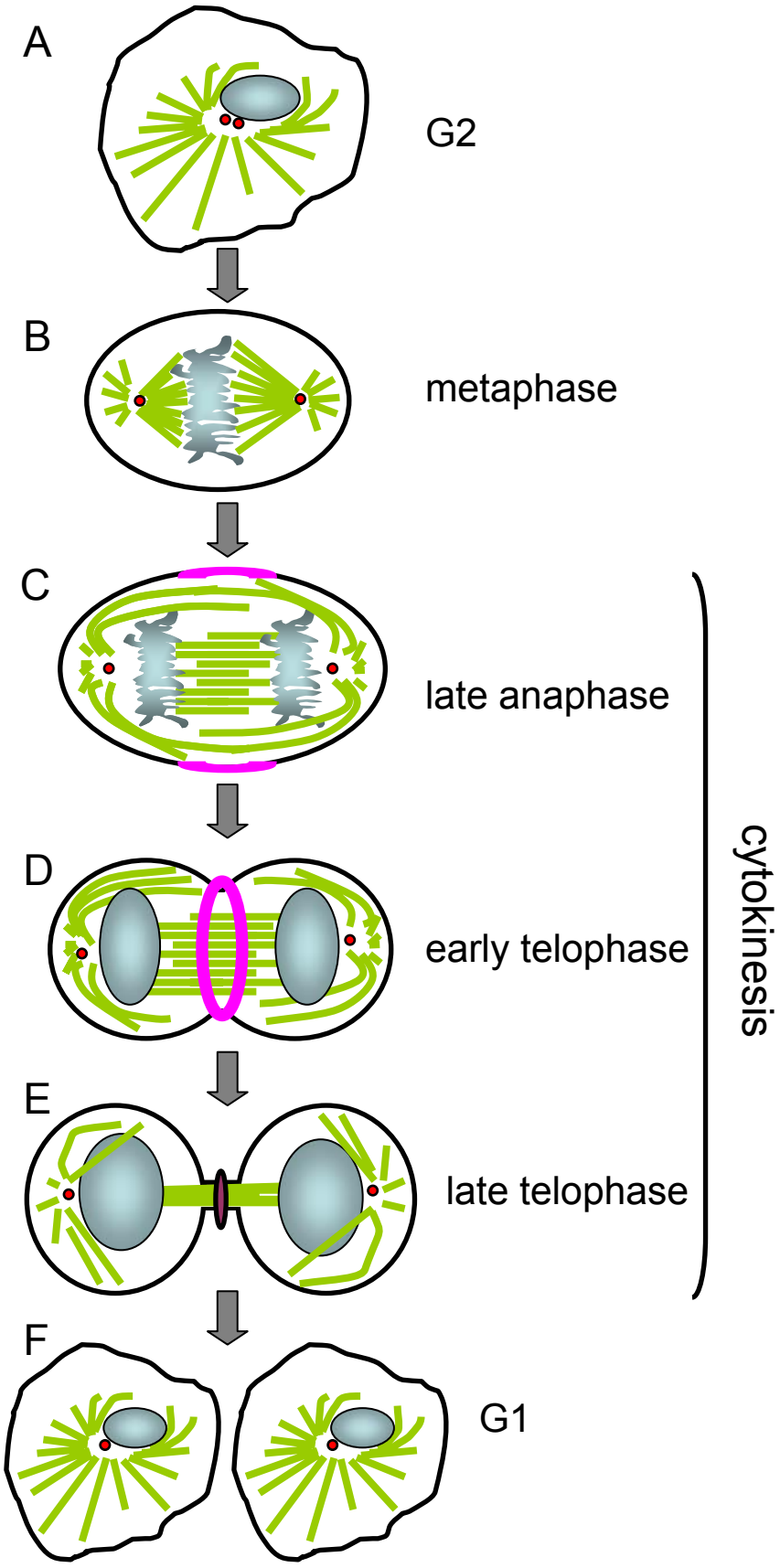
A
G2
B
metaphase
C
late anaphase
D
early telophase
E
late telophase
F
G1
cytokinesis

Figure 1. Cytokinesis in animal cells. DNA (blue), microtubules (green), centrosomes (red dots), contractile ring (pink) and midbody (purple) are shown. (A) A cell in G2. The DNA and centrosome have been duplicated. (B) A cell in metaphase. The chromosomes are aligned at the equatorial plate and attached to the spindle by microtubules. (C) A cell in late anaphase. The chromosomes are separated and move towards two poles. Microtubules contact the cell cortex and the area with bundled microtubules between the chromosomes is called the midzone. Molecules required for the cleavage furrow formation are transported and activated at the midzone. (D) A cell in early telophase. The chromosomes start decondensation. The cleavage furrow ingresses, and the contractile ring forms (pink). (E) Cell in late telophase. The cleavage furrow has completely ingressed and compressed the midzone microtubules to a condensed bundle called the midbody (purple). The contractile ring disassembles. (F) A cell in G1. Nuclei in the daughter cells have fully formed and the midbody abscises. The cell exits mitosis.

positioning of the cleavage furrow (see section 1.1.1.3 for details). There are two structural features of spindles: 1) an astral spindle is formed by radial microtubule arrays nucleated at the centrosomes found at the spindle poles (Figure 2, light green); 2) a central spindle is defined as the antiparallel arrays of microtubules formed between segregated chromatids at the midzone during anaphase (Figure 2, dark green). It is known that communication to the cell cortex through microtubules is required for cleavage plane positioning (Rappaport, 1996), suggesting that the molecules delivered by microtubules might regulate the furrow initiation in cytokinesis.

The classical model, although still debated, reveals that astral and central spindles function together to position the cleavage furrow. Negative signals from astral microtubules to the cortex prevents furrow assembly at the poles, while positive signals from midzone microtubules to the cortex stimulates furrow formation at the equator (Alsop and Zhang, 2003; D'Avino et al., 2005; Gatti et al., 2000) (Figure 2).

One of the positive signal candidates at the midzone is the small GTPase Rho, the main regulator of myosin II activation and actin polymerization (Piekny et al., 2005). Activated Rho localizes at the furrow in cells (Yonemura et al., 2004). Furthermore, depletion or inhibition of RhoA, the primary isotype in mammalian systems, prevents furrow formation (Piekny et al., 2005). The regulators of Rho are divided into two groups: the GDP-GTP exchange factor (GEF) ECT2/Pebble, and the GTPase-activating protein (GAP) CYK-4 / MacRacGAP (Piekny et al., 2005). MKLP1, a microtubule molecular motor of the kinesin-6 family, associates with CYK-4 to form a complex and transport it to the central spindle during cytokinesis and is required for

Figure 2

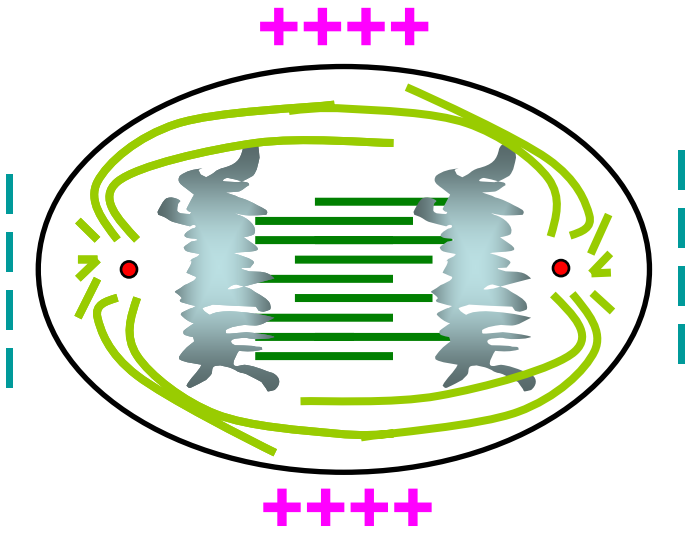

**Figure 2.** Model of how microtubule spindles determine the cleavage plane formation site. DNA (blue), centrosomes (red dots), astral spindles (light green), central spindles (dark green), polar relaxation signals (blue -) and equator stimulation signals (red +) are shown.

cytokinesis completion (Matuliene and Kuriyama, 2002; Mishima et al., 2002; Somers and Saint, 2003). Another essential protein for cytokinesis is PRC1, a microtubule associated protein. PRC1 binds multiple kinesins localized at the central spindle in mammalian cells, including MKLP1, KIF4 and KIF14. Depletion of PRC1 causes abnormal localization of these kinesins in anaphase (Gruneberg et al., 2006; Kurasawa et al., 2004; Neef et al., 2007).

Two kinases, Aurora B and Plk1 are also candidates for positive signaling at the equator (Nigg, 2001). Aurora B, which associates with chromatin in early mitosis, forms a complex with INCENP (inner centromere protein) and Survivin, This macromolecular complex concentrates at the centromere in metaphase and moves to the central spindle in anaphase (Earnshaw and Cooke, 1991; Vader et al., 2006; Vagnarelli et al., 2006). Depletion or inhibition of either Aurora B or Survivin interferes with cytokinesis, indicating that this complex is required for cell division (Yang et al., 2004; Yokoyama et al., 2005). Two likely substrates of Aurora B during cytokinesis are MgcRacGAP and the kinesin MKLP1 (Guse et al., 2005; Minoshima et al., 2003), whereas the substrates of Plk1are still undisclosed.

#### 1.1.1.3 Cleavage furrow and contractile ring

The furrow consists of the plasma membrane attached to a contractile ring, which is primarily assembled from actin and myosin II. Both actin and myosin are highly dynamic, with a fast turnover in contractile rings (Murthy and Wadsworth, 2005; Yumura, 2001). The contractile ring will be discussed below and plasma membrane dynamics will be reported in Section 1.1.1.5.

Actin filaments in the contractile ring are usually in parallel bundles, unlike the dendritic network found at the leading edge of a migrating cell (Rappaport, 1996). Whether actin molecules are nucleated in the furrow or assembled actin filaments are transported to the furrow is still unclear. In Xenopus eggs, Noguchi and Mabuchi have observed rapid growth of F-actin patches in the furrow region by live-cell imaging. These patches then align in tandem, elongate and fuse with each other to form short F-actin bundles that lengthen to form the contractile ring (Noguchi and Mabuchi, 2001). However, movement of assembled actomyosin filaments (the functional complex of actin and myosin) toward the equatorial region is observed in mammalian cells and nematode embryos (Hird and White, 1993; Murthy and Wadsworth, 2005).

Actin-nucleating proteins also localize in contractile rings and regulate actin dynamics during cytokinesis. The ARP2/3 complex, required for nucleation of branched filaments, is influential but not required for contractile ring formation (Pollard, 2007). Formins, functioning in nucleating unbranched actin filaments, are essential for contractile ring assembly and cytokinesis (Goode and Eck, 2007; Lu et al., 2007; Zigmond, 2004). They are thought to be positively regulated by the Rho pathway (Watanabe et al., 1997).

Another actin-binding protein required for cytokinesis is ADF/cofilin, which plays a role in actin filament disassembly. The activation of ADF/cofilin depends on the concentration of actin monomers and other regulators (Gunsalus et al., 1995; Ono et al., 2003). It is likely that destabilizing actin by ADF/cofilin is important for maintaining both actin dynamics and contractile ring disassembly at the late stages of cytokinesis.

Anillin, another actin-binding protein, localizes to the cleavage furrow and plays a role as a scaffold protein that links RhoA, actin, and myosin II (Field and Alberts, 1995; Gregory et al., 2008; Somma et al., 2002; Straight et al., 2005). Anillin is required to maintain active myosin II in the equatorial plane, and depletion of anillin in mammals causes contractual defects at the cleavage furrow (Gregory et al., 2008; Somma et al., 2002; Straight et al., 2005).

Myosin II is very dynamic at the furrow. During anaphase, DeBiasio and colleagues have found that myosin flows to the equator and forms a meshwork including both parallel and perpendicular fibers to the plane of cleavage in mammalian cells (DeBiasio et al., 1996). Myosin flow has also been observed in Xenopus eggs (Noguchi and Mabuchi, 2001). However, how myosin transports to the midzone remains unknown. It is suggested that microtubules are likely involved in this process (Foe et al., 2000).

Although there are several arguable models for how actomyosin aligns in the furrow, the phosphorylation of myosin II is known to be the critical step for actomyosin complex assembly and contractility. Nonmuscle myosin II is composed of a heavy and two types of light chains, the essential and regulatory light chains. In higher eukaryotes, cellular myosin is activated by phosphorylation of the myosin regulatory light chain (MLC) at Thr18/Ser19 (Figure 3) (Komatsu et al., 2000; Moussavi et al., 1993). The phosphorylation at MLC Ser19 is critical for the actomyosin filament assembly; however, diphosphorylation promotes the interaction of myosin with the actin specifically at the cleavage furrow (Ikebe et al., 1988; Scholey et al., 1980). A global phosphorylation of myosin II at serine 19 of the MLC is initiated at anaphase when cortical myosin II transport starts. The phosphorylation of myosin II remains high near the

equatorial plane through telophase and into cytokinesis, whereas the phosphorylation of myosin II at serine 19 of the MLC decreases at the poles in mammalian cells (DeBiasio et al., 1996). Komatsu and colleagues have shown that the expression of unphosphorylated MLC in mammalian cells causes failure of cytokinesis (Komatsu et al., 2000). Inhibition of MLC phosphorylation also results in the clearance of actin from the equatorial region, a reduction in myosin II at the furrow, and inhibition of cytokinesis (Murthy and Wadsworth, 2005). In *Drosophila,* unphosphorylatable MLC mutant blocks cell division (Jordan and Karess, 1997). Thus, MLC phosphorylation is one of the key essential processes regulating contractile ring formation and cytokinesis completion.

There are two groups of enzymes controlling MLC phosphorylation to ensure MLC activity is regulated at the right time, level, and position at the cleavage furrow. One group are kinases that phosphorylate MLC and promote myosin II activity; while the other is a phosphatase that dephosphorylates MLC and inhibits its activity (Glotzer, 2005; Hartshorne et al., 2004; Somlyo and Somlyo, 2003). Several kinases have been identified to phosphorylate MLC at Thr18/Ser19 *in vivo* and/or *in vitro* in mammalian cells, including myosin light chain kinase (MLCK), Rho-kinase (ROCK), citron kinase and Aurora B kinase. It is interesting that several kinases that phosphorylate myosin II can also inhibit myosin phosphatase via phosphorylation (Figure 4). These kinases and myosin phosphatase will be discussed below in detail.

MLCK has two isoforms, long and short. The short one contains the IgG modules and the actin-binding motif at the N-terminus and the catalytic domain and the $Ca^{2+}$/ calmodulin binding

Figure 3

**A**

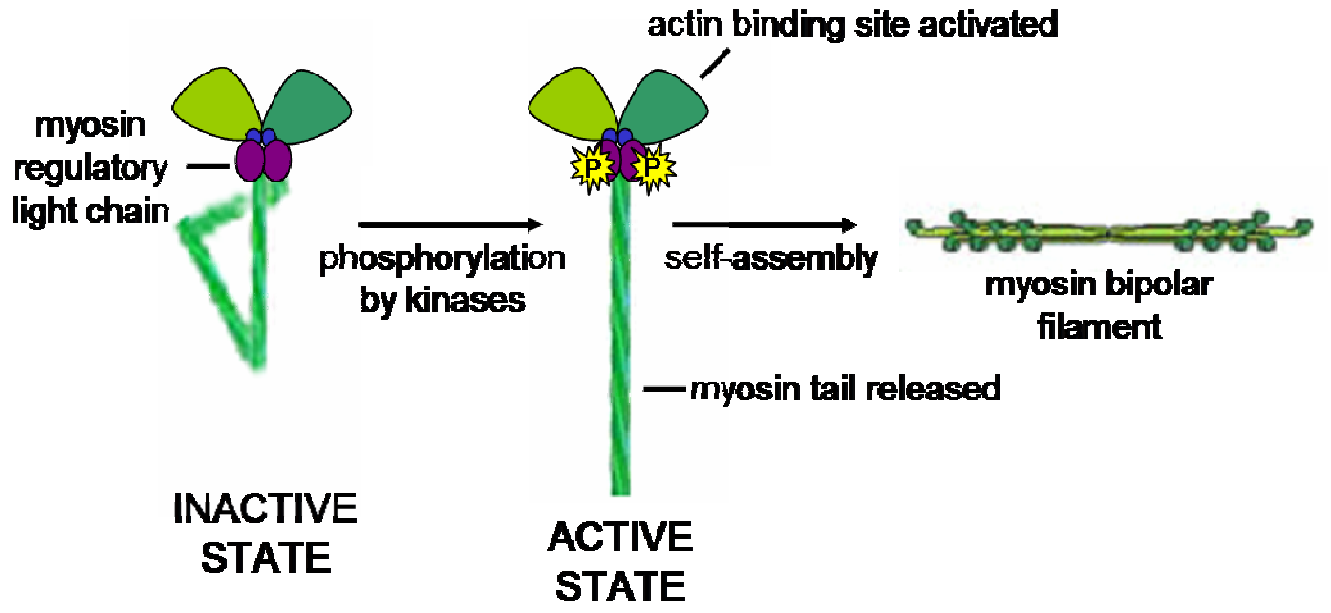
actin binding site activated
myosin
regulatory
light chain
P
P
phosphorylation
by kinases
self-assembly
myosin bipolar
filament
myosin tail released
INACTIVE
STATE
ACTIVE
STATE

**B**

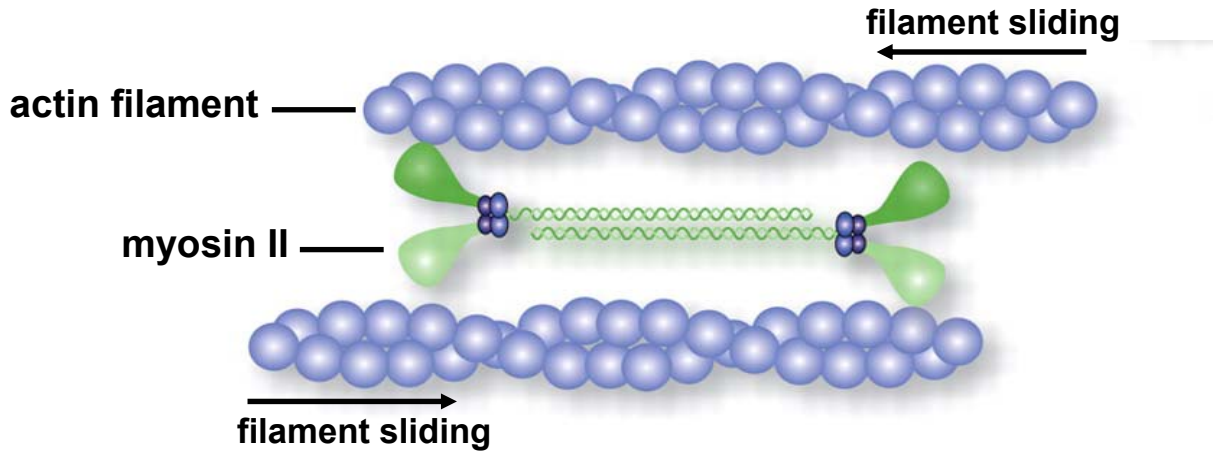
filament sliding
actin filament
myosin II
filament sliding

**Figure 3.** Myosin regulatory light chain phosphorylation and the regulation of the assembly of myosin II into actomyosin filaments. (A) Myosin heavy chain (green), myosin regulatory light chain (purple), myosin essential light chain (blue) are shown. The nonmuscle myosin II regulatory light chain phosphorylation by kinases causes a change in the conformation of the myosin head, activaing its actin-binding site and releasing the myosin tail to allow the myosin molecules to assemble as bipolar filaments. The figure is adapted from Molecular Biology of the Cell, 4th edition, Alberts et al. (B) Bipolar filaments of myosin II produce contraction by sliding actin filaments in opposite directions. The figure is adapted from (Glotzer, 2005).

Figure 4

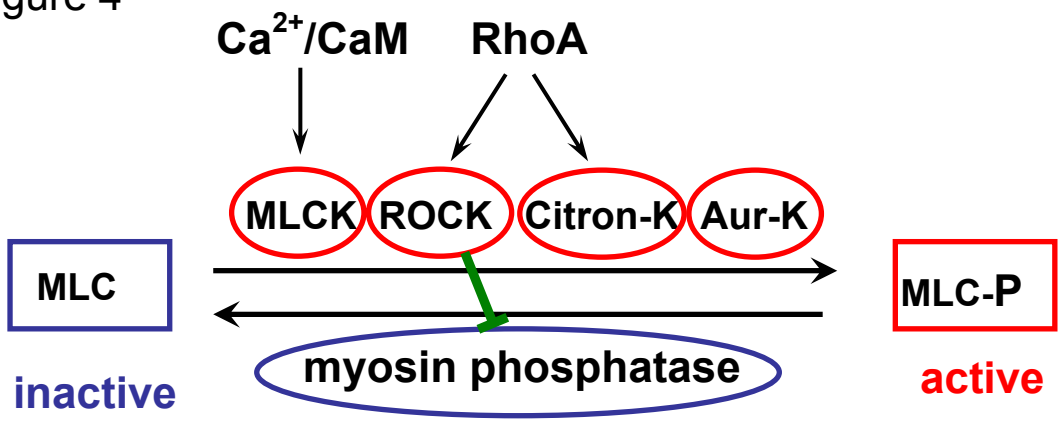


**Figure 4.** Myosin regulatory light chain phosphorylation regulation. Citron-K, citron kinase. Aru-K, Aurora kinase. The figure is adapted from (Matsumura, 2005).

domain at the C-terminus. The long isoform is the same as the short form except for six additional IgG modules and two actin-biding motif extensions at the N-terminus (Herring et al., 2006). Both MLCK isoforms are activated by $Ca^{2+}$/calmodulin. Chew et al. have used florescence resonance energy transfer (FRET) analysis to show that short MLCK is activated at the midzone immediately before the contraction at the cleavage furrow (Chew et al., 2002). However, the long isoform is preferentially localized in cleavage furrow in some cells (Poperechnaya et al., 2000). MLCK first phosphorylates MLC on Ser19, and then Thr18 at high kinase concentrations (Ikebe and Hartshorne, 1985), which is critical for cytokinesis completion in many organisms. Complete inhibition of furrow contractility is observed with either a MLCK inhibitory peptide or ML-7, a specific MLCK chemical inhibitor (Lucero et al., 2006; Silverman-Gavrila and Forer, 2001). Recent studies suggest that MLCK might be regulated by Aurora B kinase in the midzone during cytokinesis. Aurora B also localizes at the equator as discussed in Section 1.1.1.2, which has been shown to bind to and phosphorylate the MLCK IgG domain (Dulyaninova and Bresnick, 2004). Mice lacking both MLCK isoforms develop to full size and do not die until 1-5 hours after birth (Somlyo et al., 2004), suggesting , MLCK is not the only kinase that regulates myosin during cytokinesis *in vivo*.

ROCK, a Rho-effector kinase, is another regulator of myosin activity during cytokinesis through inhibiting myosin phosphatase and phosphorylating MLC (Amano et al., 1996; Eda et al., 2001; Kosako et al., 1999). There are two genes encoding ROCK in mammalian cells, ROCK-I and ROCK-II. Both forms of ROCK along with RhoA, an activator of ROCK, localize at the cleavage furrow. However, ROCK inhibitors only reduce MLC phosphorylation at the cleavage furrows and slow contraction but do not block initiation or completion of cytokinesis in HeLa

cells (Kosako et al., 2000). Neither ROCK-I nor ROCK-II knockout mice have been reported to show cytokinesis failure (Shimizu et al., 2005; Thumkeo et al., 2003).

In addition, citron kinase, another Rho-effector, also phosphorylates MLC at Thr18/Ser19 during cytokinesis (Eda et al., 2001; Yamashiro et al., 2003). Citron kinase localizes at the cleavage furrow and midbody during the early and late stages of cytokinesis, respectively (Eda et al., 2001; Gruneberg et al., 2006; Madaule et al., 1998; Paramasivam et al., 2007). This localization requires KIF14, a known mitotic kinesin (Gruneberg et al., 2006). Overxpression of citron kinase deletion mutants results in the accumulation of multinucleate cells and a kinase-active mutant causes abnormal contraction during cytokinesis in HeLa cells (Madaule et al., 1998). However, RNAi-mediated knockdown of citron kinase in *C. elegans* causes no phenotype, indicating the roles of citron kinase are different in other species (Simmer et al., 2003). Mice with inactivated citron-K gene grow at slower rates, are severely ataxic, and die before adulthood (Di Cunto et al., 2000).

Resent study reveals that AIM-1, an Aurora kinase from rat, monophosphorylates MLC at Ser19 *in vitro* and colocalizes with monophosphorylated MLC at the cleavage furrow of dividing cells. It suggests Aurora kinases may be directly involved in monophosphorylation of MLC during cytokinesis (Murata-Hori et al., 2000).

Myosin phosphatase is the only known phosphatase regulating MLC. It consists of MYPT1 (myosin targeting subunit), M20 and PP1cδ (a catalytic subunit). MYPT1 contains a PP1cδ-binding domain and a MLC-binding motif near the N-terminus and a M20-binding

domain near the C-terminus (Ito et al., 2004). MYPT1 is specifically phosphorylated at Ser432/Thr435 during prometaphase which increases its myosin phosphatase activity. When cells enter late anaphase, MYPT1 is phosphorylated primarily by ROCK at an inhibitory site (Thr696), leading to the initiation of cleavage furrow formation (Kawano et al., 1999; Totsukawa et al., 1999; Yokoyama et al., 2005). MYPT1 is activated again while the contractile ring is disassembling during the late cytokinesis. RNAi knockdown of MYPT1 increases MLC phosphorylation in HeLa cells, resulting in an increase of actin filaments assembly (Xia et al., 2005). Moreover, MYPT1 also interacts with multiple proteins, including Tau, MAP2, GTP-RhoA, cGMP-dependent protein kinase (cGKIα), phospholipids (Amano et al., 2003; Ito et al., 1997; Surks et al., 1999). Therefore, MYPT1 might also have the potential to function as a signal transducer for cytoskeletal remodeling. The function of M20 is not clear. Takizawa et al. have found that M20 associates with microtubules in living cells and enhances the rate of tubulin polymerization *in vitro*, suggesting M20 might play roles in regulating microtubule dynamics and cytokinesis signal transduction (Takizawa et al., 2003).

#### 1.1.1.4 Midbody

In late telophase, the midzone microtubules are deeply compressed by contractile ring closure. This complex structure that forms between dividing cells during cytokinesis containing tightly bundled microtubules and proteins, is called midbody (Figure 1E). It is known that MKLP1, KIF4, KIF14 and Aurora B complex, localize to the central spindle at the beginning of cytokinesis (see Section 1.1.1.2 for details), and also concentrate at the midbody. These kinesins and the complex are required for cytokinesis (Gruneberg et al., 2006; Katayama et al., 2003;

Kurasawa et al., 2004; Matuliene and Kuriyama, 2002). Recently, studies on isolated midbodies from Chinese hamster ovary (CHO) cells have revealed some new components. Interestingly, Golgi matrix protein, GM130, and cdk1 have been found, indicating that the midbody very likely functions in vesicle trafficking and cell cycle regulation, which are essential for successful cytokinesis in mammalian cells (Skop et al., 2004).

#### 1.1.1.5 Membrane dynamics during cytokinesis

The cytoplasmic membrane is very dynamic during cytokinesis in animal cells. At the early stage, while the contractile ring is closing, membrane inserts at the site of cleavage to satisfy the geometric requirement of an increase in surface area for a cell to divide (Danilchik et al., 2003; Shuster and Burgess, 2002). It is also hypothesized that vesicles transported to the furrow might contain some important transmembrane proteins whose enrichment at the cleavage site contributes to contractility (Emoto and Umeda, 2000). There are two major mechanisms for membrane transportation to the cleavage furrow: 1) the secretory pathway and 2) the endosomal recycling pathway. Some evidence to support a role for the secretory pathway in membrane insertion is that some Golgi proteins are required for cytokinesis (Sisson et al., 2000). In addition, an integral membrane protein, Strabismus (Stbm), is essential for membrane deposition during cell division in *Drosophila* and localizes primarily to the Golgi (Lee et al., 2003). Endocytosis also has been observed to occur specially at the furrow in the nematode eggs and zebrafish embryo (Danilchik et al., 2003; Feng et al., 2002).

#### 1.1.1.6 The endoplasmic reticulum function during cytokinesis

The endoplasmic reticulum (ER) is an essential cellular organelle for protein synthesis and maturation, as well as a $Ca^{2+}$ storage compartment and resource of intracellular calcium signals. Although ER has not been shown to play a role in cytokinesis, Bicknell et al. have found that an ER unfolded protein stress response disrupts cytokinesis in *S.cerevisiae*, suggesting ER function may be relevant (Bicknell et al., 2007). The hypotheses are that 1) ER stress disrupts vesicle trafficking, resulting in slow membrane deposition at the cleavage furrow (see discussion in Section 1.1.1.5); or 2) ER stress inhibits phospholipid metabolism which is required for cytokinesis (Emoto and Umeda, 2001; VerPlank and Li, 2005). It is known that phosphatidylinositol 4-phosphate 5-kinase (PIP5K) and its product phosphatidylinositol 4,5-bisphosphate (PI(4,5)P(2)) are localized to the cleavage furrow and required for normal cell division (Emoto et al., 2005; Field et al., 2005; Janetopoulos et al., 2005).

### 1.1.2 Cytokinesis defects and tumorigenesis

#### 1.1.2.1 Outcome of cytokinesis failure

As discussed previously, cytokinesis seems to be a delicate system and easily impaired. What is the outcome of cytokinesis failure? Based on the live-cell imaging studies, if cytokinesis fails, a cell with two nuclei (tetraploidy) and four centrosomes (Eggert et al., 2006; Shi and King, 2005) and the study in this dissertation) will result. These tetraploid cells have been observed to undergo a p53-dependent arrest in G1 of the cell cycle. This is likely due to the apparent risk to genome stability (Andreassen et al., 2001). However, recent studies have challenged this idea, showing that tetraploid cells from defective cytokinesis do not necessarily undergo arrest or delay in G1 (Uetake and Sluder, 2004). Furthermore, it has been known that normal hepatocytes

of the liver, which can be tetraploid, are capable of proliferation (Guidotti et al., 2003). In conclusion, the tetraploid progeny from an abortive cytokinesis have the potential to proliferate, which could be p53-dependent.

#### 1.1.2.2 Cytokinesis defects, p53 and tumorigenesis

Tetraploidy, one of the consequences of cytokinesis failure, has been considered to be a transient intermediate for aneuploidy and tumorigenesis. Although common solid tumors tend to be aneuploid, it has been shown that in some tumor tissue samples, such as myeloid leukemia, malignant gliomas, and colonic adenocarcinoma, (Lemez et al., 1998; Park et al., 1995; Takanishi et al., 1996) and in many tumor-derived cell lines (Lothschutz et al., 2002; Olaharski et al., 2006; Shi and King, 2005), tetraploidy is common. Galipeau et al. have found that premalignant Barrett's oesophagus accumulates tetraploid populations of cells and this correlates with progression to aneuploidy with inactivation of the p53 gene (Galipeau et al., 1996). This study strongly supports the link between tetraploidy and aneuploidy. Recent study from the Pellman lab has provided a direct experimental test of tumorigenesis potential of tetraploid cells accumulated from cytokinesis failure. Tetraploid p53-null mouse mammary epithelial cells (MMEC) derived from treatment with an actin inhibitor generate malignant mammary tumors after subcutaneous injection into nude mice. The tumor cells isolated from mice are aneuploid with extra centrosomes indicating that they are derived from the injected tetraploid cells (Fujiwara et al., 2005). In addition to this work, Rat1a fibroblast cells with Gp1bα overexpression, a subunit of the von Willebrand factor receptor, give rise to tetraploid cells *in vitro* as discussed further in this dissertation. These tetraploid Rat1a- Gp1bα cells are also tumorigenic in nude mice (Li et al., 2007a). Taken together, these results indicate that tetraploid

cells derived from cytokinesis defects are strongly correlated with tumorigenesis and malignant progression.

As I discussed above, normal tetraploid cells usually, but not always, undergo a p53-dependent cell cycle arrest in G1. Consistent with this, p53 +/+ tetraploids fail to propagate *in vitro* and do not induce tumors in Pellman's study (Fujiwara et al., 2005). In Li's study, human foreskin fibroblast cells (HFF) with overexpressed Gp1bα do not, but HFF cells with Gp1bα overexpression and p53 knockdown do produce tetraploid cells for a long period of time (Li et al., 2007a; Li et al., 2007b). In summary, it is possible that p53 null or deficiency is required for cytokinesis-induced tumorigenesis by promoting proliferation of tetraploids.

How does p53 play a role in leading tetraploids to tumorigenesis? p53 protein (encoded by gene *TP53*) is a transcription factor that regulates the cell cycle and functions as a tumor suppressor protein. In unstressed cells, the p53 level is low due to a continuous degradation by association with the murine double minute 2 (Mdm2) protein. Mdm2 binds to p53 and transports it from the nucleus to the cytoplasm where it is degraded by the proteasome (reviewd in Oren, 2003). In response to stress from DNA damage, a series of kinases including ATR, ATM, Chk1, Chk2, DNA-PK are activated by DNA damage response (reviewd in Bakkenist and Kastan, 2004; Pluquet and Hainaut, 2001). Subsquently, p53 is phosphorylated at multiple sites at N-terminal transcriptional activation domain by these protein kinases, and phosphorylated p53 disassociates with Mdm2 and becomes stable and active. The activation of Chk1, Chk2 and p53 lead to cell cycle checkpoints arrest. If the DNA damage is not too severe, this transient arrest gives cells time to repair the lesions. In addition, p53 also licalizes to the sites of DNA damage to

promote repair (Al Rashid et al., 2005). Alternertively, if the DNA damage repair fails, p53 induces apoptosis by transcriptionally upregulating effectors of apoptosis such as PUMA, BAX and downregulating repressors such as BCL-2 (reviewd in Oren, 2003). Instead of apoptosis, activation of p53 by severe DNA damage leads to cell senescence in fibroblast cell lines (Di Leonardo et al., 1994). Taken together, the transient arrest, apoptosis or senescence are important mechanisms for cells to eliminate DNA damage and chromosomal aberrations, which may contribute to tumorigenesis.

p53 protein is considered a guardian of the genome. If the *TP53* gene is damaged, tumor suppression is severely reduced. People who have only one functional copy of the *TP53* gene often develop tumors in early adulthood, known as Li-Fraumeni syndrome (reviewed in (Iwakuma et al., 2005). This tumor suppressor gene is mutated or deleted in approximately 50% of human cancers (reviwed in Soussi et al., 2006). Furthermore, it is believed that p53 pathway is somewhat inactivated in tumors carrying wild-type *TP53* gene through Mdm2 amplification (Michael and Oren, 2003). In terms of the p53's contribution in leading tetraploids to tumorigenesis, it appears that a defective p53 activity possibly allows tetraploids to overcome the cell cycle checkpoints and escape from apoptosis or senescence, resulting in uncontrolled cell divisions with high risks of unrepaired DNA damage.

The mechanism of how the tetraploid cells become aneuploid has been studied for years. It is known that tetraploid cells with extra centrosomes can undergo abnormal mitoses, such as multipolar cell division and anaphase bridges, and this leads to aneuploid cells and genomic instability. How this happens will be discussed in details in Section 1.2 and Section 1.3. An

interesting recent idea is that tetraploidy might enhance tumorigenesis by increasing the long-term fitness of cells with added chromosomes. In diploid budding yeast, mutators, which induce DNA damage in yeast, have a fitness advantage over nonmutators (Thompson et al., 2006). In contrast, haploid mutators have no advantage and show less fitness when competed against haploid nonmutators. In conclusion, a diploid chromosome set gave budding yeast a significant advantage over haploids in this mutation evolution experiment (Thompson et al., 2006). It is very likely that extra chromosome sets might mask the effects of deletion or mutations to allow cells with DNA damage to survive longer until a transforming mutation occurs. Therefore, tetraploidy benefits cells during tumorigenesis.

## 1.2 CENTROSOME AMPLIFICATION AND MULTIPOLAR SPINDLES (MPS)

During mitosis, centrosomes organize the spindle poles and direct the chromosome segregation into daughter cells. The accurate regulation of centrosome assembly and duplication is essential for this process. The presence of more than two centrosomes in one single cell usually leads to multipolar spindles, resulting in an elevated frequency of chromosome missegregation. It is believed that this centrosome overamplification and spindle multipolarity is associated with tumor progression (reviewed in Saunders, 2005).

### 1.2.1 Centrosome amplification

Centrosomes have to duplicate once and only once in each cell cycle. However, abnormal, especially supernumerary (more than one centrosome in G1 phase), centrosomes are widely observed in cancer cells. In this section, I will review the regulation of centrosome duplication and discuss mechanisms of how centrosomes are overamplified.

#### 1.2.1.1 Centrosome structure and duplication in cell cycle

Centrosomes, small non-membranous organelles (1-2μm in diameter), are the major microtubule organizing centers (MTOCs) of animal cells (reviewed in Bornens, 2002; Nigg, 2006). The centrosome in animal cells is composed of a pair of centrioles, connected by an intercentriolar linkage and embedded in a protein meshwork, called the pericentriolar material (PCM). Vertebrate centrioles are small cylindrical organelles composed of 9 triplet longitudinal microtubules (Figure 5). The centrioles are oriented perpendicular to each other, and the older mother centriole is studded by appendages at its distal ends (Figure 6). Appendages appear to be essential for anchoring microtubules (Bornens, 2002). The PCM contains proteins responsible for microtubule nucleation and anchoring, including γ-tubulin and centrin. It is well known that γ-tubulin forms ring complexes serving as nucleation sites for the assembly of microtubules (Zhang and Nicklas, 1995); and centrin functions in maintaining centrosome structure and regulating centriole duplication (Salisbury et al., 2002). There are several coiled-coil proteins that have been identified as PCM proteins, such as, pericentrin, that functions in centrosome replication regulation (Loncarek et al., 2008); ninein (Bouckson-Castaing et al., 1996), which is

Figure 5

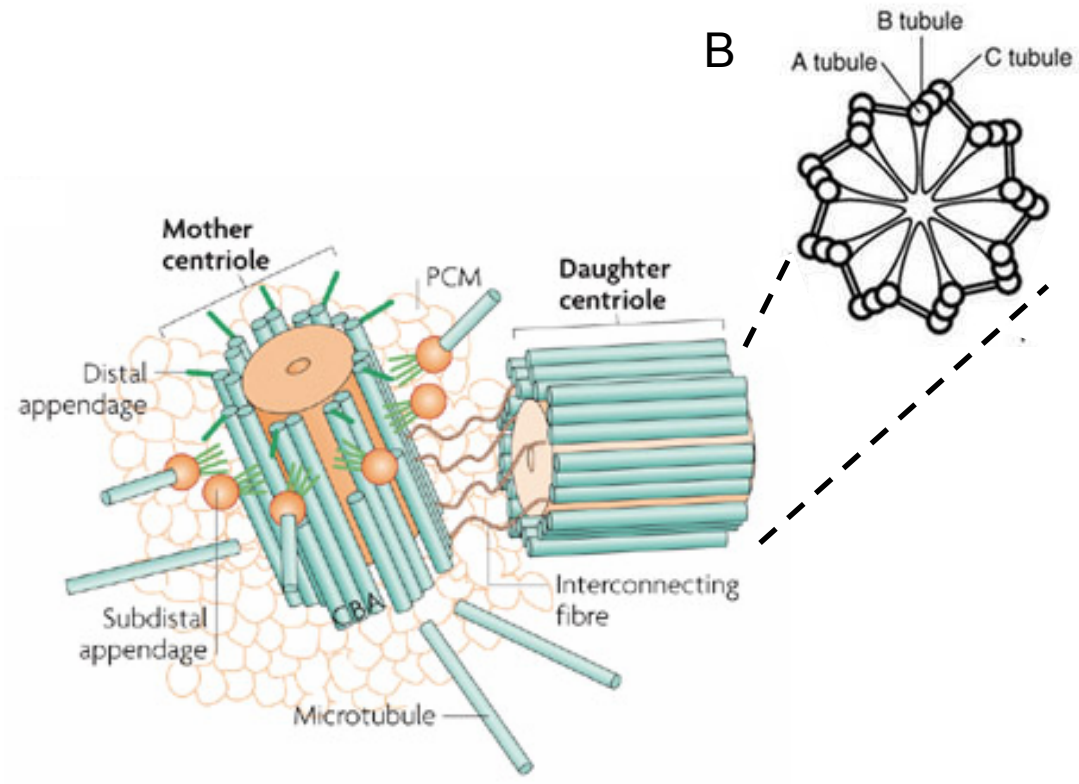
A
B
B tubule
A tubule
C tubule
Mother centriole
PCM
Daughter centriole
Distal appendage
Interconnecting fibre
Subdistal appendage
Microtubule

C

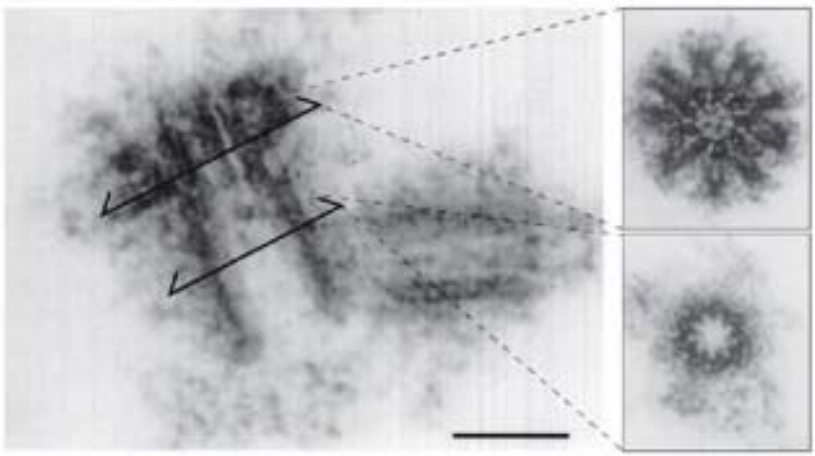

**Figure 5.** Centrosome structure. (A) Schematic cartoon of the centrosome. PCM, the pericentriolar material. (B) Schematic cartoon of centriole configuration with an array of nine microtubule triplet. In each triplet, the most internal tubule is called the A tubule; the two following ones are the B tubule and the C tubule respectively. (C) Electron microscopy graph of the centrosome. The top right figure indicates a cross-section of appendages; the right bottom shows a cross-section of the proximal part of the centriole with triplet microtubules. Bar: 0.2 μm. Figures are adapted from (Bettencourt-Dias and Glover, 2007).

required for centrosomal regulation, and Cep135 for microtubule organization (Ohta et al., 2002). Interestingly, it has been found that cyclin B1/Cdk1 is first activated on the centrosomes in prophase, suggesting that centrosomes transiently recruit components of signaling pathways to possibly enhance the efficiency of cell cycle regulation (Jackman et al., 2003; Kramer et al., 2004).

During interphase, centrosomes organize the cytoplasmic microtubule network, playing roles in vesicle transport, proper distribution of small organelles and establishments of cell shape, polarity and motility (reviewed in Nigg, 2002; Saunders, 2005). During mitosis, centrosomes direct the mitotic spindle formation at the poles. Although centrosomes are not essential for bipolar spindle formation, they are required for chromosome segregation fidelity and cleavage plane determination during cell division (Heald et al., 1996; Khodjakov et al., 2000). Therefore, the precise control of centrosome number is critical to ensure bipolarity in dividing cells. The centrosome duplication cycle is reviewed in Figure 6. In G1, a pair of centrioles is oriented orthogonally to each other. Once cells pass the G1 checkpoint, the centrioles lose their orthogonal arrangement. In early S phase, a procentriole forms perpendicular to each centriole at the proximal end, and later these new centrioles elongate. The elongation of procentrioles continues throughout G2. At the G2/M transition, the two newly formed centriole pairs disconnect and the PCM is divided between the parental centrioles. At the same time, a process known as centrosome maturation occurs, resulting in an increase of MT nucleation activity. In mitosis, two centrosomes organize bipolar spindles to direct chromosome segregation. Each daughter cell inherits only one centrosome and behaves as a mother centriole during the subsequent replication cycle. It is well known that both phosphorylation and

proteolysis are required and essential for the regulation of the centrosome replication cycle (Bornens, 2002; Brinkley, 2001; D'Assoro et al., 2002; Pihan et al., 2001; Sluder and Nordberg, 2004).

#### 1.2.1.2 Centrosome overamplification pathways

Centrosomal amplification is a common source of divisional errors in cancer cells and has been suggested to play a role in tumor formation for over a century (Wunderlich, 2002). Supernumerary centrosomes have been reported in a variety of solid tumors, including breast, brain, bone, gall bladder, lung, liver, pancreas, colon, prostate, ovary and cervix (Carroll et al., 1999; Gisselsson et al., 2004; Hsu et al., 2005; Jiang et al., 2003; Kawamura et al., 2003; Kuo et al., 2000; Lingle et al., 1998; Lingle and Salisbury, 2000; Nakajima et al., 2004; Pihan et al., 2001; Sato et al., 1999; Saunders, 2005; Skyldberg et al., 2001), and cancer-derived cell lines (Figure 7) (Pihan et al., 2003; Quintyne et al., 2005).

There are several models to explain how centrosomes become amplified (Figure 8) (Blagosklonny, 2007; Nigg, 2002; Sluder and Nordberg, 2004; Tarapore and Fukasawa, 2002). First, since centrosomes can replicate independently of chromosomal duplication, centrosomes may over-replicate during the cell cycle. For example, when cells lacking normal cell cycle checkpoints are treated with the DNA synthesis inhibitor hydroxyurea, centrosomes continue to duplicate even though the cell cycle is blocked (D'Assoro et al., 2004). Similarly, overexpression of the Cdk2/Cyclin E kinase in a p53 -/- genetic background, expression of the

Figure 6

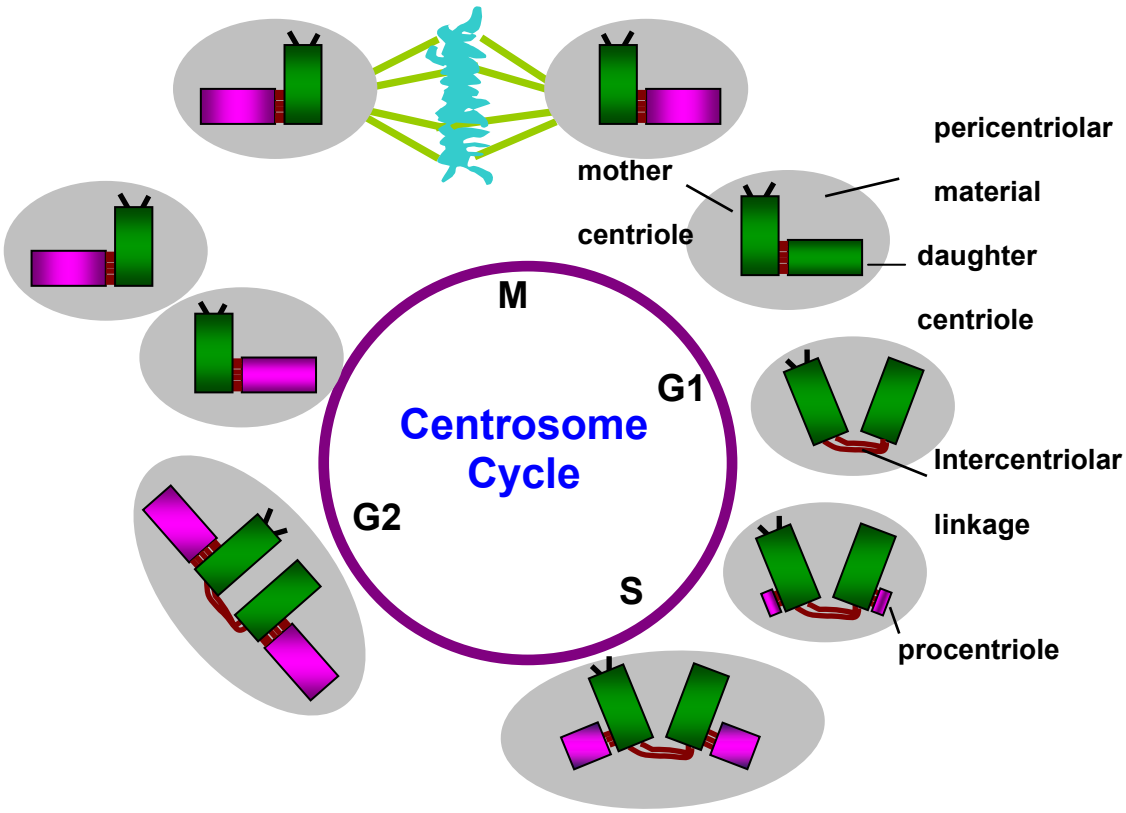


**Figure 6.** The centrosome duplication cycle. The centrosome consists of mother (green) and daughter centrioles (pink), that are connected by an intercentriolar linkage (red) and are embedded in the pericentriolar material (grey). The mother centriole can be distinguished by the presence of appendages (black lines). The figure is adapted from Crasta and Surana, Cell Division, 2006.

Figure 7

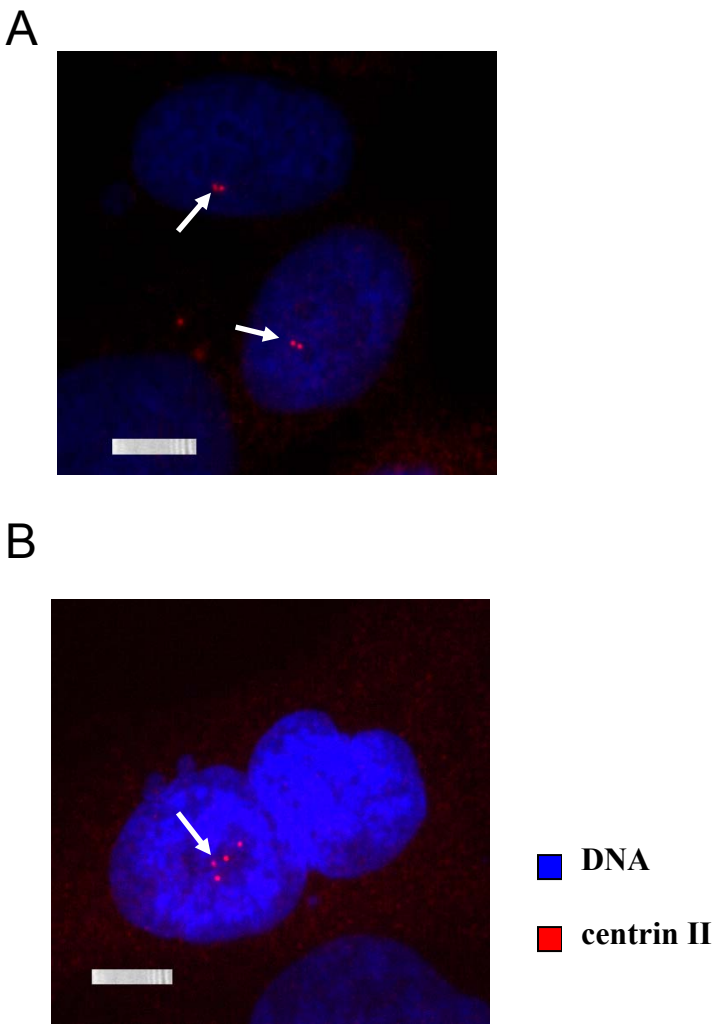


**Figure 7.** Centrosome amplification in UPCI:SCC103 cells. Centrioles and nuclei are stained in red and blue respectively. (A) A pair of centrioles in a mononulceated cell (arrows). (B) Four centrioles are observed in a binucleated cell (arrow).

Figure 8

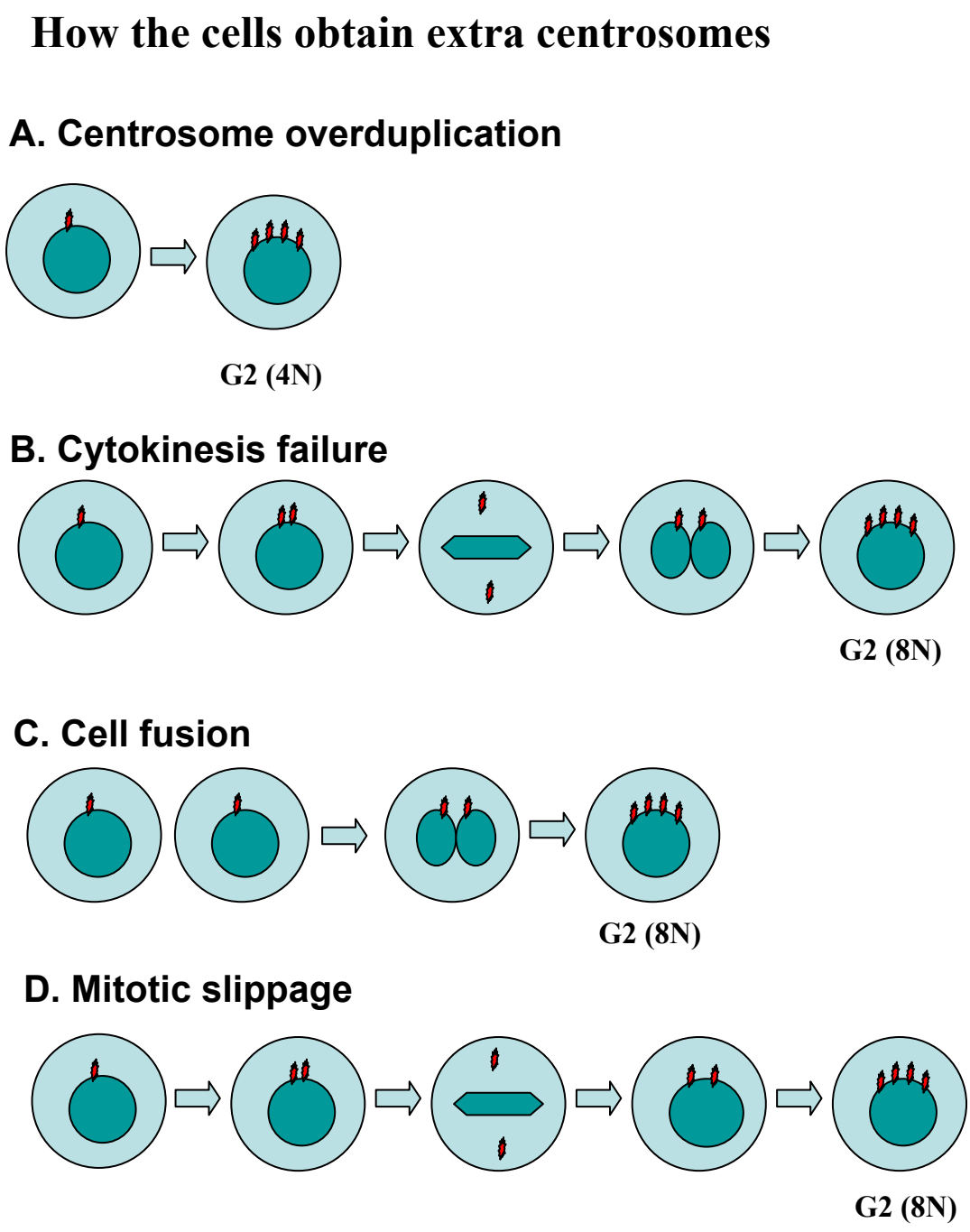


**Figure 8.** Supernumerary centrosome accumulation in cells.

human papillomavirus oncoprotein E7, the Cdk2 substrate hMps1, or the polo-like kinase-2 (plk-2), all induce additional rounds of centrosomal duplication (Chiba et al., 2000; Duensing and Munger, 2002; Fisk et al., 2003; Kawamura et al., 2004; Warnke et al., 2004). Additional to this, recent studies have shown that *de novo* genesis of centrioles could be produced in cultured cells and *Drosophila* embryos without mother centrioles (Khodjakov et al., 2002; La Terra et al., 2005; Rodrigues-Martins et al., 2007). Taken together, either centrosomal overduplication and/or *de novo* genesis is a potential important source of centrosome amplification.

The second model predicts that supernumerary centrosomes result from a failure of cytokinesis. As discussed in Section 1.1.2, if cytokinesis fails to partition the duplicated centrosomes, a single cell can inherit more than one centrosome, even though centrosomal replication is normal. Study from this dissertation has revealed that abortive cytokinesis is an important and primary mechanism for cancer cells to obtain extra centrosomes.

The third mechanism is cell-cell fusion. Although there is no good evidence supporting that this mechanism is widely involved in centrosome amplification in cancer cells, Duelli et al. have demonstrated that a primate virus (Mason-Pfizer monkey virus) is capable of inducing cell-cell fusion. This type of virus uses both viral and exosomal proteins involved in cell fusion to produce transformed proliferating human cells if the p53 is inactivated, providing a link between cell fusion and carcinogenesis (Duelli et al., 2005).

Recently, mitotic slippage has emerged as another model for centrosome amplification. If the cells arrest in mitosis for a very long time, even though the spindle checkpoint is active,

Figure 9

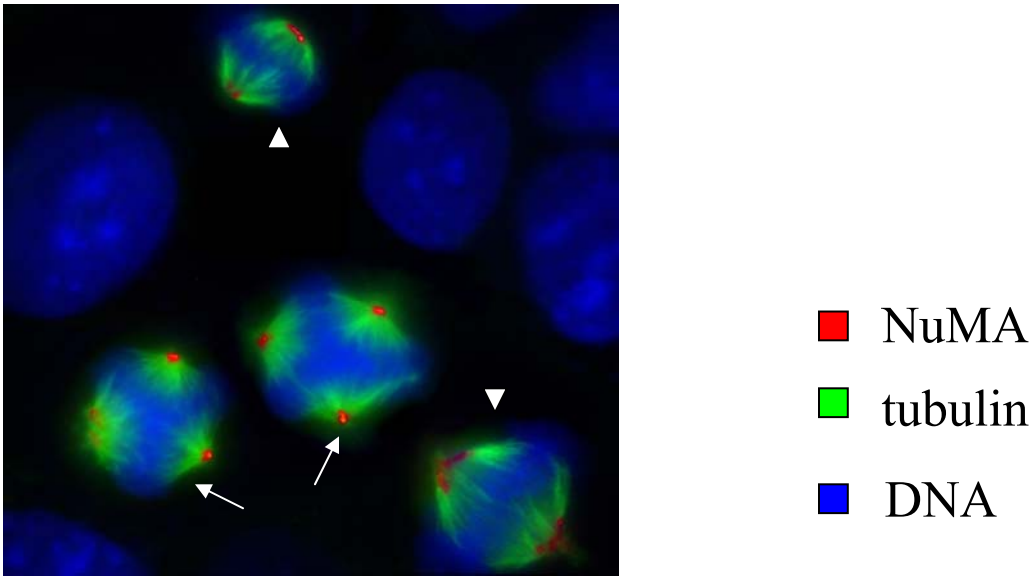


**Figure 9.** Bipolar and multipolar spindles in mitotic UPCI:SCC103 cells. Nuclei (blue), centrosome (red) and microtubules (green) are labeled. Cells with bipolar spindles (arrowheads) and multipolar spindles (arrows) are shown. Figure is from Dr. Nicholas Quintyne and Dr. William Saunders.

Figure 10

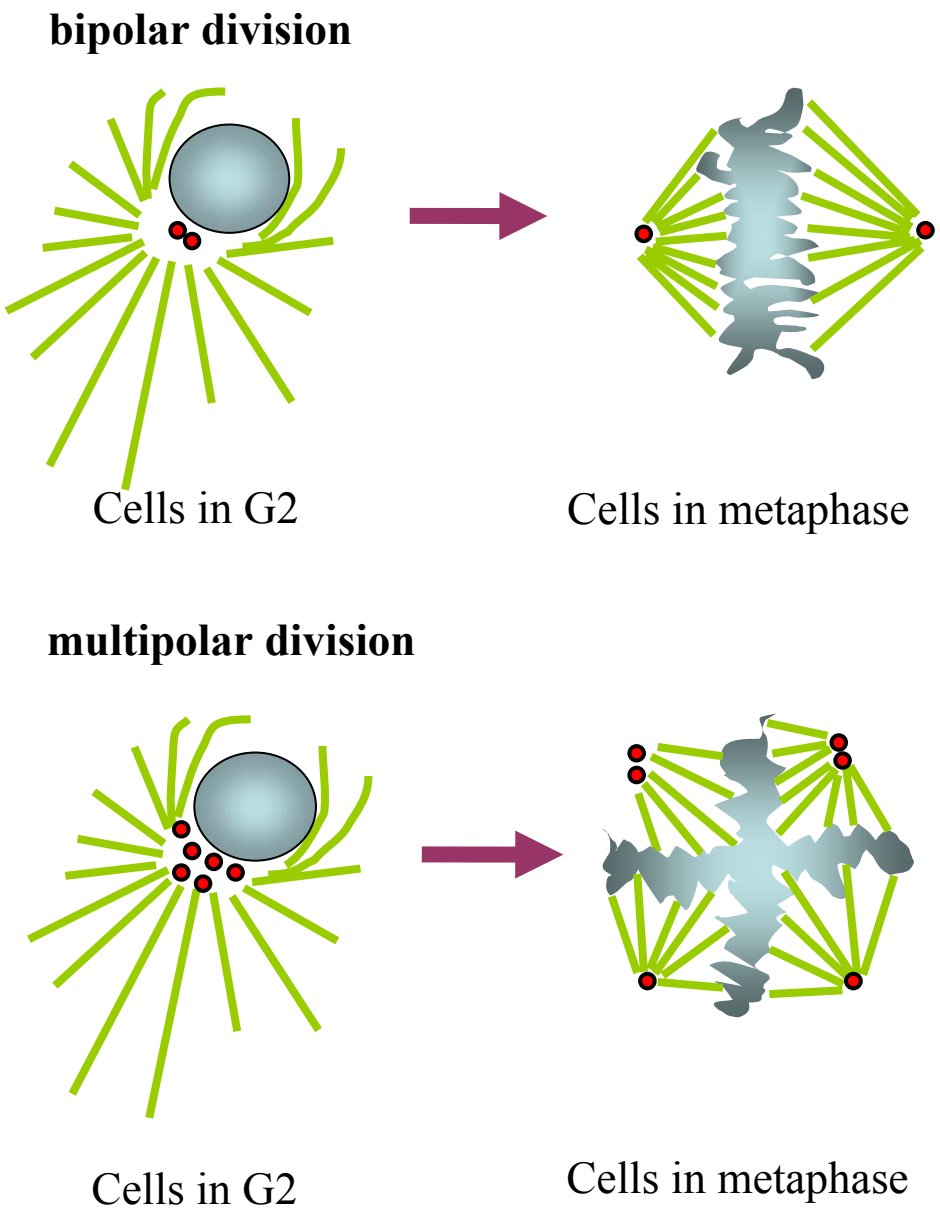


**Figure 10.** Centrosome amplification leads to multipolar spindle formation. DNA (blue), microtubules (green) and centrosomes (red) are shown.

cyclin B is slowly and continuously degraded by APC-proteolysis. Thus, the cell ultimately exits mitosis and arrests in G1 with duplicated chromosomes and two centrosomes (Blagosklonny, 2007). Theoretically, if these cells enter the next cell cycle, they will have extra centrosomes. The cells escaped from the mitotic slippage usually result in big mononucleated daughter cells due to un-segregated chromosomes, which is distinguishable from cytokinesis failure ended with binucleated daughters.

### 1.2.2 Multipolar spindles (MPS)

Multipolar spindles formation is strongly linked to centrosome amplification, especially in cancer cells. This section will discuss MPS structure and mechanisms of how MPS form in detail.

#### 1.2.2.1 MPS structure and formation

Multipolar spindles (MPS) are defined as the presence of more than two spindle poles in mitotic cells. MPS in metaphase cells were identified by irregular chromosome alignment; typically a "Y" or "T" figure for tripolar and an "X" figure for tetrapolar spindles (Figure 9). The multipolarity most likely comes from centrosome amplification. The simple rationale is that more than two active centrosomes organize microtubules to create multiple spindle poles (Figure 10). I have observed a high frequency of centrosome amplification and multipolarity in various tested cancer cell lines, and multipolar spindles mostly come from binucleated cells (data from this dissertation). It is also known that chemically inhibiting cytokinesis or overexpression of

Aurora A leads to both multinucleated cells and MPS in the absence of centrosome replication defects (Meraldi et al., 2002; Sluder and Nordberg, 2004; Uetake and Sluder, 2004). Furthermore, binucleated cells in sea urchin zygotes, and PtK1 cells, form MPS as shown by live cell microscopy (Sluder et al., 1997).

#### 1.2.2.2 Centrosome amplification and MPS

Although centrosome overamplification and MPS appear to occur together in cancer (reviewed in Gisselsson et al., 2002), not all the cells with extra centrosomes undergo multipolar mitosis. For example, in NIE115 (mouse neuroblastoma cells) and UPCI:SCC114 (human oral cancer cells), supernumerary centrosomes coalesce into two functional spindle poles at mitosis (Quintyne et al., 2005; Ring et al., 1982). Recent study from the Saunders lab reveals a model for how multipolar spindles are inhibited in normal cells, suggesting that active dynein at the spindle poles cluster the extra centrosomes together. Dynein mislocalization from the spindles in mitosis in cancer cells leads to multipolarity in some cancer cell lines (Figure 11A) (Quintyne et al., 2005).

In the second model, centrosomal splitting can also lead to MPS without amplifying centrosomes (Figure 11B). For example, the Nek2 kinase, which plays a role in centriole separation through phosphorylation of liner proteins between two centrioles, is overexpressed in breast cancer tissue and leads to centrosomal splitting and MPS (Fry et al., 1998; Hayward et al., 2004). Centrosome separation can also be induced by treatment with microtubule disrupting drugs, such as nocodazole and colcemid (Jean et al., 1999; Meraldi and Nigg, 2001). Moreover,

Figure 11

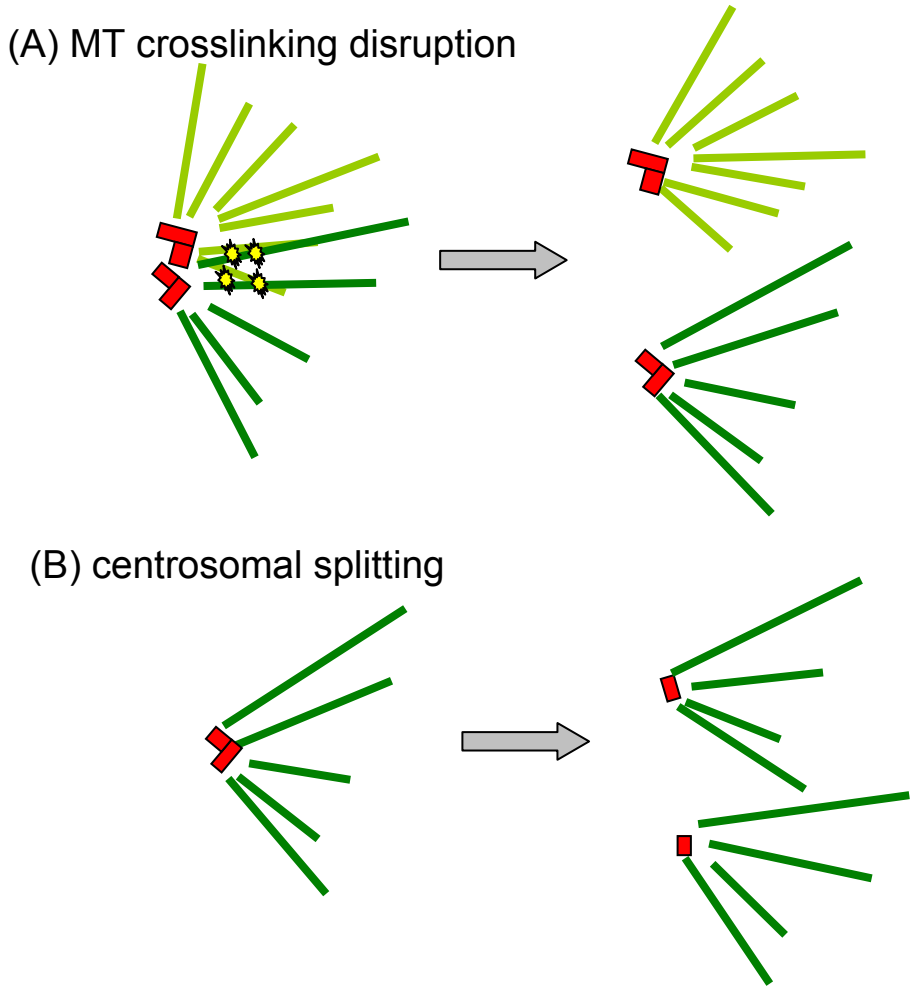


**Figure 11.** Multipolar spindle formation. (A) microtubule crosslinking disruption model. Centrioles (red rectangle), microtubules (light green, dark green), microtubule binding proteins (yellow) are shown. Centrosomes are coalesced by microtubule binding proteins at one pole. If these proteins are depleted, centrosomes split and multipolar spindles form. (B) Centrosomal splitting model. Centrioles (red rectangle) and microtubules (dark green) are shown. If a centrosome splits, centrioles are capable of organizing MT to form multiple spindle poles.

it has been shown that DNA damage leads to centrosomal splitting in mammalian cells (Hut et al., 2003). Observation from the Saunders lab also supports this pathway, as centrosomal fragmentation has been seen after the treatment of ionizing radiation in human cells (Acilan and Saunders, unpublished data).

### 1.2.3 Supernumerary centrosomes, MPS and tumorigenesis

Supernumerary centrosomes and multipolar divisions are commonly observed in a variety of solid tumors and cultured cancer cells as discussed above. Multipolarity, followed by a multipolar division, is thought to be a short-term consequence of centrosome amplification. Multipolar divisions have the potential to induce chromosomal instability because multiple spindle poles can not guarantee an even distribution of genetic material into daughter cells. Thus, the daughter cells are mostly likely aneuploid. Undoubtedly, the progeny from a multipolar division are often inviable due to a loss of essential genes. However, if these cells lose tumor suppressor genes, such as *TP53*, while retaining a viable inheritance of chromosomes, they may become malignant cells. On the other hand, some progeny may gain rather than lose oncogenes and be selected based on enhanced growth signals.

Taken together, it is possible that this gain-and-loss process gives the progeny of multipolar division a selective advantage to survive, proliferate and progressively increase malignancy. In addition, multipolar division is also associated with other chromosome segregational defects, such as anaphase bridges, promoting more genomic instability in cells (see Section 1.3.2.1 for details).

## 1.3 GENOMIC INSTABILITY AND TUMORIGENESIS

### 1.3.1 Sources of genomic instability

Cancer is a result of accumulation of mutations that accelerate cell division and/or inhibit cell death. In theory, a cell has to undergo multiple mutations before it becomes tumorigenic (Lengauer et al., 1997). Two major ways of mutation have been demonstrated in general, microsatellite instability (MIN) and chromosomal instability (CIN). MIN is typically caused by mutations in mismatch repair genes. CIN is defined as an elevated rate of gain or loss of part or whole chromosomes during mitoses. CIN is thought to be a major cause of mutational change and aneuploidy which is commonly observed in solid tumors and tumor-derived cell lines. In this section, I will discuss some events that may contribute to genomic instability.

#### 1.3.1.1 Chromosome segregation defects

Although there are numerous events that may lead to CIN, the main defects can be listed as abnormal chromosomal segregation and/or cell-cycle checkpoint regulation. These different defects usually coexist in cancer cell lines and perhaps cooperatively contribute to the multistep tumorigenesis process (Gisselsson et al., 2002; Jallepalli and Lengauer, 2001; Saunders et al., 2000). The major visible segregational defects in cancer cells can be summarized as micronuclei, lagging chromosomes, anaphase bridges and multipolar mitoses (Figure 12), which will be discussed individually below.

Figure 12

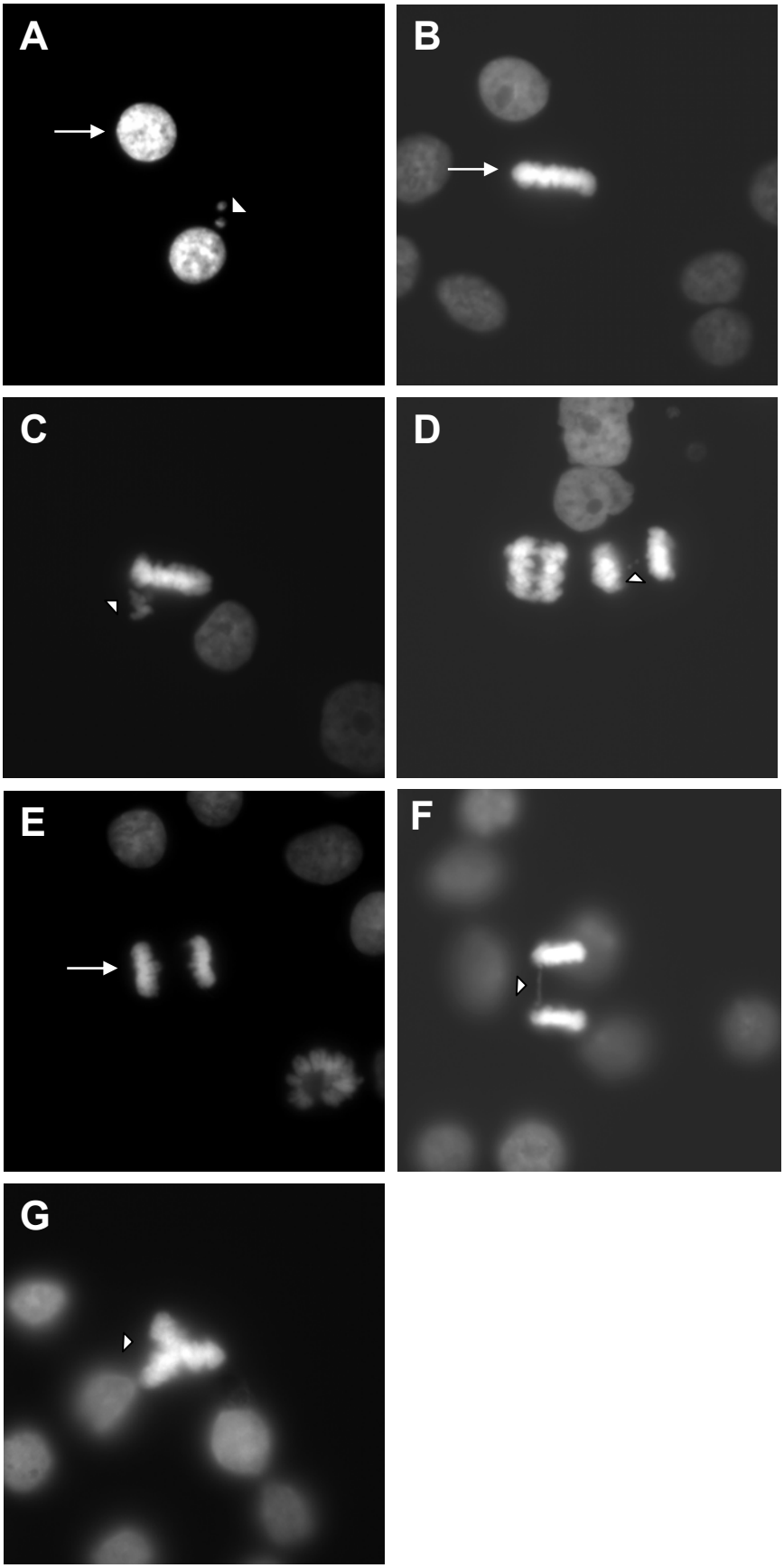

**Figure 12.** Chromosomal segregation defects in HeLa cells. (A) A normal interphase cell (arrow) and an interphase cell with two micronuclei (arrowhead) are shown. (B) A normal metaphase cell (arrow). (C) A metaphase cell with lagging chromosome (arrowhead). (D) An anaphase cell with lagging chromosome (arrowhead). (E) A normal anaphase cell (arrow). (F) An anaphase cell with an anaphase bridge (arrowhead). (G) A metaphase cell with multipolar spindles (arrowhead).

Lagging chromosomes are defined as whole chromosomes or chromosome fragments, that fail to align properly at the metaphase plates (Figure 12C) or segregate behind the separated chromosomal masses during anaphase (Figure 12D). Lagging chromosomes are thought to be caused by failure in attachment of the spindle microtubules to the kinetochore (Dulout and Olivero, 1984) or by merotelic attachment of one kinetochore to both spindle poles (Cimini et al., 2002; Cimini et al., 2001; Thompson and Compton, 2008). Saunders lab has reported another origin of lagging chromosomes. They have found that chromosomes in bridges typically resolve by breaking into multiple fragments, resulting in lagging chromosomes (Hoffelder et al., 2004). The daughter cells with lagging chromosomes are under the risk of losing a whole or part of chromosome or gaining both copies of the sister chromatids or amplified chromosomal fragments. Both events contribute to chromosomal instability.

Micronuclei are the small nuclei that form whenever a chromosome or a fragment of a chromosome is not incorporated into one of the daughter nuclei during cell division (Figure 12A). Micronuclei have nuclear envelopes and a size that is 1/16 to 1/3 of the main nucleus (Fenech, 1993). The major reason of micronuclei formation is possibly due to lagging chromosomes, however breakage of anaphase bridges has also been shown to result in micronuclei in 50% of dividing cells with bridges (Hoffelder et al., 2004). Micronuclei are thought to be biomarkers of chromosome damage due to genetic instability or exposure to environmental mutagens or carcinogens, which would be useful for prediction of cancer risk (Iarmarcovai et al., 2007; Mateuca et al., 2006).

Another frequently observed chromosomal segregation defect in cancer cells is anaphase bridges. Anaphase bridges are viewed as chromatin fibers connecting the two chromosome masses together in dividing cells (Figure 12F). A bridge is thought to form from breakage-fusion-bridge (BFB) cycles. BFB cycle starts in chromosomes when there is a DNA double stranded break (DSB), exposing telomere-free chromosome ends. These naked ends are believed to fuse with other chromosomes, or sister chromatids with a DSB (Gisselsson, 2002). DBS repair pathways are considered to be essential for the fusion of free chromosome ends. A recent study from the Saunders lab has discovered that neither of the two major DSB repair pathways, homologous recombination (HR) or non-homologous end joining (NHEJ), are required for bridge formation. The NHEJ pathway very likely plays a role in prevention of bridges. The cells appear to use HR to repair the breaks when NHEJ is compromised, resulting in an increase of anaphase bridge formation (Acilan et al., 2007). Although anaphase bridges usually break in anaphase from the tension of the spindle pulling forces and/or cytokinesis midzone contraction, bridges sometimes, but rarely, have been observed to persist until telophase, or even interphase, without interruption, suggesting that strong unresolved anaphase bridges might be a cause of cytokinesis failure in cancer cells (Luo, Wu and Saunders, unpublished data). Anaphase bridges have been shown to contribute to CIN and have been reported at high frequency in both cancer cell culture and tumor tissues (Gisselsson et al., 2000; Montgomery et al., 2003). Moreover, this abnormality has been revealed to lead to structural and numerical chromosome changes and is strongly linked to tumorigenesis (Artandi et al., 2000; Stewenius et al., 2005).

Multipolar spindles (MPS) formation is a defect observed in many cancer cell lines and solid tumors (Figure 12G). As discussed in Section 1.2 in more detail, MPS formation is

associated with abnormalities of the centrosome and account for CIN and tumorigenesis (Saunders, 2005).

Although I have discussed four major types of chromosomal segregation defects (micronuclei, lagging chromosomes, anaphase bridges and multipolar mitoses) separately above, these defects have been shown to occur together and cooperatively contribute to CIN. It is known that the breakages along the anaphase bridges typically occur at multiple sites, leading to formation of lagging chromosomes and micronuclei (Hoffelder et al., 2004). In addition, there is a very strong correlation between the frequency of MPS and the level of bridging in different tumor samples (Gisselsson et al., 2002). There are two models of how these two events are linked together. First, the initiating mechanism of these two related segregational defects might be the same. For example, ionizing radiation and X-ray exposure have been shown to induce both defects in cells (Gisselsson et al., 2001; Sato et al., 2000; Scott and Zampetti-Bosseler, 1980). Another example is expression of human papillomavirus proteins E6 or E7, that bind and inactivate tumor suppressor proteins p53 and pRb *in vivo*. Expression of these proteins leads to both formation of anaphase bridges and multipolar cell divisions after centrosome overamplification in cells (Duensing et al., 2000; Schaeffer et al., 2004). Another model is that the correlation between anaphase bridges and MPS could exist due to another abnormality in cancer cells: tetraploidy. It has been shown that a tetraploid DNA content, results in an increase in DNA damage (Storchova et al., 2006). Since abnormal DNA repair causes anaphase bridges, tetraploidy may contribute to CIN by this mechanism. On the other hand, tetraploidy is also tightly associated with centrosome amplification, leading to multipolar mitoses in tumors and cultured tumor cells (See Section 1.2 for details).

#### 1.3.1.2 Mismatch repair defects

DNA mismatch repair (MMR) is a system for recognizing and repairing erroneous insertion, deletion, mis-pair of bases and other forms of DNA damage, which usually arise during DNA replication and recombination. Failure in the mismatch repair system has been shown to elevate the rate of DNA mutation destabilize simple repeat sequences, which is known as microsatellite instability (MIN) (Christmann et al., 2003). Mutations in the essential genes of MMR, such as, the MutS and MutL homologues, are found in most hereditary non-polyposis colon cancers (HNPCC) (Aaltonen et al., 1993; Christmann et al., 2003). A subtype of HNPCC, known as Muir-Torre Syndrome (MTS), is associated with skin tumors. MIN cannot be detected by karyotype analysis and does not involve the large scale genomic changes due to CIN.

### 1.3.2 Consequences of genomic instability

After summarizing origins of genomic instability above, in this section, I will discuss some outcomes of chromosome segregation and mismatch repair defects. The common consequence in cancer cells is to contribute to genomic instability and aneuploidy.

#### 1.3.2.1 Outcomes of chromosomal instability

Segregational defects in mitosis usually induce some large scale chromosomal alterations. There are two types of changes: 1) chromosome number, and 2) chromosome structure, including gene amplification, gene deletion and translocation.

Changes in chromosome number can be described as the gain or loss of an entire chromosome during chromosome segregation, which leads to a state of aneuploidy. Aneuploidy is known to be associated with almost all cancer types (Mitelman, 1983) and its severity is correlated with tumorigenesis (Cavalli et al., 1989).

Gene amplifications involve an increase in the copy number of oncogenes, which may lead to over production of the associated gene product and drive the cells to overcome checkpoints and proliferate uncontrollably. For instance, amplification of the Myc oncogene, which encodes for a transcription factor that regulates expression of 15% of all genes, has been reported in 30% of neuroblastomas (Ruf et al., 2001; Seeger et al., 1985). When Myc is overexpressed, it increases cell proliferation (Ruf et al., 2001).

DNA deletions are another phenotype of chromosomal instability. Loss of tumor suppressor genes is strongly associated with tumorigenesis. For example, the phosphatase and tensin homolog (PTEN) gene is one of the most commonly lost tumor suppressors in human cancers (Tamguney and Stokoe, 2007). PTEN acts by opposing the action of PI3K, which is essential for anti-apoptotic, pro-tumorogenic Akt activation (Leslie and Downes, 2004). Homozygous deletion of the PTEN gene has been detected in a subset of prostate adenocarcinomas (Wang et al., 1998).

Another type of chromosomal instability is DNA translocations. A translocation is most commonly seen as the rearrangement of regions of nonhomologous chromosomes. Translocations may create a fusion of two genes with a change in the activity of the hybrid

sequence. One famous example is the Philadelphia translocation which is associated with chronic myelogenous leukemia (CML). It is due to a reciprocal translocation designated as an exchange of genetic material between region q34 of chromosome 9 and region q11 of chromosome 22, by which the nuclear protein Bcr is translocationally juxtaposed to the Abl kinase, producing a hybrid Bcr-Abl protein with increased kinase activity (Ben-Neriah et al., 1986; Jeffs et al., 1998; Kurzrock et al., 2003).

#### 1.3.2.2 Outcomes of microsatellite instability

In addition to chromosomal instability, microsatellite instability is another reason for genomic instability. Changes in nucleotide sequence are widely observed in tumors including substitution, addition or deletion of nucleotides. For instance, mutations at codon 12 of c-K-Ras gene are found in most pancreatic carcinomas (Almoguera et al., 1988). Mutations in BRCA1/2 genes are associated with 30-50% of the heritable breast cancer cases (Nathanson et al., 2001; Rahman and Stratton, 1998), and the tumor suppressor gene p53 is defective in ~50% of all human cancers by various mutations (Hainaut and Hollstein, 2000; Hollstein et al., 1991; Soussi and Beroud, 2001).

### 1.3.3 Cytokinesis failure, genomic instability and tumorigenesis

It has been reported that cytokinesis failure, ending with a doubled genome and amplified centrosomes, induces tumor formation in mice (Fujiwara et al., 2005). However, it is still not clear how it contributes to the cellular hyper proliferation associated with cancer. In this section,

I will discuss the model of how cytokinesis failure contributes to aneuploidy and tumorigenesis by elevating genomic instability.

Recent studies from the Compton lab has revealed that chromosome missegregation only leads to transient aneuploidy in stable diploid cell lines. These aneuploids are selected and diluted out of the population after some time in culture (Thompson and Compton, 2008). Probably, this could be due to genetic imbalances in aneuploids created by gain or loss of whole chromosomes associate with reduction in viability. Moreover, in unstable aneuploid cancer cell lines, induced chromosome missegregation further promotes genome instability as a long-term effect, suggesting that additional changes are required for the persistence of aneuploid cells in tumors. For example, p53 mutation or deletion reduces cell cycle checkpoints and inhibits cell apoptosis (Hainaut and Hollstein, 2000), which might be required to maintain transient aneuploidy as a long-term defect.

Although these "additional changes" are poorly defined, cytokinesis failure might play some roles in these events. Cytokinesis, the last step of mitosis, is essential for the daughter cells to inherit only one set of chromosomes. Failure of cytokinesis is observed in tumor-derived cell lines (data from this dissertation). Theoretically, cells in tumors could fail at cytokinesis at a high frequency because of the elevated proliferation rates and tetraploidy that have been observed in many instances (Hainaut and Hollstein, 2000; Olaharski et al., 2006). Incomplete cytokinesis leads to two major abnormalities in cells. First, the DNA content is doubled to 4N; second, the centrosome is duplicated already and can be amplified again in the next cell cycle. These two consequences satisfy the prerequisites of multipolar spindle formation. Unsurprisingly and

supportively, MPS is a common phenotype of tumor and cultured cancer cells (Saunders, 2005). It is known cytokinesis failure is not the only pathway for cells to form MPS (Figure 8). However, it is believed that cytokinesis failure would give cells an advantage for multipolar cell division due to the large size of the genome. Typically, multipolarity means that cells divide in three or four or even more directions. If the cell starts with a diploid genome, it is very likely each progeny would inherit about half the genetic material. Undoubtedly, these cells possibly arrest or apoptose, however, tetraploid mother cells could overcome this disadvantage.

In addition, multipolarity not only increases the rate of gene gain or loss, but also elevates DNA damage (Storchova et al., 2006), resulting in bridge formation, lagging chromosomes and micronuclei in mitosis. The daughter cells from multipolar mitosis are very likely aneuploid due to a series of chromosome segregational defects. Therefore, a good explanation of why the majority of cancer cells are not tetraploid but aneuploid (Fujiwara et al., 2005; Li et al., 2007a) is that tetraploids possibly play a role as precursors of aneuploid cells in tumorigenesis and tumor progression. As discussed above, tetraploidy could enhance the fitness of cells undergoing chromosome missegregation through a buffer-like effect. This event would allow cells to survive until a critical mutation occurs, such as, loss of the p53 gene and/or amplification of the myc gene. These changes could possibly further contribute to aneuploidy in tumorigenesis.

It is not surprising if aneuploidy formation and selection might encourage cells to fail in cytokinesis, and undergo multipolar divisions and anaphase bridges. For instance, the mitotic arrest deficient 2 (MAD2) protein is suggested to play a key role in a functional mitotic

checkpoint during mitosis. Decreased MAD2 expression has been reported in several types of human cancer cell lines derived from lung, breast and ovarian carcinomas, which is associated with impaired mitotic checkpoints (Li and Benezra, 1996; Takahashi et al., 1999; Wang et al., 2002). Recent studies have found that a MAD2 variant with 10 residues deleted in the C terminal is able to induce aneuploidy by promoting chromosomal duplication. This is a result from an impaired mitotic checkpoint and subsequent cytokinesis, suggesting an essential role of MAD2-mediated mitotic checkpoint and prevention of genomic instability in human cells. Another example is the NuMA gene, which has been shown to be amplified via breakage-fusion-bridge cycles in cancer cell lines (Huang et al., 2002; Quintyne et al., 2005). Overexpression of this spindle protein NuMA depletes dynein localization at the spindle poles and promotes multipolarity in some cancer cell types (Quintyne et al., 2005). Furthermore, the study from this dissertation suggests that MLCK protein, required for cytokinesis completion, is widely down-regulated in carcinomas and cancer cells, which might be caused by chromosomal segregational defects .

This dissertation will focus on the mechanism of why cancer cells fail in cytokinesis and how these defects contribute to genomic instability and tumorigenesis.

# 2.0 CHAPTER II: MULTIPOLAR SPINDLE FORMATION IS ASSOCIATED WITH FAILURE OF CYTOKINESIS

## 2.1 INTRODUCTION

Chromosomal instability, defined as a continuous change in the structure or number of chromosomes, is proposed to be a key mechanism driving the genomic changes associated with tumorigenesis (Jallepalli and Lengauer, 2001). A major cause of chromosomal instability in cells appears to be segregational defects during mitosis, resulting in a high frequency of chromosomal aberrations. Centrosomal amplification is a common source of divisional errors in cancer cells and has been suggested to play a role in tumor formation for over a century (Wunderlich, 2002). Supernumerary centrosomes have been reported in a variety of solid tumors, including breast, brain, bone, gall bladder, lung, liver, pancreas, colon, prostate, ovary and cervix carcinomas (Carroll et al., 1999; Gisselsson et al., 2004; Hsu et al., 2005; Jiang et al., 2003; Kawamura et al., 2003; Kuo et al., 2000; Lingle et al., 2002; Lingle et al., 1998; Nakajima et al., 2004; Pihan et al., 2001; Sato et al., 1999; Skyldberg et al., 2001).The main impact of supernumerary centrosomes is to increase the chances that the microtubule spindle formed in the subsequent mitosis will be multipolar and that the chromosomes will be unequally distributed to multiple daughter cells (Brinkley, 2001; Nigg, 2002; Sluder and Nordberg, 2004). Indeed, centrosomal changes, including amplification, are strongly linked to aneuploidy and

chromosomal instability in numerous studies (Ghadimi et al., 2000; Lingle et al., 2002; Lingle et al., 1998; Pihan et al., 2003).

There are several models to explain how centrosomes become amplified, as discussed in Section 1.2 in detail (Nigg, 2002; Sluder and Nordberg, 2004; Tarapore and Fukasawa, 2002). However, it is currently unknown which pathway is most relevant for centrosome amplification and MPS formation in cancer cells. In addition, how multipolarity survives and contributes to aneuploidy and tumorigenesis is unclear. I have investigated MPS formation in real-time in human embryonic kidney cells (HEK-293) and oral cancer cells (UPCI:SCC103) using a histone-GFP marker for chromosomes and a farnesylated-GFP marker for the plasma membrane (Haigo et al., 2003; Kanda et al., 1998). In both cell lines, nearly all the MPS arose from cells that were multinucleated in interphase, suggesting that multipolarity arose from failure of cytokinesis rather than over-replication of centrosomes. The corollary was also true, as expected, that failure of cytokinesis always gave rise to multinucleation. Significantly, many cells with MPS not only survived mitosis but divided again, indicating MPS did not reduce the chromosome number enough to block further division. This paradox may be explained by my observation that cells with MPS nearly always had an incomplete cytokinesis, combining two or more segregated chromosome sets into the same cell. I suggest a model whereby failure of cytokinesis may give rise to a self-perpetuating population of cells that contain supernumerary centrosomes, MPS and multiple nuclei. This proposed pool of cells is suggested to serve as a testing ground for generating viable, though aneuploid, mononucleated cells that comprise the majority of tumor cells.

## 2.2 RESULTS

### 2.2.1 MPS arose in cells with more than one nuclei

In order to investigate the origin and impact of MPS, both tumor and non-tumor cells grown in culture were examined by live-cell microscopy. Human embryonic kidney cells (HEK-293) and a human oral squamous cell carcinoma cell line (UPCI:SCC103) were chosen because they had both high levels of multipolarity and a high transfection efficiency. Both cell lines were transiently transfected with a plasmid expressing GFP-histone H2B (Kanda et al., 1998), and MPS in metaphase cells were identified by irregular chromosome alignment; typically a "Y" or "T" figure for tripolar and an "X" figure for tetrapolar spindles (Figure 13A, top right panel). Immunofluorescence studies of fixed cells confirmed that these abnormal alignments were only observed in cells with MPS ((Lingle et al., 2002; Saunders et al., 2000) and data not shown). Strikingly, in both cell lines > 90% of MPS arose in multinucleated cells by live cell imaging, which is defined as cells with two or more nuclei (Figure 13A top left panel, Figure 13B).

### 2.2.2 High frequency of cytokinesis defects in cells with MPS

Since MPS correlated with multinucleation, I wanted to know how these multinucleated cells formed. It is known that multinucleates can result from a failure of cytokinesis (Rigby and Papadimitriou, 1984) or the fusion of two or more cells (Brathen et al., 2000). To determine which mechanism is more common in HEK-293 and UPCI:SCC103 cells, I monitored cell activities by live cell microscopy.

Figure 13

A

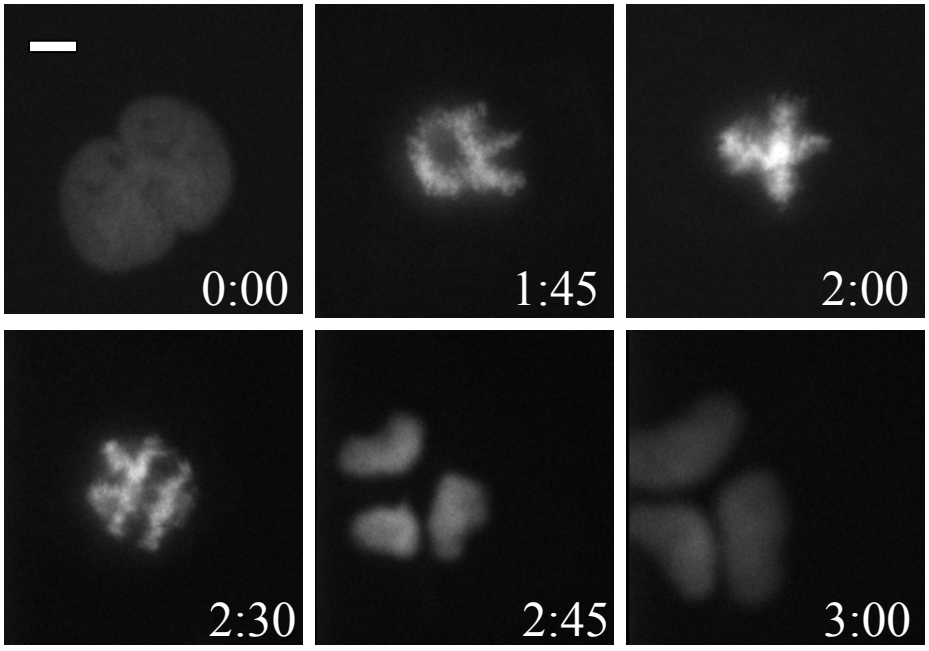
0:00
1:45
2:00
2:30
2:45
3:00

B

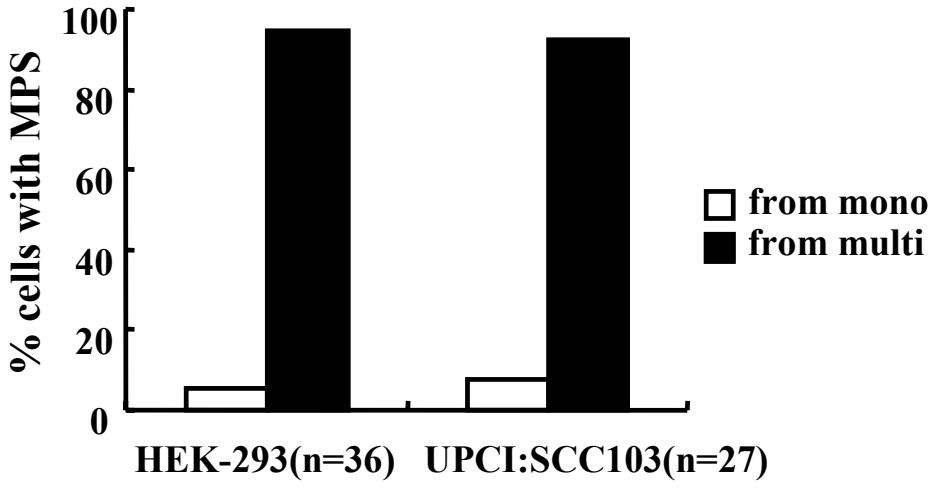
100
80
60
40
20
0
% cells with MPS
from mono
from multi
HEK-293(n=36)
UPCI:SCC103(n=27)

**Figure 13.** MPS arose primarily in multinucleated cells. (A) An example of multipolar mitosis in UPCI:SCC103 cells. Cells were transfected with a plasmid expressing GFP-histone H2B and viewed at 15 minute intervals by live cell epifluorescence microscopy. In this and subsequent figures, only selected images are shown. A binucleated cell in interphase (0 minutes) began chromosome condensation and aligned its chromosomes on a single MPS (2 hours), and divided in multiple directions into a trinucleated cell (3 hours). The bar in this and all subsequent figures is 1μm and time is in hours:minutes format. (B) The frequency of live cells with multipolar spindles arising from interphase mononucleated or multinucleated cells is shown for the HEK-293 and UPCI:SCC103 cell lines.

#### 2.2.2.1 Cytokinesis failure was the major cause of multinucleation

I transfected both cell lines with two plasmids: one is GFP-histone H2B to label nucleus and the other is a farnesylated membrane-GFP marker to indicate the position of the plasma membrane (Haigo et al., 2003). By live cell analysis, I found that the great majority of multinucleated cells in these cell lines resulted from a failure in cytokinesis (19 out of 20 in HEK-293 cells, and 15 out of 16 in UPCI:SCC103 cells) (Figure 14). The rest resulted from apparent cell-cell fusion.

#### 2.2.2.2 Cytokinesis failure led to multinucleation and MPS

When cytokinesis failed, a MPS was invariably seen in the next cell division (Figure 15). Nine cases of cytokinesis failure were imaged through a second division in GFP-labeled HEK-293 cells, and all of them formed MPS in the following mitosis. Three similar cases were observed in UPCI:SCC103 cells. In contrast, none of 34 HEK-293 cells with complete cytokinesis showed multipolar division in the next cell cycle. These observations indicate that a failure of cytokinesis usually leads to MPS formation in the subsequent division due to the overamplification of centrosomes.

Due to the difficulty in imaging two successive divisions and endogenous low MPS frequency in HEK-293 UPCI:SCC 103 cells, I could not get a large sample size of cytokinesis failure that directly led to multipolarity. Therefore, I looked at the frequency of incomplete cytokinesis from bipolar division in GFP-labeled HEK-293 and UPCI:SCC103 cells. Cytokinesis failed in ~10% of mononucleated cells that underwent a bipolar division (Figure 16C). This

compares with published frequencies of ~5% in both BSC1 monkey kidney cells (Piel et al., 2001) and p53 -/- mouse embryonic fibroblasts (Sluder and Nordberg, 2004). In conclusion, cytokinesis failed at a measurable frequency in HEK-293 and oral cancer cells.

To rule out that these results were influenced by transfection conditions, GFP expression, or UV exposure on the microscope, I also measured the frequency of cytokinesis failure by differential interference contrast (DIC) imaging of live cells. Examples of successful and abortive cytokinesis following bipolar division in UPCI:SCC103 cells are shown in Figure 16A and Figure 16B respectively. The HEK-293 cells did not grow flat enough in culture to be visualized by DIC. The frequency of cytokinesis failure in UPCI:SCC103 determined by DIC optics was 10%, (n= 69 total divisions, Figure 16C), and is consistent with that observed by fluorescence microscopy. Is this frequency sufficient to account for the multipolarity observed in the cells? MPS frequency in fixed cells stained with antibodies to γ-tubulin were ~11% in UPCI:SCC103 and ~10% in HEK-293 cells. Moreover, I found that by live cell fluorescent imaging, 9.9% (n=192 total divisions) of the HEK-293 cells, and 8.7% (n= 115) of the UPCI:SCC103 cells underwent a multipolar division (Figure 16C). Thus, the frequency of failure of cytokinesis is sufficient to account for all of the spindle multipolarity observed in both cell lines.

Cultured cells grow in an environment lacking the normal tissue architecture found *in situ,* and late-stage events in cytokinesis are influenced by tension generated through interactions of the dividing cell with its extracellular environment (Burton and Taylor, 1997). To confirm that the observed cytokinesis failures in these cells were not an artifact of the culture conditions,

Figure 14

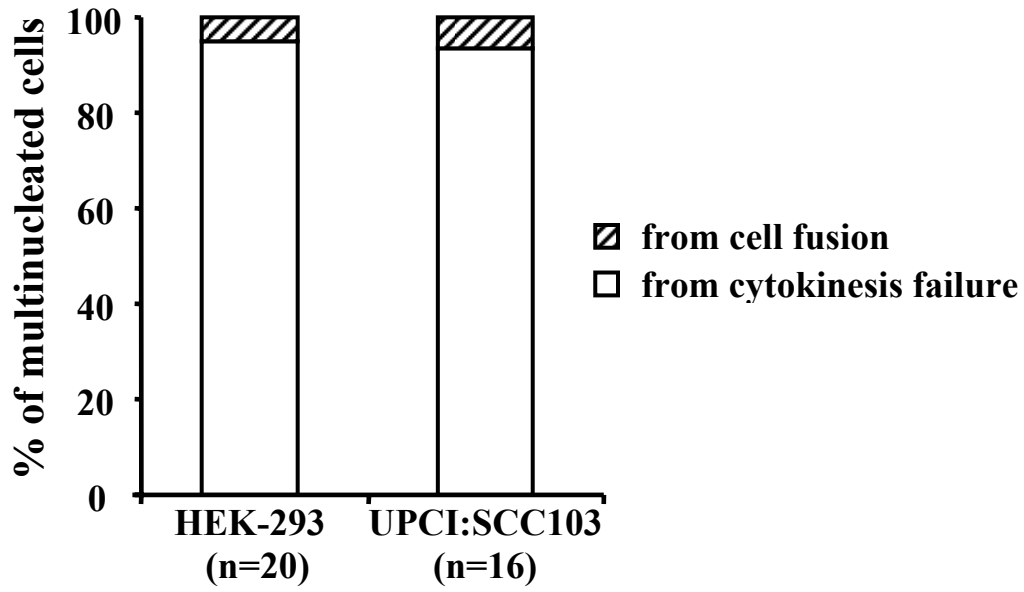


**Figure 14.** Majority multinucleated cells came from cytokinesis failure in HEK-293 and UPCI:SCC103 cells.

Figure 15

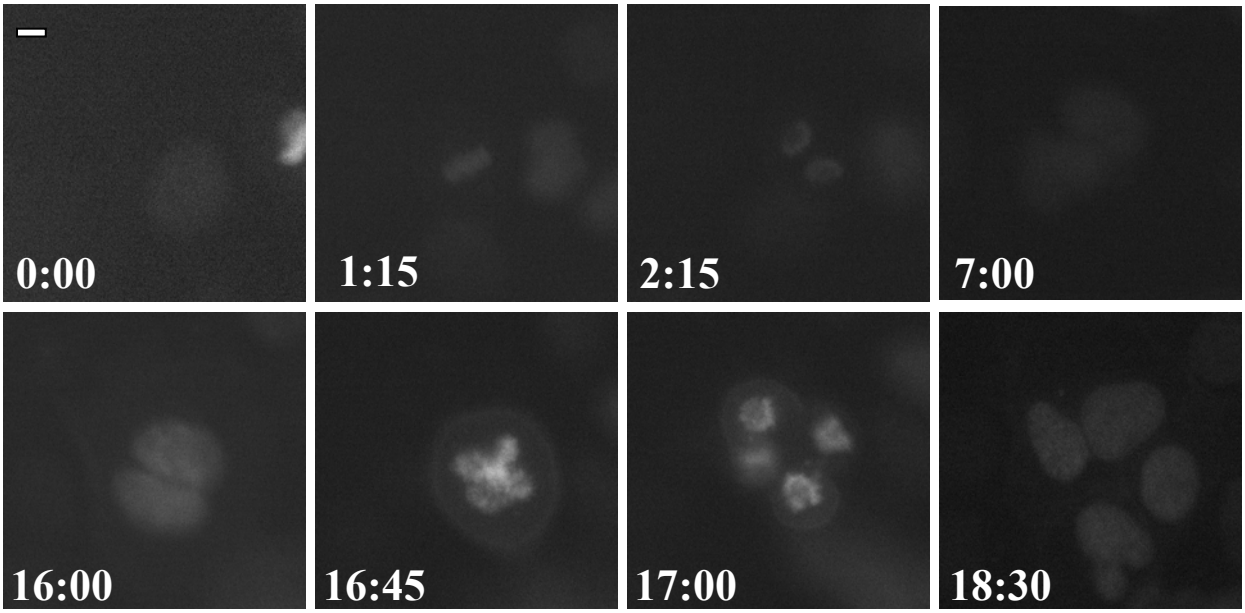


**Figure 15.** Cytokinesis defects in bipolar cells were followed by multipolar division. UPCI:SCC103 cells were transfected with GFP-histone H2B and GFP-membrane marker and viewed at 15 minute intervals by live cell epifluorescence microscopy. A mononucleated cell in interphase (0 minutes) began bipolar cell division and failed in cytokinesis with a binucleated cell (7 hours). This binucleated cell divided again in multipolar fashion (16 hours and 45 minutes) and finished cell division as a tetranucleated cell (18 hours and 30 minutes). Time: hours:minutes; bar :1μm

Figure 16

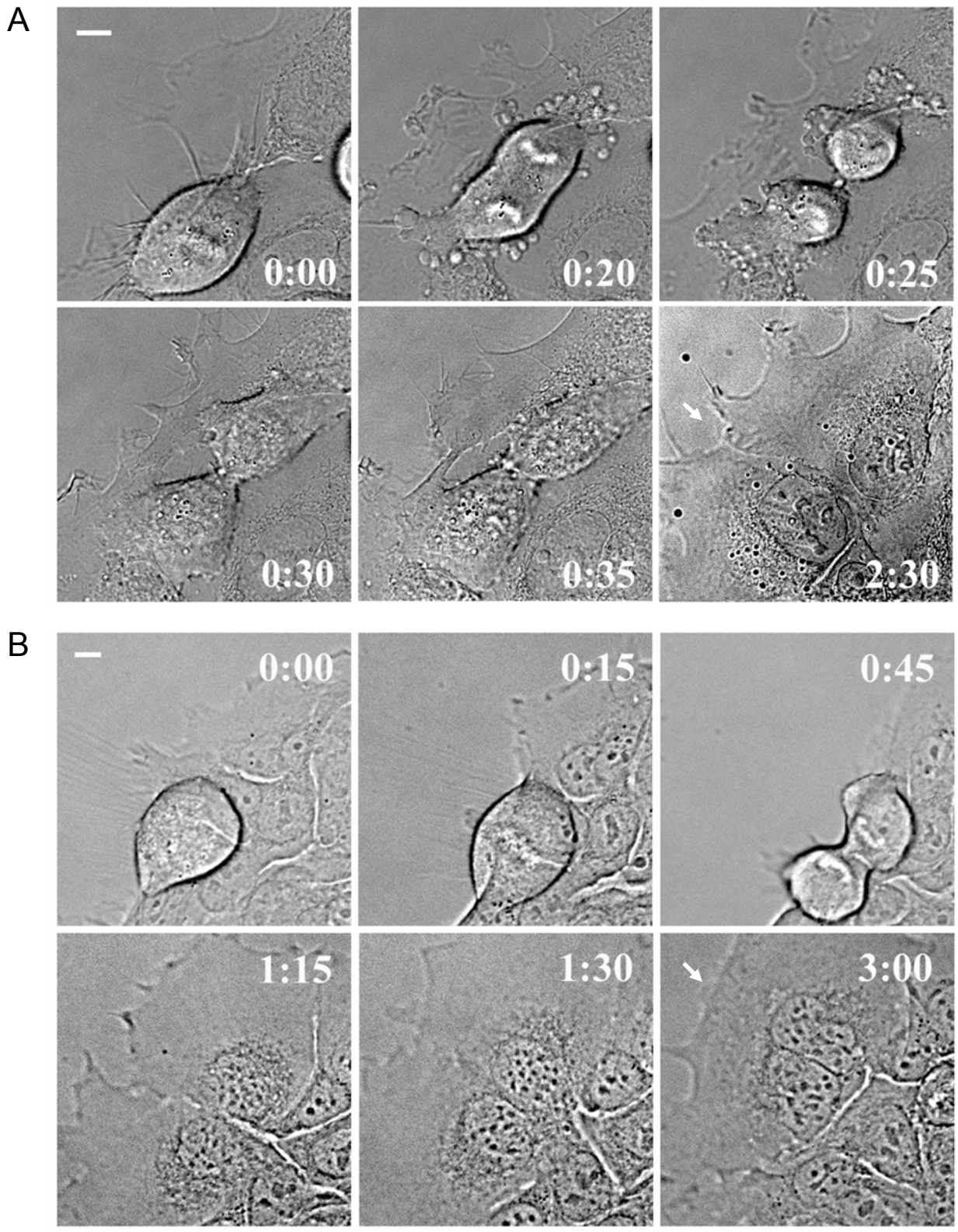

Figure 16

C

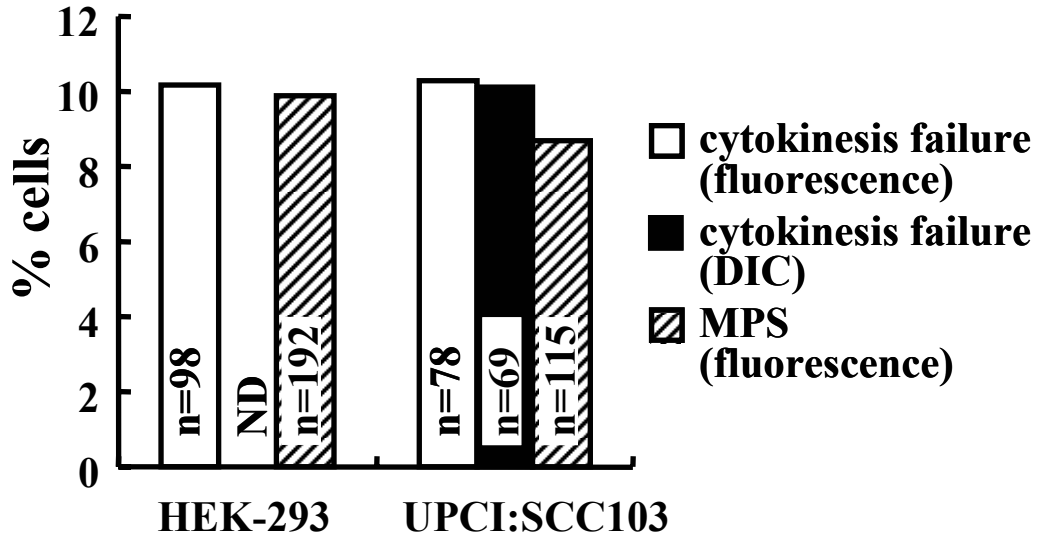


**Figure 16.** Failure of cytokinesis in HEK-293 and UPCI:SCC103 cells. (A) An example of a successful cytokinesis in UPCI:SCC103 cells as viewed by DIC microscopy every 5 minutes. The cell completed cytokinesis in 2 hours and 30 minutes. A plasma membrane border was clearly observed between daughter cells (arrow) and the nuclei were separated. (B) An example of an abortive cytokinesis in UPCI:SCC103 cells. The cell initiated and failed in cytokinesis at 3 hours with a binucleated cell formation. Note the continuous plasma membrane at 3 hours (arrow) and the close proximity of the two nuclei in the binucleated cell. Time: hours:minutes; bar: 1μM. (C) The frequency of cells with cytokinesis failure by real-time DIC or fluorescence microscopy compared to the frequency of multipolarity as determined by real-time fluorescence microscopy. ND = not determined.

I also examined uvulopalatopharyngoplasty specimens from surgical samples of normal human tissue grown (UP3 cells) and viewed under similar conditions to HEK-293 and UPCI:SCC103 cells (Rubin Grandis et al., 1996). The tissue samples are a mixture of cell types, including fibroblasts and keratinocytes (data not shown). I examined 47 mitotic divisions in real-time by DIC in these untransformed cells and each completed cytokinesis normally. Consistent with the absence of cytokinesis defects, no multipolar divisions were observed in real-time. In addition, retinal pigment epithelium cells stable transformed with human telomerase reverse transcriptase (RPE-hTERT cells) showed no cytokinesis defects by DIC live cell analysis (n=62). In conclusion, although I cannot rule out that long term growth in culture may affect the frequency of cytokinesis failure, the cytokinesis defects I observed were apparently not a consequence of the immediate *in vitro* culturing or microscopic imaging conditions.

**2.2.2.3 Cytokinesis failure was a common defect in a variety of cancer cells**

I have observed two nuclei in close proximity in one intact cell (defined as binucleated cell) as the product of cytokinesis failure in HEK-293 and UPCI:SCC103 cell lines. Also, it is well known that different cancer cells have an increase in ploidy. Therefore, I wanted to test whether cytokinesis failure occurred at high frequency in other cancer cell lines from other tissue types (Table 1). Percentages of multinucleation, defined as two or more than two nuclei in a single cell, were examined via immunofluorescent labeling of nuclei and the cell cortex in different cancer cell lines. In this and the following experiments, human fibroblast and RPE-hTERT cells were used as normal controls (referred to as “normal cells” in the following context). Human fibroblast cells are tissue-cultured primary cells with stable diploid genome. However, the low rate of division and a fast senescence period in fibroblast cells are limitations

for mitosis and cytokinesis studies in this dissertation. Therefore, RPE-hTERT cell line, which is commonly used (Kim et al., 2007), is employed as another normal control here. Although these epithelium cells were modified to be immortalized from primary cells, they consistently maintain stable diploid genome and do not behave transformed phenotypes (Jiang et al., 1999). In addition, very few mitotic defects such as anaphase bridges, micronuclei, lagging chromosomes and cytokinesis failure can be observed in RPE-hTERT cells at early passages (data not shown). Thus, RPE-hTERT cell line is considered as an example of normal cells. Unsurprisingly, all the tested cancer cells showed a higher frequency of multinucleation when compared to normal cells, ranging from approximately 5% to 9% (Figure 17). Consistent with this, multipolarity ratios are also high in these cell lines (Quintyne et al., 2005). These results suggest that cytokinesis failure is possibly a primary cause of MPS formation in different cancer cells.

### 2.2.3 Fate of multipolar cell divisions

It is predicted that multipolar mitosis contributes to genomic instability and aneuploidy due to unequal inheritance genomes by the daughter cells. However, it is not very clear how this occurs. In the following sections I will investigate the fate of cells that undergo multipolar cell divisions and propose a model that predicts how this is related to aneuploidy in cancer cells.

**Table 1.** Cancer cell lines in this dissertation.

| Cell line | Tissue source |
|---|---|
| UPCI:SCC103 | oral carcinoma(tongue) |
| UPCI:SCC78 | oral carcinoma (floor of mouth) |
| MES-SA | uterine sarcoma |
| SK-HEP1 | liver adenocarcinoma |
| A549 | lung carcinoma |
| HeLa | cervical carcinoma |
| U2OS | bone osteosarcoma |
| HCT116 | colon carcinoma |

Figure 17

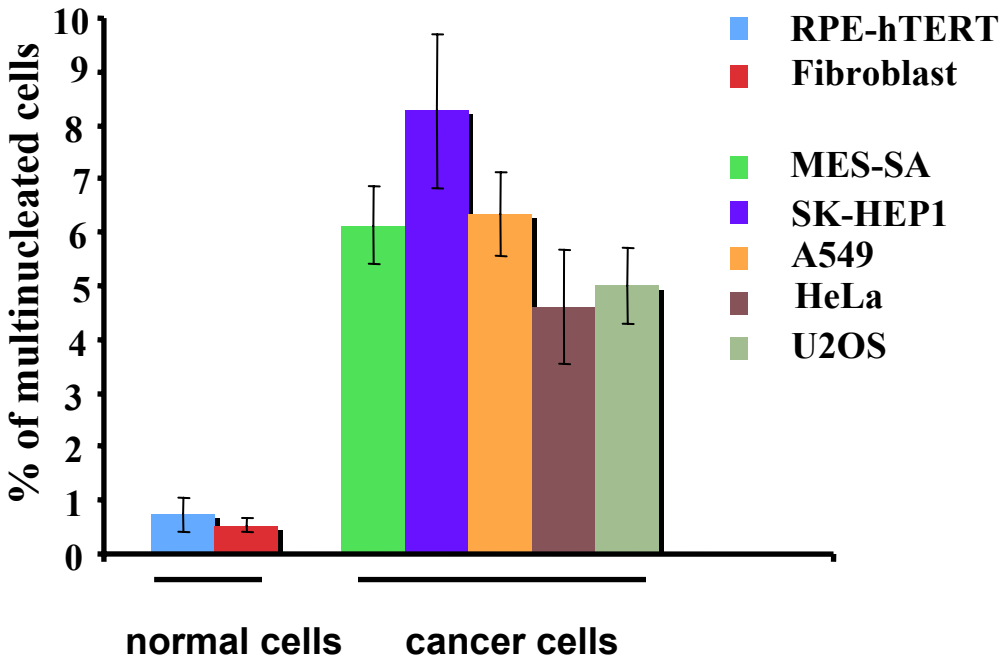


**Figure 17.** Multinucleation was a common phenotype in cancer cells. Cells were stained with DAPI and MHC indicating nuclei and cell boundary respectively. Normal cells showed low multinucleation frequency, while cancer cells exhibited a high frequency. Data and error bars represent mean and standard deviation of more than three different experiments, respectively.

Figure 18

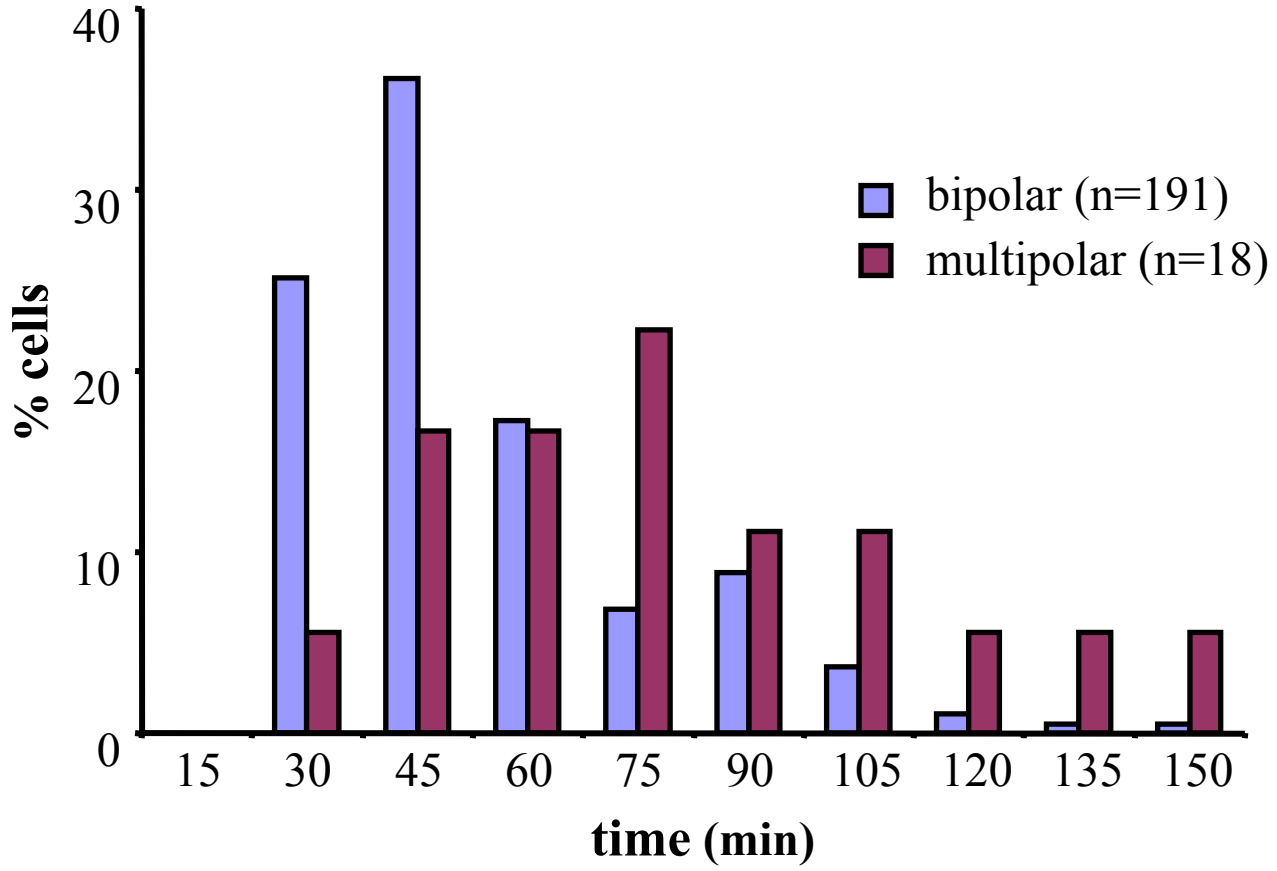


**Figure 18.** Mitoses delayed in multipolar divisions in UPCI:SCC103 cells. Cells undergoing bipolar or multipolar mitoses were followed every 15 minutes by live cell imaging. Minutes from nuclear envelope breakdown to anaphase onset are shown.

#### 2.2.3.1 Multipolar cell divisions delayed mitosis exit and have a high potential to cause cytokinesis failure

As shown in Section 2.2.2.2, the frequency of MPS is lower in live cells than fixed cells. One possibility may be that the mitosis is delayed in multipolar cells compared to bipolar cells; therefore, in a fixed window I would observe more cells with MPS due to the elongated process. To test this hypothesis, I compared the time from nuclear envelope breakdown to anaphase onset in cells with bipolar and multipolar divisions. The majority of bipolar cells took 45 minutes to finish this process. In contrast, most multipolar cells took 75 minutes, confirming that the multipolar cell division delayed the exit from mitosis (Figure 18). This may result from that increased time is required to catch and align chromosomes at the metaphase plate where there are multipolar spindles.

I next examined in more detail the ability of cells with MPS to complete a normal mitosis and divide again. In HEK-293 cells, those with a bipolar division completed anaphase and exited mitosis 100% of the time (n= 93), as determined by GFP fluorescent imaging of chromosome decondensation. By comparison, 88% (n= 40) of cells with MPS completed anaphase and exited mitosis. The multipolar cells that were unable to proceed usually arrested in metaphase for various periods of time before exiting mitosis and apparently undergoing mitotic slippage (Blagosklonny, 2007), as determined by the appearance of nuclear fragmentation. Similarly, when I examined UPCI:SCC103 cultures by DIC and GFP-fluorescence I saw 72% (n= 46) of cells with MPS were able to complete anaphase. Thus, cells with multipolar spindles are typically able to complete mitosis, consistent with previous observations indicating the lack

of a mitotic checkpoint to block division in cells with spindle polarity defects (Sluder et al., 1997).

Starting with dividing cells may bias the sample towards more viable members of the cell population. To avoid this, I also measured the frequency that multinucleated cells divide. Multinucleated cells in interphase were identified and observed by live-cell imaging. The average duration of the cell cycle is ~ 15 hours for the UPCI:OSCC103 cells and ~ 16 hours for the HEK-293 cells, as determined by fluorescent live cell imaging. I observed 45% (n=22) of multinucleated UPCI:OSCC103 cells and 83% (n=30) of the HEK-293 cells divide within 18 hours. While these numbers are lower than the frequency of MPS in cells exiting mitosis, they indicate that nearly 1/2 or more of multinucleated cells remain capable of further division.

In a related assay, I also investigated whether HEK-293 cells that undergo multipolar division were able to divide again. I began imaging cells in interphase by GFP fluorescence and the maximum safe viewing time under the conditions I employed is ~30 hours. At greater times, cells visibly deteriorated (data not shown). 100% (n=34) of the daughters of bipolar divisions divided again within 27 hours. Of the cells that divided with a multipolar division, at least one or more of the daughters from 50% (n=8) of the divisions entered mitosis again within 27 hours. (This sample size is necessarily low because of the requirement to view a rare cell type through two successive divisions within a 30 hour window.) Thus, as predicted there appears to be a substantial loss in viability from multipolar division. However, in this limited sample size, many of the multipolar divisions produced at least one cell able to divide again. Thus, the progeny of MPS division can potentially contribute to future generations of the cell culture population.

Figure 19

A Cytokinesis Completion

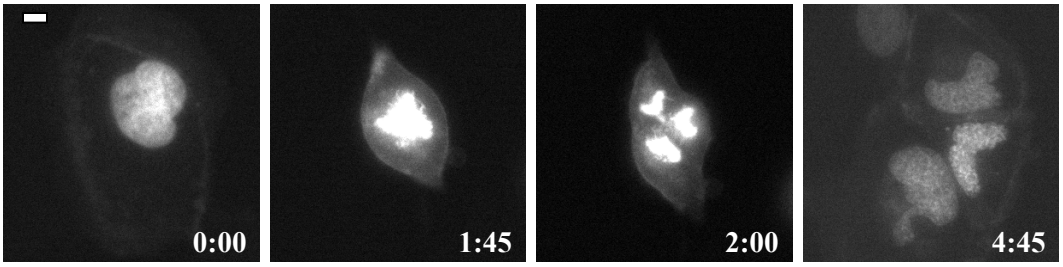


Partial Cytokinesis Failure

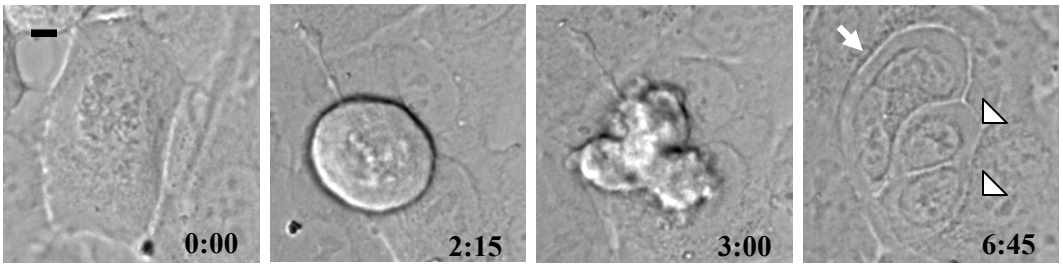


Total Cytokinesis Failure

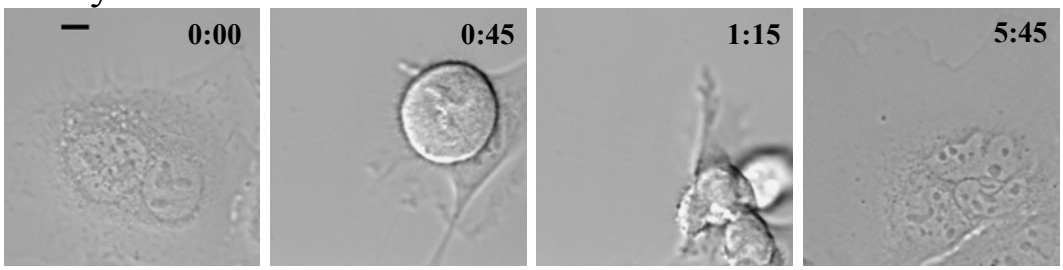


B

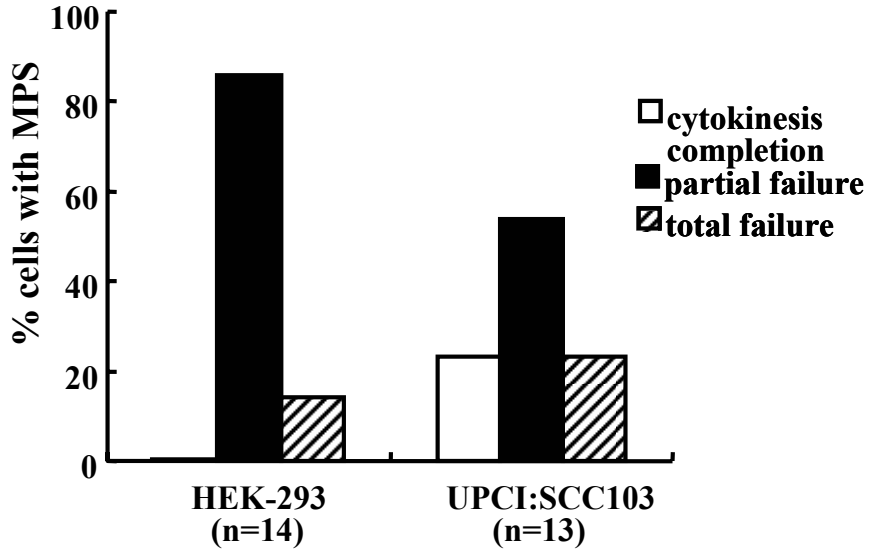

**Figure 19.** Majority of multipolar cells failed in cytokinesis in HEK-293 and UPCI:SCC103 cells. (A) Examples of cytokinesis in UPCI:SCC103 cells. Top panel, an example of cytokinesis completion. The GFP-labeled cell was recorded every 15 minutes. Multipolar division completed and formed three separated mononulceated daughter cells. Middle panel, an example of partial cytokinesis failure. The cell was observed every 5 minutes by DIC optics. Multipolar division completed and formed three separated daughter cells: two mononulceated cells (arrowhead) and one binucleated cell (arrow). Bottom panel, an example of partial cytokinesis failure. The cell was observed every 5 minutes by DIC optics. Multipolar division completed and formed one trinucleated daughter cell. Time: hours:minutes; bar: 1μM. (B) Frequency of MPS cells with complete cytokinesis, partial or total cytokinesis failure in HEK-293 cells and UPCI:SCC103 cells.

Although most cells with MPS were able to exit mitosis, and in some cases divide again, I found that they consistently had difficulties in completing cytokinesis (Figure 19). In all the cases of HEK-293 cells with MPS that were clearly imaged throughout mitosis by fluorescence, either a partial or a complete failure of cytokinesis was observed. Similarly, the majority of UPCI:SCC103 cells with MPS did not complete cytokinesis when viewed by either fluorescence or DIC optics (Figure 19B). In some cases, cytokinesis was completely blocked. But in many cases, a partial failure of cytokinesis was observed, giving rise to a mixture of mononucleated and multinucleated cells (Figure 19A). Thus, the frequency of cytokinesis failure jumps dramatically with MPS, so that when the cells exhibits multipolar divisions they may regain some or even all of the chromosomes that would have been lost by the multipolar division.

#### 2.2.3.2 Most mononulceated cells from multipolar division inherited single centrosomes

Due to chaotic chromosome segregation in MPS cells, I assume that the daughter cells are aneuploid or polyploid. Since the results above suggest some of the daughter cells from MPS are viable, I hypothesize that mononulceated progenies divide bipolarly and form a stable aneuploid clonal cell line, contributing to genomic instability in tumorigenesis. Due to the difficulties of following live cell activities for a long time, I examined the centrosome distribution in multipolar cell divisions. If a mononulceated daughter cell inherits one single centrosome, it might have high potential to divide bipolarly in the next cell cycle.

Centrosome numbers were examined in mitotic UPCI:SCC103 cells. The movements of GFP-labeled centrosomes were observed in multipolar mitoses by live cell imaging. Mononucleated daughter cells from multipolar divisions usually retained zero, one or two

Figure 20

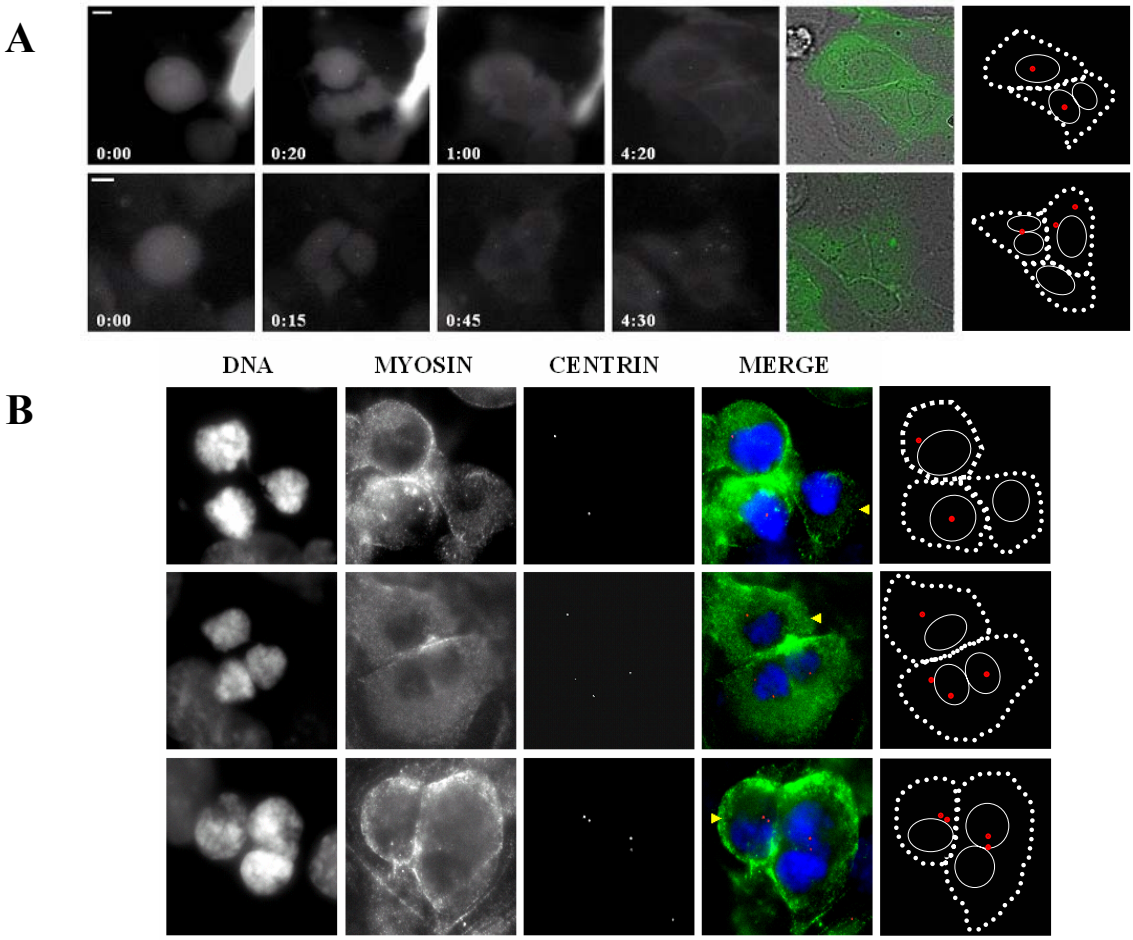
A
0:00
0:20
1:00
4:20
0:00
0:15
0:45
4:30
B
DNA
MYOSIN
CENTRIN
MERGE
C
centrosome number of mononucleated cells after multipolar divisions in live cells
% cells
100
80
60
40
20
0
0
1
2
>2
centrosome number (n=23)
D
centrosome number of mononucleated cells after multipolar divisions in fixed cells
% cells
100
80
60
40
20
0
0
1
2
>2
centrosome number (n=63)

**Figure 20.** Majority of mononucleated daughter cells from multipolar cell divisions inherited single centrosomes. (A) Examples of centrosome numbers in mononucleated UPCI:SCC103 cells by live cell imaging. Cells were transfected with a plasmid expressing pEGFP-Hs-Centrin. Multipolar cell divisions were examined by fluorescent and DIC microscopy. The top panel is an example of a mononucleated cell with one centrosome. The bottom panel is an example of a mononulceated cell with zero or two centrosomes. The fluorescent and DIC images are merged in the second column on the right to confirm the numbers of nuclei in each daughter cell. The last column shows the schematic pictures of merged images. (B) Examples of centrosome numbers in mononucleated UPCI:SCC103 cells by immunofluorescence. Telophase UPCI:SCC103 cells were collected by synchronization and release. Myosin (green), centrioles (red) and DNA (blue) were labeled by immunofluorescence. Arrowheads point the examples of mononulceated daughter cells with zero, one or two centrosomes from multipolar divisions. The last column shows the schematic pictures of merged images. (C) The quantification of centrosome number in mononulceated daughter cells from (A). (D) The quantification of centrosome number in mononulceated daughter cells from (B).

centrosomes (Figure 20A). As expected, among these mononulceated cells, about 83% inherit single centrosome as products from bipolar cell division (n=23, Figure 20C), suggesting that these mononulceated cells with one centrosome may go into a normal bipolar mitosis in the next cell cycle. To reduce the experimental errors resulting from small sample size of this work, I also investigated the centrosome number in fixed dividing UPCI:SCC103 cells. Cells were synchronized and fixed in telophase and centrosomes were labeled and quantified by immunofluorescence (Figure 20B). Consistent with live cell analysis, the majority (~ 70%, n=63) of mononulceated cells from multipolar divisions received only a single centrosome (Figure 20D). Only 15% of the daughters inherited no centrosomes (Figure 20C and D), some of that may be collected by false negative results from immunofluorescence assay. The cells with no centrosomes might not undergo mitosis in the next cell cycle. Besides, about 10% of mononulceated cells obtained two or more centrosomes (Figure 20C and D), and possibly enter multipolar cell division in the next cell cycle.

## 2.3 DISCUSSION

My results address an important question about the centrosomal and chromosomal inheritance of cells with multipolar spindles. Strikingly, ~50% of the cells with MPS gave rise to at least one daughter capable of further division. Since division into more than two sets of chromosomes would seemingly invariably lead to chromosome loss, can cells with MPS remain viable and contribute to genomic instability in the tumor? I have shown that MPS most frequently arise in

multinucleated cells and only rarely in mononucleated cells in the two cell lines tested. Multinucleated cells were observed to arise from a failure of cytokinesis, and the frequency of aborted cytokinesis was similar to the frequency of MPS. Therefore, a failure of cytokinesis appears to be the main source of MPS in these cell lines. This has important implications for the survivability of cells arising from multipolar division. A diploid cell with supernumerary centrosomes is unlikely to survive a multipolar division. But if a multipolar division acts on a tetraploid rather than a diploid set of chromosomes, the chances of completing cell division and obtaining viable progeny is likely to increase. My results support a model that cytokinesis failure not only destabilizes the genome through centrosomal amplification, but also provides the added chromosome complement to potentially survive the multipolar division of the next cell cycle.

A second mechanism for surviving multipolar division is revealed by the observation that cytokinesis commonly fails at least one cleavage furrow site following multipolar division, suggesting that MPS do not necessarily lead to a loss of chromosomes. I interpret my data to indicate that the chromosomal complement a daughter of a MPS cell receives is determined not only by the outcome of spindle segregation, but also by whether a cleavage furrow forms between adjacent chromosome sets. Since this typically fails in cells with MPS, daughter cells from multipolar divisions frequently receive more than the one set of segregated chromosomes, possibly enough genetic material to divide again. Previously, cytokinesis failure following multipolar spindles has been shown in p53 -/- mouse embryonic fibroblasts (Sluder and Nordberg, 2004). Tetraploid p53-null (p53-/-) mouse mammary epithelial cells, derived from chemical-induced cytokinesis failure, lead to malignant mammary epithelial cancers when transplanted subcutaneously into nude mice (Fujiwara et al., 2005). My results are consistent

Figure 21

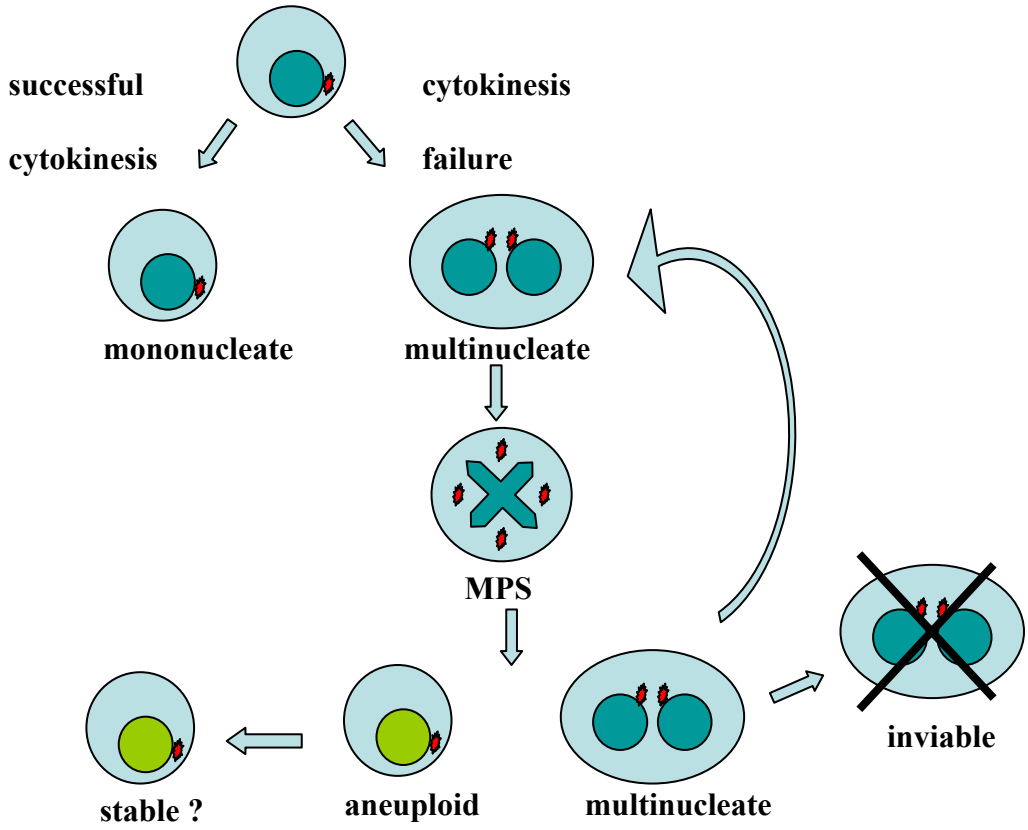


**Figure 21.** A model is shown to describe the maintenance of a pool of multinucleated and multipolar cells. Cells enter the pool following failure of cytokinesis, which in the populations examined occurred ~ 10% of the time. Multinucleated cells then divide multipolar due to the presence of amplified centrosomes but usually fail to complete cytokinesis, giving rise to multinucleated daughters. Some of these multinucleated cells apoptose or arrest, but others are able to divide, giving rise to another generation of multipolar and multinucleated daughters. Occasional mononucleated cells are derived from the multipolar division (chartreuse). I speculate that some of these may give rise to stable mononucleated, but aneuploid, clonal lines.

with and expand upon these earlier observations. These results can explain the viability of daughters of multipolar division and reveal the interplay between the resolution of spindle multipolarity, the completion of cytokinesis and tumorigenesis.

I propose that the cells with MPS may exist as a cycling pool of multinucleated cells (Figure 21). The population is sustained by cytokinesis defects, both in preexisting multinucleated cells, and also arising *de novo* in mononucleated cells. A subset of multinucleated cells are lost from the pool by cell death or arrest. But my observations that a portion are viable enough for additional divisions and that they will likely fail again at cytokinesis suggests a self-renewing population. In support of this model, many tumor-derived cultures and tumor tissue samples contain a subset of binucleated cells (Prasad et al., 1993) and tetraploidization appears to be an early event in tumorigenesis (Fujiwara et al., 2005; Galipeau et al., 1996). Taken together, the observation that failure of cytokinesis, followed by tetraploidization, centrosomal amplification and subsequent rounds of multipolar division, induces multiple rounds of faulty chromosome segregation in tumor cells. These mitotically unstable cells are suggested to give rise to genetic variability in the tumor cells population by escaping cycles of cytokinesis failure, therefore, allowing clonal selection to act to favor specific genomic combinations. What remains to be determined is why cytokinesis fails in the tumor cells, which will be discussed in the next chapter.

# 3.0 CHAPTER III: DEFICIENCY IN MYOSIN LIGHT CHAIN (MLC) PHOSPHORYLATION IS A CAUSE OF CYTOKINESIS FAILURE IN CANCER CELLS

## 3.1 INTRODUCTION

Chromosomal instability is a key mechanism for genomic changes associated with tumorigenesis (reviewed in Jallepalli and Lengauer, 2001). In many cancer cells, mitotic spindles have more than two poles, which can cause chromosome segregational defects and aneuploidy, leading to chromosome instability (reviewed in Pihan et al., 2003; Saunders et al., 2000). Spindle multipolarity is strongly related to amplification of the centrosome, the microtubule organizing center of the cell. There are four major models to explain how centrosomes get amplified: 1) centrosome replication defects; 2) cell division defects; 3) cell fusion; and 4) mitotic slippage (Blagosklonny, 2007; Brinkley, 2001; Nigg, 2002; Sluder and Nordberg, 2004). Results in Chapter II support the model that failure of cytokinesis is a major cause of amplified centrosomes and multipolarity in the tested human embryonic kidney cells (HEK-293) and human oral squamous carcinoma cells ( UPCI:SCC103). It also has been shown that in some tumor tissue samples, such as myeloid leukemia, malignant gliomas, colonic adenocarcinoma, (Lemez et al., 1998; Park et al., 1995; Takanishi et al., 1996) and many tumor-derived cell lines (Lothschutz et al., 2002; Olaharski et al., 2006; Shi and King, 2005), tetraploidy is common.

Additionally, Pellman and coworkers recently found that blocking cytokinesis causes primary cells lacking p53 to become much more tumorigenic in mice (Fujiwara et al., 2005). Therefore, failure of cytokinesis, and the resulting polyploidy, may contribute to human cancer.

However, the origin of the abortive cytokinesis is still unclear. Resent microarray analyses have shown that myosin light chain kinase (MLCK) transcription is low in various tumors, such as colon, lung, prostate, bladder, brain, breast, ovarian, liver, melanoma and myeloma, compared to normal controls, but high in head-neck and lymphonma (www.oncomine.org, (Rhodes et al., 2007)). Down-regulated MLCK transcription and expression are also observed in mesenchymal tumor cells and transformed chicken embryo fibroblasts, respectively (Schenker and Trueb, 1998; Van Eldik et al., 1984). These results suggest the MLCK may play an important role in cytokinesis failure and tetraploidy in tumor tissue. To test this hypothesis, I used tumor-derived cells as a model system to investigate the role of myosin regulatory light chain (MLC) phosphorylation in the failure of cytokinesis of cancer cells.

Cytokinesis begins at late anaphase with the assembly of a transient structure called the contractile ring at the equator between the spindle poles. Contraction of the contractile ring occurs at telophase, from an actin-myosin molecular motor system, and results in the formation of a cleavage furrow. Nonmuscle myosin II is composed of a heavy and two types of light chains, essential and regulatory light chains. In higher eukaryotes, cellular myosin is activated by phosphorylation of MLC at Thr18/Ser19 (Komatsu et al., 2000; Moussavi et al., 1993). Komatsu and colleagues showed that the expression of unphosphorylated MLC in mammalian cells caused

failure of cytokinesis (Komatsu et al., 2000). Thus, MLC phosphorylation is one of the key processes regulating contractile ring formation and cytokinesis completion.

MLCK and myosin phosphatase are known as critical enzymes to regulate myosin phosphorylation. MLCK primarily phosphorylates MLC on Ser19, and then Thr18 at high concentrations (Ikebe and Hartshorne, 1985). MLCK is activated by $Ca^{2+}$/calmodulin and localizes at cleavage furrows (Poperechnaya et al., 2000) which is critical for cytokinesis completion in many organisms. Complete inhibition of furrow contractility is observed with either the MLCK inhibitory peptide or ML-7, a specific MLCK inhibitor (Lucero et al., 2006; Silverman-Gavrila and Forer, 2001). However, why MLCK expression is decreased and whether this contributes to cytokinesis defects in cancer cells is still unclear.

Myosin phosphatase also regulates MLC. It consists of MYPT1 (myosin targeting subunit), M20 and PP1cδ (a catalytic subunit) (Ito et al., 2004). MYPT1 is phosphorylated during prometaphase which increases myosin phosphatase activity. When cells enter late anaphase, MYPT1 is phosphorylated by ROCK1 at an inhibitory site, leading to the inhibition of myosin phosphatase and initiation of cleavage furrow formation (Kawano et al., 1999; Totsukawa et al., 1999; Yokoyama et al., 2005). MYPT1 also interacts with multiple proteins, including Tau, MAP2, GTP-RhoA, cGMP-dependent protein kinase (cGKIα), phospholipids (Amano et al., 2003; Ito et al., 1997; Surks et al., 1999). It suggests that MYPT1 might have the potential to function as a signal transducer for cytoskeletal remodeling.

Previous studies in the Saunders lab have documented the failure of cytokinesis in cancer

cells, resulting in multinucleated cells (a single cell with two or more than two nuclei). Furthermore, multinucleated cells divided with multipolar spindles in real time microscopic imaging (See Chapter II for details). In this chapter, I investigate the causes of defective cytokinesis in cancer cells. I show here that the failure of cytokinesis in cancer cell lines is correlated with low levels of MLC phosphorylation. The phosphorylation reduction is caused by increased MYPT1 and decreased MLCK in oral cancer cells. When MLC phosphorylation was restored to high levels, cytokinesis failure and multipolar division were reduced in oral and liver cancer cells. Additionally, both overexpression of MYPT1 and inhibition of MLCK in primary cells elevated multinucleation and multipolar spindles defects. In conclusion, my results show for the first time that cytokinesis failure in cancer cells is caused by deficiencies in myosin light chain phosphorylation, which is due to the reduction of MLCK, as well as elevation of myosin phosphatase.

## 3.2 RESULTS

### 3.2.1 Oral cancer cells failed at an early stage of cytokinesis

Previous results have shown that approximately 10% of human embryonic kidney cells (HEK-293) and human oral squamous carcinoma cells (UPCI:SCC103) failed in cytokinesis resulting in multinucleated cells (see Chapter II). It is known that cytokinesis is a continuous multistep program: central spindle formation, cleavage furrow and contractile ring assembly, midbody formation and contractile ring disassembly, midbody abscission and membrane events. In order

to dissect where the cells failed in cytokinesis, I started with the examinations of the central spindle and contractile ring formation in UPCI:SCC103 cells.

#### 3.2.1.1 Central spindle proteins localized properly in oral cancer cell

The central spindle is an important structure in cytokinesis, defined as the antiparallel arrays of microtubules formed between segregated chromatids at the midzone during anaphase. There are a number of proteins localizing at central spindles. One group is a subset of kinesin motors including MKLP1, KIF4 and KIF14, which are required for protein transportation (Gruneberg et al., 2006; Kurasawa et al., 2004; Neef et al., 2007). The other group are kinases, such as Aurora B kinase, which is essential for the whole process of cytokinesis. These proteins stay at the central spindle from the beginning of cytokinesis and concentrate in the midbody at the late stage. Since these central spindle proteins are required for early cytokinesis, I initiated the studies by investigating the localization of Aurora B, KIF14 and MKLP1. Immunofluorescence assays in UPCI:SCC103 cells indicated that all of these proteins localize properly at the central spindle in early cytokinesis and the midbody in late cytokinesis (Figure 22). No difference of MKLP1 localization was detected in these oral cancer cells compared to normal UP3 cells. Thus, I found no data indicating that cytokinesis failure was caused by defects in the central spindle or diminished central spindle protein mislocalization.

#### 3.2.1.2 Myosin heavy chain (MHC) mislocalized at the cleavage furrows

It has been discussed in Chapter I that the central spindle and astral spindle regulate cleavage plane positioning (Rappaport, 1996). After the furrow initiates, the contractile ring assembles and the furrow starts ingression at the beginning of the cytokinesis. It is well known

that myosin is a component of the contractile ring, which concentrates at the furrow to facilitate contractility (DeBiasio et al., 1996). Therefore, myosin II localization at the furrow in cytokinesis became the next candidate to look at. In both UP3 and RPE-hTERT cells (normal controls), over 95% of the anaphase cells exhibit normal localization of myosin, concentrated at the midzone of the cell cortex (Figure 23A and C). About 5% abnormal myosin localization observed in these two normal cell lines might be caused by immunofluorescence artifacts. In UPCI:SCC103 cells, two categories of abnormal myosin localization were observed at a higher frequency compared to normal cells. One is categorized as no contractile ring formation and the other is identified as even myosin distribution along the cortex, and not concentrated of the furrow (Figure 23A). Interestingly, I observed myosin disappeared at the furrows in 16.9% UPCI:SCC103 cells and myosin evenly distributed in 14.3% cells (Figure 23C). In addition, even though 68.8% myosin localized normally, it was not as intense as normal cells. One possibility is that the MHC protein is more abundant in normal cells. However, I ruled this out by immunoblotting analysis (Figure 23B). In conclusion, these data suggested that UPCI:SCC103 cells failed early in cytokinesis due to reduced levels or mis-regulation of myosin localization or activation.

#### 3.2.1.3 Cells with defective contractile ring failed in cytokinesis

Due to the uncondensed and mislocalized nature of MHC in fixed oral cancer cells, I next asked whether the cells with defective contractile rings eventually failed in cytokinesis. In order to answer this question, UPCI:SCC103 cells were transiently transfected with a plasmid expressing GFP-actin and examined by live-cell microscopy to view cleavage furrow and

Figure 22

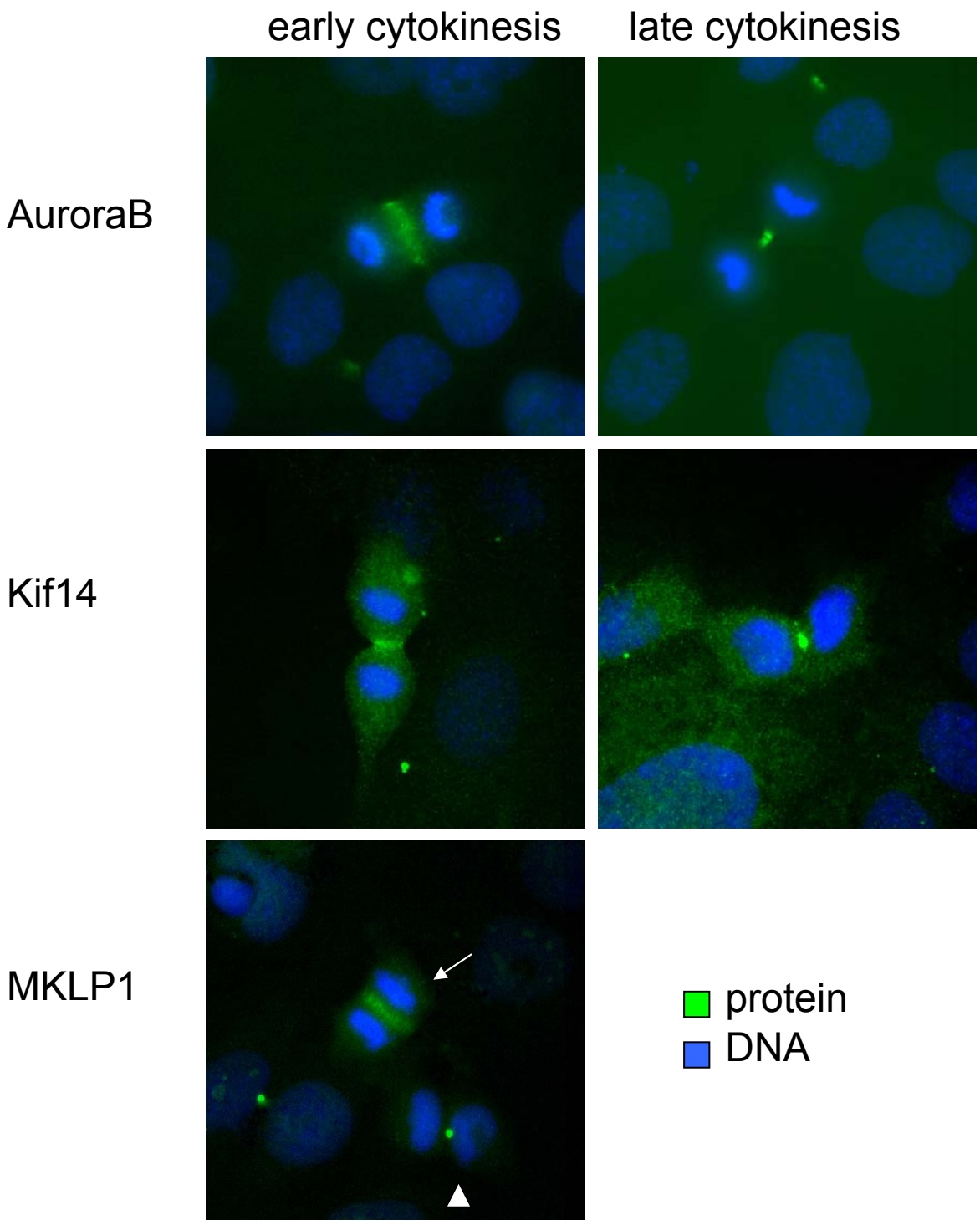
early cytokinesis
late cytokinesis
AuroraB
Kif14
MKLP1
protein
DNA

**Figure 22.** Central spindle proteins localized properly in UPCI:SCC103 cells during cytokinesis. Top panel, Aurora B kinase (green) concentrates at the central spindle in early cytokinesis (left) and midbody in late cytokinesis (right). Middle panel, KIF 14 (green) localizes at the central spindle in early cytokinesis (left) and midbody in late cytokinesis (right). Bottom panel, MKLP1 (green) localizes at the central spindle in early cytokinesis (arrow) and midbody in late cytokinesis (arrowhead).

Figure 23

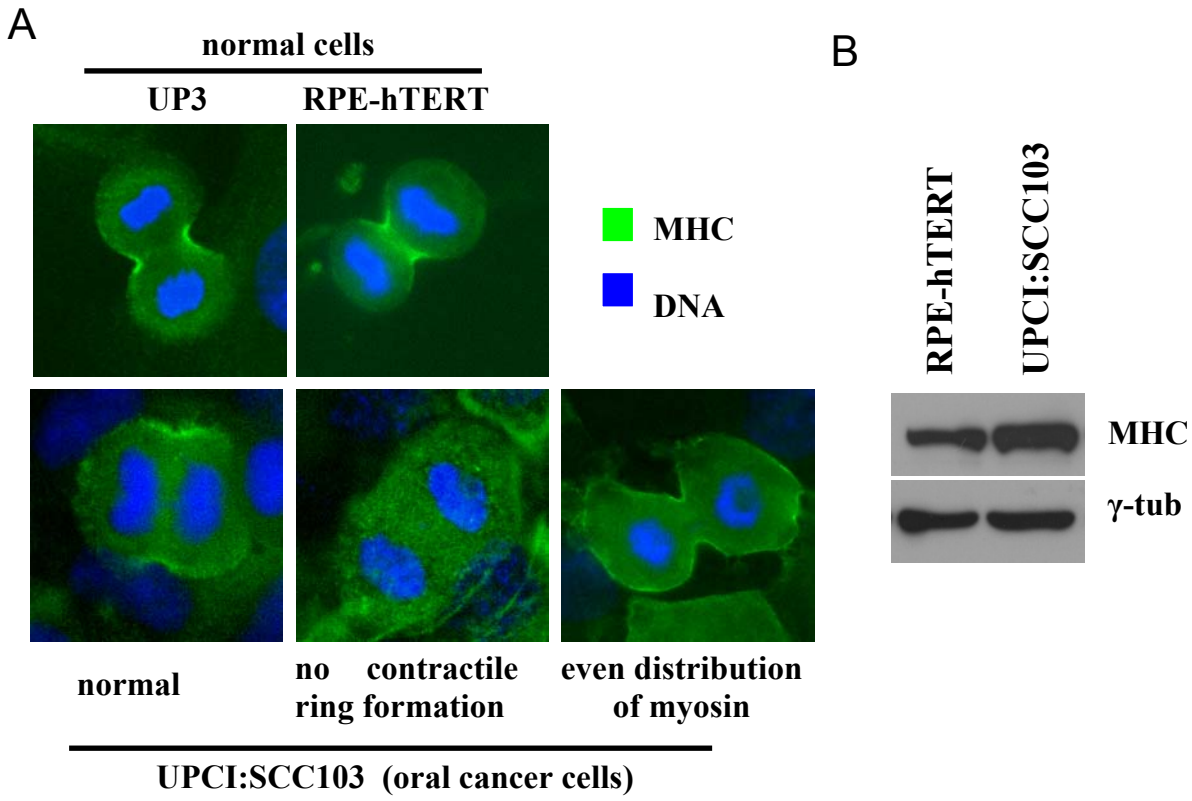
A
normal cells
UP3
RPE-hTERT
MHC
DNA
normal
no contractile ring formation
even distribution of myosin
UPCI:SCC103 (oral cancer cells)
B
RPE-hTERT
UPCI:SCC103
MHC
γ-tub

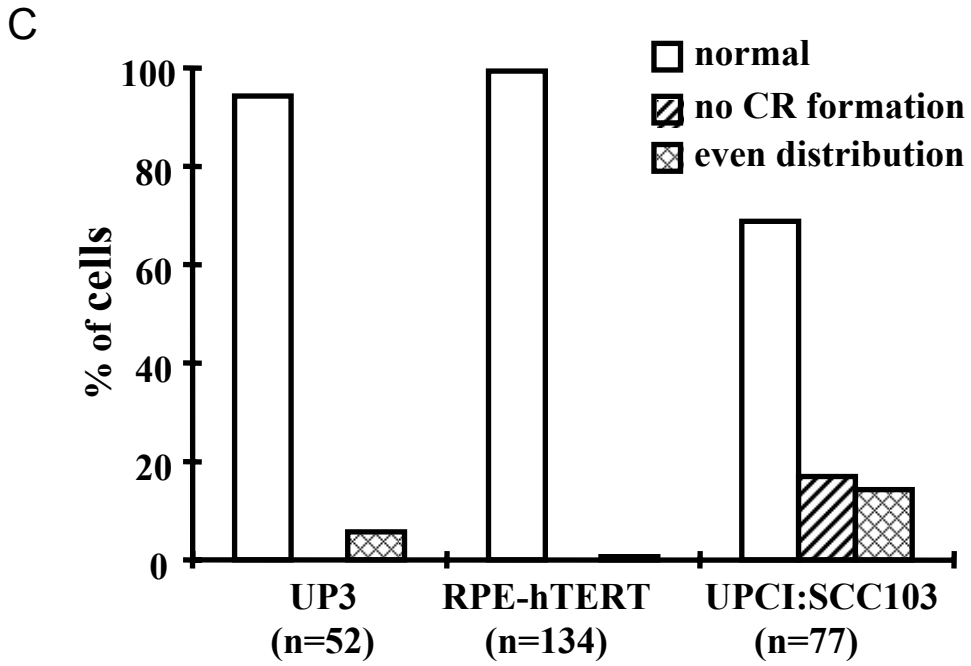
C
normal
no CR formation
even distribution
% of cells
100
80
60
40
20
0
UP3
(n=52)
RPE-hTERT
(n=134)
UPCI:SCC103
(n=77)

**Figure 23.** Myosin mislocalized in UPCI:SCC103 cells. (A) The localization of MHC in UP3, RPE-hTERT and UPCI:SCC103 cells were shown by immunofluorescence. (B) MHC expression level was similar in RPE-hTERT and UPCI:SCC103 cells. (C) The quantification of the localization of MHC in those cell lines.

Figure 24

A

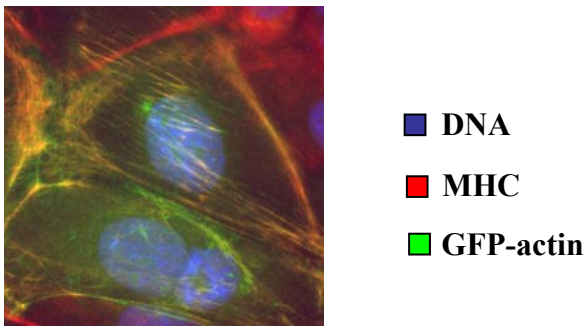
DNA
MHC
GFP-actin

B

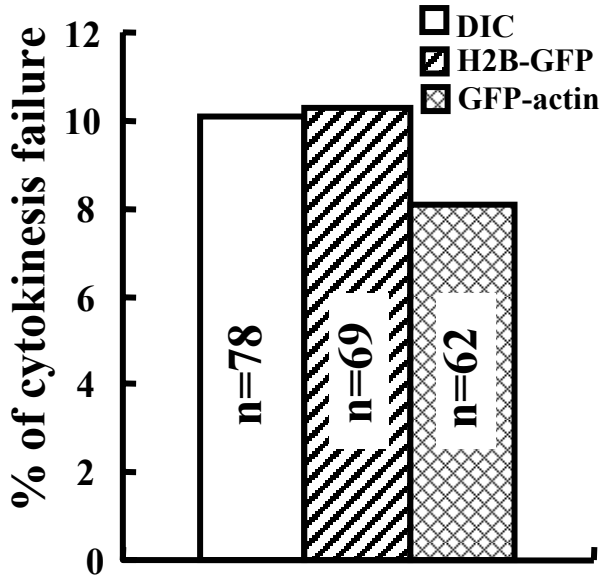
% of cytokinesis failure
0
2
4
6
8
10
12
n=78
n=69
n=62
DIC
H2B-GFP
GFP-actin

C

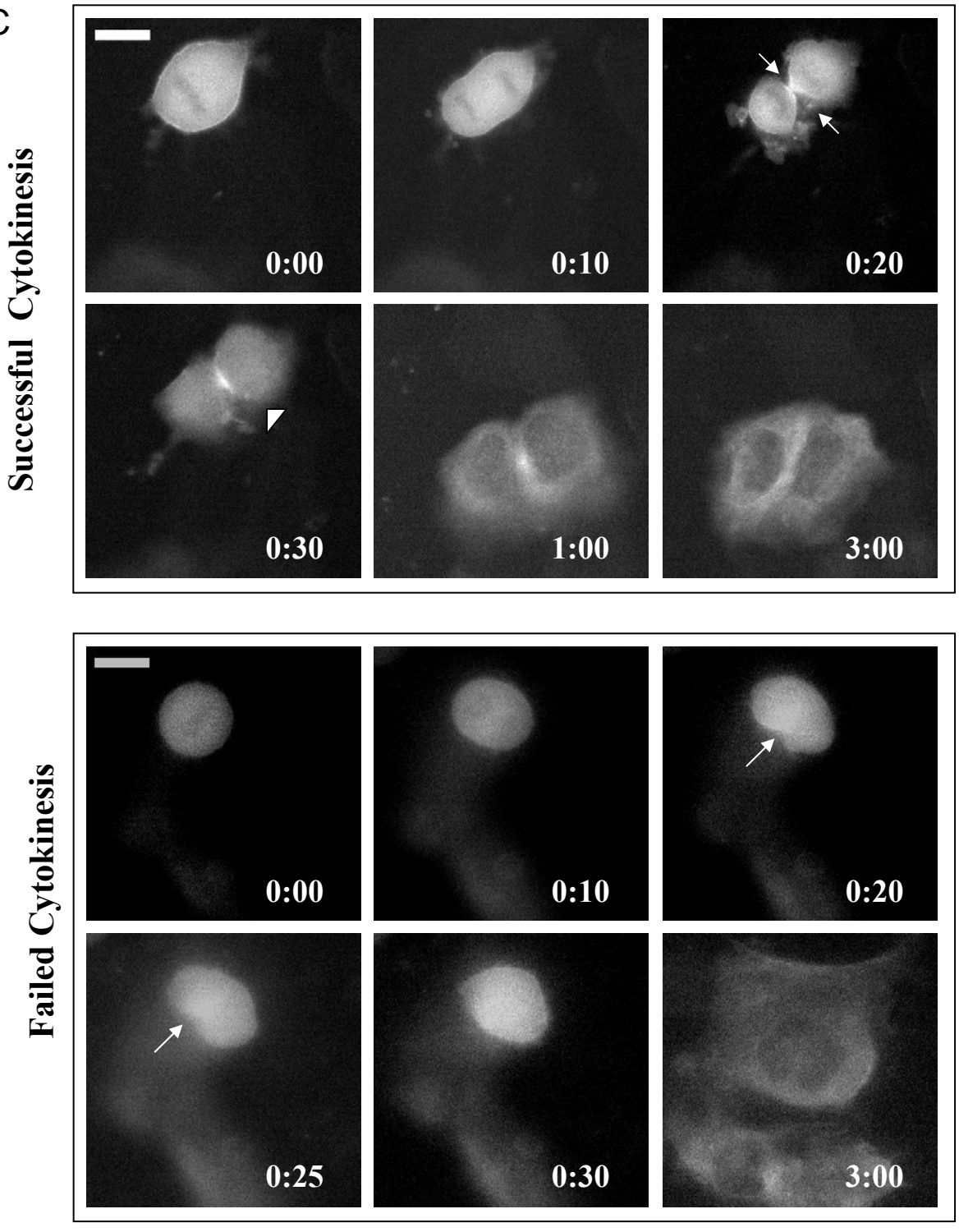
Successful Cytokinesis
0:00
0:10
0:20
0:30
1:00
3:00
Failed Cytokinesis
0:00
0:10
0:20
0:25
0:30
3:00

**Figure 24.** Majority of oral cancer cells failed in cytokinesis at an early stage with defective contractile ring formation. (A) GFP-actin localized properly in UPCI:SCC103 cells. (B) Cytokinesis failure frequency in GFP-actin transfected UPCI:SCC103 cells was comparable to untreated cells. (C) UPCI:SCC103 cells were transfected with GFP-actin plasmids and bipolar cell division was followed by live cell imagining. Top panel: an example of successful cytokinesis. Cleavage furrow started forming 10 minutes after metaphase (arrows) and contractile ring assembles at 30 minutes (arrowhead). The cell finally completed cytokinesis with two separated daughter cells (3 hours). Bottom panel: an example of failed cytokinesis. Cleavage furrow started forming on one side 20 minutes after metaphase (arrow) and regressed completely at 30 minutes. The cell failed in cytokinesis and formed one binucleated daughter cell (3 hours). Photos were taken every 5 minutes. Time: hours: minutes; bar: 1μm.

contractile ring formation. The recombinant GFP-actin colocalized with myosin, suggesting the protein is active (Figure 24A). Consistent with previous observations of ~10% abortive cytokinesis, 8.1% (n=62) UPCI:SCC103 cells transfected with GFP-actin failed in cytokinesis (Figure 24B). Eighty percent (n=5) exhibited cleavage furrow and contractile ring formation defects (Figure 24C), suggesting that these cancer cells primarily failed at an early stage of cytokinesis with defective contractile ring assembly. Consistently, in the example of one MPS cell division, normal and defective contractile ring were both observed (labeled by arrow and arrowhead respectively), ending with a partial cytokinesis failure and a mixture with mononulceated and binucleated progenies (labeled by one star and two stars respectively, Figure 25).

### 3.2.2 MLC phosphorylation was deficient in cancer cells

MLC phosphorylation at Thr18/Ser19 is one of the key regulatory steps of contractile ring formation and contractility (Komatsu et al., 2000; Moussavi et al., 1993). Therefore, I asked whether the phosphorylation of MLC in cancer cells was different from normal cells.

#### 3.2.2.1 MLC phosphorylation was downregulated and was correlated with multinucleation in cancer cells

MLC phosphorylation was detected by electrophoresis on a urea glycerol gel (Xia et al., 2005). The unphosphorylated, monophosphorylated and diphosphorylated MLC were separated and MLC phosphorylation ratios were determined by immunoblotting and calculated the ratios of

the intensities of monophosphorylated and diphosphorylated bands over total MLC (Figure 26A). Interestingly, the cancer cells universally showed a reduction in MLC phosphorylation compared to normal cells ($p<0.001$) (Figure 26B).

Results in Chapter II have revealed that cancer cells accumulate multinucleated cells resulted from cytokinesis failure (Figure 17). Here, I observed a correlation between the ratios of MLC phosphorylation and frequencies of multinucleation by a statistical analysis (Figure 27). These observations suggest that the deficiency of MLC phosphorylation could be a cause of cytokinesis failure in a variety of cancer cell lines.

#### 3.2.2.2 Timing of MLC phosphorylation in cytokinesis was normal, but phosphorylation levels were low during cytokinesis in oral cancer cells

Previous data from this dissertation indicate that defective MLC phosphorylation might account for abortive cytokinesis in cancer cells. To test this hypothesis, I used human oral squamous cancer cells UPCI:SCC103 as a representative cancer cell type for the following studies. The phosphorylation of MLC would be examined in dividing UPCI:SCC103 cells and compared to dividing primary RPE-hTERT cells. First, I determined if MLC phosphorylation was induced during mitosis in the cancer cells. UPCI:SCC103 and RPE-hTERT cells were synchronized at metaphase by colcemid and released for different time points. Comparing within the cell line, the phosphorylation of MLC was elevated in RPE-hTERT cells and so was in cancer cells, when anaphase and telophase were accumulated (Figure 28A). It seemed that the levels of MLC phosphorylation were similar in UPCI:SCC103 and RPE-hTERT cells (Figure 28B). This is possibly due to the increased frequency of anaphase/telophase cells in the tumor

Figure 25

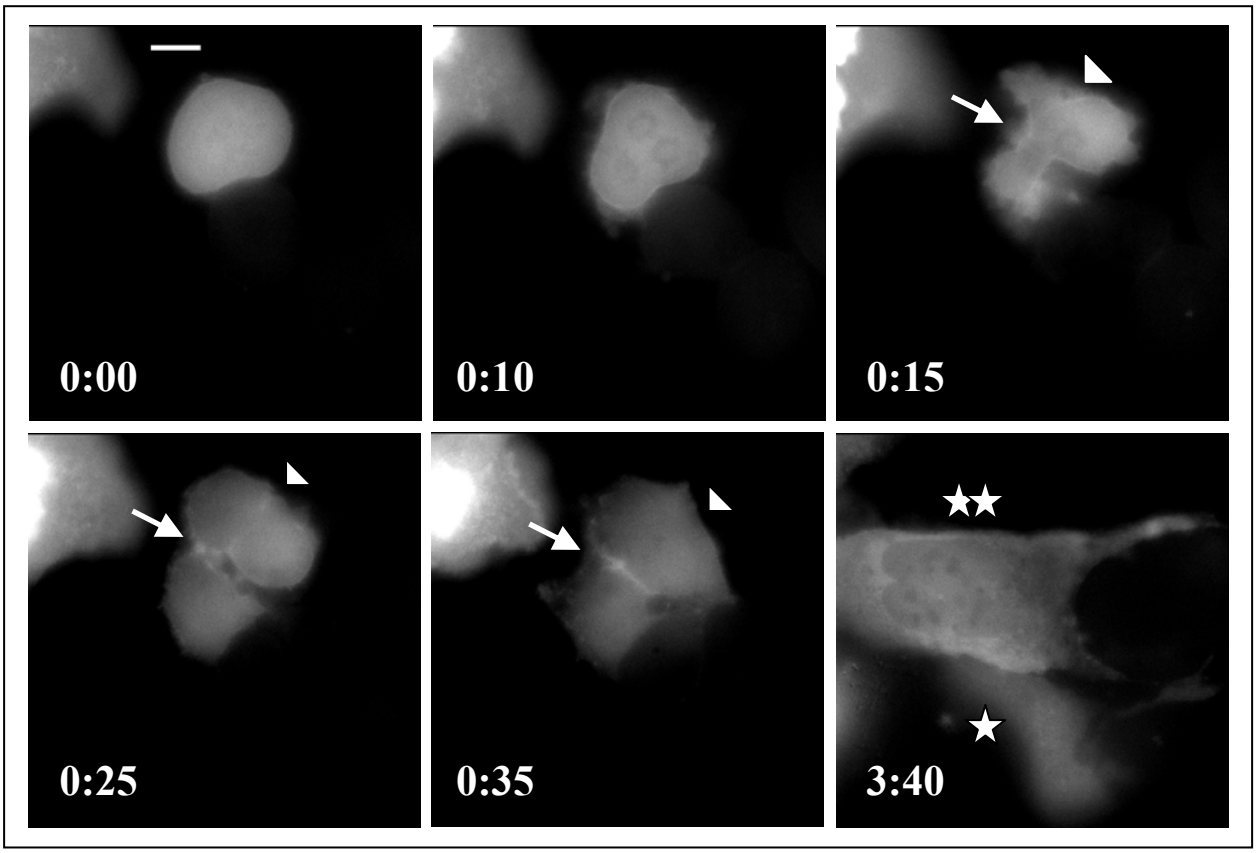


**Figure 25.** MPS cell division failed with defective contractile ring formation in UPCI:SCC103 cells. Oral cancer cells were transfected with GFP-actin plasmid. A cell with multipolarity was recorded every 5 minutes. Cleavage furrow and contractile ring formed normally between two daughter cells (arrow), but not others (arrowhead). 3 hours and 40 minutes later, the top spindle without a contractile ring failed in cytokinesis with a binucleated cell as an end-product (two stars). The bottom part underwent proper contraction, completed cytokinesis and gave rise to a mononulceated daughter cell (one star).

Figure 26

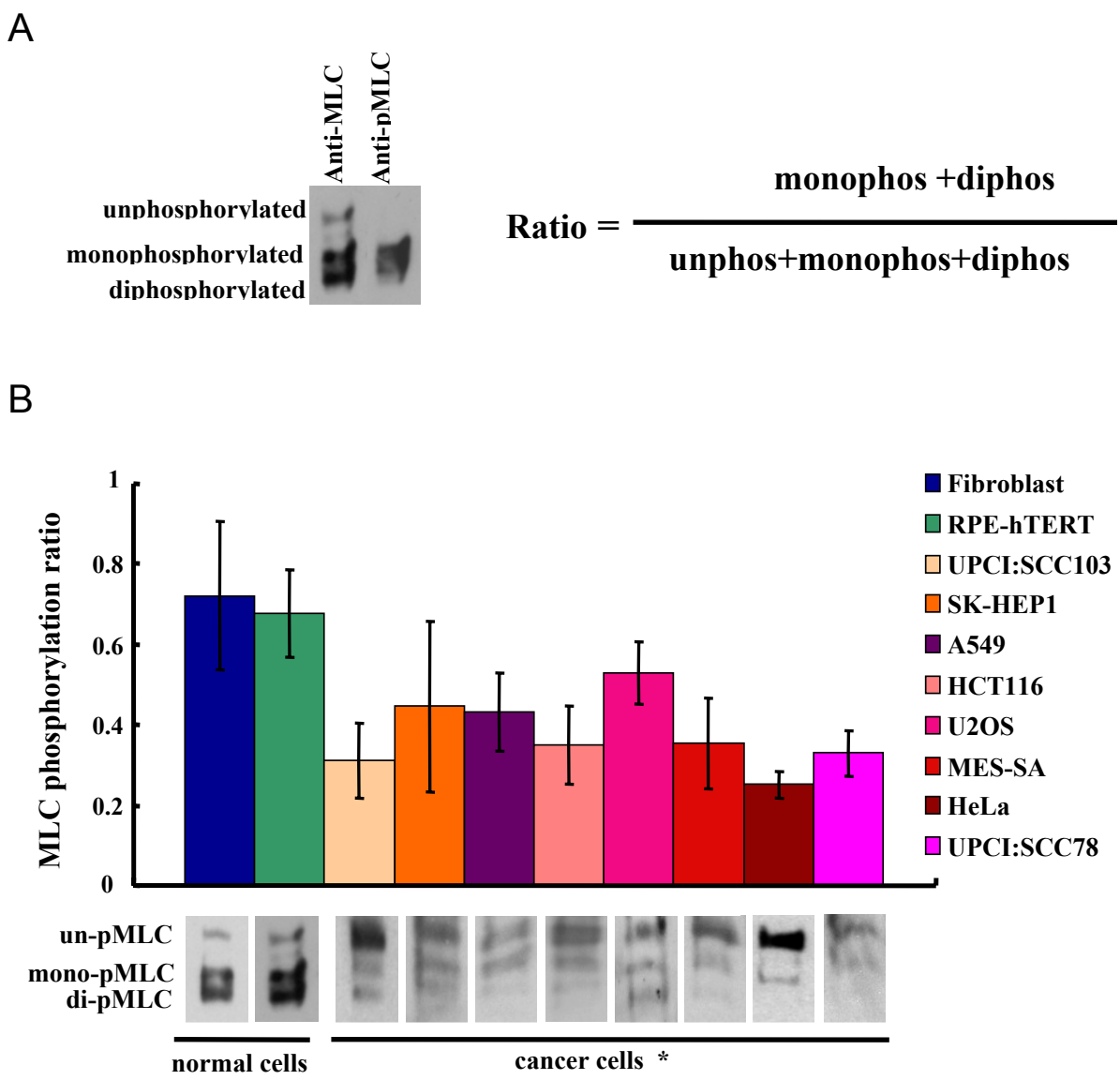


**Figure 26.** The phosphorylated MLC levels in cancer cells were low compared to normal cells (*p <0.001). (A) MLC phosphorylation was analyzed by urea glycerol gel electrophoresis. Ratio = (monopMLC + dipMLC ) / (unpMLC + monopMLC + dipMLC ). (B) The phosphorylated MLC ratios in tested cell lines. Data and error bars represent mean and standard deviation of more than three different experiments, respectively.

Figure 27

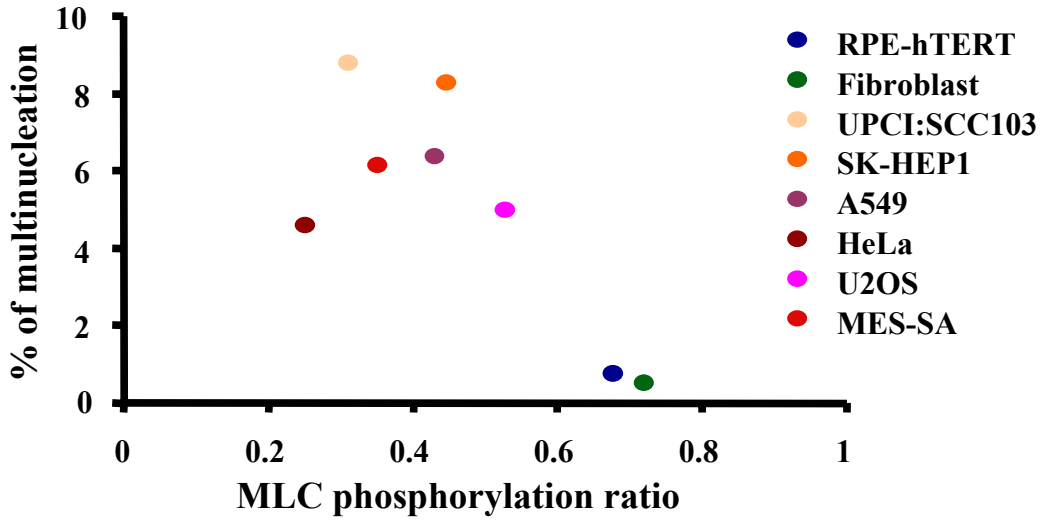


**Figure 27.** The ratio of MLC phosphorylation was correlated with the frequency of multinucleation in various cell lines. Data represent mean of more than three different experiments.

Figure 28

A

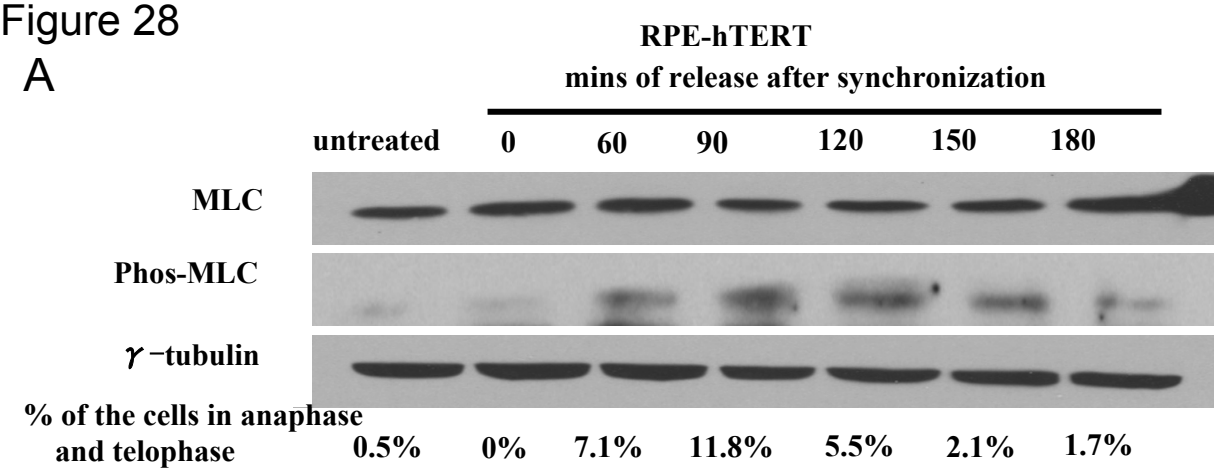


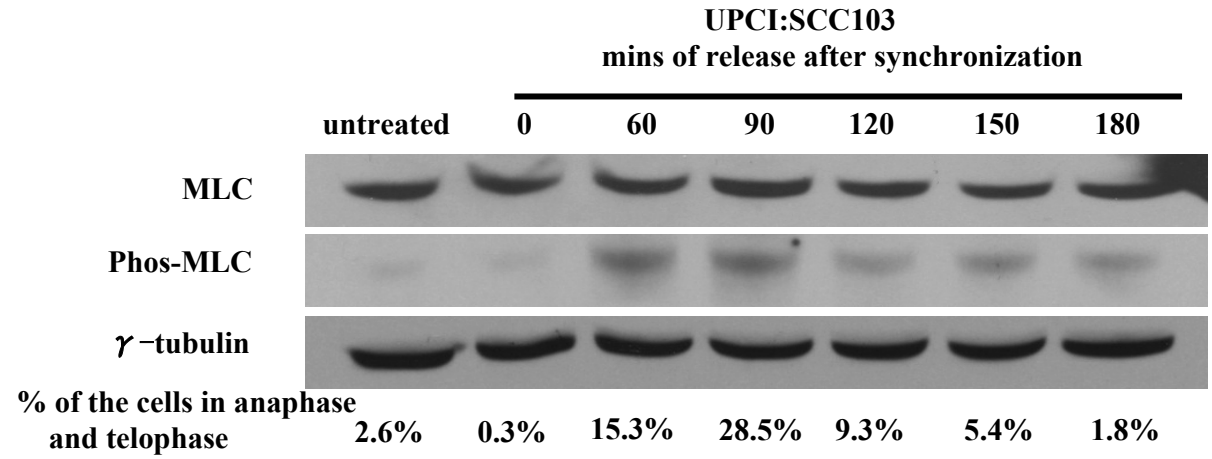


B

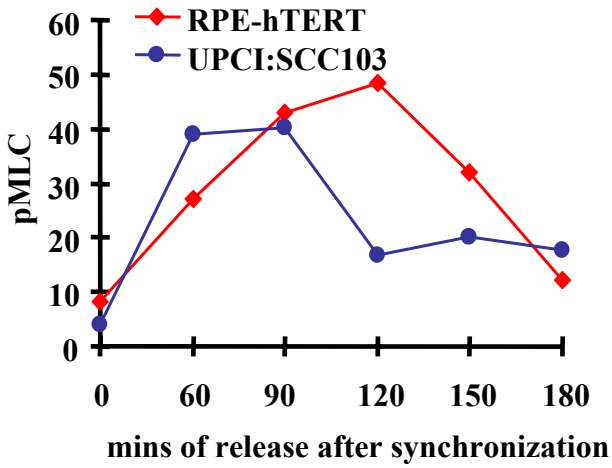


C

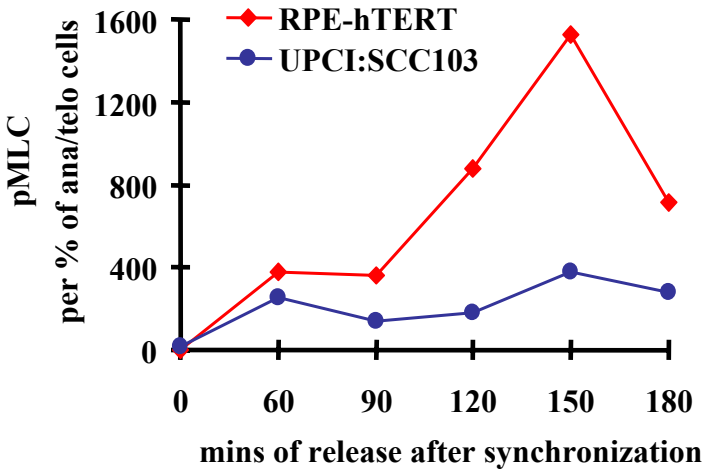

**Figure 28.** Timing of MLC phosphorylation in cytokinesis was normal but phosphorylation level was low during cytokinesis in oral cancer cells. (A) MLC in UPCI:SCC103 cells were able to be phosphorylated at the right time. The levels of phosphorylated MLC in UPCI:SCC103 and RPE-hTERT cells were tested at different time points after synchronization. The numbers on the bottom represent the percentages of cells in anaphase and telophase after release. (B) Quantification of MLC phosphorylation at each time points from (A). The measurement is in arbitrary unit. (C) Quantification of MLC phosphorylation per percentage of anaphase/telophase cells at each time points from (A). The measurement is in arbitrary unit.

cell population after the colcemid release (Figure 28A). Therefore, if the MLC phosphorylation level was normalized by the percentage of anaphase/telophase cells, MLC phosphorylation was reduced in oral cancer cells compared to normal cells. Together with urea glycerol gel results, it suggested that the level of MLC phosphorylation remained low in not only interphase cells, but also anaphase and telophase cells, which might be the reason for cytokinesis failure in the cancer cells.

#### 3.2.2.3 Phosphorylated MLC was missing from cleavage furrow in cancer cells

To confirm this conclusion, I compared the localization of phosphorylated MLC (Ser19) in normal versus cancer cells by immunofluorescence. In contrast to normal cells, the phosphorylated MLC was diminished at the cleavage furrow in most of the cancer cell lines (Figure 29A). Furthermore, taking a deeper look at these cells, the phosphorylated MLC in cancer cells was not colocalized with the contracted MHC. I presented HeLa and MES-SA cells in Figure 29B as examples. In conclusion, I observed that failure of cytokinesis in cancer cell lines was associated with decreased phosphorylation of MLC.

### 3.2.3 MLC phosphorylation deficiency was the cause of cytokinesis failure in oral cancer cells

MLC phosphorylation at Thr18/Ser19 promotes assembly of actin and myosin which is important for the contractility of the contractile ring (Moussavi et al., 1993). To test whether the deficiency of phosphorylation of MLC is the cause of defective contractile ring and failed

Figure 29

A

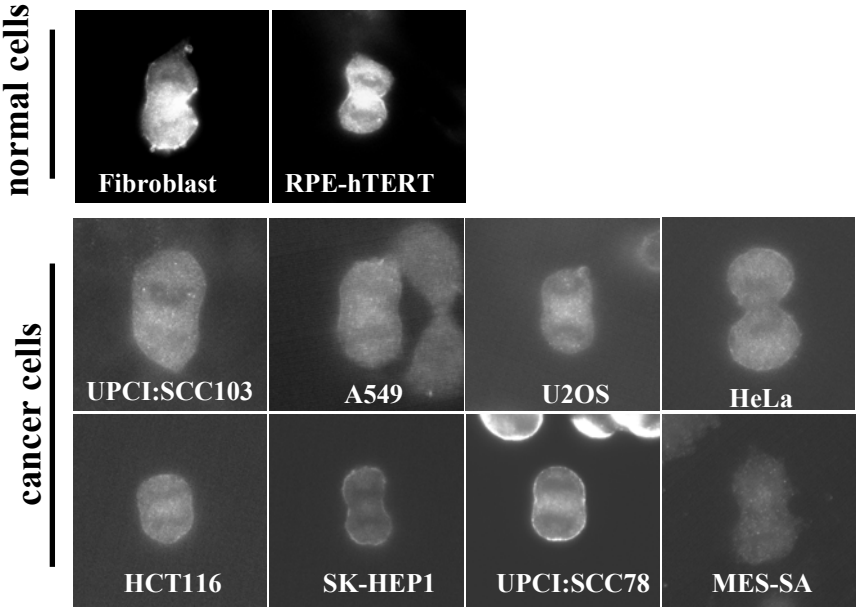
normal cells
Fibroblast
RPE-hTERT
cancer cells
UPCI:SCC103
A549
U2OS
HeLa
HCT116
SK-HEP1
UPCI:SCC78
MES-SA

B

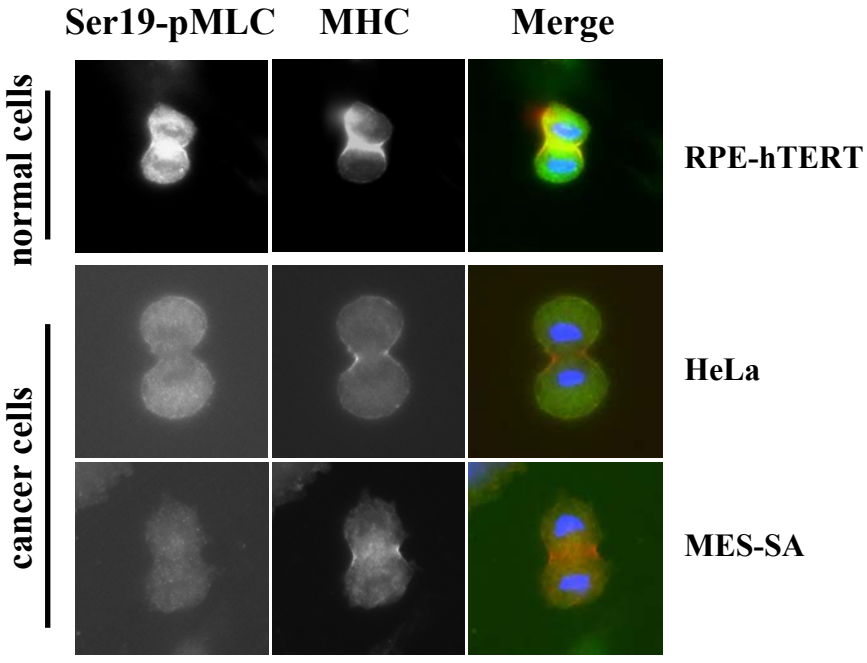
Ser19-pMLC
MHC
Merge
normal cells
RPE-hTERT
cancer cells
HeLa
MES-SA

**Figure 29.** Mislocalization of phosphorylated MLC in anaphase cancer cells. (A) Ser19-phosporylated MLC in anaphase cells from different cell lines were viewed by immunofluorescence. In normal cells (top panel), Ser19-phosphorylated MLC was concentrated at the midzones. In cancer cells (bottom panel), phosphorylated MLC were missing at the midzones. (B) MHC but not Ser19-phosphorylated MLC concentrated at the furrows in cancer cells. Merge panel: blue, DNA; red, MHC; green, Ser19-phosphorylated MLC.

Figure 30

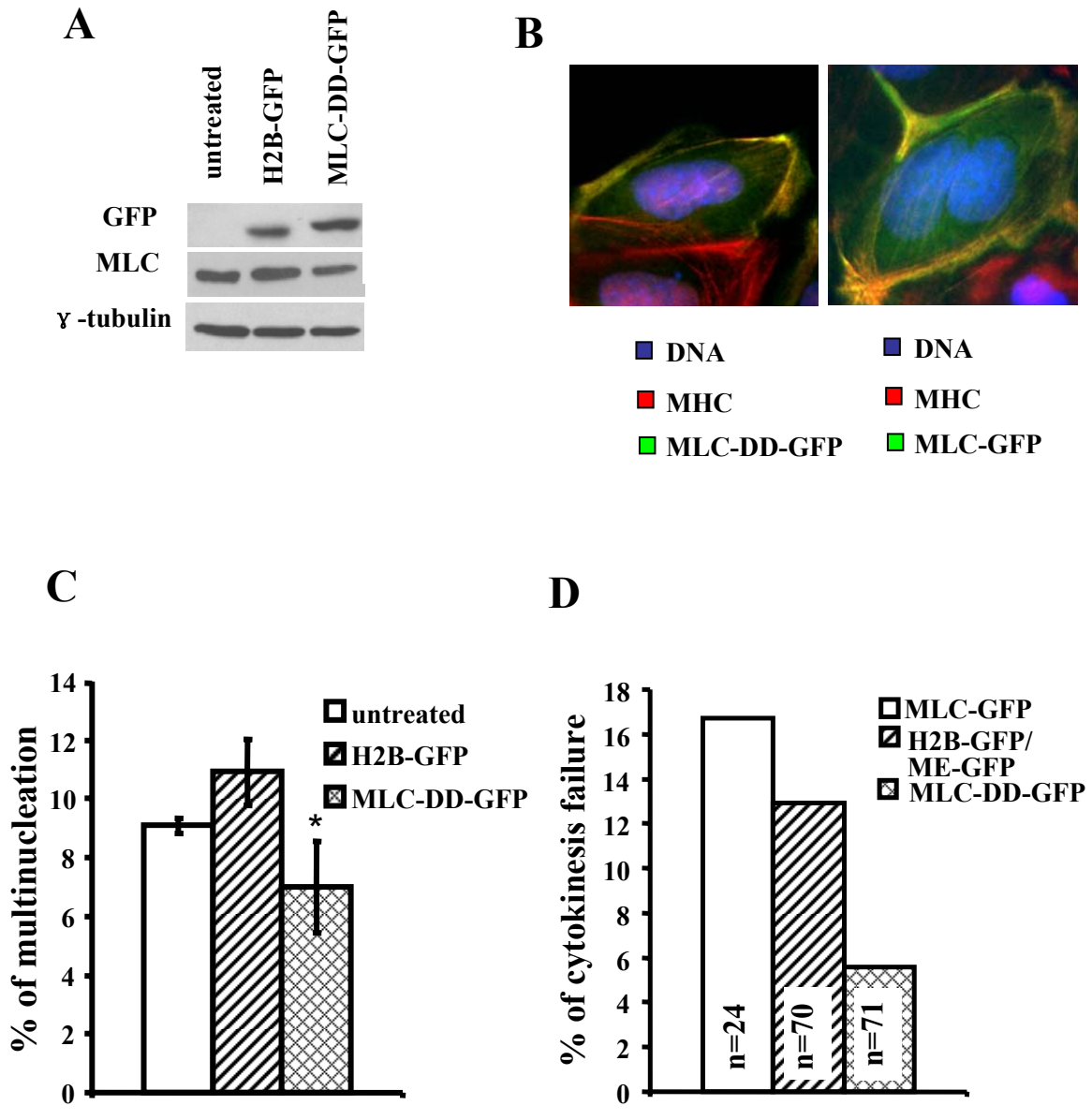
A
untreated
H2B-GFP
MLC-DD-GFP
GFP
MLC
ɣ -tubulin
B
DNA
MHC
MLC-DD-GFP
DNA
MHC
MLC-GFP
C
% of multinucleation
14
12
10
8
6
4
2
0
untreated
H2B-GFP
MLC-DD-GFP
*
D
% of cytokinesis failure
18
16
14
12
10
8
6
4
2
0
MLC-GFP
H2B-GFP/
ME-GFP
MLC-DD-GFP
n=24
n=70
n=71

**Figure 30.** Expression of phosphomimetic MLC rescued the cytokinesis failure in oral cancer cells. (A) MLC-DD-GFP was overexpressed in UPCI:SCC103 cells. (B) MLC-DD-GFP and MLC-GFP both colocalized with endogenous myosin fibers in UPCI:SCC103 cells. (C) Multinucleation was reduced after phosphomimetic MLC expression in UPCI:SCC103 cells (* $p < 0.01$). Data and error bars represent mean and standard deviation of more than three different experiments, respectively. (D) Cytokinesis failure was rescued by phosphomimetic MLC overexpression. UPCI:SCC103 were transfected with different plasmids as shown and bipolar cell divisions were followed by live cell imaging.

Figure 31

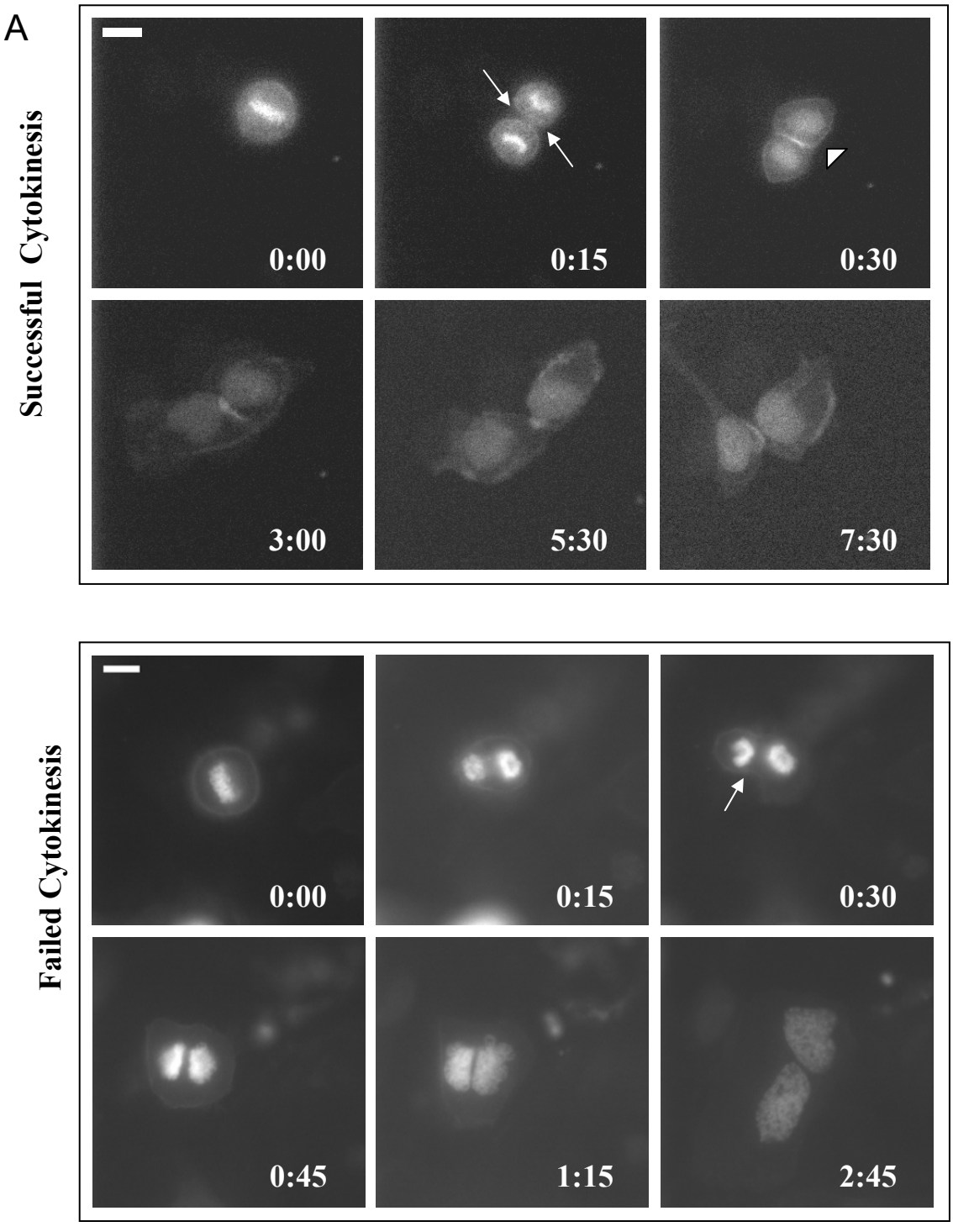
A
Successful Cytokinesis
0:00
0:15
0:30
3:00
5:30
7:30
Failed Cytokinesis
0:00
0:15
0:30
0:45
1:15
2:45

Figure 31

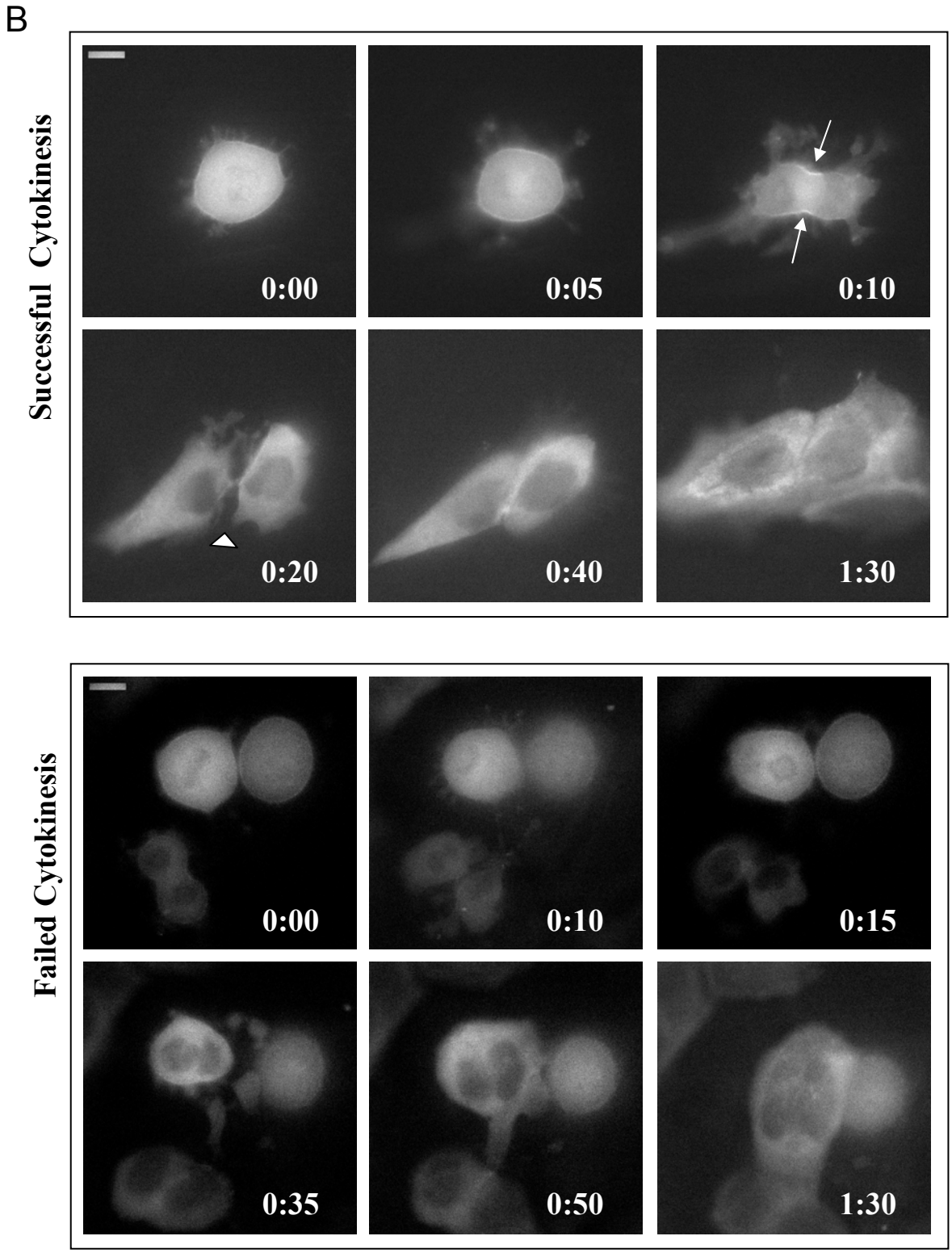
B
Successful Cytokinesis
0:00
0:05
0:10
0:20
0:40
1:30
Failed Cytokinesis
0:00
0:10
0:15
0:35
0:50
1:30

**Figure 31.** Cytokinesis failed with defective contractile ring formation in oral cancer cells. UPCI:SCC103 cells were transfected with (A) histone H2B-GFP and membrane-associated farnesylated-GFP plasmids or (B) wild-type MLC-GFP plasmids, and bipolar cell division were followed by live cell imaging. Arrows: cleavage furrows; Arrowheads: contractile rings. Time: hours: minutes; bar: 1μm.

cytokinesis, a plasmid encoding phosphomimetic MLC (Thr18 and Ser19 were replaced with Asp) was transfected into UPCI:SCC103 cells. This recombinant MLC protein expressed abundantly and localized properly with MHC, the same as wild-type MLC (Figure 30A and B). The multinucleation frequency decreased marginally, but significantly, after phosphomimetic MLC expression in oral cancer cells (Figure 30C, $p<0.01$). However, the frequency of cytokinesis failure decreased markedly by introduction of the phosphomimetic MLC (Figure 30C) compared to the cells with wild-type MLC-GFP or H2B-GFP and farnesylated-GFP expression (Figure 31). These observations indicated that cytokinesis failure in these cells was caused by deficient phosphorylation of MLC.

### 3.2.4 Myosin phosphatase was a key regulator of MLC phosphorylation and cytokinesis completion in cells

The next question I addressed was why the phosphorylation of MLC was decreased in the tested malignant cells. It has been shown that myosin phosphorylation is regulated by a number of kinases and one phosphatase. Hence, the study started with examining the expressions of these proteins by immunoblotting.

#### 3.2.4.1 Expression of MLC phosphorylation regulators

Immunoblotting in Figure 32 summarized the expressions of kinases and phosphatase involved in MLC phosphorylation regulation. ROCK1 expressions showed no consistent

Figure 32

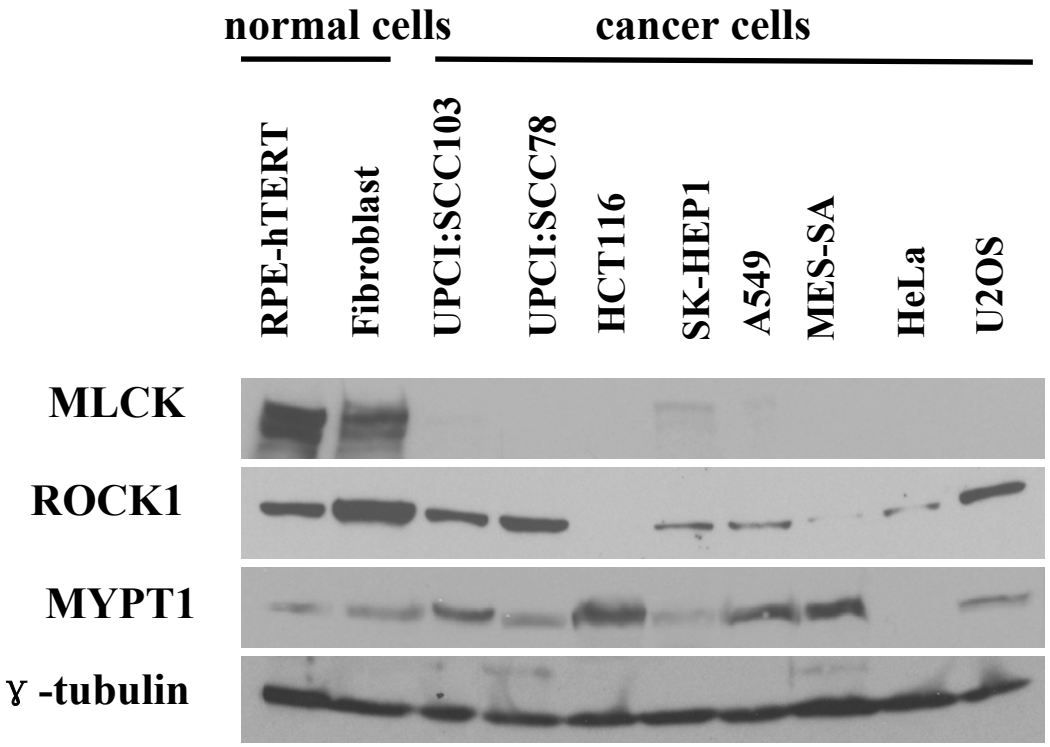


**Figure 32.** Expression of kinases and phosphatase involved in regulation of MLC phosphorylation in different cell lines. Cells were lysed and MLCK, ROCK1,MYPT1 and γ-tubulin expressions were examined by immunoblotting. γ-tubulin was used as a loading control.

differences between normal and cancer cells (Figure 32) and citron kinase expression was overall low among all cell lines (data not shown). Since defective ROCK1 or overexpression of citron kinase did not previously cause contractile ring defects (Kosako et al., 1999; Madaule et al., 1998), I turned my focus on another important kinase: myosin light chain kinase (MLCK). Interestingly and surprisingly, MLCK expression is down-regulated in all the tested cancer cell lines (Figure 32). On the other hand, the myosin targeting subunit (MYPT1) of myosin phosphatase, was up-regulated for expression in many of the tested cell lines (Figure 32), consistent with my developing model that deficient MLC phosphorylation caused cytokinesis failure in cancer cells. I will discuss the results about how phosphatase overexpression plays a role in cytokinesis in this section and how defective MLCK effects cytokinesis in cancer cells in Section 3.2.5.

#### 3.2.4.2 Myosin phosphatase knockdown in cancer cells increased MLC phosphorylation

It was indicated that the MYPT1 overexpression could be a cause of the deficient MLC phosphorylation in oral cancer cells. Hence, I designed an siRNA targeting MYPT1 to knock down myosin phosphatase in tumor cells (Figure 33A middle lane and Figure 33B red). After siMYPT treatment, the phosphorylation ratio of MLC in UPCI:SCC103 cells elevated to approximately 80%, which was comparable to normal cells, showing phosphorylation was limited due to the activity of this protein (Figure 33D, $p<0.01$). In addition, this increase was not caused by the up-regulation of MLC expression after siRNA treatment (Figure 33D).

#### 3.2.4.3 Myosin phosphatase knockdown rescued cytokinesis failure in oral cancer cells

The next question I addressed was whether the cytokinesis would be rescued when the MLC phosphorylation levels increased by MYPT1 knockdown. As expected, the multinucleation frequency decreased after MYPT1 knockdown (Figure 34A, $p<0.01$). In order to confirm this reduction is due to down-regulation of phosphatase and not other off-target effects, a recombinant siRNA-resistant chicken MYPT1 protein was expressed in the siMYPT1-treated UPCI:SCC103 cells (Figure 33A and B). This recombinant MYPT1-GFP protein colocalized with endogenous MHC and the expression restored multinucleation to untreated levels (Figure 34B and C). Phosphatase knockdown did not cause significant apoptosis or changes in the mitotic index (data not shown). These results indicated that the multinucleation in the oral cancer cell line was caused by decreased MLC phosphorylation, resulting from myosin phosphatase overexpression. To confirm that the reduction in multinucleation was caused by improved cytokinesis efficiency, I examined cell divisions by live cell imaging. The frequency of cytokinesis failure in bipolar cell divisions in UPCI:SCC103 cells dropped from 8.4% to 3.2% after MYPT1 down-regulation by siRNA treatment (Figure 34D). I hypothesized the extended siMYPT1 treatment in UPCI:SCC103 cells should sharply reduce the multinucleation and spindle multipolarity defects in these cells. I observed that both multinucleation and multipolarity were markedly decreased after 20 days of siMYPT1 treatment compared to scramble siRNA treatment controls, indicating that defective MLC phosphorylation and failed cytokinesis is a major cause of multinucleation and multipolarity in these oral cancer cells (Figure 34E and F, $p < 0.005$).

It is believed that tetraploidy and multipolarity contributes to chromosomal instability. Therefore, I investigated whether the genome was more stable after the cytokinesis defects were corrected by myosin phosphatase knockdown in oral cancer cells. Collaborators Dale Lewis and Dr. Susanne Gollin examined the stability of chromosome 6 and chromosome 20 in UPCI:SCC103 cells. Compared to scramble siRNA treated cells, both chromosomes deviated less from modes in the cells with 20-day consecutive MYPT1 knockdown, indicating the genome is more stable after the cytokinesis failure was rescued in oral cancer cells (unpublished data, Lewis and Gollin).

#### 3.2.4.4 Myosin phosphatase knockdown rescued cytokinesis failure in liver cancer cells

I observed that not all cancer cell lines showed high levels of myosin phosphatase expression (Figure 32). Therefore, another cancer cell line, SK-HEP1, with a relatively low level of MYPT1 expression was tested with siRNA knockdown. Similar to oral cancer cells, these liver cancer cells showed decreased multinucleation and multipolarity percentages after 20-day siMYPT1 treatment (Figure 35), suggesting that elevated myosin phosphatase activity is a cause of cytokinesis failure in different tumor cell types.

#### 3.2.4.5 Myosin phosphatase overexpression induced cytokinesis failure in normal and cancer cells

I next asked whether the overexpression of MYPT1 was sufficient to cause cytokinesis failure and result in multinucleation in non-malignant cells. Full-length chicken MYPT1 fused with GFP was transiently expressed in RPE-hTERT cells. After cMYPT1-GFP overexpression,

Figure 33

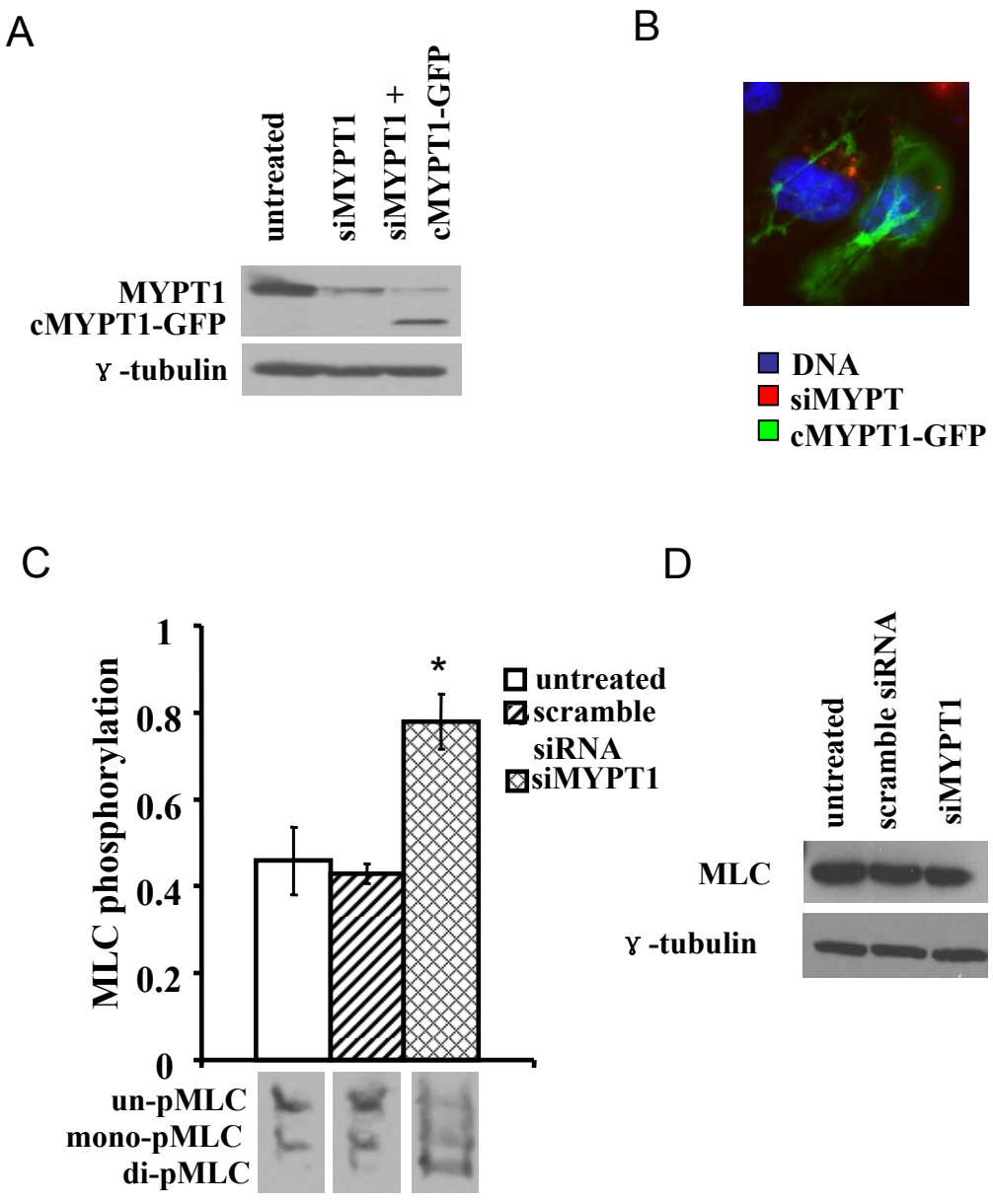
A
untreated
siMYPT1
siMYPT1 +
cMYPT1-GFP
MYPT1
cMYPT1-GFP
γ -tubulin
B
DNA
siMYPT
cMYPT1-GFP
C
MLC phosphorylation
1
0.8
0.6
0.4
0.2
0
*
untreated
scramble siRNA
siMYPT1
un-pMLC
mono-pMLC
di-pMLC
D
untreated
scramble siRNA
siMYPT1
MLC
γ -tubulin

**Figure 33.** Myosin phosphatase knockdown increased MLC phosphorylation in oral cancer cells. (A) and (B) MYPT1 knockdown and resistant-cMYPT1-GFP expression in UPCI:SCC103 cells by immunoblotting and immunofluorescence respectively. (C) MYPT1 knockdown elevated MLC phosphorylation in oral cancer cells (*$p < 0.01$). UPCI:SCC103 cells were treated by siMYPT1 and phosphorylation of MLC was examined by urea glycerol gel electrophoresis. Data and error bars represent mean and standard deviation of more than three different experiments, respectively. (D) MYPT1 knockdown did not change MLC expressions in UPCI:SCC103 cells.

Figure 34

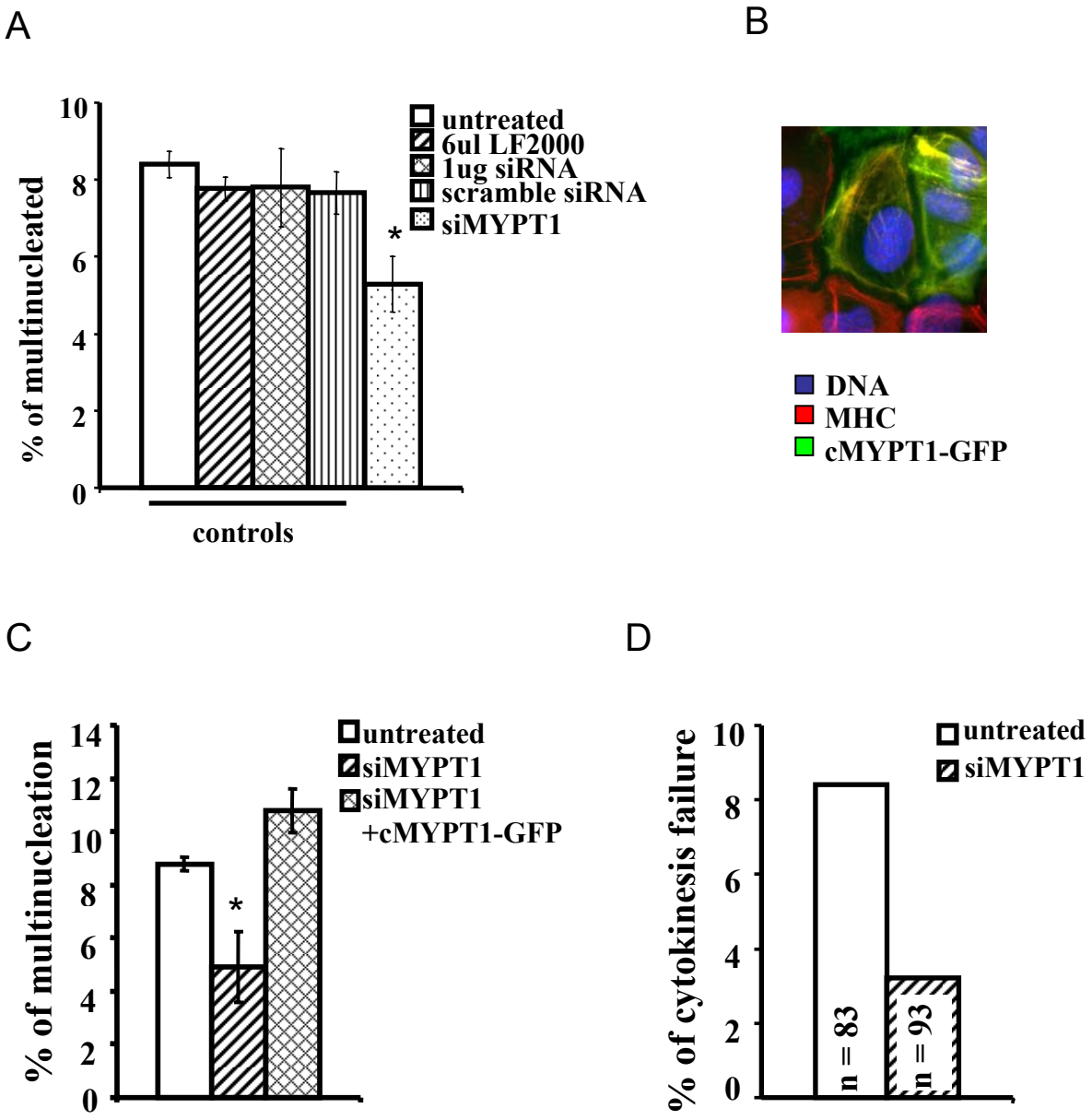
A
B
C
D
% of multinucleated
untreated
6ul LF2000
1ug siRNA
scramble siRNA
siMYPT1
*
controls
DNA
MHC
cMYPT1-GFP
% of multinucleation
siMYPT1
+cMYPT1-GFP
% of cytokinesis failure
n = 83
n = 93

E

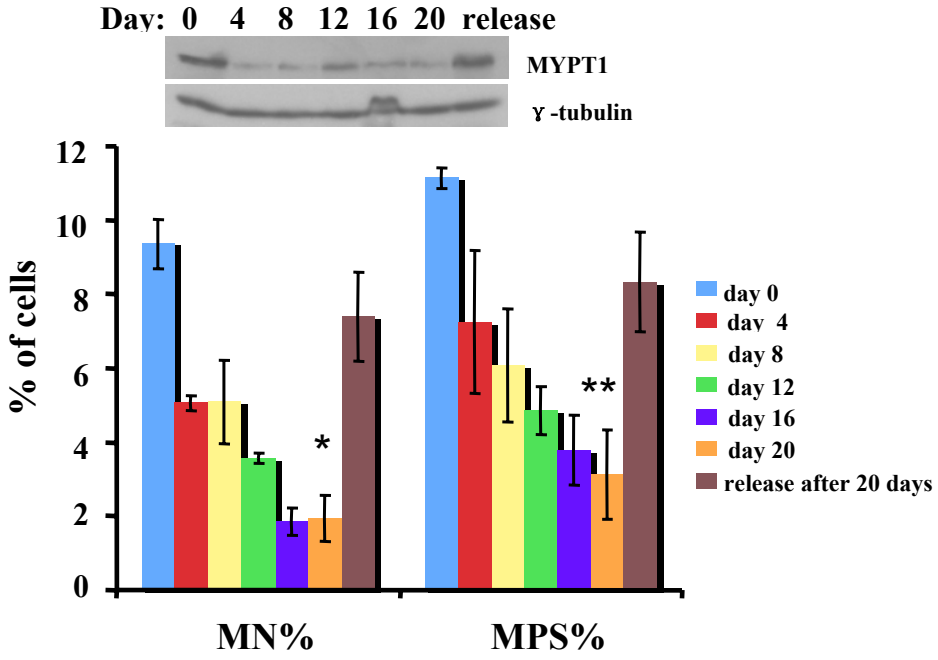
Day: 0 4 8 12 16 20 release
MYPT1
ɣ -tubulin
% of cells
12
10
8
6
4
2
0
*
**
MN%
MPS%
day 0
day 4
day 8
day 12
day 16
day 20
release after 20 days

F

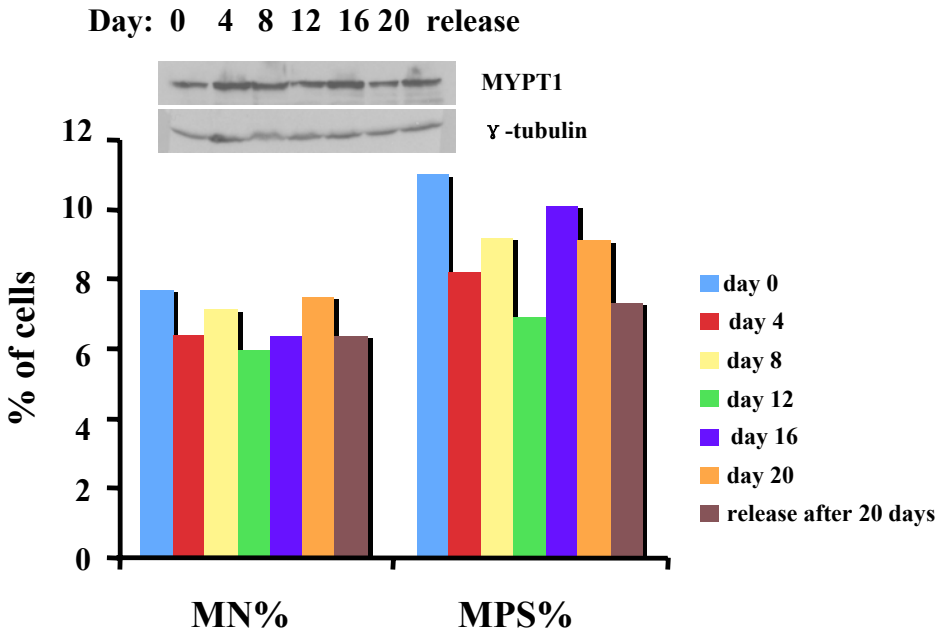
Day: 0 4 8 12 16 20 release
MYPT1
ɣ -tubulin
% of cells
12
10
8
6
4
2
0
MN%
MPS%
day 0
day 4
day 8
day 12
day 16
day 20
release after 20 days

**Figure 34.** siRNA-mediated myosin phosphatase knockdown reduced cytokinesis failure, multinucleation and multipolar mitosis. (A) Multinucleation frequency was reduced by siMYPT1 knockdown in oral cancer cells but not control treatments (*$p < 0.01$). UPCI:SCC103 cells were treated by identical amount of tranfection reagent or siRNA alone, or scramble siRNA or siMYPT1. Cells were counted for multinucleation. (B) cMYPT1-GFP colocalized with MHC in UPCI:SCC103 cells. (C) Multinucleation frequency was reduced by siMYPT1 knockdown and was restored by resistant MYPT1-GFP protein expression in oral cancer cells (*$p < 0.01$). UPCI:SCC103 cells were treated by siMYPT1 and transfected with resistant MYPT-GFP plasmids. Cells with both siRNA and plasmid were quantitated for multinucleation. (D) MYPT1 knockdown markedly rescued cytokinesis failure in oral cancer cells. UPCI:SCC103 cells were transfected with siMYPT1. Bipolar cell divisions were examined by DIC time-lapse microscopy. (E) Multinucleation and multipolarity levels were reduced after 20-day siMYPT1 treatment in oral cancer cells (*$p < 0.005$, **$p < 0.005$). UPCI:SCC103 cells were treated with siMYPT1 for 20 days. Multinucleation and multipolarity were quantified every four days. (F) Multinucleation and multipolarity levels were consistent after 20-day scramble siRNA treatment in oral cancer cells. UPCI:SCC103 cells with multinucleation and multipolar spindles were quantitated after various times treatment with scramble siRNA. Data and error bars represent mean and standard deviation of three different experiments, respectively.

Figure 35

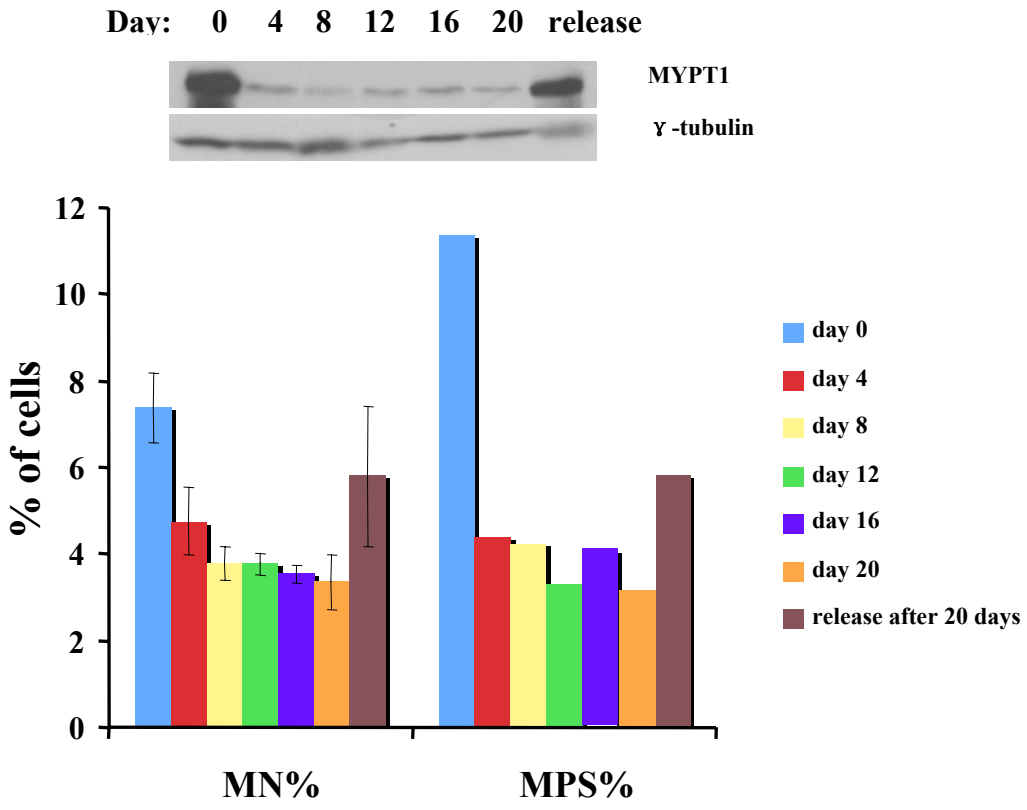


**Figure 35.** Multinucleation and multipolarity levels were reduced after 20-day siMYPT1 treatment in liver cancer cells. SK-HEP1 cells were treated by siMYPT1 for 20 days. Cells with multinucleation and multipolar spindles were quantitated after the siMYPT1 treatment of various days. Data and error bars represent mean and standard deviation of two different experiments, respectively.

Figure 36

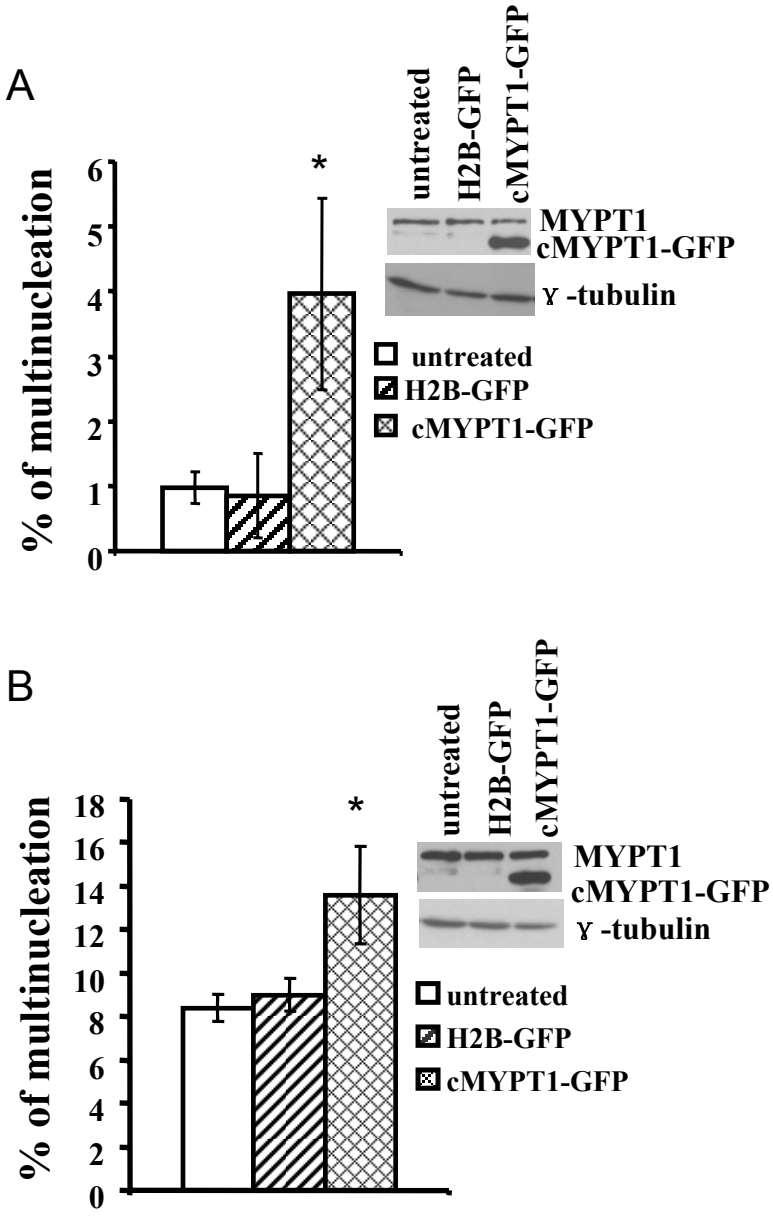
A
% of multinucleation
0
1
2
3
4
5
6
*
untreated
H2B-GFP
cMYPT1-GFP
MYPT1
cMYPT1-GFP
ϒ -tubulin
untreated
H2B-GFP
cMYPT1-GFP
B
% of multinucleation
0
2
4
6
8
10
12
14
16
18
*
untreated
H2B-GFP
cMYPT1-GFP
MYPT1
cMYPT1-GFP
ϒ -tubulin
untreated
H2B-GFP
cMYPT1-GFP

**Figure 36.** Overexpression of MYPT1 in cells increased the multinucleation and multipolarity. (A) RPE-hTERT cells (*p <0.005) (B) UPCI:SCC103 cells (*p <0.005). Data and error bars represent mean and standard deviation of three different experiments, respectively.

Figure 37

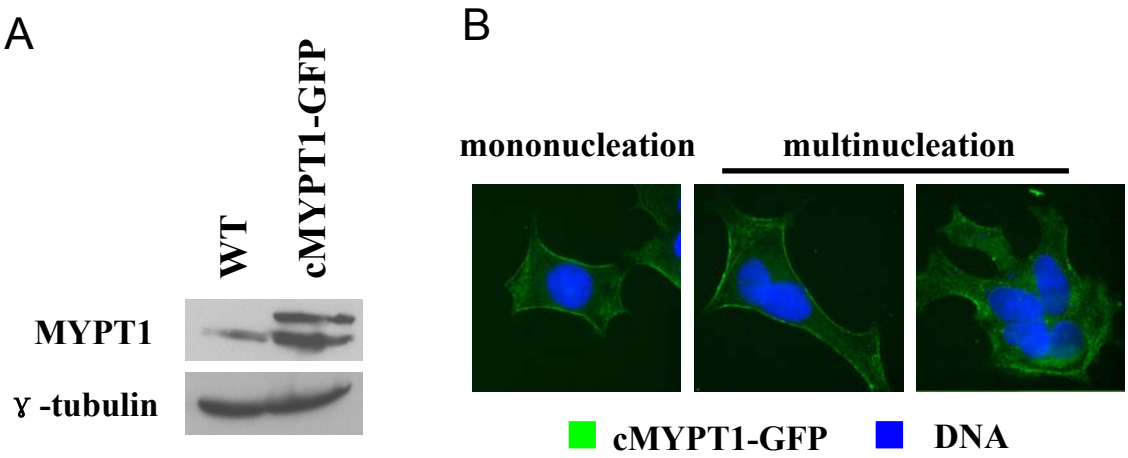
A
WT
cMYPT1-GFP
MYPT1
ɣ -tubulin
B
mononucleation
multinucleation
cMYPT1-GFP
DNA

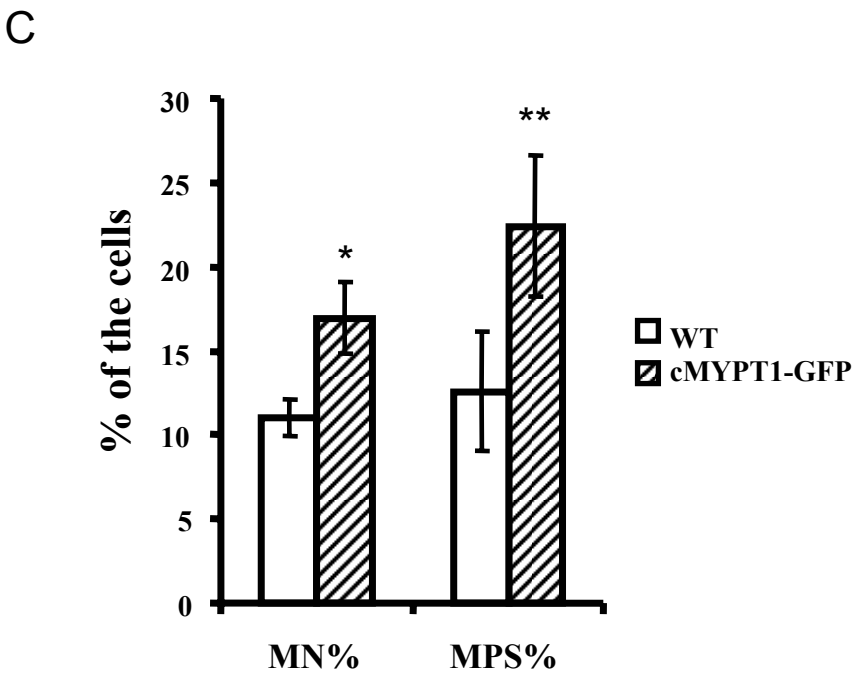
C
% of the cells
30
25
20
15
10
5
0
*
**
MN%
MPS%
WT
cMYPT1-GFP

**Figure 37.** Multinucleation and multipolarity increased in HEK-293 cells with stable cMYPT1-GFP overexpression. (A) HEK-293 cells stably express cMYPT1-GFP. (B) Examples of multinucleated cells in HEK-293 cells with cMYPT1-GFP overexpression. (C) Multinucleation and multipolarity were quantitated in wild-type and cMYPT1-GFP overexpressed HEK-293 cells (*$p<0.005$, **$p<0.005$). Data and error bars represent mean and standard deviation of three different experiments, respectively.

multinucleation frequency increased approximately four fold (Figure 36A, $p<0.005$). Similarly, the overexpression of cMYPT1 in UPCI:SCC103 cells gave rise to additional multinucleated cells (Figure 36B, $p<0.005$), indicating that cancer cells have high potential to tolerate the presence of multinucleation. To confirm this was not the only effect from transient transfection, HEK-293 cells stably expressing MYPT1-GFP protein were used for study (Figure 37A). With overexpressed MYPT1, HEK-293 cells showed elevated multinucleation and multipolarity (Figure 37B and C, $p< 0.005$). Taken together, these results indicate that the overexpression of phosphatase is a primary cause of cytokinesis failure, multinucleation and multipolarity in cancer cell lines.

### 3.2.5 Myosin light chain kinase (MLCK) was downregulated and inhibited in oral cancer cells

It is well known that MLCK is a primary and essential kinase to regulate MLC phosphorylation in cytokinesis during the cell division (Ikebe and Hartshorne, 1985; Sellers, 1991). Strikingly, the MLCK expression levels in all of the tested cancer cell lines were much lower than in normal cell lines (Figure 32). This is consistent with microarray analyses from other labs, showing that myosin light chain kinase (MLCK) transcription is low in various tumors, such as colon, lung, prostate, bladder, brain, breast, ovarian, liver, melanoma and myeloma, compared to normal controls, and only high in head-neck cancer and lymphonma (www.oncomine.org, Rhodes et al., 2007).

In order to confirm that the activity of MLCK is also reduced, endogenous MLCK was immunoprecipitated from equal amount of whole cell lysates and MLCK activity assays were performed *in vitro* (Poperechnaya et al., 2000). The results showed that MLCK activity from same number of the cells was lower in oral cancer cells than normal cells, suggesting both MLCK expression and activity are down-regulated in oral cancer cells (unpublished data, Sahasrabudhe and Saunders).

#### 3.2.5.1 MLCK overexpression did not increase MLC phosphorylation in oral cancer cells

I observed that MLC phosphorylation was defective in oral cancer cells and resulted in cytokinesis failure. Therefore, I hypothesized that cytokinesis would be rescued if I restored the expression and activity of MLCK in oral cancer cells. To test this hypothesis, full-length MLCK-GFP protein was expressed in UPCI:SCC103 cells (Figure 38A). Exogenous MLCK localized along the cytoskeletal fibers in UPCI:SCC103 and RPE-hTERT cells and the activity of this GFP-fused MLCK was confirmed by kinase activity assay *in vitro* (Dulyaninova et al., 2004) and data not shown). These data suggested MLCK-GFP functioned properly in oral cancer cells, however, the MLC phosphorylation ratio did not increase (Figure 38B and C).

#### 3.2.5.2 MLCK overexpression did not correct defective cytokinesis in oral cancer cells

I observed the presence of multinucleated oral cancer cells with MLCK-EGFP overexpression (Figure 38B). Consistent with no increase of MLC phosphorylation, I found no reduction, and even a slight increase in multinucleation (Figure 39B). Furthermore, there was no change in the frequency of cytokinesis failure or contractile ring defects, even though the MLCK-EGFP was overexpressed in these oral cancer cells (Figure 39C). This suggested that

Figure 38

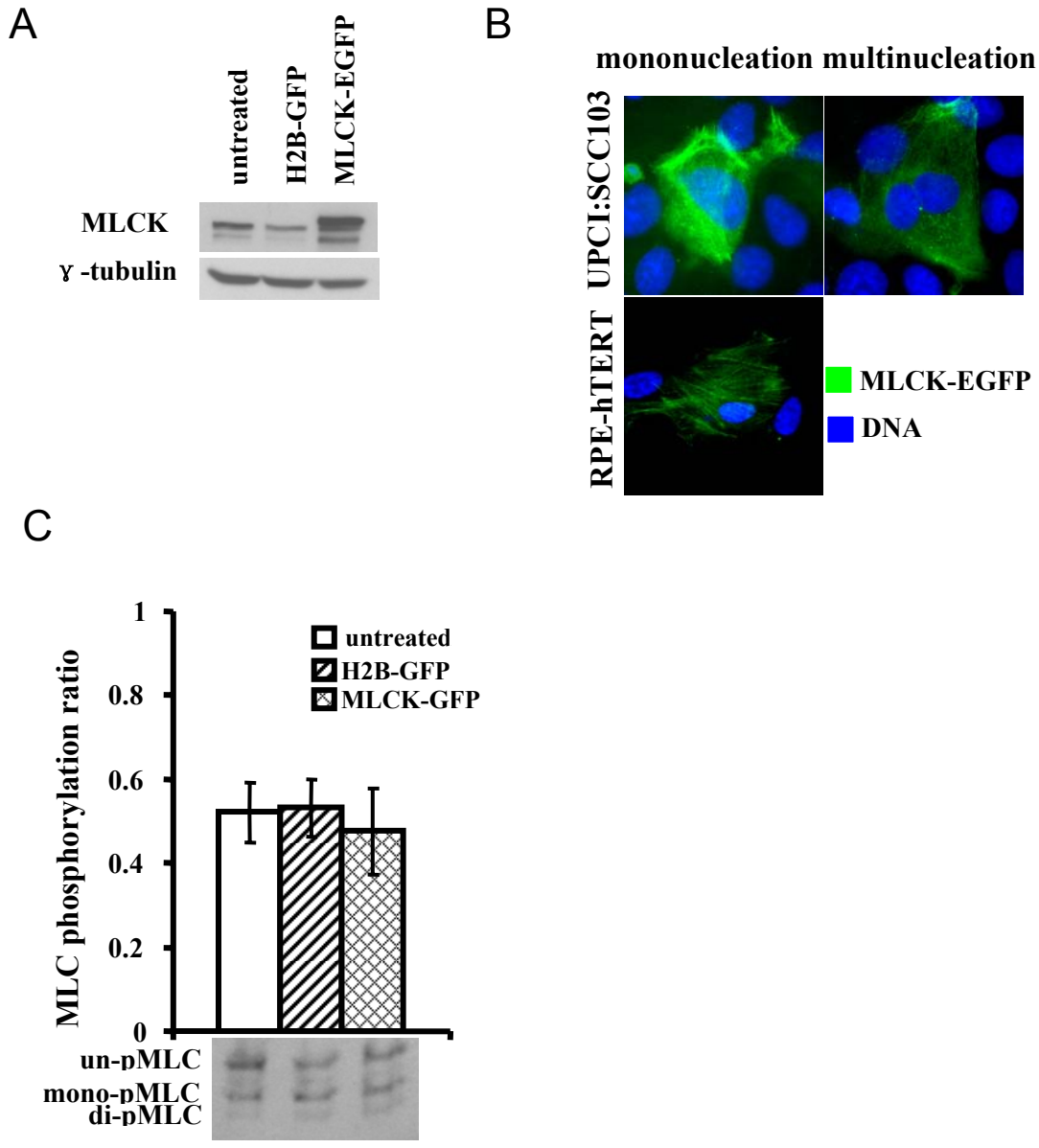
A
untreated
H2B-GFP
MLCK-EGFP
MLCK
γ -tubulin
B
mononucleation multinucleation
UPC1:SCC103
RPE-hTERT
MLCK-EGFP
DNA
C
MLC phosphorylation ratio
1
0.8
0.6
0.4
0.2
0
untreated
H2B-GFP
MLCK-GFP
un-pMLC
mono-pMLC
di-pMLC

**Figure 38.** Overexpression of MLCK was not able to increase MLC phosphorylation in oral cancer cells. (A) MLCK protein was overexpressed in UPCI:SCC103 cells. (B) MLCK-EGFP was expressed in UPCI:SCC103 and RPE-hTERT cells. Mononucleated and multinucleated cells were observed in MLCK-EGFP expressed UPCI:SCC103 cells. (C) MLC phosphorylation ratio was unchanged after MLCK overexpression in UPCI:SCC103 cells. Data and error bars represent mean and standard deviation of more than three different experiments, respectively.

Figure 39

A

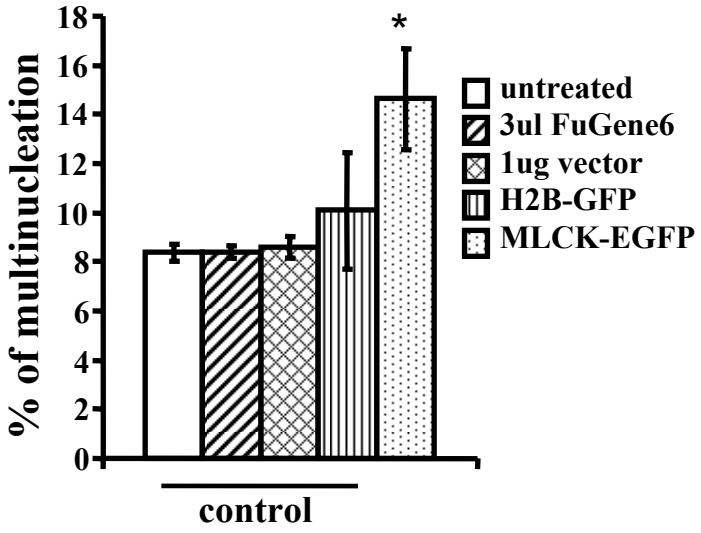
% of multinucleation
18
16
14
12
10
8
6
4
2
0
*
untreated
3ul FuGene6
1ug vector
H2B-GFP
MLCK-EGFP
control

B

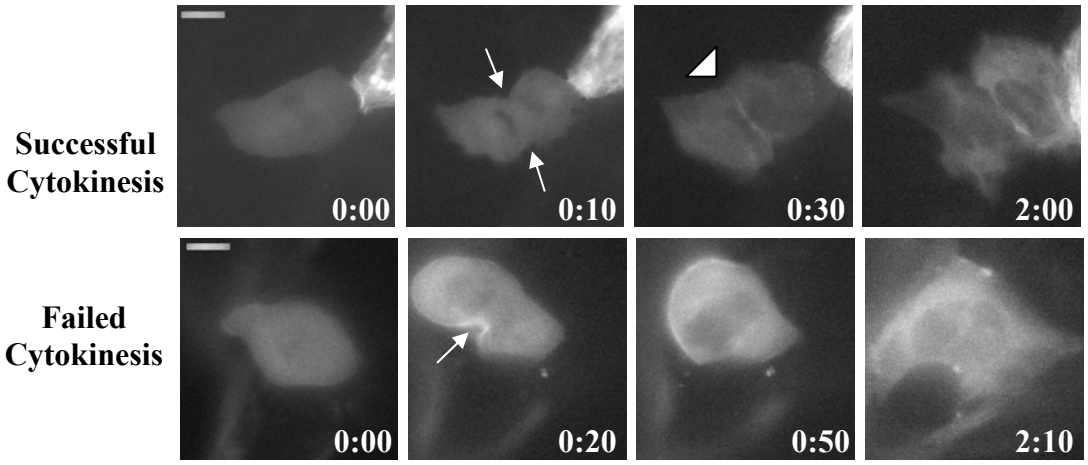
Successful Cytokinesis
0:00
0:10
0:30
2:00
Failed Cytokinesis
0:00
0:20
0:50
2:10

**Figure 39.** Overexpression of MLCK did not rescue the cytokinesis defects in oral cancer cells. (A) The multinucleation frequency slightly increased after MLCK overexpression in UPCI:SCC103 cells. Cells were treated with transfection reagent alone or DNA only or H2B-GFP plasmid as controls. Data and error bars represent mean and standard deviation of more than three different experiments, respectively.(B) The deficiency of cleavage furrow formation was not rescued by MLCK overexpression in UPCI:SCC103 cells. UPCI:SCC103 cells were transfected with MLCK-EGFP plasmids and bipolar cell divisions were followed by live cell imaging. Arrows: cleavage furrows; Arrowheads: contractile rings; Time: hours: minutes; bar: 1μm.

Figure 40

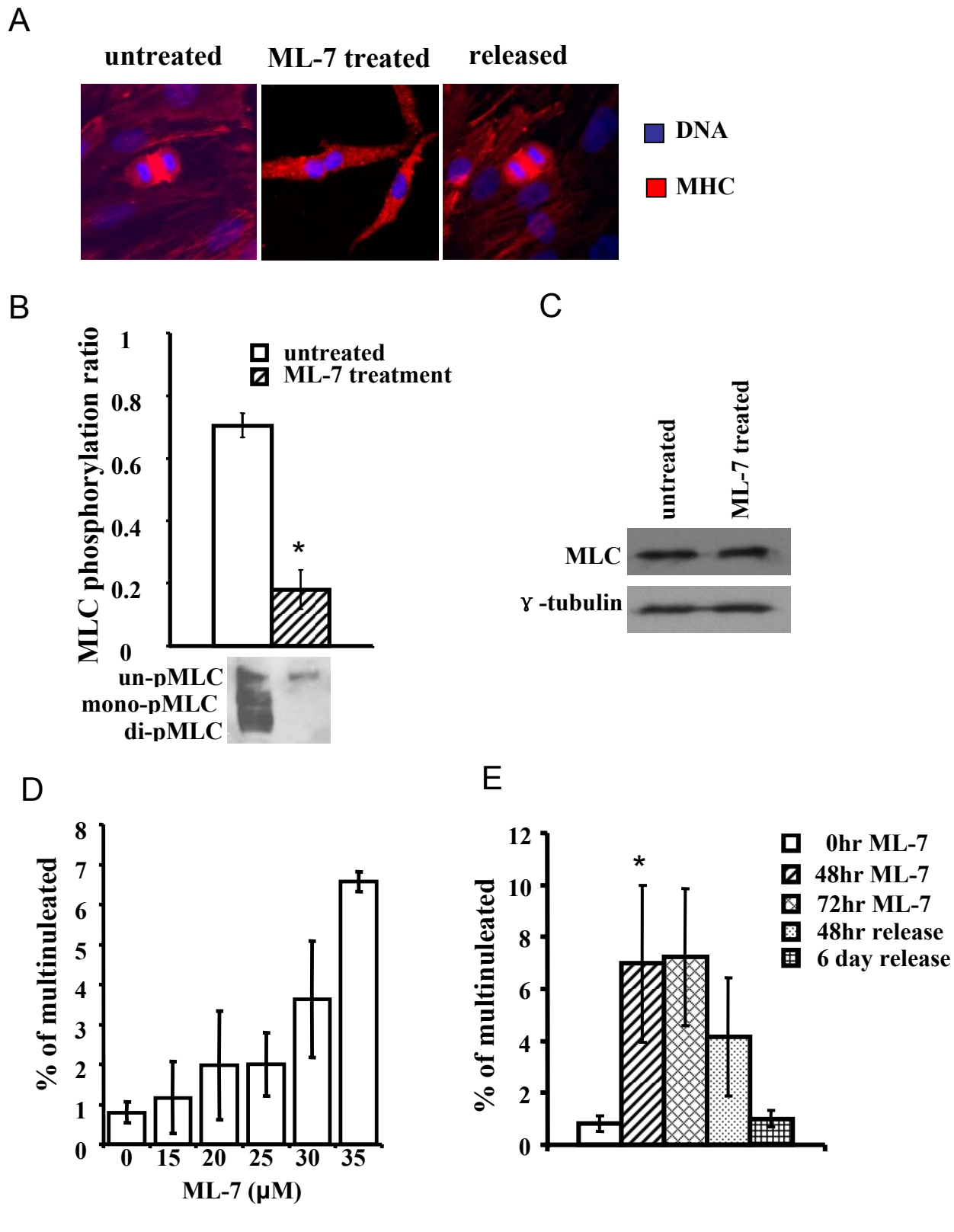
A
untreated
ML-7 treated
released
DNA
MHC
B
MLC phosphorylation ratio
1
0.8
0.6
0.4
0.2
0
untreated
ML-7 treatment
*
un-pMLC
mono-pMLC
di-pMLC
C
untreated
ML-7 treated
MLC
ɣ -tubulin
D
% of multinuleated
8
7
6
5
4
3
2
1
0
0
15
20
25
30
35
ML-7 (μM)
E
% of multinuleated
12
10
8
6
4
2
0
*
0hr ML-7
48hr ML-7
72hr ML-7
48hr release
6 day release

**Figure 40.** Multinucleation increased by ML-7 treatment in normal cells. (A) Actin-myosin filaments were destroyed by 3μM ML-7 treatment after 48 hours and restored after 48 hr release. (B) MLC phosphorylation ratio was reduced after 48-hour 35μM ML-7 in RPE-hTERT cells (*$p < 0.01$). Cells were treated with 35μM ML-7 for 48 hours and MLC phosphorylation was detected by urea glycerol gel. (C) MLC expression level did not decrease after 48-hour 35μM ML-7 treatment in RPE-hTERT cells. (D) Multinucleation frequency increased after 48 hr ML-7 treatment at different concentrations. (E) Multinucleation frequency increased after ML-7 treatment and recovers after release (*$p < 0.005$). Data and error bars represent mean and standard deviation of more than three different experiments, respectively.

MLCK might be inhibited in UPCI:SCC103 cells. To confirm this hypothesis, equal amounts of endogenous MLCK were immunoprecipitated from UPCI:SCC103 and RPE-hTERT cells and MLCK activity was compared *in vitro*. The MLCK activity in oral cancer cells was lower than normal cells, indicating that MLCK was inhibited in UPCI:SCC103 cells. The mechanism is currently under investigation (unpublished data, Sahasrabudhe and Saunders).

#### 3.2.5.3 MLCK inhibition in normal cells resulted in multinucleation

To examine if MLCK inhibition is sufficient to block cytokinesis completion in non-malignant cells, RPE-hTERT cells were treated with ML-7, a specific inhibitor of MLCK. A low dosage of 15μM of ML-7 could induce an accumulation of multinucleated cells in RPE-hTERT cells. As ML-7 concentration increased, multinucleation frequency increased up to 6.6% by 35μM ML-7 treatment for 48 hours (Figure 40D). Stress fibers disappeared and MLC phosphorylation decreased sharply (Figure 40A middle panel and Figure 40B), which was not due to reduced expression of endogenous MLC (Figure 40C). Furthermore, if RPE-hTERT cells were treated with 35μM ML-7 for different periods of time, the multinucleation approximately increased to 7% after 48- and 72-hour ML-7 treatment (Figure 40E, $p<0.005$). This phenotype was reversed when the RPE-hTERT cells were released after 72-hour of treatment (Figure 40A right panel and Figure 40E). These results confirmed that a reduction on MLCK activity could reproduce the MLC phosphorylation defects and multinucleation in normal cells to a comparable level as malignant cells.

## 3.3 DISCUSSION

Polyploidy is an important characteristic of major solid tumor tissues and tumor-derived cells (Lemez et al., 1998; Lothschutz et al., 2002; Olaharski et al., 2006; Park et al., 1995; Shi and King, 2005; Takanishi et al., 1996). It has been shown that cytokinesis failure is a mechanism for the increased ploidy of oral carcinoma cells (see detail in Chapter II). The data presented here elaborate some of the molecular defects leading to cytokinesis failure in these and other cancer cell types. I conclude that the ratios of MLC phosphorylation are universally reduced, and this reduction is correlated to the increased multinucleation in the cancer cell lines tested in these studies (Figure 26B and Figure 27). Although my results show that MLC is able to be phosphorylated in oral cancer cells with normal timing at late anaphase and/or telophase, the phosphorylation of MLC in mitosis is reduced compared to normal cells (Figure 28). Furthermore, phosphomimetic MLC overexpression overcomes the endogenous defective MLC phosphorylation and rescues cytokinesis failure (Figure 30). When MLC phosphorylation is restored to normal levels by phosphatase knockdown, cytokinesis failure and multinucleation also decrease (Figure 33 and 34). Finally, the reduction of MLC phosphorylation by phosphatase overexpression or MLCK inhibition causes multinucleation and multipolar mitoses in nonmalignant cells (Figure 36A and Figure 40). These results demonstrate that decreased MLC phosphorylation is a necessary and sufficient cause of cytokinesis failure and subsequent multinucleation and multipolar division.

Interestingly, Ser19-phosphorylated MLC does not localize to the cleavage furrow in cancer cells despite the fact that myosin heavy chain still does concentrate normally at the same

position (Figure 29). DeBiasio et al. have found that myosin fibers flow to the equatorial plate during anaphase and form a network (DeBiasio et al., 1996). It also has been shown that phosphorylation of MLC is essential for maintenance and activity of myosin in the furrow but not for initial recruitment of myosin to the furrow in HeLa cells (Miyauchi et al., 2006). These observations suggest that the myosin can move to the metaphase plate, but the fibers are not contractive enough to complete cytokinesis due to reduced phosphorylation in the cancer cells. Consistent with this conclusion, I observe an increase frequency of cytokinesis failure in oral cancer cells after wild-type MLC is overexpressed (Figure 30D). I believe this could be caused by the availability of more MLCK substrate, resulting in further reduction of the MLC phosphorylation ratio.

Pellman and colleagues have shown that the tetraploid p53-null cells generate malignant myoepitheliomas in nude mice. They link cytokinesis failure to carcinogenesis for the first time *in vivo* (Fujiwara et al., 2005). However, how cytokinesis fails in cancer cells remains unclear. In this study, I propose a model of the mechanism for the accumulation of multinucleated cells (Figure 41). In normal cells, MLC phosphorylation is regulated by MLCK and myosin phosphatase at the appropriate time during the mitosis to ensure the completion of cytokinesis. If the balance of MLC phosphorylation is changed by MLCK inhibition or myosin phosphatase overexpression, cytokinesis fails early in division, leading to multinucleated cells. These cells inherit extra centrosomes leading to divide multipolarly in the next mitosis.

Figure 41

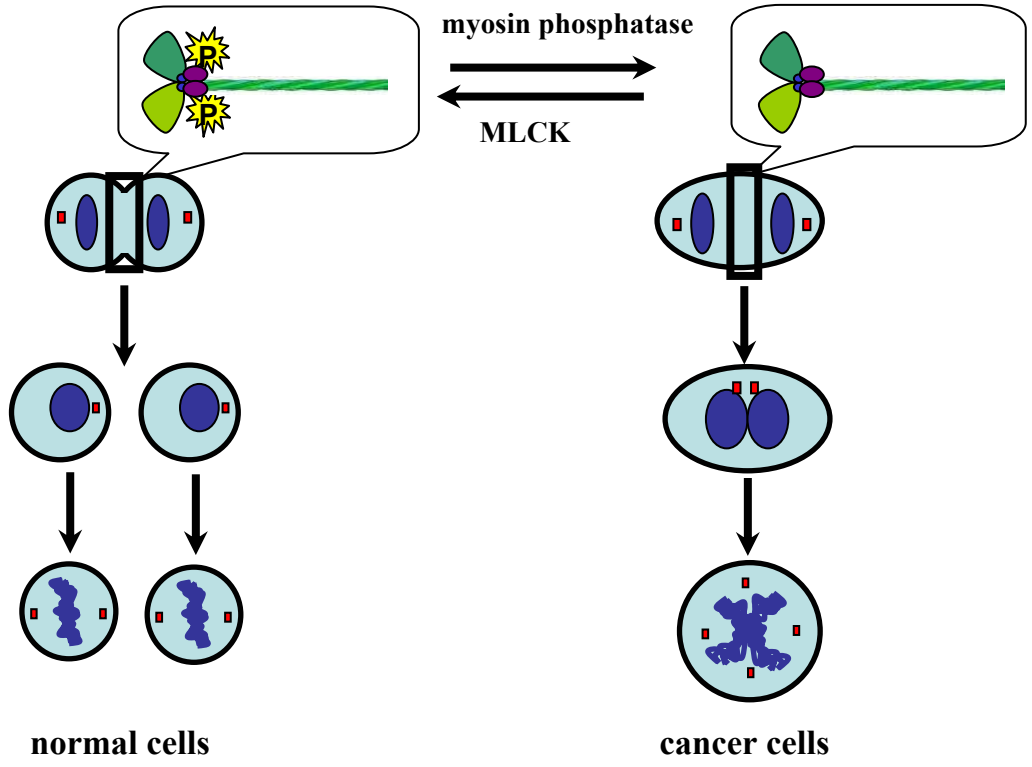


**Figure 41.** **A** model of the mechanism for the accumulation of multinucleated cells in cancer cells. In normal cells, MLC phosphorylation is regulated by MLCK and myosin phosphatase at the appropriate time during the mitosis to ensure the completion of cytokinesis. Theses cells divide bipolarly in the next cell cycle. In cancer cells, the balance of MLC phosphorylation is changed by MLCK inhibition or myosin phosphatase overexpression. Therefore, cytokinesis fails early in division, leading to multinucleated cells. These cells inherit extra centrosomes leading to multipolarity in the next mitosis.

Consistent with my observations, down-regulated MLCK transcription and expression is also observed in transformed cells and various tumor tissue samples (www.oncomine.org, (Rhodes et al., 2007; Schenker and Trueb, 1998; Van Eldik et al., 1984). Strikingly, I observe that not only the MLCK expression is low, but the MLCK activity is also inhibited in the tested cancer cells. How MLCK is inhibited in these cells is still under investigation. Resent studies have shown that Aurora B, which is usually overexpressed in cancer cells (Katayama et al., 2003), binds and phosphorylates MLCK *in vitro* (Dulyaninova and Bresnick, 2004). Additionally, MLCK can be phosphorylated and inhibited by p21-activated protein kinases (Conti and Adelstein, 1981; Goeckeler et al., 2000; Sanders et al., 1999). Therefore, both Aurora B and PAK are potential candidates of MLCK inhibitors involved in cytokinesis.

In the last decade, additional myosin light chain kinases including Rho-kinase and citron kinase have been shown to localize to the cleavage furrow (Amano et al., 1996; Eda et al., 2001; Kosako et al., 1999). However, I did not detect significant consistent differences of ROCK1 and citron kinase expressions in the tested cell lines (Figure 32 and data not shown). Moreover, I have also examined the RhoA expression, which is the activator of ROCK and citron kinase, and observed the same levels in cancer cells compared to normal cells (data not shown). But I can not rule out that the defective cytokinesis in cancer cells is also influenced by abnormal regulations of these kinases.

The activity of these kinases is balanced by myosin phosphatase, which also plays an important role in cytokinesis. The expression of MYPT1, the targeting subunit, varied in the

tested cells (Figure 4) and this is consistent with the microarrays results in different tumors (www.oncomine.org, Rhodes et al., 2007). When I increased the level of phosphorylated MLC in the MLCK-downregulation background by knockdown MYPT1, I rescued the cytokinesis failure in oral cancer cells. Thus, I conclude that the overexpression of MYPT1 in cancer cells is a cause of low MLC phosphorylation and cytokinesis failure. In addition to regulating MLC phosphorylation levels, MYPT1 may also play other roles in carcinogenesis. MYPT1 has been shown to interact with retinoblastoma protein (Rb) *in vitro* (Wu et al., 2005). There is a possibility that MYPT1 sequesters Rb to release transcription factor E2F and over-activate gene transcriptions. Furthermore, MYPT1 also binds to Tau and Map2 (microtubule associated proteins) and dephosphorylates Tau. The dephosphorylation increases Tau activity to promote microtubule assembly *in vitro* (Amano et al., 2003). Hence, overexpression of MYPT1 could also disrupt dynamic microtubules at the midbody, which is essential for vesicle fusion, at late cytokinesis, giving rise to multinucleation.

The apparent consequences of cytokinesis failure are doubled genetic material and centrosomes. It is known that supernumerary centrosomes lead to the formation of a multipolar spindle in the next cell division. Consistent with this, I observe a decrease of multipolar spindles after cytokinesis is rescued by depletion of myosin phosphatase in cancer cells (Figure 34E and Figure 35). Multipolar divisions are believed to contribute to chromosomal instability, and are associated with tumor formation and progression. My results suggest that a correction of cytokinesis defects could reduce genomic instability and possibly limit tumor development. Due to a common MLC phosphorylation defects in tested cancer cells, the upregulation of MLC phosphorylation could be a major target of cancer therapeutics. However, this is not that simple

because myosin activity functions in many aspects besides cytokinesis. Cancer cells may need high phosphorylation of MLC for invasiveness of metastasis, but low phosphorylation for abortive cytokinesis. In fact, I observe that phosphorylated MLC primarily localizes at cell periphery in the interphase and dis-localizes to the cleavage furrows during cytokinesis in oral cancer cells (Figure 29 and data not shown). It has been shown that ML-7 inhibits MLCK and prevents the growth of tumors in mice and rats. This prevention might be caused by less motility and adhesion due to decreased MLC phosphorylation and increased apoptosis (Gu et al., 2006; Kaneko et al., 2002; Tohtong et al., 2003). However, it is possible that therapeutic MLCK inhibition might also give rise to an increase in cytokinesis defects and aneuploidy, which would cause severe problems in long-term human treatment. In my studies, I have concluded that downregulation of myosin phosphatase rescues cytokinesis failure, possibly reducing aneuploidy in cancer cells. Interestingly, Xia et al. have shown that knockdown of MYPT1 in HeLa cells inhibit cell migration and adhesion (Xia et al., 2005). Taking these together, it suggests that inhibitors of MYPT1 could be valuable agents for cancer therapeutics.

# 4.0 CHAPTER IV: PROTEIN GPIB-A INDUCES TUMOREGENESIS BY CAUSING CYTOKINESIS FAILURE

## 4.1 INTRODUCTION

c-Myc, a proto-oncogene, encodes a transcription factor that activates expression of 15% of genes in genomes from flies to humans (reviewed in Dang et al., 2006). c-Myc regulates numerous biological events including cell proliferation, apoptosis, cell differentiation and stem cell self-renewal. c-Myc is very often found to be upregulated in many types of cancers and Myc overexpression leads to genomic instability (Li and Dang, 1999; Nesbit et al., 1999; Wade and Wahl, 2006; Yin et al., 1999). The Prochownik lab (Section of Hematology/Oncology, Children's Hospital of Pittsburgh) has identified one c-Myc target, MT-MC1, a nuclear protein with the unique ability to recapitulate multiple c-Myc functions (Yin et al., 2002). Recently, they focus studies on protein GpIbα, which is a common transcriptional and regulational target of c-Myc and MT-MC1 respectively.

GpIbα, a membrane glycoprotein, is expressed largely by megakaryocytes and platelets. GpIbα is an integral subunit of the von Willebrand factor receptor (vWFR) and is required for megakaryocytic differentiation, apoptosis, proliferation and endomitosis (Feng et al., 1999; Kanaji et al., 2004; Lepage et al., 2000) as well as platelet adhesion, aggregation and activation

(Lopez and Dong, 1997; Ruggeri, 1991). Li et al. have revealed that GpIbα is overexpressed in solid tumors and many tested cancer cell lines due to c-Myc upregulation (Li et al., 2007a; Li et al., 2007b). This overexpression induces tetraploidy and multinucleation in multiple normal cell lines. Interestingly, Rat1a-GpIbα (rat fibroblast cells with GpIbα overexpression) cells form colonies on soft agar and tumors in nude mice. Consistent with the proposed significance of tetraploidy, tetraploid Rat1a-GpIbα cells develop tumors more rapidly and of larger size than from diploid Rat1a-GpIbα cells. This is likely caused by enhanced cell growth and survival after GpIbα overexpression in Rat1a cells. Interestingly, in human primary HFF (human foreskin fibroblast) cells, GpIbα overexpression and p53 knockdown together (HFF-shp53-GpIbα cells) can induce a large increase in tetraploidy and multinucleation (Li et al., 2007a). In this report, I investigate how and why HFF-shp53-GpIbα cells become tetraploid.

In this chapter, I have demonstrated that cytokinesis failure is the primary cause of elevated tetraploidization in HFF-hTERT-shp53-GpIbα cells. When GpIbα is knocked down in HeLa and OS (osteosarcoma) cells, the frequency of multinucleation is reduced markedly, suggesting cytokinesis failure in different cancer cell types can be caused by GpIbα overexpression. In addition, chromosome segregational defects were reduced significantly, which may be a result of the restoration of normal cytokinesis in these GpIbα-knockdown cells. Further study disclosed that endogenous GpIbα proteins concentrated and colocalized with actin at the contractile rings. However, overexpressed GpIbα mislocalized from the contractile ring in p53 defective HFF cells 60% of the time, which might account for the abnormal cytoskeleton and division observed in these dividing cells. In conclusion, GpIbα has been shown for the first time here to play a role in cytokinesis possibly through regulating cytoskeleton rearrangements.

Taken together, the GpIbα-overexpression-induced cytokinesis failure through defective cytokinesis remodeling contributes to tetraploidization and genomic instability in tumorigenesis.

## 4.2 RESULTS

### 4.2.1 GpIbα overexpression caused cytokinesis failure and genomic instability

GpIbα overexpression with p53 knockdown in HFF cells induces a high frequency of tetraploidy and multinucleation (Li et al., 2007a and Figure 42A); and one of the mechanisms to induce multinucleation is cytokinesis failure (See Section 1.1.2.1 for details). Therefore, I first decided to examine whether cytokinesis was compromised in these cells.

#### 4.2.1.1 GpIbα overexpression caused cytokinesis failure

A series of HFF-hTERT (human foreskin fibroblast cells stably transformed with human telomerase reverse transcriptase) cell lines were used for this study, including HFF-hTERT-vector (cells stably expressing empty vector), HFF-hTERT-shp53 (p53 is stably suppressed by short hairpin RNA), HFF-hTERT-GpIbα (cells stably expressing GpIbα), and HFF-hTERT-shp53- GpIbα (cells stably expressing GpIbα and suppressing p53 expression) (Li et al., 2007a). I examined cell divisions by live DIC microscopy. Approximately 8.8% of cytokinesis failure was recorded in HFF-hTERT-shp53-GpIbα cells, but not in the other cell lines (Figure 42B and C), suggesting that defective cell division is the primary cause of tetraploid accumulation in

Figure 42

A

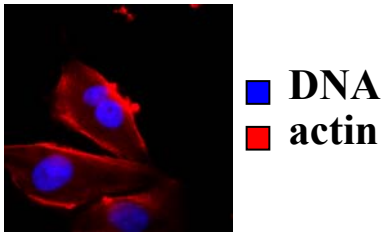
DNA
actin

B

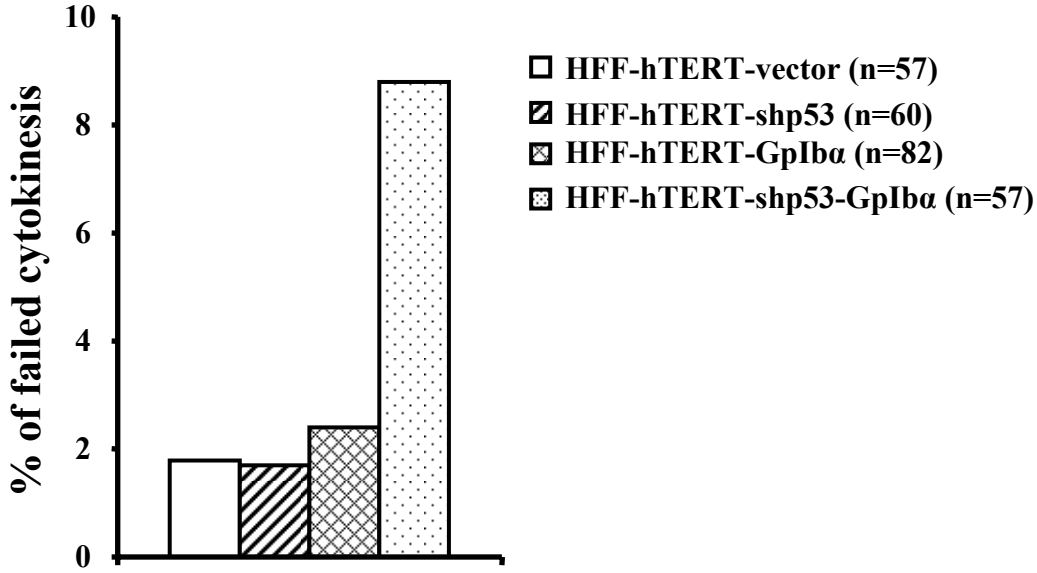
% of failed cytokinesis
0
2
4
6
8
10
HFF-hTERT-vector (n=57)
HFF-hTERT-shp53 (n=60)
HFF-hTERT-GpIbα (n=82)
HFF-hTERT-shp53-GpIbα (n=57)

C

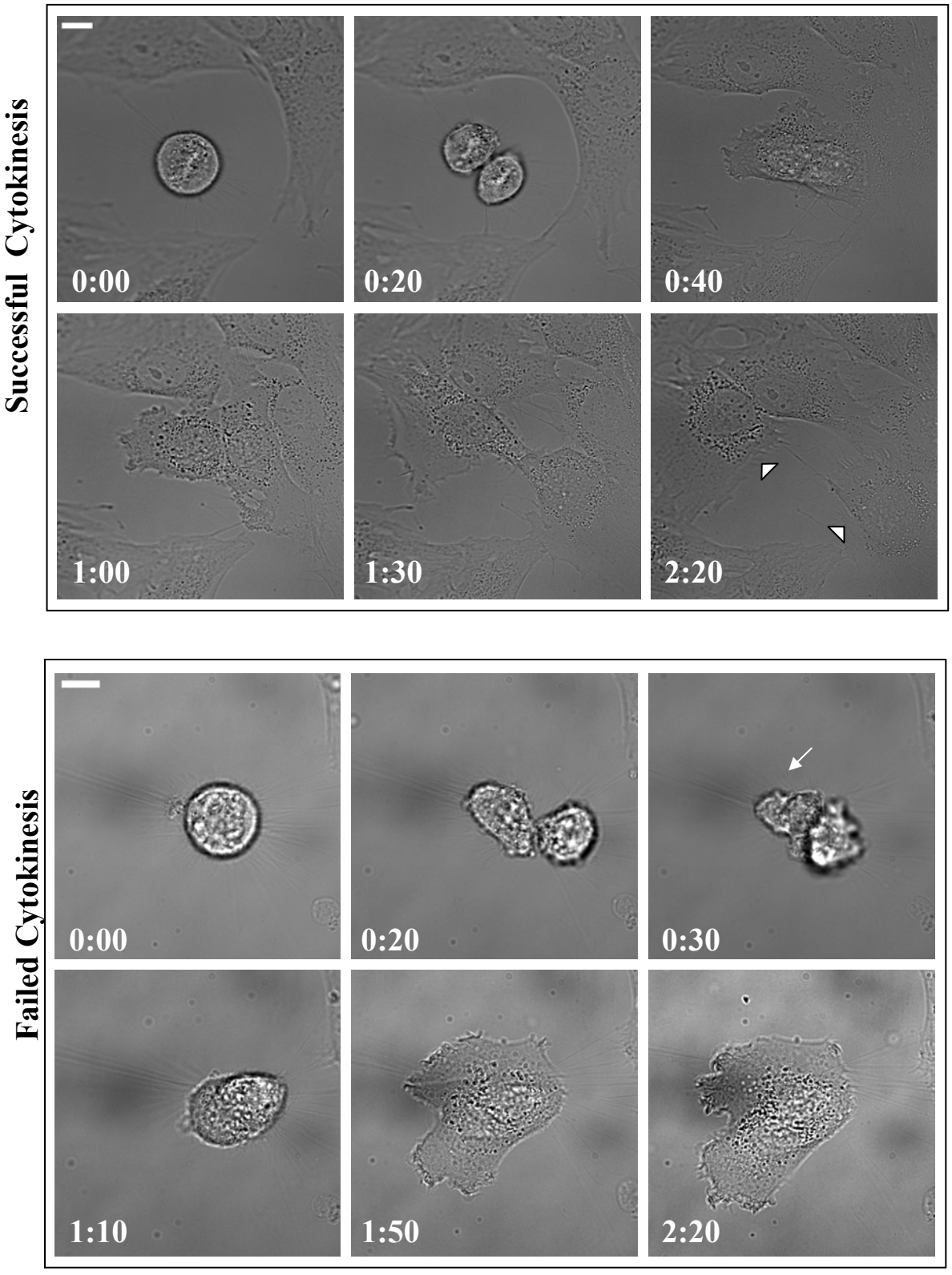
Successful Cytokinesis
0:00
0:20
0:40
1:00
1:30
2:20
Failed Cytokinesis
0:00
0:20
0:30
1:10
1:50
2:20

**Figure 42.** Overexpression of GpIbα led to cytokinesis failure in p53-knockdown HFF cells. (A) Multinuleated cells are observed in HFF-hTERT-shp53-GpIbα cells. DNA and actin are shown in blue and red respectively. (B) Cytokinesis fails at a high frequency in HFF-hTERT-shp53-GpIbα cells. Bipolar cell division is followed by live DIC optics. (C) Examples of successful and failed cytokinesis in HFF-hTERT-shp53-GpIbα cells. Top: The cell divides and daughter cells (arrowheads) separate apart after 2 hours and 20 minutes. Bottom: The cell fails in division and produces a binucleated daughter cell after 2 hours and 20 minutes. Arrowhead indicates abnormal blebbed cytoskeleton in the dividing cell. Time: hours: minutes; bar: 1μm.

these cells. In the cases of defective cytokinesis in HFF-hTERT-shp53-GpIbα cells, I observed abnormal shapes of the cell cortex (Figure 42C arrow). This suggests that the actin cytoskeleton rearrangement might be defective resulting in abortive cytokinesis.

#### 4.2.1.2 Cytokinesis failure and genomic instability decreased after GpIbα knockdown in cancer cells

GpIbα is widely overexpressed in a variety of tumors and tumor cell lines (Li et al., 2007a; Li et al., 2007b). GpIbα overexpression gives rise to tetraploidy in many tested cell lines and leads to genomic instability in HFF cells. Here, I want to address a question whether suppressing GpIbα could reduce cytokinesis failure and genomic instability in cancer cells. GpIbα proteins were stably knocked down at mRNA and protein levels by short hairpin RNA in HeLa cells (HeLa-shGpIbα) and Osteosarcoma cells (OS- shGpIbα) (Figure 43A and not shown). As expected, multinucleation was greatly reduced in these two cell lines (Figure 43B and C, $p<0.01$), suggesting that the cytokinesis failure was rescued. In addition, the chromosome segregational defects, including lagging chromosomes, anaphase bridges, micronuclei and multipolar mitoses, also decreased after GpIbα was knocked down in HeLa and OS cells (Figure 43B). Consistently, less colony formation was observed in HeLa-shGpIbα and OS-shGpIbα cells in softer agar assays (unpublished data, Li and Prochownik). Taken together, genomic destabilization can be partially, but significantly, corrected by inhibition of GpIbα in cancer cells.

Figure 43

A

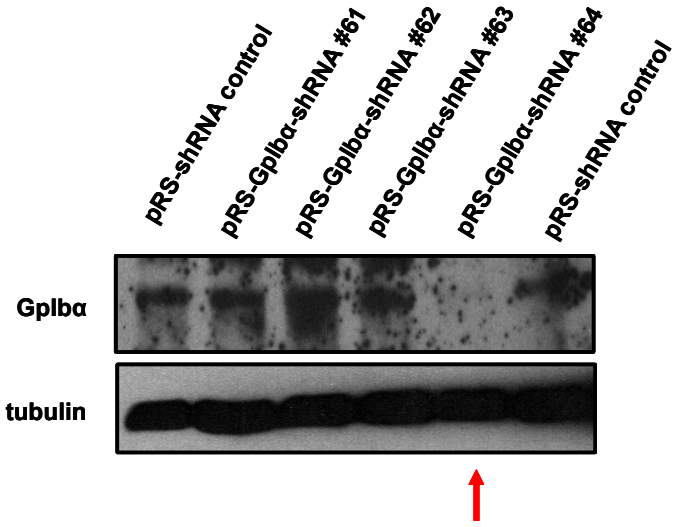


| | Value of Gplbα/GADPH |
|---|---|
| HeLa-vector | 5.36E-3 |
| HeLa-shGplbα | 2.32E-3 |

B

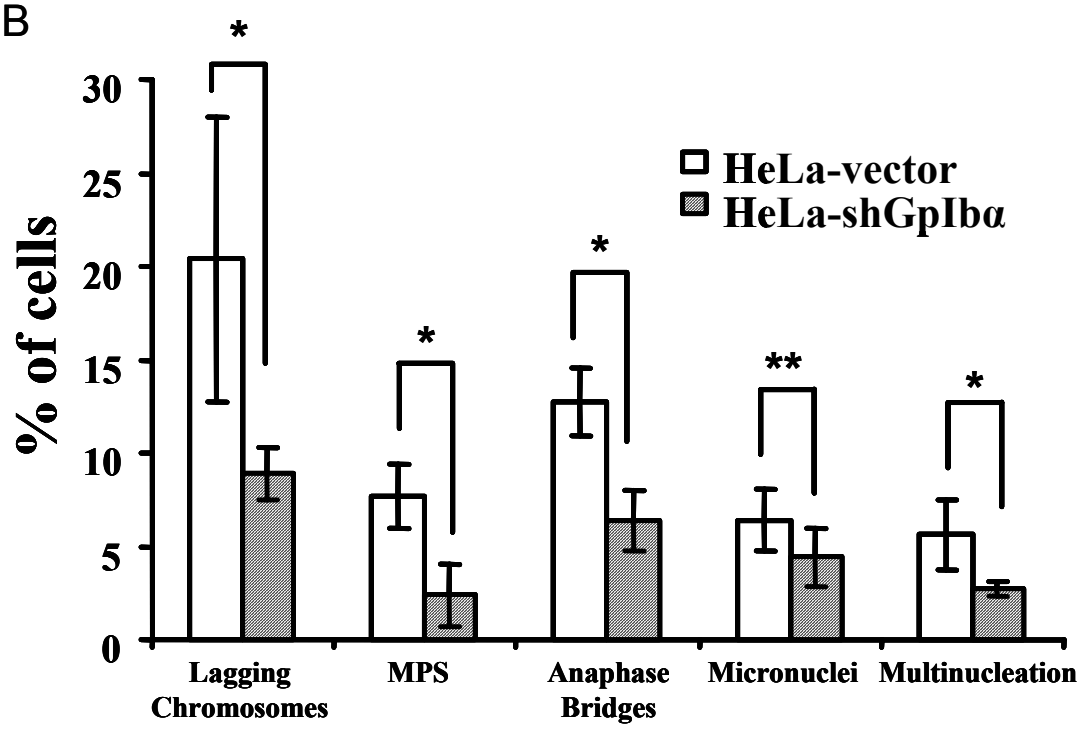

C

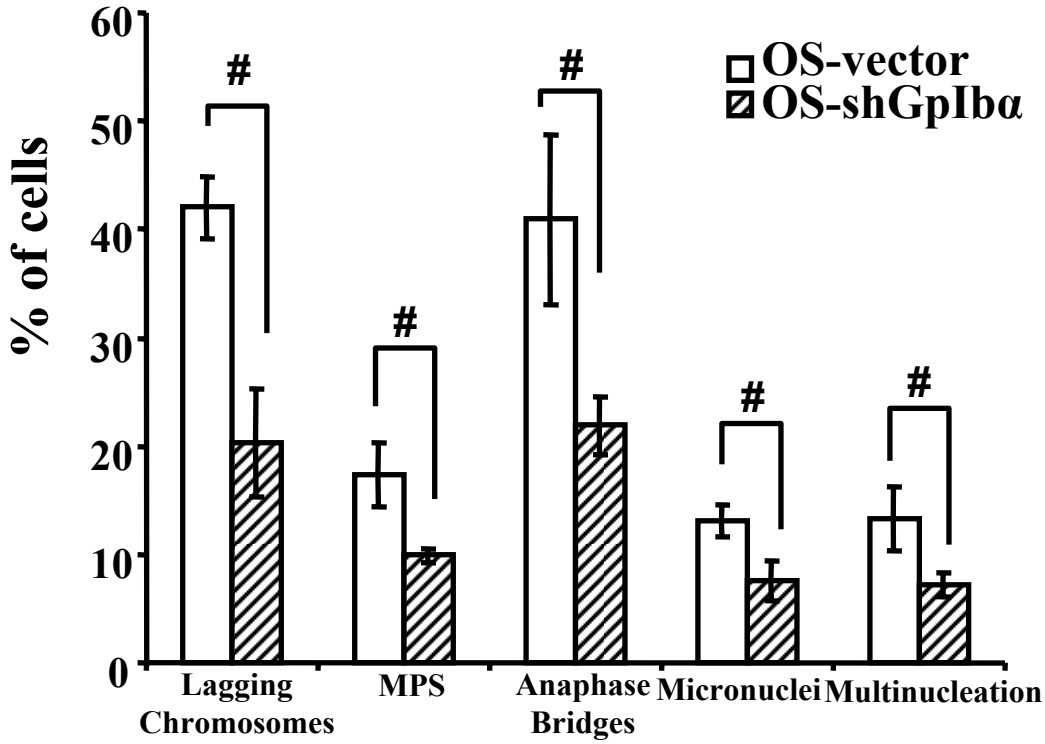


**Figure 43.** GpIbα knockdown reduces multinucleation and chromosomal instability in HeLa and OS cells. (A) GpIbα is stably knocked down by short hairpin RNA in HeLa cells. Different siRNA sequences were used to knock down GpIbα in HeLa cells. Reduced GpIbα protein expression and mRNA transcription levels were detected by immunoblotting and quantitative RT-PCR in a clone from siRNA sequence 64 (Experiments and Figure were done by Dr. Youjun Li and Dr. Edward Prochownik). (B) and (C) Multinucleation and chromosomal instability decrease in (B) HeLa cells and (C) OS cells with GpIbα knockdown (*$p<0.01$, **$p<0.07$, #$p<0.01$). Frequencies of lagging chromosomes, MPS, anaphase bridges, micronuclei and multinucleation were counted in HeLa-vector and HeLa-shGpIbα cells. Data and error bars represent mean and standard deviation of three different experiments, respectively.

### 4.2.2 GpIbα might play a role in cytokinesis

How does GpIbα function in cytokinesis? It is known that GpIbα is one subunit of the von Willebrand factor receptor presents on the surface of platelet. Its extracellular domain binds von Willebrand factor and thrombin, while its intracellular domain associates tightly with the cytoskeleton through the actin-binding protein filamin (Meyer et al., 1997; Xu et al., 1998). Since actin plays a critical role in cytokinesis, therefore, I hypothesized that GpIbα functions in cytokinesis through regulating cytoskeleton remodeling.

#### 4.2.2.1 GpIbα localized at the cleavage furrow and mis-localized by overexpression

To test this hypothesis, GpIbα localization was evaluated by immunofluorescence in HFF cells. Interestingly, GpIbα did not localize to the cell membrane, but was found in the cytoplasm in interphase cells. In late mitosis, GpIbα concentrated at the contractile ring in the midzone, colocalizing with actin in HFF-hTERT-vector cells (Figure 44A top penal and Figure 45A). Surprisingly, GpIbα was missing from the contractile rings in HFF cells with GpIbα overexpression and p53 knockdown (Figure 44A, bottom panel), which occurred in about 60% of all the anaphase cells I observed (Figure 44B). Exogenously overexpressed GpIbα localized normally in most cells (Figure 44B). These data indicate that overexpressed GpIbα is mis-localized from the contractile ring in a p53-dependent manner, which may be a cause of cytokinesis failure in HFF-hTERT-shp53- GpIbα cells.

Figure 44

A

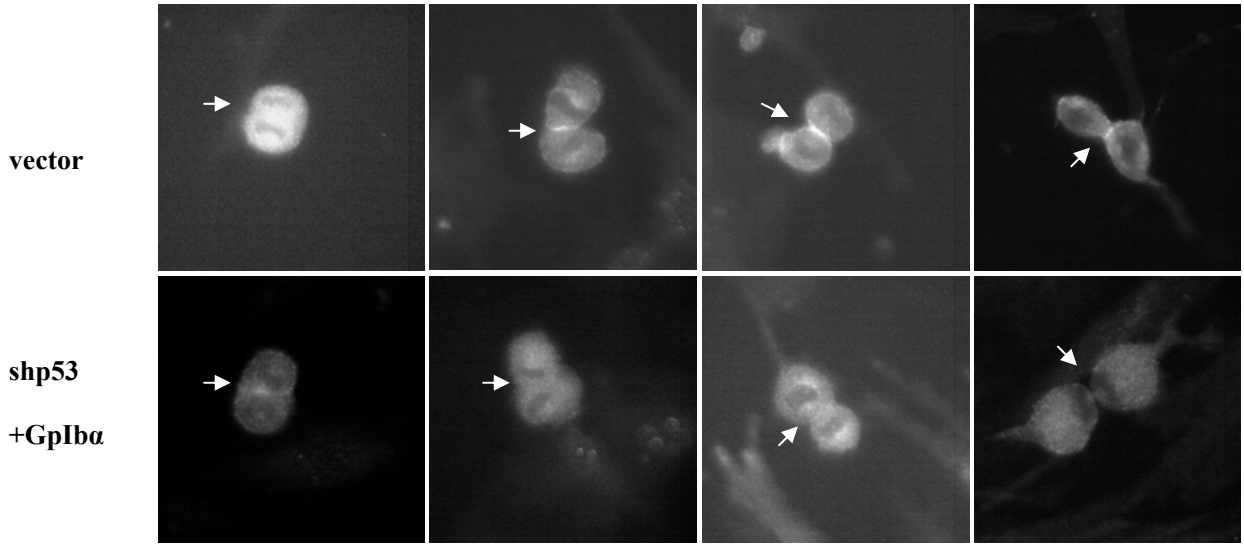
vector
shp53
+GpIbα

B

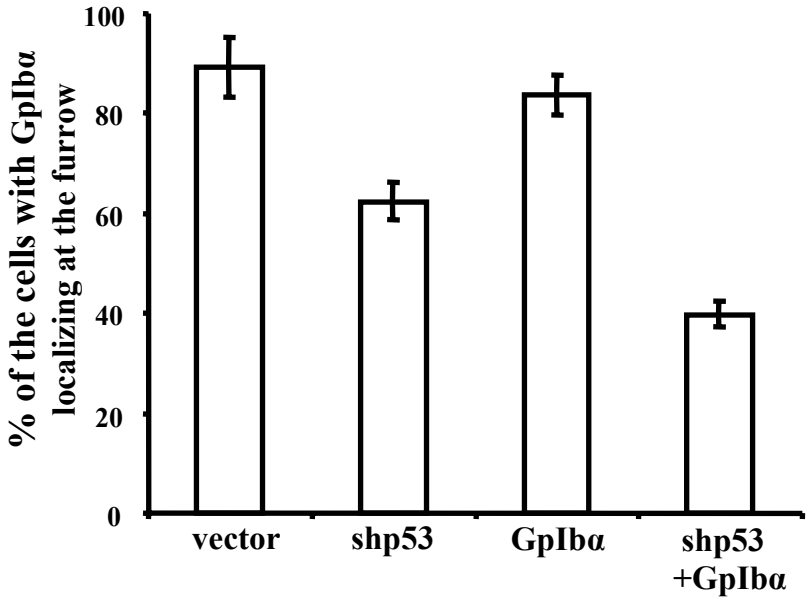
% of the cells with GpIbα localizing at the furrow
100
80
60
40
20
0
vector
shp53
GpIbα
shp53 +GpIbα

**Figure 44.** GpIbα localized to the contractile ring in HFF-hTERT-vector cells but not HFF-hTERT-shp53-GpIbα cells. (A) GpIbα accumulated at the contractile rings during cytokinesis in HFF-hTERT-vector cells, but this specific localization disappeared when GpIbα was overexpressed and p53 was knocked down (arrows). (B) Quantifications of GpIbα localization at the contractile rings in four types of HFF cells. Data and error bars represent mean and standard deviation of three different experiments, respectively.

Figure 45

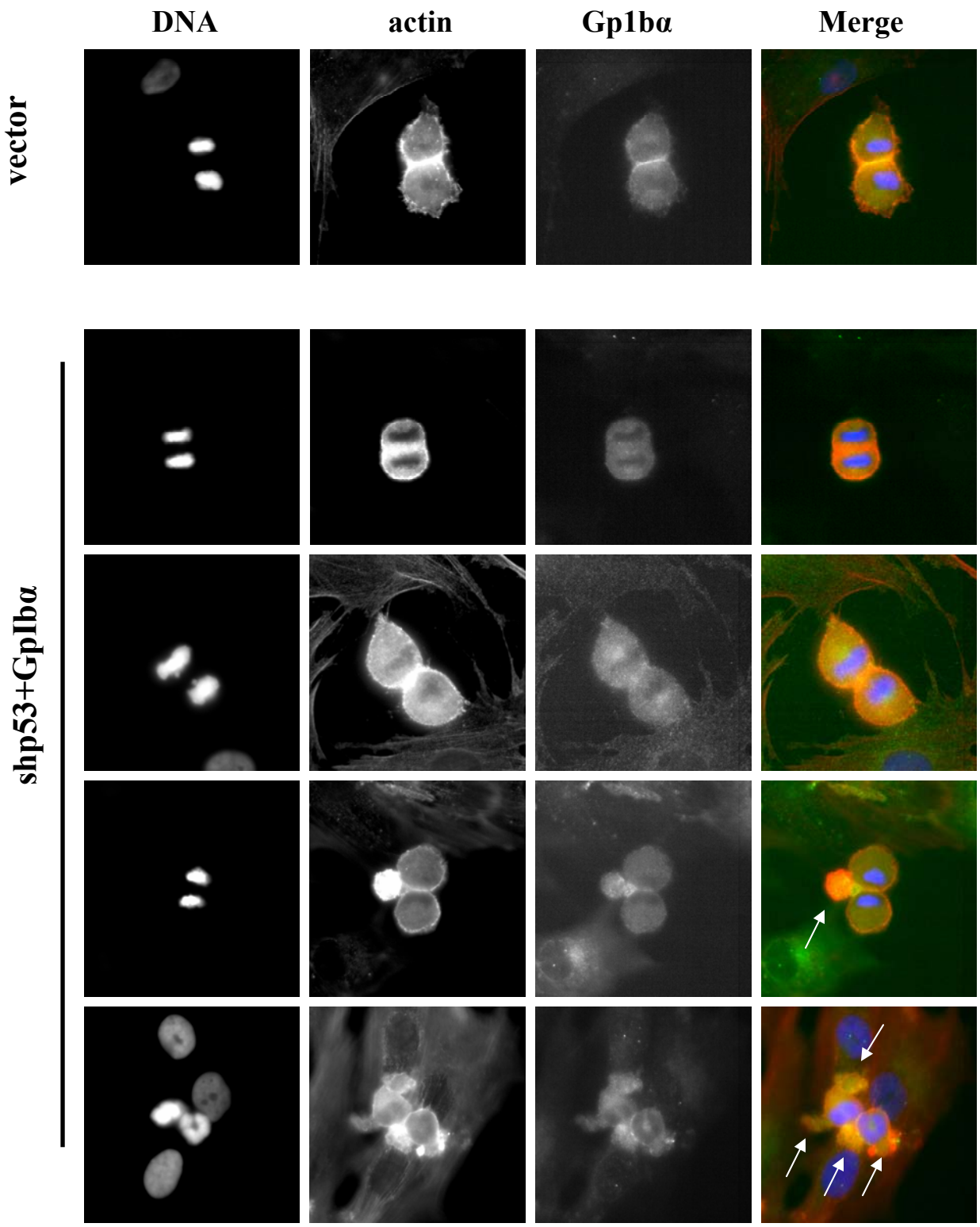

**Figure 45.** GpIbα colocalized with actin perfectly at the contractile rings in HFF-hTERT-vector cells, but not in HFF-hTERT-shp53-GpIbα cells. (A) GpIbα concentrated at the contractile rings along with actin in HFF-hTERT-vector cells. In the merge column, actin and GpIbα are shown in red and green respectively. (B) Actin accumulated at abnormal sites on the cell cortex when GpIbα was missing from the contractile rings in HFF-hTERT-shp53-GpIbα cells (arrows). In the merge column, actin and GpIbα are shown in red and green, respectively.

Figure 46

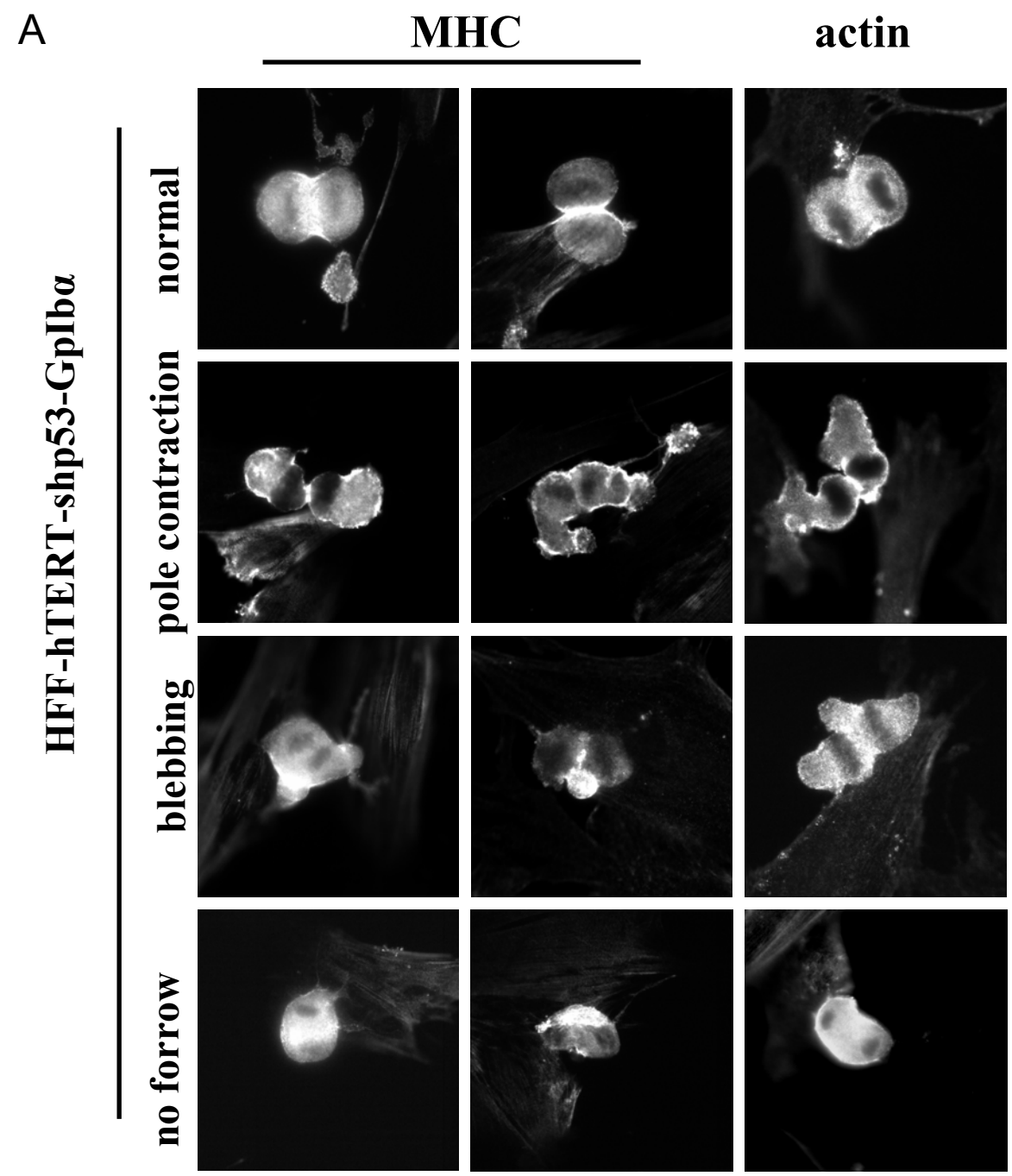
A
MHC
actin
HFF-hTERT-shp53-GpIbα
normal
pole contraction
blebbing
no forrow

B

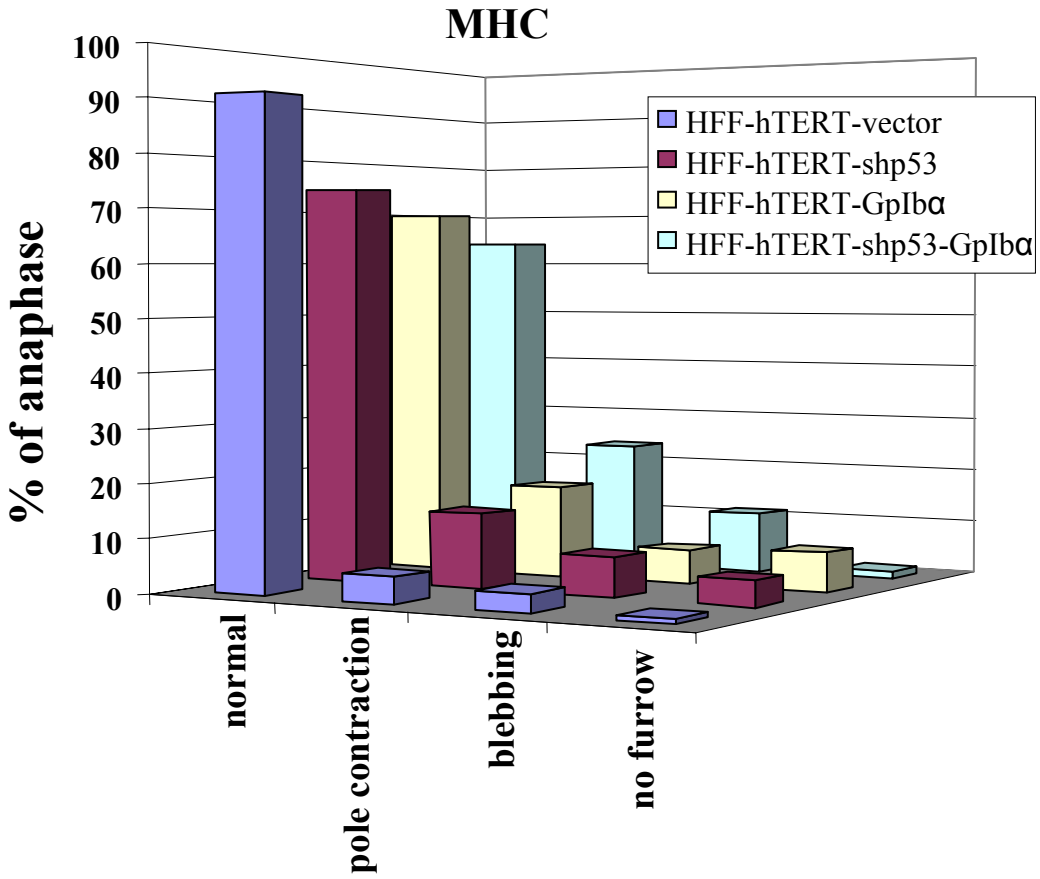
MHC
% of anaphase
100
90
80
70
60
50
40
30
20
10
0
HFF-hTERT-vector
HFF-hTERT-shp53
HFF-hTERT-GpIbα
HFF-hTERT-shp53-GpIbα
normal
pole contraction
blebbing
no furrow

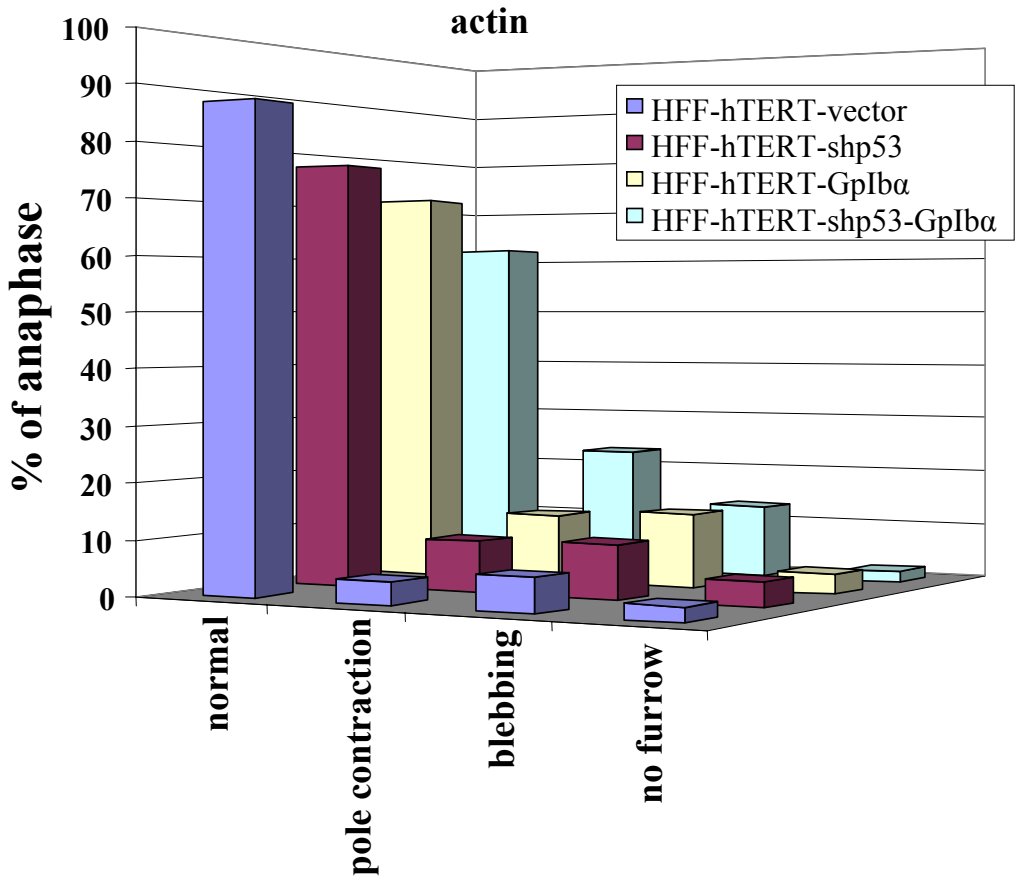
actin
% of anaphase
100
90
80
70
60
50
40
30
20
10
0
HFF-hTERT-vector
HFF-hTERT-shp53
HFF-hTERT-GpIbα
HFF-hTERT-shp53-GpIbα
normal
pole contraction
blebbing
no furrow

**Figure 46.** Abnormal cytoskeleton was observed in HFF-hTERT-shp53-GpIbα cells. (A) The cytoskeleton is labeled with MHC or actin by immunofluorescence in HFF-hTERT-shp53-GpIbα cells. Three major types of cortex abnormalities were recorded as pole contraction, blebbing or no furrow. (B) The frequency of cytoskeleton abnormalities increased in HFF-hTERT-shp53-GpIbα cells. Quantifications of the frequencies of cytoskeleton abnormalities in HFF cells. Assays based on MHC and actin stain are shown on the top and bottom panels respectively. Bars stand for means of three different experiments. Means and standard deviations data are shown in the following tables (Table 2 and 3).

**Table 2.** Cytoskeleton morphology in HFF cells detected by MHC antibody.

| | | normal | pole contraction | blebbing | no furrow |
|---|---|---|---|---|---|
| HFF-hTERT-vector | avg (%) | 90.93 | 4.80 | 3.43 | 0.83 |
| | stdv (%) | 10.45 | 4.19 | 5.95 | 1.44 |
| HFF-hTERT-shp53 | avg (%) | 73.97 | 13.90 | 7.40 | 4.73 |
| | stdv (%) | 20.07 | 12.21 | 8.38 | 4.70 |
| HFF-hTERT-GpIbα | avg (%) | 69.43 | 17.10 | 6.27 | 7.20 |
| | stdv (%) | 27.09 | 18.30 | 9.34 | 7.96 |
| HFF-hTERT-shp53-GpIbα | avg (%) | 63.93 | 23.53 | 11.17 | 1.37 |
| | stdv (%) | 20.15 | 11.17 | 9.76 | 1.17 |

**Table 3.** Cytoskeleton morphology in HFF cells detected by actin antibody.

| | | normal | pole contraction | blebbing | no furrow |
|---|---|---|---|---|---|
| HFF-hTERT-vector | avg (%) | 87.17 | 4.17 | 6.10 | 2.57 |
| | stdv (%) | 7.92 | 1.67 | 7.36 | 3.16 |
| HFF-hTERT-shp53 | avg (%) | 76.73 | 9.20 | 9.67 | 4.40 |
| | stdv (%) | 16.27 | 4.67 | 9.46 | 3.82 |
| HFF-hTERT-GpIbα | avg (%) | 71.10 | 12.07 | 13.27 | 3.57 |
| | stdv (%) | 21.78 | 10.25 | 9.21 | 3.11 |
| HFF-hTERT-shp53-GpIbα | avg (%) | 62.03 | 22.87 | 13.10 | 2.03 |
| | stdv (%) | 12.80 | 8.55 | 5.21 | 1.10 |

#### 4.2.2.2 Cytoskeleton abnormalities in GpIbα overexpressing cells

Next I asked whether this GpIbα mislocalization changed the cytoskeleton morphology and resulted in cytokinesis failure in HFF-hTERT-shp53-GpIbα cells. In the live cell analysis, abnormal cytoskeleton was observed in HFF-hTERT-shp53-GpIbα cells (Figure 42C, arrows). Therefore, actin and MHC distributions were examined in HFF cells. In both immunofluorescence studies, abnormal cytoskeleton blebbing at the cleavage furrows and poles was detected at high frequencies in HFF-hTERT-shp53-GpIbα cells compared to control cells (Figure 46, Table 2 and Table 3). Interestingly, when GpIbα was overexpressed, actin colocalizes with GpIbα at the abnormal blebbing sites instead of the contractile rings during cytokinesis (Figure 45B). It suggests that contraction defects at the midzone could account for cytokinesis failure in these cells. To rule out these cytoskeleton abnormalities were the consequences (rather than the cause) of abortive cytokinesis, cytokinesis failure was induced by MLCK inhibition in control (HFF-hTERT-vector) cells. No blebbed cell cortex was observed, suggesting that blebbing at furrows and contraction at poles were not simply the result of defective cell division and could be a specific cause of failed cytokinesis by GpIbα overexpression (data not shown). In conclusion, it is very likely that overexpression of GpIbα in p53 defective HFF cells causes GpIbα disappearance from the contractile rings following with mislocalization of actin as well as abnormal cytoskeleton structures, possibly resulting in cytokinesis failure in these cells.

#### 4.2.2.3 GpIbα overexpression did not induce unfolded protein response (UPR) in HFF cells

Some, but not all of the overexpressed GpIbα accumulated in the endoplasmic reticulum (ER) (unpublished data, Li and Prochownik). Recently, some studies show that defective calcium channels in the ER cause improper contraction of oocyte division in *C. elegans* (personal

communication with Jayne M. Squirrell). In addition, unfolded protein response (UPR) activity is required for cytokinesis completion through maintaining ER homeostasis and capacity in yeast (Bicknell et al., 2007). Thus, I began to study whether the ER is functional in HFF-hTERT cells. The localization of calnexin, an integral chaperone protein of the ER, was examined first. Interestingly, aggregated calnexin stain was observed in HFF-hTERT-shp53 and HFF-hTERT-shp53-GpIbα cells, but not in HFF-hTERT-vector and HFF-hTERT-Gp1bα cells (Figure 47A top panel). However, another chaperone protein, Bip, localized properly in all the tested HFF cells (Figure 47A bottom panel). In addition, the structure of the Golgi apparatus was normal in these cells (Figure 47B). Taken together so far, GpIbα overexpression might accumulate in the ER, but did not cause any detected ER and Golgi dysfunction in the HFF cells. In addition, I treated HFF cells with DTT, which induces ER stress and activates the UPR. Increased sensitivity to DTT treatment was observed in HFF-hTERT-shp53 and HFF-hTERT-shp53-GpIbα cells, compared to vector alone (data not shown). However, UPR activities, evaluated by XBP1 mRNA splicing, were at the similar levels among four cell lines before and after DTT treatment (Figure 47C). In conclusion, neither GpIbα overexpression nor p53 down-regulation, caused ER dysfunction; neither did it activate the UPR pathway. At this time, I have no evidence that overexpression of GpIbα gives rise to the abnormal cytokinesis by affecting ER functions and UPR pathways.

#### 4.2.2.4 GpIbα overexpression did not effect endocytosis in cells

GpIbα is a transmembrane protein and appropriate membrane dynamics is required for cytokinesis completion. Therefore, endocytosis, a process that cells absorb material from the outside by engulfing it with their cell membrane, was detected in the HFF cells. Cells were treated by fluorescent labeled transferrin, and transferrin movements were recorded by live cell

imagining. Functional endocytosis was observed in all the HFF cells with or without GpIbα overexpression (Figure 48), indicating that GpIbα overexpression did not lead to cytokinesis failure by effecting endocytosis in HFF cells.

## 4.3 DISCUSSION

GpIbα, a membrane glycoprotein, is expressed largely in different cancer cells and tumor samples. Overexpression of GpIbα leads to tetraploid in normal human cells in a p53 knockdown background. In this report, I have investigated for the first time that GpIbα functions in cytokinesis possibly through regulating actin-directed cytoskeleton dynamics during cell division. Overexpression changes the GpIbα position at the cleavage furrow and gives rise to abnormal actin localization and contraction in the cell cortex during cytokinesis. This is very likely to be a cause of cytokinesis failure in some cancers.

Although excessive GpIbα accumulates in the cytoplasm and ER when it is overexpressed, this did not cause defective ER and UPR, which might lead to cytokinesis failure. Interestingly, Prochownik lab has shown that GpIbα localization across the membrane is required for tetraploid induction (Li et al., 2007a; Li et al., 2007b) . Moreover, recent study revealed that overexpression of GpIbα without filamin binding domain does not cause tetraploidy (unpublished data, Li and Prochownik), further proving my conclusion that the filamin-mediated

Figure 47

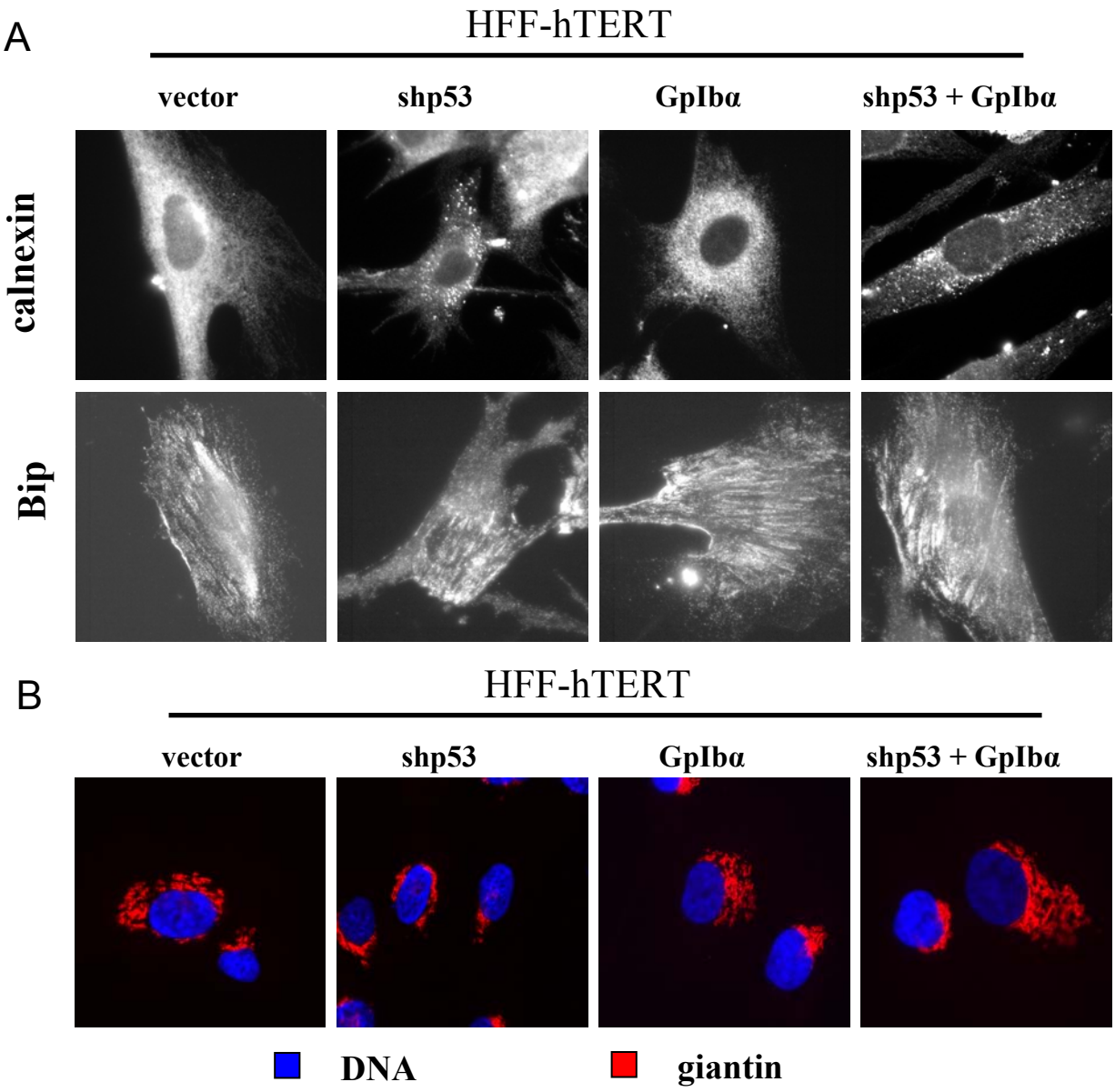
A
HFF-hTERT
vector
shp53
GpIbα
shp53 + GpIbα
calnexin
Bip
B
HFF-hTERT
vector
shp53
GpIbα
shp53 + GpIbα
DNA
giantin
C
HFF-hTERT
vector
shp53
GpIbα
shp53+ GpIbα
no primer control
2mM
- + - + - + - +
unspliced
spliced

**Figure 47.** GpIbα overexpression and/or p53 knockdown did not induce ER dysfunction and UPR in HFF cells. (A) Calnexin, but not Bip, accumulated in the ER in HFF-hTERT-shp53 and HFF-hTERT-shp53-GpIbα cells. Each type of HFF cell line was immuno-stained by calnexin and bip antibodies and viewed by epifluorescent microscope. (B) Golgi apparatus was normal in HFF cells as shown by anti-giantin antibodies. DNA and giantin are shown in blue and red respectively. (C) UPR pathway was normal and could be activated at the appropriate time. RT-PCR of XBP1 was performed in all four types of HFF cells with and without 2mM DTT treatment for 1 hour. UPR activity is evaluated by the ratio of spliced XBP1 mRNA.

Figure 48

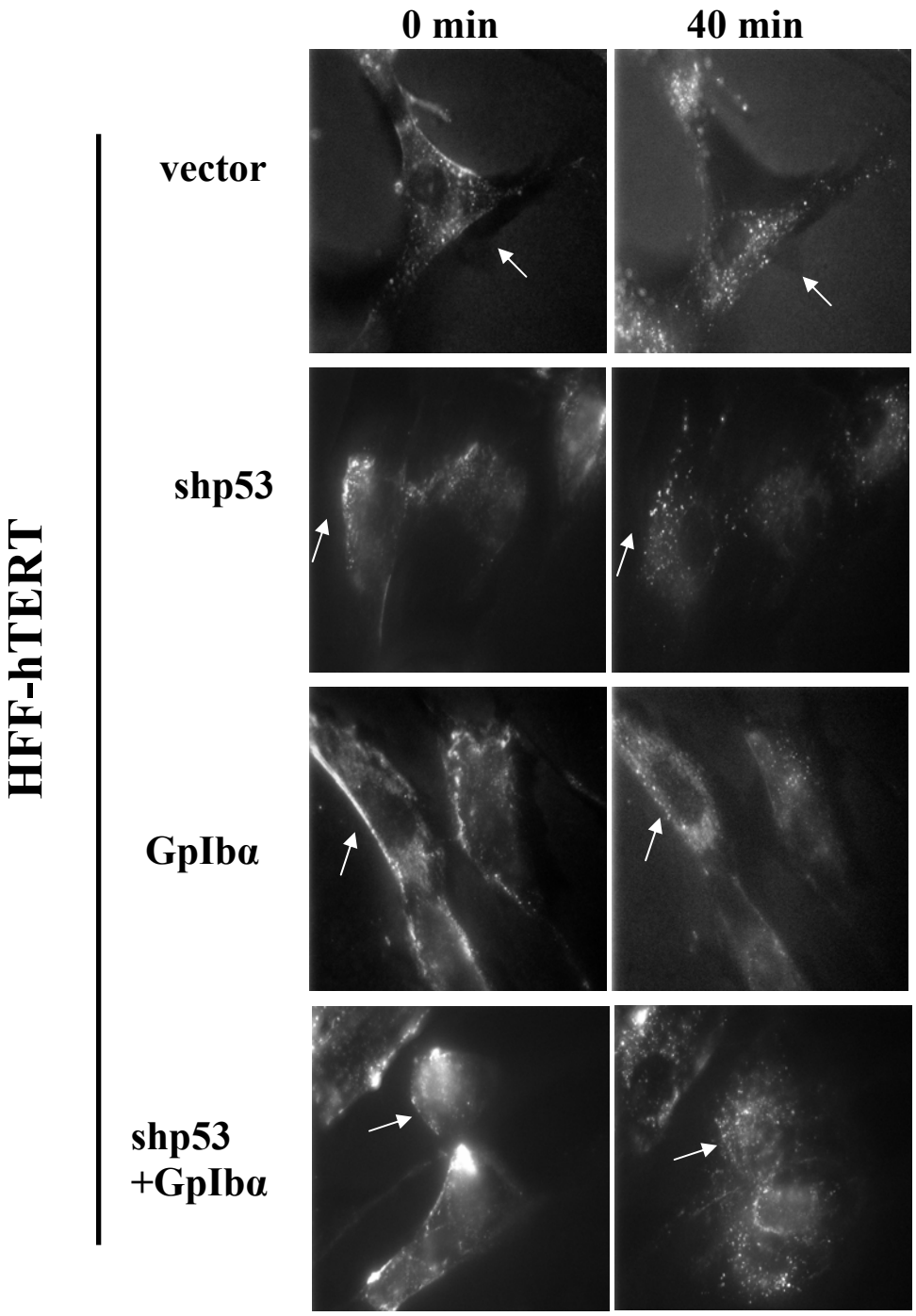

**Figure 48.** GpIbα overexpression and/or p53 knockdown did not affect endocytosis in HFF cells. All four types of HFF cells were incubated with FITC-transferrin. FITC-tranferrin loaded on the cell membrane and was engulfed into the cell after 40 minutes (arrows).

Figure 49

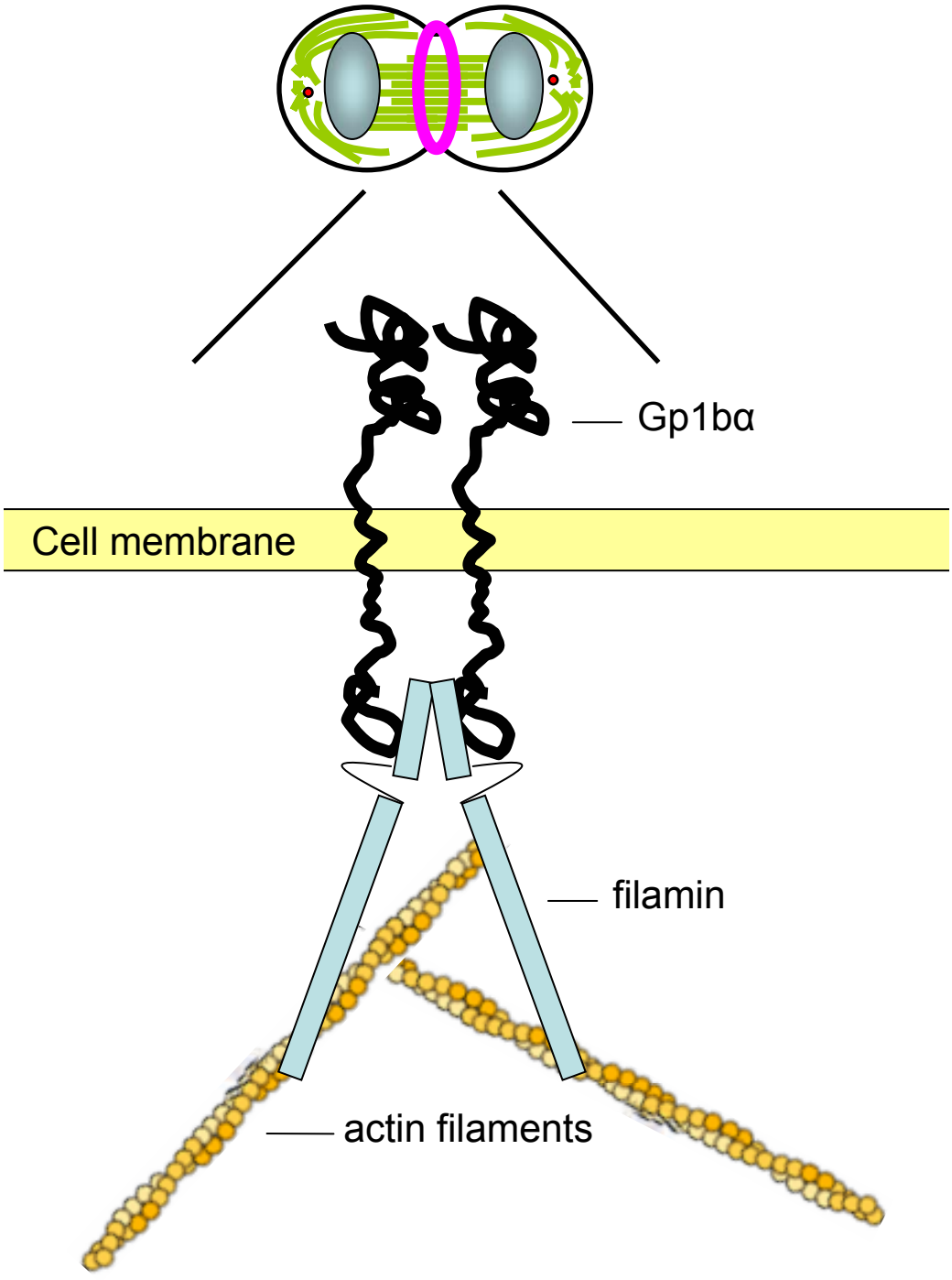

**Figure 49.** A model of how GpIbα regulates the actin cytoskeleton during cytokinesis. The cytoplasmic side of GpIbα (black) binds to dimerized filamin (light blue) at the C terminus. The N terminus of filamin associates with actin filaments (yellow) to promote actin-filament branching. In this manner, GpIbα may play a role at the contractile ring during cell division. Figure is adapted from (Stossel et al., 2001).

interaction of GpIbα and actin is important for cytokinesis regulation. Here, I propose a model of how GpIbα plays a role in cytokinesis. The cytoplasmic tail of GpIbα contains a filamin binding domain, interacting with filamin just beneath the cell membrane. Filamin is an actin binding protein, crosslinking actin filaments to form networks. Therefore, GpIbα protein possibly regulates cytokinesis by binding actin through filamin association (Figure 49). Consistent with this, it is known that bone marrow megakaryocytes, the precursors of blood platelets, undergo endomitosis (continuous rounds of DNA replication but no cell division) resulting in giant cells with a DNA content ranging 8N to 128N (reviewed in Ravid et al., 2002). Since GpIbα is abundant in megakaryocytes and platelets, I guess these excessive GpIbα might inhibit cytokinesis in these cells.

Both the protooncogene c-Myc, and its target MT-MC1, are upregulated in almost all types of carcinomas. GpIbα is a target of both c-Myc and MT-MC1, and is overexpressed in a variety of tested cancer cells. This overexpression leads to the mislocalization of GpIbα at the contractile ring and inappropriate cytoskeleton contraction in the cell cortex and ends with cytokinesis failure and tetraploidy. Although c-Myc plays multiple roles in tumorigenesis, my study reveals that one of these pathways is that c-Myc induces malignant cancers through regulating GpIbα, resulting in tetraploidization and genomic instability through cytokinesis failure and the following multipolar mitoses.

Another issue is why p53 is required for the GpIbα overexpression phenotype. Previous studies have shown that GpIbα overexpression causes DNA damage and induces senescence in HFF cells, and that p53 deficiency is required for GpIbα overexpressing HFF cells to pass the

DNA damage checkpoint and senescence barrier to survive and proliferate at high rates (Li et al., 2007a). This could explain why tetraploids are accumulated only in HFF-hTERT-shp53-GpIbα cells, but not with GpIbα expression alone. However, cytokinesis failure from GpIbα expression also required p53 inhibition. I have observed that calnexin accumulated in p53-defecient HFF cells, suggesting that the ER may be under some stress, although it is not enough to induce the UPR. Consistent with these observations, electron microscopy analysis reveals the abnormal enlarged ER in HFF-hTERT-shp53 cells (unpublished data, Rbaibi and Kiselyov). Although this type of abnormality is not obvious in other p53-defective cell lines, it still indicates that p53 possibly plays a role in ER homeostasis maintenance. ER in a p53-knockdown cell may have impaired GpIbα modification and abnormal function, thereby facilitating cytokinesis failure in HFF cells.

# 5.0 CHAPTER V: SUMMARY AND SPECULATIONS

Cancer is a class of diseases that results from cells displaying the traits of 1) uncontrolled growth beyond normal limits; 2) invasion into adjacent normal tissues and 3) sometimes metastasis to other locations in the body via lymph or blood. According to the American Cancer Society, a total of 1,444,920 new cancer cases and 559,650 deaths for cancers are estimated to occur in the United States in 2007. This number of deaths is presently responsible for about 23.1% of all deaths in the United States during 2007, indicating that cancer is a major threat to public health (Jemal et al., 2007).

Cancer, once diagnosed, is usually treated with surgery, chemotherapy and/or radiotherapy. However, these treatments are not specific to kill only malignant cancer cells but also destroy normal cells. Thus, it is very important to develop drugs that act specifically on certain tumors and minimize damage to normal tissues. It is believed that dissecting the molecular abnormalities and the mechanism of carcinogenesis would significantly contribute to cancer therapy development. In this study, I use tissue-cultured cells as a model system to understand the molecular defects in cancers and the pathways of how normal cells change to malignantly transformed cells.

Nearly all cancers have gene mutations and defects in DNA repair machinery. These damages may be inherited from parents or randomly acquired through errors in DNA replication or environmentally induced damage. There are approximately 10,000 lesions that occur spontaneously in a mammalian cell per day (Lindahl, 1993), which can be efficiently removed. However, in the transformed cells, DNA repair pathways are more or less impaired leading to catastrophic outcomes. For instance, p53, a tumor suppressor gene, has been mutated in almost all cancer types, inactivating DNA repair proteins, shutting off the repair machinery and inhibiting apoptosis to allow uncontrolled cell growth (Hainaut and Hollstein, 2000; Soussi and Beroud, 2001).

In addition to the small mutations, cancer cells typically have unstable genomes that exhibit aneuploidy or polyploidy. These changes play an important part of malignant transformation in most tumor models (reviewed in Ried et al., 1999). In this study, I focus on chromosomal segregation and cytokinesis in cancer cells and investigate how the defects of these processes contribute to genomic instability and tumorigenesis. A mouse model from the Pellman lab strongly supports the pathway that the tetraploid p53-/- cells resulting from cytokinesis failure in culture generate tumors in mice and the tumor cells isolated from the mice are aneuploid (Fujiwara et al., 2005). However, how the tetraploids progress to aneuploids is still not very clear. For this study, mice model has some limitations. For example, cell division is hard to follow *in vivo*. Therefore, I use tissue-cultured human cells as a system to understand more about it. My study reveals that incomplete cytokinesis after chromosome segregation in a cancer cell causes tetraploidy. Some of these cells can undergo multipolar divisions in the next cell cycle if the amplified centrosomes are not clustered. Multipolarity is considered a type of

chromosome segregational defect, which has a high probability of causing genomic changes in the daughter cell due to an asymmetrical cell division. The genetic gain-or-loss very likely brings growth advantages to the daugher cells to make them transformed and malignant. Under selection, this small population of transformed cells might become dominant due to uncontrolled proliferation and out grow the normal cells in the tissue and form tumors (Figure 50, major vertical pathway).

In addition, in multinucleated cancer cells, I have also observed that multipolarity always occurs with other segregational defects, such as, lagging chromosomes, anaphase bridges (Figure 50, pathway c), and for most cases, cells with multipolar division partially or completely fail in cytokinesis at a high frequency (Figure 50, pathway b). It suggests that all of these defects are very likely to promote yet more genomic instability to give the cancer cells the many genetic changes needed to become more malignant.

The defects I have found in cancer cells resulting in cytokinesis failure are all related to cytoskeletal defects. I have demonstrated that myosin regulatory light chain is phosphorylated at a low level in eight different types of cancer cell lines and this is a major cause for these cells failing in normal contraction at the midzone and consequently aborting cytokinesis. The deficiency of MLC phosphorylation could be due to 1) downregulated MLCK expression and inhibited MLCK activity or 2) upregulated myosin phosphatase expression (Figure 50). If I elevated the MLC phosphorylation by knockdown of myosin phosphatase, the defective cytokinesis, as well as multipolar mitosis, is rescued in oral cancer and liver cancer cells. Another protein I have found to play a role in cytokinesis for the first time is GpIbα, which

localizes at the contractile ring in normal cells. When it is overexpressed in p53-deficient normal cell, GpIbα disappears from the contractile rings and cells fail in cytokinesis. This GpIbα mislocalization possibly triggers cytoskeleton contraction at other sites on the cell cortex via binding filamin to regulate actin filaments networks (Figure 50).

However, whether filamin functions during cytokinesis is still unknown. Filamin is well known to crosslink actin filaments into orthogonal networks in cortical cytoplasm and participates in the anchoring of membrane proteins for the actin cytoskeleton (Stossel et al., 2001). But actin filaments in the contractile ring are usually in parallel bundles, unlike the dendritic network found at the leading edge of a migrating cell (Rappaport, 1996). However, filamin has been observed at the contractile ring at ~16% frequency in dividing chick embryo cells, comparing to ~14% actin localization (Nunnally et al., 1980). Filamin also binds to Rho family GTPases, including Cdc42, RhoA and Rac1 (Bishop and Hall, 2000; Marti et al., 1997; Ohta et al., 1999). It suggests that filamin may recruit these Rho factors to regulate actin assembly and myosin activation during cytokinesis. Therefore, further studies of GpIbα-filamin regulation during cytokinesis are required.

Cancer is not only a mass of cells. *In vivo,* cancer cells attach to extracellular matrix or adhere to each other to form a three-dimensional structure, which is known to be essential for cancer proliferation, invasion and metastasis (Tlsty and Coussens, 2006). To rule out that the conclusions above are only due to a growth in culture, I also looked carefully at how these genes are regulated in tumor tissues and found the similar results in human tissues compared to cultured cells (www.oncomine.org, Rhodes et al., 2007). More importantly, my collaborators

have shown that the GpIbα-overexpression induced tetraploid Rat1a cells generates tumors in mice (Li et al., 2007a), which supports the model that cytokinesis failure is a critical pathway for tumorigenesis *in vivo*.

Why do cancer cells require many mutations to impair cytokinesis? It is interesting that although tetraploids contribute to genomic instability more than diploids, different cancer cells only show around 10% multinucleation. It is possible that this low level of multinucleation allows genetic variation without completely eliminating normal division. My studies suggest that cancer cells modify different effectors to achieve this balance.

In the GpIbα-mediated cytokinesis failure pathway, two transcription factors are very critical, c-Myc and p53. It is well known that c-Myc is a protooncogene which is overexpressed in a wide range of human cancers. Deregulated c-Myc activity in cancer can lead to excessive activation of its downstream pathways, such as stimulation of changes in gene expression and cellular signaling to promote genomic abnormalities and tumorigenesis (Figure 50, pathway d) (Wade and Wahl, 2006). MT-MC1 had been identified as a downstream gene of c-Myc which is highly upregulated in cancers and functions as a potential oncogene (Yin et al., 1999). Interestingly, GpIbα is abundantly expressed in a number of tested cancer cells due to the regulation by c-Myc and MT-MC-1 (Li et al., 2007b), suggesting that GpIbα overexpression could be a target, although not the only one, for c-Myc functioning in increasing genomic instability via regulating cytokinesis in tumorigenesis.

Figure 50

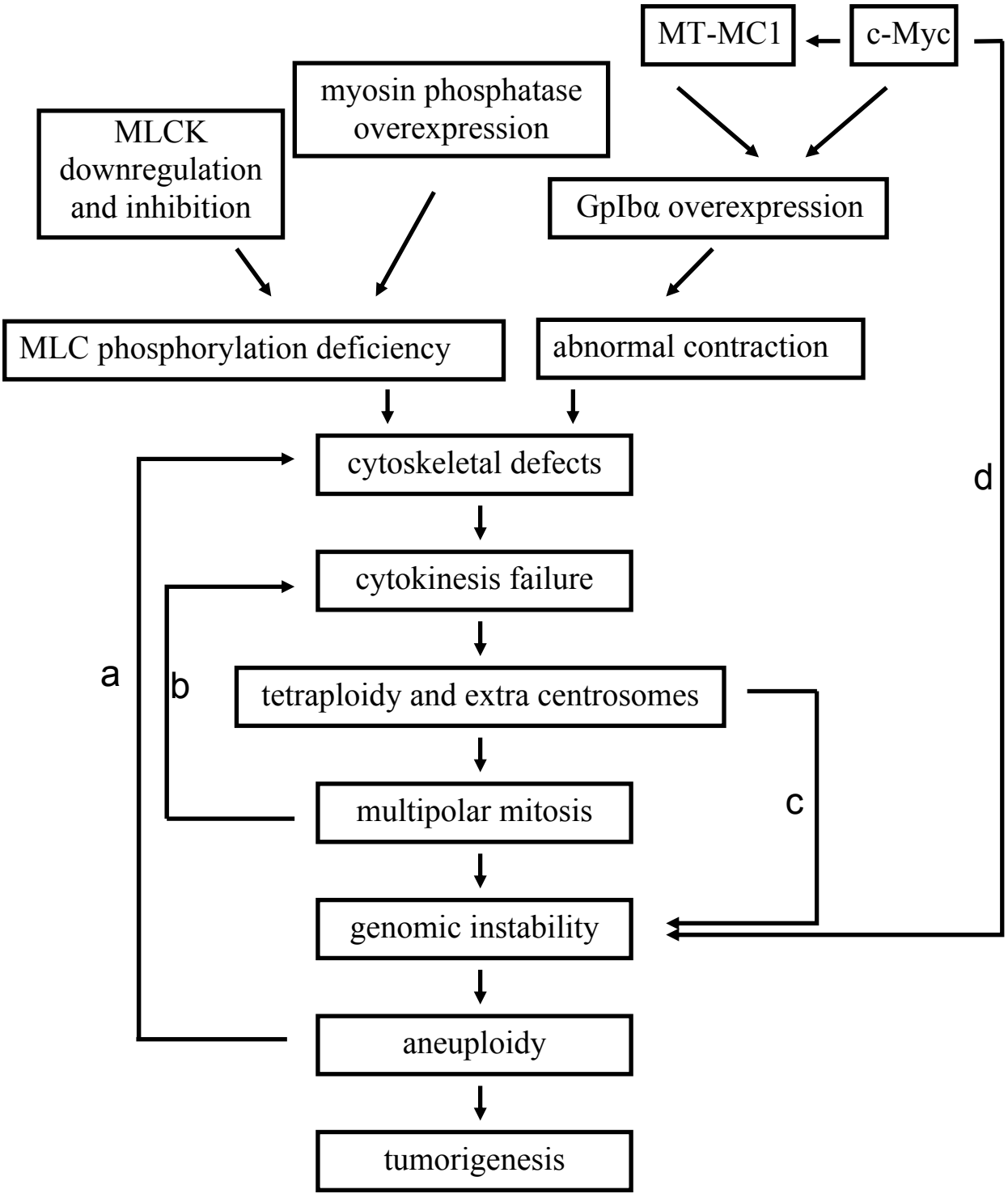


**Figure 50.** A model of how cytoskeletal defects lead to tumorigenesis.

However, GpIbα overexpression alone is not sufficient to induce failed cytokinesis in HFF cells. p53 is another critical effecter in this process. My data suggest that p53 may function in ER homeostasis to regulate GpIbα modification during cytokinesis. Generally speaking, p53 plays an extremely important role in cytokinesis failure mediated tumorigenesis. This is supported by results from the Pellman lab that p53+/+ tetraploid cells do not lead to tumor formation in mice (Fujiwara et al., 2005). The idea behind this observation is that p53 regulates cell cycle and apoptosis in cells, which ensures only the normal cells could survive and defective cells die. Thus, if p53 positive cells fail in cytokinesis and end with tetraploid daughter cells, these binucleated cells would die, limiting the damaging consequences. However, if p53 is inactive, the tetraploids very likely survive, divide and fall into the vicious cycle of tumorigenesis as shown in Figure 50.

As discussed above, cytokinesis failure is a distinguishable phenotype of cancer cells. The study from this dissertation has shown that defective MLC phosphorylation is a cause of cytokinesis failure in cancer cells. Thus, the biochemical examination of MLC phosphorylation can be a potential diagnostic indicator of cancer. For example, urea glycerol gel electrophoresis can be used to test phosphorylation levels of MLC in tissues. Low ratio of MLC phosphorylation in the tissue suggests high potential for malignancy.

In addition, cytokinesis failure is a cause for cells to be transformed; therefore, cytokinesis can be one possible therapeutic target in cancer. My studies have shown that knockdown of myosin phosphatase or GpIbα can correct cytokinesis failure and stabilize the

genome in cancer cells, suggesting that the inhibitors of these molecules possibly are good candidates, such as CPI-17 (Eto et al., 1997; Yamawaki et al., 2001), a myosin phosphatase inhibitory protein. On the other hand, chemicals that lead to cytokinesis failure, likely activating apoptosis pathway in cancers, are also considered as potential drugs of cancer therapy. For example, Aurora kinase inhibitors have recently begun clinical trials (Harrington et al., 2004). This kinase inhibition causes tetraploid accumulation resulting in cell death. However, given that blocking cytokinesis in p53-/- cells causes tumor in mice and discussion above, it is a high risk for this treatment in cancer therapy. Therefore, I believe that the drugs that selectively correct cytokinesis failure in cancers are promising targets for therapeutics.

# 6.0 CHAPTER VI: MATERIALS AND METHODS

## 6.1.1 Cell culturing

American Type Culture Collection (ATCC) cell lines, HCT116, SK-HEP1, U2OS, HeLa, MES-SA, A549, HEK-293, Human fibroblast, were cultured in the medium recommended by the supplier. Oral cancer cell lines, UPCI:SCC103 and UPCI:SCC78, are gifts from Dr. Susanne M. Gollin (University of Pittsburgh). These cells were maintained in minimal essential medium (Sigma), supplemented with 10% fetal bovine serum (FBS) (Atlanta Biologicals), 2mM L-Glutamine, 0.05 mg/ml Gentamycin and 1% non-essential amino acids (Invitrogen). Uvulopalatopharyngoplasty biopsy cell samples were cultured in KGM2 medium (Clonetics, Walkersville, MD). RPE-hTERT were cultured in Dulbecco's modified eagle's medium (DMEM)/nutrient mixture F-12 ham (Sigma), supplemented with 10% FBS. HFF-hTERT cells are gifts from Dr. Edward Prochownik (University of Pittsburg) and cultured in DMEM medium with 2mM L-Glutamine and 10% FBS. OS cells are also the gifts from Dr. Edward Prochownik (University of Pittsburg) and cultured in DMEM medium with 10% FBS. All cells were incubated at $37^{o}C$ in 5% $CO_2$.

### 6.1.2 DNA transfections

$2x10^5$ cells were grown on 22mm x 22mm sterile glass coverslips in six-well plates or 35mm dishes in OPTI-MEM. After 16-18 hours in culture, cells were transfected with 1-2μg of DNA plasmids (see Section 6.1.12) by using 3-6μl FuGENE6 transfection reagent (Roche Diagnostics) per coverslip according to the manufacture's protocol. Cells were transfected for 22 hours and cultured in fresh medium for 8 hours before lysing or fixation.

### 6.1.3 RNA transfection

$2x10^5$ cells were grown on sterile glass coverslips in six-well plates or 35mm dishes. Transfection with siMYPT1 (5'-GAG ACA AGA AAG ATT TGC T-3',Dharmacon) (Xia et al., 2005) or the control rhodamine siRNA (Qiagen) was performed using Lipofectamine 2000 reagent (Invitrogen) according to the manufacturer's recommendations. Cells were transfected 18-20 hours after being seeded on the coverslips and cultured for another 22 hours. After transfection, cells were maintained in medium for 24 hours. For long-term siRNA treatment, these treated cells were seeded on the coverslips or dishes again and treated with siMYPT1 as shown above.

### 6.1.4 Immunofluorescence staining

Cells on coverslips were fixed in -20°C cold methanol or in 3.7% formaldehyde at room temperature and washed in PBS. Coverslips were blocked in 1.5% BSA/PBST or 5% goat serum/PBST and immunostained with a variety of primary antibodies (see Section 6.1.11). Primary antibodies were diluted in the blocking solution and incubated on cells for 1h at 37°C. Then, cells were incubated with fluorescent labeled goat anti-rabbit IgG (Invitrogen, 1:250) for 1 hour at room temperature and stained with 4,6-diamidino-2-phenylindole (DAPI) at 1 μg/ml (Sigma). The coverslips were mounted and viewed by Olympus BX60 epifluorescence microscope with 100x oil immersion objectives. Hamamatsu Argus-20 CCD camera was used to capture images.

### 6.1.5 Live microscopy analysis

Cells were seeded with a density of $2x10^5$ cells on 35mm glass-bottom Petri dishes (MatTek Corp.) and viewed after DNA transfection or siRNA treatment. Cells were maintained at 37°C with a moisturized-warm air microscope chamber (Life Imaging Services, Reinach, Switzerland). Differential interference contrast (DIC) microscopy and epifluorescence microscopy was performed on a Nikon TE2000-U inverted microscope with a Coolsnap HQ digital camera (Roper Scientific Photometrics). Images were taken by MetaMorph (Molecular Devices) and converted to TIFF format and exported to Adobe Photoshop.

### 6.1.6 Immunoblotting

Cells were cultured on 150 mm dishes were collected, washed twice with PBS and resuspended in 400 μl of RIPA buffer (Tris-HCL pH 7.4, 1% NP-40, 150 mM NaCl and protease inhibitors leupeptin, pepstatin and PMSF at 1μg/ml each). After 15 minutes on ice, the lysates were clarified by centrifugation at $4^0$ C for 15 min at 10,000g and supernatant was collected. Protein concentration was measured using Bradford assay (Bio-Rad). Proteins were separated by SDS-polyacrylamide gel electrophoresis, transferred to PVDF membranes (Bio-Rad), and incubated with primary antibodies (see Section 6.1.11), diluted in 5% milk/TBST for overnight at 4°C. ECL anti-mouse IgG-HRP linked F(ab')α fragment and ECL anti-rabbit IgG-HRP linked F(ab')α fragment (1:10000, Amersham, GE Healthcare, UK) were diluted in 5% milk and used as secondary antibodies with 1-hour incubation. The membranes were visualized by chemiluminescence assay (Pierce) and Kodak M35A X-OMAT Processors (Kodak). The protein amounts were quantified by ImageGuage software program.

### 6.1.7 MLC phosphorylation analysis

MLC phosphorylation was measured by urea/glycerol-PAGE and immunoblotting as previously described (Word et al., 1991). Cells were seeded on 6-well plates and harvested by 0.5 ml ice-cold trichloroacetic acid containing 10 mM dithiothreitol (DTT). The pellets were washed three times with diethyl ether and resuspended with 8 M urea, 20 mM Tris–HCl, 23 mM glycine, 10% glycerol, 10 mM EGTA, 1 mM EDTA, and 0.2% bromophenol blue (pH 8.6). The supernatant fractions were subjected to gel electrophoresis and rAb-MLC (gift from Dr. James T. Stull,

University of Texas Southwestern Medical Center, Dallas, TX, 1:5000) was used as immunoblotting.

### 6.1.8 UPR activity assay

HFF cells were cultured and lysed in a RNase-free environment. Total RNA extract was purified by RNeasy Mini kit (Qiagen) and mRNA was synthesized by SuperScript III First-Strand Synthesis System for RT-PCR (Invitrogen). Standard PCR was performed with purified total mRNA. Primers 5'-GAATGAAGTGAGGCCAGTGG-3' and 5'-GGGGCTTGGTATATATGT-GG-3' were designed to target both unspliced and spliced XPB1 mRNA. PCR products were resolved on 2% agrose gel electrophoresis and viewed by ethidium bromide stain and Kodak Image Station 440 (Kodak).

### 6.1.9 Endocytosis assay

HFF cells were seeded on the 35mm petri dishes and incubated with FITC-transferrin (Sigma) with a dilution of 1:500 at 37°C. After 25 minutes, cells were washed by 1XPBS (pH = 4.0) and recorded 0 minutes and 40 minutes after wash by Nikon TE2000-U inverted microscope with a Coolsnap HQ digital camera.

### 6.1.10 Cell synchronization and drugs treatment

#### 6.1.10.1 Cell synchronization and release

To synchronize the cells, 20ng/ml of colcemid (Irvine Scientific) was added to the cells for 18 hours. Cells were released by washing twice with FBS and incubating in medium.

#### 6.1.10.2 ML-7 treatment

Cells were seeded on coverslips and treated with 35μM ML-7 (Sigma) for 48 or 72 hours. Cells were washed and released in medium up to 6 days. Samples were fixed and immuno-stained for multinucleation frequency quantification.

#### 6.1.10.3 DTT treatment

HFF cells were treated with 2mM DTT for 1 hour and fixed or lysed.

### 6.1.11 Antibodies

#### 6.1.11.1 Immunofluorescence

rAb-MHC (Sigma, 1:500); mAb-actin (Sigma, 1:300); mAb-Ser19-MLC (Cell Signaling, 1:50); mAb-centrinII (a gift from Dr. Jeffrey L. Salisbury, Mayo Clinic and Foundation, 1:5000); mAb-γ-tubulin (Sigma, 1:1000); ratAb-Gp1ba (a gift from Dr. Edward Prochownik, University of Pittsburgh, 1:100); rAb-calnexin (1:100, Stressgen, MI); rAb-bip (Abcam, 1:200); mAb-giantin (a gift from Dr. Adam D Linstedt, Carnegie Mellon University, 1:200) were used.

#### 6.1.11.2 Immunoblotting

mAb-γ-tubulin (Sigma, 1:5000); rAb-MLC (gift from Dr. James T. Stull, University of Texas Southwestern Medical Center,1:5000); rAb-MYPT1 (Upstate, 1:1000), rAb-GFP (Abcam, 1:3000); mAb-MLCK (Sigma, 1:5000); mAb-ROCK1 (Santa Cruz, 1:100); mAb-CRIK (BD Transduction Laboratories, 1:300); mAb-pMLC (Cell Signaling, 1:1000); mAb-Ser19-MLC (Cell Signaling, 1:1000) were used.

### 6.1.12 Plasmids

pBOS-H2B-GFP (BD Pharmingen) and pEGFP-Hs-Centrin are from commercial resources. Farnesylated-GFP and GFP-actin expressing plasmids are gifts from Dr. Jeffrey D. Hildebrand (University of Pittsburgh) and the MLCK-GFP plasmid is a gift of Dr. Anne R. Bresnick (Albert Einstein College of Medicine) (Dulyaninova et al., 2004). GFP-MLC and GFP-MLC-DD plasmids are gifts from Dr. Kathleen Kelly (National Cancer Institute) (Ward et al., 2002).GFP-MYPT1 plasmid coding full length of chicken MYPT1 is a gift from Dr. David J. Hartshorne (University of Arizona) (Wu et al., 2005). Site-directed mutagenesis to create the siRNA-resistant silent mutant of GFP-MYPT1was performed using primers 5'-CAG AGA CAA GAG CGG TTT GCT GAC AG-3' and 5'-CTG TCA GCA AAC CGC TCT TGT CTC TG-3'. The construct was verified by sequencing. GpIbα overexpression and p53 knockdown plasmids were generated in the Prochownik lab (Universitity of Pittsburgh) as described previously (Li et al., 2007a; Li et al., 2007b). GpIbα knockdown plasmid was constructed by bi-cistronic retroviral vectors encoding GpIbα shRNA in the Prochownik lab (Universitity of Pittsburgh).

### 6.1.13 Statistical methods

All statistical analyses were performed using R statistical package (R version 2.4.1; R Foundation for Statistical Computing). The group comparisons were conducted by non-parametric Wilcox test. All p-values are one-sided. The Spearman's correlation coefficient was calculated for describing the relationship between levels of MLC phosphorylation and multinucleation frequencies.

## BIBLIOGRAPHY


Aaltonen, O, Tuomainen, J, Laine, M, Niemi, P. 1993. Cortical differences in tonal versus vowel processing as revealed by an ERP component called mismatch negativity (MMN). *Brain Lang*, 44: 139-152.

Acilan, C, Potter, DM, Saunders, WS. 2007. DNA repair pathways involved in anaphase bridge formation. *Genes Chromosomes Cancer*, 46: 522-531.

Al Rashid, ST, Dellaire, G, Cuddihy, A, Jalali, F, Vaid, M, Coackley, C, Folkard, M, Xu, Y, Chen, BP, Chen, DJ, Lilge, L, Prise, KM, Bazett Jones, DP, Bristow, RG. 2005. Evidence for the direct binding of phosphorylated p53 to sites of DNA breaks in vivo. *Cancer Res*, 65: 10810-10821.

Almoguera, C, Shibata, D, Forrester, K, Martin, J, Arnheim, N, Perucho, M. 1988. Most human carcinomas of the exocrine pancreas contain mutant c-K-ras genes. *Cell*, 53: 549-554.

Alsop, GB, Zhang, D. 2003. Microtubules are the only structural constituent of the spindle apparatus required for induction of cell cleavage. *J Cell Biol*, 162: 383-390.

Amano, M, Ito, M, Kimura, K, Fukata, Y, Chihara, K, Nakano, T, Matsuura, Y, Kaibuchi, K. 1996. Phosphorylation and activation of myosin by Rho-associated kinase (Rho-kinase). *J Biol Chem*, 271: 20246-20249.

Amano, M, Kaneko, T, Maeda, A, Nakayama, M, Ito, M, Yamauchi, T, Goto, H, Fukata, Y, Oshiro, N, Shinohara, A, Iwamatsu, A, Kaibuchi, K. 2003. Identification of Tau and MAP2 as novel substrates of Rho-kinase and myosin phosphatase. *J Neurochem*, 87: 780-790.

Andreassen, PR, Lohez, OD, Lacroix, FB, Margolis, RL. 2001. Tetraploid state induces p53-dependent arrest of nontransformed mammalian cells in G1. *Mol Biol Cell*, 12: 1315-1328.

Artandi, SE, Chang, S, Lee, SL, Alson, S, Gottlieb, GJ, Chin, L, DePinho, RA. 2000. Telomere dysfunction promotes non-reciprocal translocations and epithelial cancers in mice. *Nature*, 406: 641-645.

Bakkenist, CJ, Kastan, MB. 2004. Initiating cellular stress responses. *Cell*, 118: 9-17.

Ben-Neriah, Y, Daley, GQ, Mes-Masson, AM, Witte, ON, Baltimore, D. 1986. The chronic myelogenous leukemia-specific P210 protein is the product of the bcr/abl hybrid gene. *Science*, 233: 212-214.

Bettencourt-Dias, M, Glover, DM. 2007. Centrosome biogenesis and function: centrosomics brings new understanding. *Nat Rev Mol Cell Biol*, 8: 451-463.

Bicknell, AA, Babour, A, Federovitch, CM, Niwa, M. 2007. A novel role in cytokinesis reveals a housekeeping function for the unfolded protein response. *J Cell Biol*, 177: 1017-1027.

Bishop, AL, Hall, A. 2000. Rho GTPases and their effector proteins. *Biochem J*, 348 Pt 2: 241-255.

Blagosklonny, MV. 2007. Mitotic arrest and cell fate: why and how mitotic inhibition of transcription drives mutually exclusive events. *Cell Cycle*, 6: 70-74.

Bornens, M. 2002. Centrosome composition and microtubule anchoring mechanisms. *Curr Opin Cell Biol*, 14: 25-34.

Bouckson-Castaing, V, Moudjou, M, Ferguson, DJ, Mucklow, S, Belkaid, Y, Milon, G, Crocker, PR. 1996. Molecular characterisation of ninein, a new coiled-coil protein of the centrosome. *J Cell Sci*, 109 ( Pt 1): 179-190.

Brathen, M, Banrud, H, Berg, K, Moan, J. 2000. Induction of multinucleated cells caused by UVA exposure in different stages of the cell cycle. *Photochem Photobiol*, 71: 620-626.

Brinkley, BR. 2001. Managing the centrosome numbers game: from chaos to stability in cancer cell division. *Trends Cell Biol*, 11: 18-21.

Burton, K, Taylor, DL. 1997. Traction forces of cytokinesis measured with optically modified elastic substrata. *Nature*, 385: 450-454.

Carroll, PE, Okuda, M, Horn, HF, Biddinger, P, Stambrook, PJ, Gleich, LL, Li, YQ, Tarapore, P, Fukasawa, K. 1999. Centrosome hyperamplification in human cancer: chromosome instability induced by p53 mutation and/or Mdm2 overexpression. *Oncogene*, 18: 1935-1944.

Cavalli, C, Danova, M, Gobbi, PG, Riccardi, A, Magrini, U, Mazzini, G, Bertoloni, D, Rutigliano, L, Rossi, A, Ascari, E. 1989. Ploidy and proliferative activity measurement by flow cytometry in non-Hodgkin's lymphomas. Do speculative aspects prevail over clinical ones? *Eur J Cancer Clin Oncol*, 25: 1755-1763.

Chew, TL, Wolf, WA, Gallagher, PJ, Matsumura, F, Chisholm, RL. 2002. A fluorescent resonant energy transfer-based biosensor reveals transient and regional myosin light chain kinase activation in lamella and cleavage furrows. *J Cell Biol*, 156: 543-553.

Chiba, S, Okuda, M, Mussman, JG, Fukasawa, K. 2000. Genomic convergence and suppression of centrosome hyperamplification in primary p53-/- cells in prolonged culture. *Exp Cell Res*, 258: 310-321.

Christmann, M, Tomicic, MT, Roos, WP, Kaina, B. 2003. Mechanisms of human DNA repair: an update. *Toxicology*, 193: 3-34.

Cimini, D, Fioravanti, D, Salmon, ED, Degrassi, F. 2002. Merotelic kinetochore orientation versus chromosome mono-orientation in the origin of lagging chromosomes in human primary cells. *J Cell Sci*, 115: 507-515.

Cimini, D, Howell, B, Maddox, P, Khodjakov, A, Degrassi, F, Salmon, ED. 2001. Merotelic kinetochore orientation is a major mechanism of aneuploidy in mitotic mammalian tissue cells. *J Cell Biol*, 153: 517-527.

Conti, MA, Adelstein, RS. 1981. The relationship between calmodulin binding and phosphorylation of smooth muscle myosin kinase by the catalytic subunit of 3':5' cAMP-dependent protein kinase. *J Biol Chem*, 256: 3178-3181.

Dang, CV, O'Donnell, KA, Zeller, KI, Nguyen, T, Osthus, RC, Li, F. 2006. The c-Myc target gene network. *Semin Cancer Biol*, 16: 253-264.

Danilchik, MV, Bedrick, SD, Brown, EE, Ray, K. 2003. Furrow microtubules and localized exocytosis in cleaving Xenopus laevis embryos. *J Cell Sci*, 116: 273-283.

D'Assoro, AB, Busby, R, Suino, K, Delva, E, Almodovar-Mercado, GJ, Johnson, H, Folk, C, Farrugia, DJ, Vasile, V, Stivala, F, Salisbury, JL. 2004. Genotoxic stress leads to centrosome amplification in breast cancer cell lines that have an inactive G1/S cell cycle checkpoint. *Oncogene*, 23: 4068-4075.

D'Assoro, AB, Lingle, WL, Salisbury, JL. 2002. Centrosome amplification and the development of cancer. *Oncogene*, 21: 6146-6153.

D'Avino, PP, Savoian, MS, Glover, DM. 2005. Cleavage furrow formation and ingression during animal cytokinesis: a microtubule legacy. *J Cell Sci*, 118: 1549-1558.

DeBiasio, RL, LaRocca, GM, Post, PL, Taylor, DL. 1996. Myosin II transport, organization, and phosphorylation: evidence for cortical flow/solation-contraction coupling during cytokinesis and cell locomotion. *Mol Biol Cell*, 7: 1259-1282.

Di Cunto, F, Imarisio, S, Hirsch, E, Broccoli, V, Bulfone, A, Migheli, A, Atzori, C, Turco, E, Triolo, R, Dotto, GP, Silengo, L, Altruda, F. 2000. Defective neurogenesis in citron kinase knockout mice by altered cytokinesis and massive apoptosis. *Neuron*, 28: 115-127.

Di Leonardo, A, Linke, SP, Clarkin, K, Wahl, GM. 1994. DNA damage triggers a prolonged p53-dependent G1 arrest and long-term induction of Cip1 in normal human fibroblasts. *Genes Dev*, 8: 2540-2551.

Duelli, DM, Hearn, S, Myers, MP, Lazebnik, Y. 2005. A primate virus generates transformed human cells by fusion. *J Cell Biol*, 171: 493-503.

Duensing, S, Lee, LY, Duensing, A, Basile, J, Piboonniyom, S, Gonzalez, S, Crum, CP, Munger, K. 2000. The human papillomavirus type 16 E6 and E7 oncoproteins cooperate to induce mitotic defects and genomic instability by uncoupling centrosome duplication from the cell division cycle. *Proc Natl Acad Sci U S A*, 97: 10002-10007.

Duensing, S, Munger, K. 2002. The human papillomavirus type 16 E6 and E7 oncoproteins independently induce numerical and structural chromosome instability. *Cancer Res*, 62: 7075-7082.

Dulout, FN, Olivero, OA. 1984. Anaphase-telophase analysis of chromosomal damage induced by chemicals. *Environ Mutagen*, 6: 299-310.

Dulyaninova, NG, Bresnick, AR. 2004. The long myosin light chain kinase is differentially phosphorylated during interphase and mitosis. *Exp Cell Res*, 299: 303-314.

Dulyaninova, NG, Patskovsky, YV, Bresnick, AR. 2004. The N-terminus of the long MLCK induces a disruption in normal spindle morphology and metaphase arrest. *J Cell Sci*, 117: 1481-1493.

Earnshaw, WC, Cooke, CA. 1991. Analysis of the distribution of the INCENPs throughout mitosis reveals the existence of a pathway of structural changes in the chromosomes during metaphase and early events in cleavage furrow formation. *J Cell Sci*, 98 ( Pt 4): 443-461.

Eda, M, Yonemura, S, Kato, T, Watanabe, N, Ishizaki, T, Madaule, P, Narumiya, S. 2001. Rho-dependent transfer of Citron-kinase to the cleavage furrow of dividing cells. *J Cell Sci*, 114: 3273-3284.

Eggert, US, Mitchison, TJ, Field, CM. 2006. Animal cytokinesis: from parts list to mechanisms. *Annu Rev Biochem*, 75: 543-566.

Emoto, K, Inadome, H, Kanaho, Y, Narumiya, S, Umeda, M. 2005. Local change in phospholipid composition at the cleavage furrow is essential for completion of cytokinesis. *J Biol Chem*, 280: 37901-37907.

Emoto, K, Umeda, M. 2000. An essential role for a membrane lipid in cytokinesis. Regulation of contractile ring disassembly by redistribution of phosphatidylethanolamine. *J Cell Biol*, 149: 1215-1224.

Emoto, K, Umeda, M. 2001. Membrane lipid control of cytokinesis. *Cell Struct Funct*, 26: 659-665.

Eto, M, Senba, S, Morita, F, Yazawa, M. 1997. Molecular cloning of a novel phosphorylation-dependent inhibitory protein of protein phosphatase-1 (CPI17) in smooth muscle: its specific localization in smooth muscle. *FEBS Lett*, 410: 356-360.

Fenech, M. 1993. The cytokinesis-block micronucleus technique: a detailed description of the method and its application to genotoxicity studies in human populations. *Mutat Res*, 285: 35-44.

Feng, B, Schwarz, H, Jesuthasan, S. 2002. Furrow-specific endocytosis during cytokinesis of zebrafish blastomeres. *Exp Cell Res*, 279: 14-20.

Feng, S, Christodoulides, N, Kroll, MH. 1999. The glycoprotein Ib/IX complex regulates cell proliferation. *Blood*, 93: 4256-4263.

Field, CM, Alberts, BM. 1995. Anillin, a contractile ring protein that cycles from the nucleus to the cell cortex. *J Cell Biol*, 131: 165-178.

Field, SJ, Madson, N, Kerr, ML, Galbraith, KA, Kennedy, CE, Tahiliani, M, Wilkins, A, Cantley, LC. 2005. PtdIns(4,5)P2 functions at the cleavage furrow during cytokinesis. *Curr Biol*, 15: 1407-1412.

Fisk, HA, Mattison, CP, Winey, M. 2003. Human Mps1 protein kinase is required for centrosome duplication and normal mitotic progression. *Proc Natl Acad Sci U S A*, 100: 14875-14880.

Foe, VE, Field, CM, Odell, GM. 2000. Microtubules and mitotic cycle phase modulate spatiotemporal distributions of F-actin and myosin II in Drosophila syncytial blastoderm embryos. *Development*, 127: 1767-1787.

Fry, AM, Meraldi, P, Nigg, EA. 1998. A centrosomal function for the human Nek2 protein kinase, a member of the NIMA family of cell cycle regulators. *Embo J*, 17: 470-481.

Fujiwara, T, Bandi, M, Nitta, M, Ivanova, EV, Bronson, RT, Pellman, D. 2005. Cytokinesis failure generating tetraploids promotes tumorigenesis in p53-null cells. *Nature*, 437: 1043-1047.

Galipeau, PC, Cowan, DS, Sanchez, CA, Barrett, MT, Emond, MJ, Levine, DS, Rabinovitch, PS, Reid, BJ. 1996. 17p (p53) allelic losses, 4N (G2/tetraploid) populations, and progression to aneuploidy in Barrett's esophagus. *Proc Natl Acad Sci U S A*, 93: 7081-7084.

Gatti, M, Giansanti, MG, Bonaccorsi, S. 2000. Relationships between the central spindle and the contractile ring during cytokinesis in animal cells. *Microsc Res Tech*, 49: 202-208.

Ghadimi, BM, Sackett, DL, Difilippantonio, MJ, Schrock, E, Neumann, T, Jauho, A, Auer, G, Ried, T. 2000. Centrosome amplification and instability occurs exclusively in aneuploid, but not in diploid colorectal cancer cell lines, and correlates with numerical chromosomal aberrations. *Genes Chromosomes Cancer*, 27: 183-190.

Gisselsson, D. 2002. Tumour morphology--interplay between chromosome aberrations and founder cell differentiation. *Histol Histopathol*, 17: 1207-1212.

Gisselsson, D, Jonson, T, Petersen, A, Strombeck, B, Dal Cin, P, Hoglund, M, Mitelman, F, Mertens, F, Mandahl, N. 2001. Telomere dysfunction triggers extensive DNA fragmentation and evolution of complex chromosome abnormalities in human malignant tumors. *Proc Natl Acad Sci U S A*, 98: 12683-12688.

Gisselsson, D, Jonson, T, Yu, C, Martins, C, Mandahl, N, Wiegant, J, Jin, Y, Mertens, F, Jin, C. 2002. Centrosomal abnormalities, multipolar mitoses, and chromosomal instability in head and neck tumours with dysfunctional telomeres. *Br J Cancer*, 87: 202-207.

Gisselsson, D, Palsson, E, Yu, C, Mertens, F, Mandahl, N. 2004. Mitotic instability associated with late genomic changes in bone and soft tissue tumours. *Cancer Lett*, 206: 69-76.

Gisselsson, D, Pettersson, L, Hoglund, M, Heidenblad, M, Gorunova, L, Wiegant, J, Mertens, F, Dal Cin, P, Mitelman, F, Mandahl, N. 2000. Chromosomal breakage-fusion-bridge events cause genetic intratumor heterogeneity. *Proc Natl Acad Sci U S A*, 97: 5357-5362.

Glotzer, M. 2005. The molecular requirements for cytokinesis. *Science*, 307: 1735-1739.

Goeckeler, ZM, Masaracchia, RA, Zeng, Q, Chew, TL, Gallagher, P, Wysolmerski, RB. 2000. Phosphorylation of myosin light chain kinase by p21-activated kinase PAK2. *J Biol Chem*, 275: 18366-18374.

Goode, BL, Eck, MJ. 2007. Mechanism and function of formins in the control of actin assembly. *Annu Rev Biochem*, 76: 593-627.

Gregory, SL, Ebrahimi, S, Milverton, J, Jones, WM, Bejsovec, A, Saint, R. 2008. Cell division requires a direct link between microtubule-bound RacGAP and Anillin in the contractile ring. *Curr Biol*, 18: 25-29.

Gruneberg, U, Neef, R, Li, X, Chan, EH, Chalamalasetty, RB, Nigg, EA, Barr, FA. 2006. KIF14 and citron kinase act together to promote efficient cytokinesis. *J Cell Biol*, 172: 363-372.

Gu, LZ, Hu, WY, Antic, N, Mehta, R, Turner, JR, de Lanerolle, P. 2006. Inhibiting myosin light chain kinase retards the growth of mammary and prostate cancer cells. *Eur J Cancer*, 42: 948-957.

Guidotti, JE, Bregerie, O, Robert, A, Debey, P, Brechot, C, Desdouets, C. 2003. Liver cell polyploidization: a pivotal role for binuclear hepatocytes. *J Biol Chem*, 278: 19095-19101.

Gunsalus, KC, Bonaccorsi, S, Williams, E, Verni, F, Gatti, M, Goldberg, ML. 1995. Mutations in twinstar, a Drosophila gene encoding a cofilin/ADF homologue, result in defects in centrosome migration and cytokinesis. *J Cell Biol*, 131: 1243-1259.

Guse, A, Mishima, M, Glotzer, M. 2005. Phosphorylation of ZEN-4/MKLP1 by aurora B regulates completion of cytokinesis. *Curr Biol*, 15: 778-786.

Haigo, SL, Hildebrand, JD, Harland, RM, Wallingford, JB. 2003. Shroom induces apical constriction and is required for hingepoint formation during neural tube closure. *Curr Biol*, 13: 2125-2137.

Hainaut, P, Hollstein, M. 2000. p53 and human cancer: the first ten thousand mutations. *Adv Cancer Res*, 77: 81-137.

Harrington, EA, Bebbington, D, Moore, J, Rasmussen, RK, Ajose-Adeogun, AO, Nakayama, T, Graham, JA, Demur, C, Hercend, T, Diu-Hercend, A, Su, M, Golec, JM, Miller, KM. 2004. VX-680, a potent and selective small-molecule inhibitor of the Aurora kinases, suppresses tumor growth in vivo. *Nat Med*, 10: 262-267.

Hartshorne, DJ, Ito, M, Erdodi, F. 2004. Role of protein phosphatase type 1 in contractile functions: myosin phosphatase. *J Biol Chem*, 279: 37211-37214.

Hayward, DG, Clarke, RB, Faragher, AJ, Pillai, MR, Hagan, IM, Fry, AM. 2004. The centrosomal kinase Nek2 displays elevated levels of protein expression in human breast cancer. *Cancer Res*, 64: 7370-7376.

Heald, R, Tournebize, R, Blank, T, Sandaltzopoulos, R, Becker, P, Hyman, A, Karsenti, E. 1996. Self-organization of microtubules into bipolar spindles around artificial chromosomes in Xenopus egg extracts. *Nature*, 382: 420-425.

Herring, BP, El-Mounayri, O, Gallagher, PJ, Yin, F, Zhou, J. 2006. Regulation of myosin light chain kinase and telokin expression in smooth muscle tissues. *Am J Physiol Cell Physiol*, 291: C817-827.

Hird, SN, White, JG. 1993. Cortical and cytoplasmic flow polarity in early embryonic cells of Caenorhabditis elegans. *J Cell Biol*, 121: 1343-1355.

Hoffelder, DR, Luo, L, Burke, NA, Watkins, SC, Gollin, SM, Saunders, WS. 2004. Resolution of anaphase bridges in cancer cells. *Chromosoma*, 112: 389-397.

Hollstein, M, Sidransky, D, Vogelstein, B, Harris, CC. 1991. p53 mutations in human cancers. *Science*, 253: 49-53.

Hsu, LC, Kapali, M, DeLoia, JA, Gallion, HH. 2005. Centrosome abnormalities in ovarian cancer. *Int J Cancer*, 113: 746-751.

Huang, X, Gollin, SM, Raja, S, Godfrey, TE. 2002. High-resolution mapping of the 11q13 amplicon and identification of a gene, TAOS1, that is amplified and overexpressed in oral cancer cells. *Proc Natl Acad Sci U S A*, 99: 11369-11374.

Hut, HM, Lemstra, W, Blaauw, EH, Van Cappellen, GW, Kampinga, HH, Sibon, OC. 2003. Centrosomes split in the presence of impaired DNA integrity during mitosis. *Mol Biol Cell*, 14: 1993-2004.

Iarmarcovai, G, Botta, A, Orsiere, T. 2007. [Micronuclei and genetic polymorphisms: from exposure to susceptibility]. *Ann Biol Clin (Paris)*, 65: 357-363.

Ikebe, M, Hartshorne, DJ. 1985. Phosphorylation of smooth muscle myosin at two distinct sites by myosin light chain kinase. *J Biol Chem*, 260: 10027-10031.

Ikebe, M, Koretz, J, Hartshorne, DJ. 1988. Effects of phosphorylation of light chain residues threonine 18 and serine 19 on the properties and conformation of smooth muscle myosin. *J Biol Chem*, 263: 6432-6437.

Ito, M, Feng, J, Tsujino, S, Inagaki, N, Inagaki, M, Tanaka, J, Ichikawa, K, Hartshorne, DJ, Nakano, T. 1997. Interaction of smooth muscle myosin phosphatase with phospholipids. *Biochemistry*, 36: 7607-7614.

Ito, M, Nakano, T, Erdodi, F, Hartshorne, DJ. 2004. Myosin phosphatase: structure, regulation and function. *Mol Cell Biochem*, 259: 197-209.

Iwakuma, T, Lozano, G, Flores, ER. 2005. Li-Fraumeni syndrome: a p53 family affair. *Cell Cycle*, 4: 865-867.

Jackman, M, Lindon, C, Nigg, EA, Pines, J. 2003. Active cyclin B1-Cdk1 first appears on centrosomes in prophase. *Nat Cell Biol*, 5: 143-148.

Jallepalli, PV, Lengauer, C. 2001. Chromosome segregation and cancer: cutting through the mystery. *Nat Rev Cancer*, 1: 109-117.

Janetopoulos, C, Borleis, J, Vazquez, F, Iijima, M, Devreotes, P. 2005. Temporal and spatial regulation of phosphoinositide signaling mediates cytokinesis. *Dev Cell*, 8: 467-477.

Jean, C, Tollon, Y, Raynaud-Messina, B, Wright, M. 1999. The mammalian interphase centrosome: two independent units maintained together by the dynamics of the microtubule cytoskeleton. *Eur J Cell Biol*, 78: 549-560.

Jeffs, AR, Benjes, SM, Smith, TL, Sowerby, SJ, Morris, CM. 1998. The BCR gene recombines preferentially with Alu elements in complex BCR-ABL translocations of chronic myeloid leukaemia. *Hum Mol Genet*, 7: 767-776.

Jemal, A, Siegel, R, Ward, E, Murray, T, Xu, J, Thun, MJ. 2007. Cancer statistics, 2007. *CA Cancer J Clin*, 57: 43-66.

Jiang, F, Caraway, NP, Sabichi, AL, Zhang, HZ, Ruitrok, A, Grossman, HB, Gu, J, Lerner, SP, Lippman, S, Katz, RL. 2003. Centrosomal abnormality is common in and a potential biomarker for bladder cancer. *Int J Cancer*, 106: 661-665.

Jiang, XR, Jimenez, G, Chang, E, Frolkis, M, Kusler, B, Sage, M, Beeche, M, Bodnar, AG, Wahl, GM, Tlsty, TD, Chiu, CP. 1999. Telomerase expression in human somatic cells does not induce changes associated with a transformed phenotype. *Nat Genet*, 21: 111-114.

Jordan, P, Karess, R. 1997. Myosin light chain-activating phosphorylation sites are required for oogenesis in Drosophila. *J Cell Biol*, 139: 1805-1819.

Kanaji, T, Russell, S, Cunningham, J, Izuhara, K, Fox, JE, Ware, J. 2004. Megakaryocyte proliferation and ploidy regulated by the cytoplasmic tail of glycoprotein Ibalpha. *Blood*, 104: 3161-3168.

Kanda, T, Sullivan, KF, Wahl, GM. 1998. Histone-GFP fusion protein enables sensitive analysis of chromosome dynamics in living mammalian cells. *Curr Biol*, 8: 377-385.

Kaneko, K, Satoh, K, Masamune, A, Satoh, A, Shimosegawa, T. 2002. Myosin light chain kinase inhibitors can block invasion and adhesion of human pancreatic cancer cell lines. *Pancreas*, 24: 34-41.

Katayama, H, Brinkley, WR, Sen, S. 2003. The Aurora kinases: role in cell transformation and tumorigenesis. *Cancer Metastasis Rev*, 22: 451-464.

Kawamura, K, Izumi, H, Ma, Z, Ikeda, R, Moriyama, M, Tanaka, T, Nojima, T, Levin, LS, Fujikawa-Yamamoto, K, Suzuki, K, Fukasawa, K. 2004. Induction of centrosome amplification and chromosome instability in human bladder cancer cells by p53 mutation and cyclin E overexpression. *Cancer Res*, 64: 4800-4809.

Kawamura, K, Moriyama, M, Shiba, N, Ozaki, M, Tanaka, T, Nojima, T, Fujikawa-Yamamoto, K, Ikeda, R, Suzuki, K. 2003. Centrosome hyperamplification and chromosomal instability in bladder cancer. *Eur Urol*, 43: 505-515.

Kawano, Y, Fukata, Y, Oshiro, N, Amano, M, Nakamura, T, Ito, M, Matsumura, F, Inagaki, M, Kaibuchi, K. 1999. Phosphorylation of myosin-binding subunit (MBS) of myosin phosphatase by Rho-kinase in vivo. *J Cell Biol*, 147: 1023-1038.

Khodjakov, A, Cole, RW, Oakley, BR, Rieder, CL. 2000. Centrosome-independent mitotic spindle formation in vertebrates. *Curr Biol*, 10: 59-67.

Khodjakov, A, Rieder, CL, Sluder, G, Cassels, G, Sibon, O, Wang, CL. 2002. De novo formation of centrosomes in vertebrate cells arrested during S phase. *J Cell Biol*, 158: 1171-1181.

Kim, JS, Lee, C, Bonifant, CL, Ressom, H, Waldman, T. 2007. Activation of p53-dependent growth suppression in human cells by mutations in PTEN or PIK3CA. *Mol Cell Biol*, 27: 662-677.

King, RW, Deshaies, RJ, Peters, JM, Kirschner, MW. 1996. How proteolysis drives the cell cycle. *Science*, 274: 1652-1659.

Komatsu, S, Yano, T, Shibata, M, Tuft, RA, Ikebe, M. 2000. Effects of the regulatory light chain phosphorylation of myosin II on mitosis and cytokinesis of mammalian cells. *J Biol Chem*, 275: 34512-34520.

Kosako, H, Goto, H, Yanagida, M, Matsuzawa, K, Fujita, M, Tomono, Y, Okigaki, T, Odai, H, Kaibuchi, K, Inagaki, M. 1999. Specific accumulation of Rho-associated kinase at the cleavage furrow during cytokinesis: cleavage furrow-specific phosphorylation of intermediate filaments. *Oncogene*, 18: 2783-2788.

Kosako, H, Yoshida, T, Matsumura, F, Ishizaki, T, Narumiya, S, Inagaki, M. 2000. Rho-kinase/ROCK is involved in cytokinesis through the phosphorylation of myosin light chain and not ezrin/radixin/moesin proteins at the cleavage furrow. *Oncogene*, 19: 6059-6064.

Kramer, A, Lukas, J, Bartek, J. 2004. Checking out the centrosome. *Cell Cycle*, 3: 1390-1393.

Kuo, KK, Sato, N, Mizumoto, K, Maehara, N, Yonemasu, H, Ker, CG, Sheen, PC, Tanaka, M. 2000. Centrosome abnormalities in human carcinomas of the gallbladder and intrahepatic and extrahepatic bile ducts. *Hepatology*, 31: 59-64.

Kurasawa, Y, Earnshaw, WC, Mochizuki, Y, Dohmae, N, Todokoro, K. 2004. Essential roles of KIF4 and its binding partner PRC1 in organized central spindle midzone formation. *Embo J*, 23: 3237-3248.

Kurzrock, R, Kantarjian, HM, Druker, BJ, Talpaz, M. 2003. Philadelphia chromosome-positive leukemias: from basic mechanisms to molecular therapeutics. *Ann Intern Med*, 138: 819-830.

La Terra, S, English, CN, Hergert, P, McEwen, BF, Sluder, G, Khodjakov, A. 2005. The de novo centriole assembly pathway in HeLa cells: cell cycle progression and centriole assembly/maturation. *J Cell Biol*, 168: 713-722.

Lee, OK, Frese, KK, James, JS, Chadda, D, Chen, ZH, Javier, RT, Cho, KO. 2003. Discs-Large and Strabismus are functionally linked to plasma membrane formation. *Nat Cell Biol*, 5: 987-993.

Lemez, P, Michalova, K, Zemanova, Z, Marinov, I, Trpakova, A, Moravcova, J, Jelinek, J. 1998. Three cases of near-tetraploid acute myeloid leukemias originating in pluripotent myeloid progenitors. *Leuk Res*, 22: 581-588.

Lengauer, C, Kinzler, KW, Vogelstein, B. 1997. Genetic instability in colorectal cancers. *Nature*, 386: 623-627.

Lepage, A, Leboeuf, M, Cazenave, JP, de la Salle, C, Lanza, F, Uzan, G. 2000. The alpha(IIb)beta(3) integrin and GPIb-V-IX complex identify distinct stages in the maturation of CD34(+) cord blood cells to megakaryocytes. *Blood*, 96: 4169-4177.

Leslie, NR, Downes, CP. 2004. PTEN function: how normal cells control it and tumour cells lose it. *Biochem J*, 382: 1-11.

Li, Q, Dang, CV. 1999. c-Myc overexpression uncouples DNA replication from mitosis. *Mol Cell Biol*, 19: 5339-5351.

Li, Y, Benezra, R. 1996. Identification of a human mitotic checkpoint gene: hsMAD2. *Science*, 274: 246-248.

Li, Y, Lu, J, Cohen, D, Prochownik, EV. 2007a. Transformation, genomic instability and senescence mediated by platelet/megakaryocyte glycoprotein Ibalpha. *Oncogene*,

Li, Y, Lu, J, Prochownik, EV. 2007b. c-Myc-mediated genomic instability proceeds via a megakaryocytic endomitosis pathway involving Gp1balpha. *Proc Natl Acad Sci U S A*, 104: 3490-3495.

Lindahl, T. 1993. Instability and decay of the primary structure of DNA. *Nature*, 362: 709-715.

Lindon, C, Pines, J. 2004. Ordered proteolysis in anaphase inactivates Plk1 to contribute to proper mitotic exit in human cells. *J Cell Biol*, 164: 233-241.

Lingle, WL, Barrett, SL, Negron, VC, D'Assoro, AB, Boeneman, K, Liu, W, Whitehead, CM, Reynolds, C, Salisbury, JL. 2002. Centrosome amplification drives chromosomal instability in breast tumor development. *Proc Natl Acad Sci U S A*, 99: 1978-1983.

Lingle, WL, Lutz, WH, Ingle, JN, Maihle, NJ, Salisbury, JL. 1998. Centrosome hypertrophy in human breast tumors: implications for genomic stability and cell polarity. *Proc Natl Acad Sci U S A*, 95: 2950-2955.

Lingle, WL, Salisbury, JL. 2000. The role of the centrosome in the development of malignant tumors. *Curr Top Dev Biol*, 49: 313-329.

Loncarek, J, Hergert, P, Magidson, V, Khodjakov, A. 2008. Control of daughter centriole formation by the pericentriolar material. *Nat Cell Biol*,

Lopez, JA, Dong, JF. 1997. Structure and function of the glycoprotein Ib-IX-V complex. *Curr Opin Hematol*, 4: 323-329.

Lothschutz, D, Jennewein, M, Pahl, S, Lausberg, HF, Eichler, A, Mutschler, W, Hanselmann, RG, Oberringer, M. 2002. Polyploidization and centrosome hyperamplification in inflammatory bronchi. *Inflamm Res*, 51: 416-422.

Lu, J, Meng, W, Poy, F, Maiti, S, Goode, BL, Eck, MJ. 2007. Structure of the FH2 domain of Daam1: implications for formin regulation of actin assembly. *J Mol Biol*, 369: 1258-1269.

Lucero, A, Stack, C, Bresnick, AR, Shuster, CB. 2006. A global, myosin light chain kinase-dependent increase in myosin II contractility accompanies the metaphase-anaphase transition in sea urchin eggs. *Mol Biol Cell*, 17: 4093-4104.

Madaule, P, Eda, M, Watanabe, N, Fujisawa, K, Matsuoka, T, Bito, H, Ishizaki, T, Narumiya, S. 1998. Role of citron kinase as a target of the small GTPase Rho in cytokinesis. *Nature*, 394: 491-494.

Marti, A, Luo, Z, Cunningham, C, Ohta, Y, Hartwig, J, Stossel, TP, Kyriakis, JM, Avruch, J. 1997. Actin-binding protein-280 binds the stress-activated protein kinase (SAPK) activator SEK-1 and is required for tumor necrosis factor-alpha activation of SAPK in melanoma cells. *J Biol Chem*, 272: 2620-2628.

Mateuca, R, Lombaert, N, Aka, PV, Decordier, I, Kirsch-Volders, M. 2006. Chromosomal changes: induction, detection methods and applicability in human biomonitoring. *Biochimie*, 88: 1515-1531.

Matsumura, F. 2005. Regulation of myosin II during cytokinesis in higher eukaryotes. *Trends Cell Biol*, 15: 371-377.

Matuliene, J, Kuriyama, R. 2002. Kinesin-like protein CHO1 is required for the formation of midbody matrix and the completion of cytokinesis in mammalian cells. *Mol Biol Cell*, 13: 1832-1845.

Meraldi, P, Honda, R, Nigg, EA. 2002. Aurora-A overexpression reveals tetraploidization as a major route to centrosome amplification in p53-/- cells. *Embo J*, 21: 483-492.

Meraldi, P, Nigg, EA. 2001. Centrosome cohesion is regulated by a balance of kinase and phosphatase activities. *J Cell Sci*, 114: 3749-3757.

Meyer, SC, Zuerbig, S, Cunningham, CC, Hartwig, JH, Bissell, T, Gardner, K, Fox, JE. 1997. Identification of the region in actin-binding protein that binds to the cytoplasmic domain of glycoprotein IBalpha. *J Biol Chem*, 272: 2914-2919.

Michael, D, Oren, M. 2003. The p53-Mdm2 module and the ubiquitin system. *Semin Cancer Biol*, 13: 49-58.

Minoshima, Y, Kawashima, T, Hirose, K, Tonozuka, Y, Kawajiri, A, Bao, YC, Deng, X, Tatsuka, M, Narumiya, S, May, WS, Jr., Nosaka, T, Semba, K, Inoue, T, Satoh, T, Inagaki, M, Kitamura, T. 2003. Phosphorylation by aurora B converts MgcRacGAP to a RhoGAP during cytokinesis. *Dev Cell*, 4: 549-560.

Mishima, M, Kaitna, S, Glotzer, M. 2002. Central spindle assembly and cytokinesis require a kinesin-like protein/RhoGAP complex with microtubule bundling activity. *Dev Cell*, 2: 41-54.

Mitelman, F. 1983. Catalogue of chromosome aberrations in cancer. *Cytogenet Cell Genet*, 36: 1-515.

Miyauchi, K, Yamamoto, Y, Kosaka, T, Hosoya, H. 2006. Myosin II activity is not essential for recruitment of myosin II to the furrow in dividing HeLa cells. *Biochem Biophys Res Commun*, 350: 543-548.

Montgomery, E, Wilentz, RE, Argani, P, Fisher, C, Hruban, RH, Kern, SE, Lengauer, C. 2003. Analysis of anaphase figures in routine histologic sections distinguishes chromosomally unstable from chromosomally stable malignancies. *Cancer Biol Ther*, 2: 248-252.

Moussavi, RS, Kelley, CA, Adelstein, RS. 1993. Phosphorylation of vertebrate nonmuscle and smooth muscle myosin heavy chains and light chains. *Mol Cell Biochem*, 127-128: 219-227.

Murata-Hori, M, Fumoto, K, Fukuta, Y, Iwasaki, T, Kikuchi, A, Tatsuka, M, Hosoya, H. 2000. Myosin II regulatory light chain as a novel substrate for AIM-1, an aurora/Ipl1p-related kinase from rat. *J Biochem*, 128: 903-907.

Murthy, K, Wadsworth, P. 2005. Myosin-II-dependent localization and dynamics of F-actin during cytokinesis. *Curr Biol*, 15: 724-731.

Nakajima, T, Moriguchi, M, Mitsumoto, Y, Sekoguchi, S, Nishikawa, T, Takashima, H, Watanabe, T, Katagishi, T, Kimura, H, Okanoue, T, Kagawa, K. 2004. Centrosome aberration accompanied with p53 mutation can induce genetic instability in hepatocellular carcinoma. *Mod Pathol*, 17: 722-727.

Nathanson, KL, Wooster, R, Weber, BL. 2001. Breast cancer genetics: what we know and what we need. *Nat Med*, 7: 552-556.

Neef, R, Gruneberg, U, Kopajtich, R, Li, X, Nigg, EA, Sillje, H, Barr, FA. 2007. Choice of Plk1 docking partners during mitosis and cytokinesis is controlled by the activation state of Cdk1. *Nat Cell Biol*, 9: 436-444.

Nesbit, CE, Tersak, JM, Prochownik, EV. 1999. MYC oncogenes and human neoplastic disease. *Oncogene*, 18: 3004-3016.

Nigg, EA. 2001. Mitotic kinases as regulators of cell division and its checkpoints. *Nat Rev Mol Cell Biol*, 2: 21-32.

Nigg, EA. 2002. Centrosome aberrations: cause or consequence of cancer progression? *Nat Rev Cancer*, 2: 815-825.

Nigg, EA. 2006. Origins and consequences of centrosome aberrations in human cancers. *Int J Cancer*, 119: 2717-2723.

Niiya, F, Xie, X, Lee, KS, Inoue, H, Miki, T. 2005. Inhibition of cyclin-dependent kinase 1 induces cytokinesis without chromosome segregation in an ECT2 and MgcRacGAP-dependent manner. *J Biol Chem*, 280: 36502-36509.

Noguchi, T, Mabuchi, I. 2001. Reorganization of actin cytoskeleton at the growing end of the cleavage furrow of Xenopus egg during cytokinesis. *J Cell Sci*, 114: 401-412.

Nunnally, MH, D'Angelo, JM, Craig, SW. 1980. Filamin concentration in cleavage furrow and midbody region: frequency of occurrence compared with that of alpha-actinin and myosin. *J Cell Biol*, 87: 219-226.

Ohta, T, Essner, R, Ryu, JH, Palazzo, RE, Uetake, Y, Kuriyama, R. 2002. Characterization of Cep135, a novel coiled-coil centrosomal protein involved in microtubule organization in mammalian cells. *J Cell Biol*, 156: 87-99.

Ohta, Y, Suzuki, N, Nakamura, S, Hartwig, JH, Stossel, TP. 1999. The small GTPase RalA targets filamin to induce filopodia. *Proc Natl Acad Sci U S A*, 96: 2122-2128.

Olaharski, AJ, Sotelo, R, Solorza-Luna, G, Gonsebatt, ME, Guzman, P, Mohar, A, Eastmond, DA. 2006. Tetraploidy and chromosomal instability are early events during cervical carcinogenesis. *Carcinogenesis*, 27: 337-343.

Ono, K, Parast, M, Alberico, C, Benian, GM, Ono, S. 2003. Specific requirement for two ADF/cofilin isoforms in distinct actin-dependent processes in Caenorhabditis elegans. *J Cell Sci*, 116: 2073-2085.

Oren, M. 2003. Decision making by p53: life, death and cancer. *Cell Death Differ*, 10: 431-442.

Paramasivam, M, Chang, YJ, LoTurco, JJ. 2007. ASPM and citron kinase co-localize to the midbody ring during cytokinesis. *Cell Cycle*, 6: 1605-1612.

Park, SH, Maeda, T, Mohapatra, G, Waldman, FM, Davis, RL, Feuerstein, BG. 1995. Heterogeneity, polyploidy, aneusomy, and 9p deletion in human glioblastoma multiforme. *Cancer Genet Cytogenet*, 83: 127-135.

Piekny, A, Werner, M, Glotzer, M. 2005. Cytokinesis: welcome to the Rho zone. *Trends Cell Biol*, 15: 651-658.

Piel, M, Nordberg, J, Euteneuer, U, Bornens, M. 2001. Centrosome-dependent exit of cytokinesis in animal cells. *Science*, 291: 1550-1553.

Pihan, GA, Purohit, A, Wallace, J, Malhotra, R, Liotta, L, Doxsey, SJ. 2001. Centrosome defects can account for cellular and genetic changes that characterize prostate cancer progression. *Cancer Res*, 61: 2212-2219.

Pihan, GA, Wallace, J, Zhou, Y, Doxsey, SJ. 2003. Centrosome abnormalities and chromosome instability occur together in pre-invasive carcinomas. *Cancer Res*, 63: 1398-1404.

Pluquet, O, Hainaut, P. 2001. Genotoxic and non-genotoxic pathways of p53 induction. *Cancer Lett*, 174: 1-15.

Pollard, TD. 2007. Regulation of actin filament assembly by Arp2/3 complex and formins. *Annu Rev Biophys Biomol Struct*, 36: 451-477.

Poperechnaya, A, Varlamova, O, Lin, PJ, Stull, JT, Bresnick, AR. 2000. Localization and activity of myosin light chain kinase isoforms during the cell cycle. *J Cell Biol*, 151: 697-708.

Prasad, CJ, Sheets, E, Selig, AM, McArthur, MC, Crum, CP. 1993. The binucleate squamous cell: histologic spectrum and relationship to low-grade squamous intraepithelial lesions. *Mod Pathol*, 6: 313-317.

Quintyne, NJ, Reing, JE, Hoffelder, DR, Gollin, SM, Saunders, WS. 2005. Spindle multipolarity is prevented by centrosomal clustering. *Science*, 307: 127-129.

Rahman, N, Stratton, MR. 1998. The genetics of breast cancer susceptibility. *Annu Rev Genet*, 32: 95-121.

Rappaport, R. 1961. Experiments concerning the cleavage stimulus in sand dollar eggs. *J Exp Zool*, 148: 81-89.

Rappaport, R. 1996. Cytokinesis in Animal Cells.

Ravid, K, Lu, J, Zimmet, JM, Jones, MR. 2002. Roads to polyploidy: the megakaryocyte example. *J Cell Physiol*, 190: 7-20.

Rhodes, DR, Kalyana-Sundaram, S, Mahavisno, V, Varambally, R, Yu, J, Briggs, BB, Barrette, TR, Anstet, MJ, Kincead-Beal, C, Kulkarni, P, Varambally, S, Ghosh, D, Chinnaiyan, AM. 2007. Oncomine 3.0: genes, pathways, and networks in a collection of 18,000 cancer gene expression profiles. *Neoplasia*, 9: 166-180.

Ried, T, Heselmeyer-Haddad, K, Blegen, H, Schrock, E, Auer, G. 1999. Genomic changes defining the genesis, progression, and malignancy potential in solid human tumors: a phenotype/genotype correlation. *Genes Chromosomes Cancer*, 25: 195-204.

Rigby, PJ, Papadimitriou, JM. 1984. Cytoskeletal control of nuclear arrangement in Langhans multinucleate giant cells. *J Pathol*, 143: 17-29.

Ring, D, Hubble, R, Kirschner, M. 1982. Mitosis in a cell with multiple centrioles. *J Cell Biol*, 94: 549-556.

Rodrigues-Martins, A, Riparbelli, M, Callaini, G, Glover, DM, Bettencourt-Dias, M. 2007. Revisiting the role of the mother centriole in centriole biogenesis. *Science*, 316: 1046-1050.

Rubin Grandis, J, Zeng, Q, Tweardy, DJ. 1996. Retinoic acid normalizes the increased gene transcription rate of TGF-alpha and EGFR in head and neck cancer cell lines. *Nat Med*, 2: 237-240.

Ruf, IK, Rhyne, PW, Yang, H, Borza, CM, Hutt-Fletcher, LM, Cleveland, JL, Sample, JT. 2001. EBV regulates c-MYC, apoptosis, and tumorigenicity in Burkitt's lymphoma. *Curr Top Microbiol Immunol*, 258: 153-160.

Ruggeri, ZM. 1991. The platelet glycoprotein Ib-IX complex. *Prog Hemost Thromb*, 10: 35-68.

Salisbury, JL, Suino, KM, Busby, R, Springett, M. 2002. Centrin-2 is required for centriole duplication in mammalian cells. *Curr Biol*, 12: 1287-1292.

Sanders, LC, Matsumura, F, Bokoch, GM, de Lanerolle, P. 1999. Inhibition of myosin light chain kinase by p21-activated kinase. *Science*, 283: 2083-2085.

Sato, N, Mizumoto, K, Nakamura, M, Nakamura, K, Kusumoto, M, Niiyama, H, Ogawa, T, Tanaka, M. 1999. Centrosome abnormalities in pancreatic ductal carcinoma. *Clin Cancer Res*, 5: 963-970.

Sato, N, Mizumoto, K, Nakamura, M, Tanaka, M. 2000. Radiation-induced centrosome overduplication and multiple mitotic spindles in human tumor cells. *Exp Cell Res*, 255: 321-326.

Saunders, W. 2005. Centrosomal amplification and spindle multipolarity in cancer cells. *Semin Cancer Biol*, 15: 25-32.

Saunders, WS, Shuster, M, Huang, X, Gharaibeh, B, Enyenihi, AH, Petersen, I, Gollin, SM. 2000. Chromosomal instability and cytoskeletal defects in oral cancer cells. *Proc Natl Acad Sci U S A*, 97: 303-308.

Schaeffer, AJ, Nguyen, M, Liem, A, Lee, D, Montagna, C, Lambert, PF, Ried, T, Difilippantonio, MJ. 2004. E6 and E7 oncoproteins induce distinct patterns of chromosomal aneuploidy in skin tumors from transgenic mice. *Cancer Res*, 64: 538-546.

Schenker, T, Trueb, B. 1998. Down-regulated proteins of mesenchymal tumor cells. *Exp Cell Res*, 239: 161-168.

Scholey, JM, Taylor, KA, Kendrick-Jones, J. 1980. Regulation of non-muscle myosin assembly by calmodulin-dependent light chain kinase. *Nature*, 287: 233-235.

Scott, D, Zampetti-Bosseler, F. 1980. The relationship between cell killing, chromosome aberrations, spindle defects and mitotic delay in mouse lymphoma cells of differential sensitivity to X-rays. *Int J Radiat Biol Relat Stud Phys Chem Med*, 37: 33-47.

Seeger, RC, Brodeur, GM, Sather, H, Dalton, A, Siegel, SE, Wong, KY, Hammond, D. 1985. Association of multiple copies of the N-myc oncogene with rapid progression of neuroblastomas. *N Engl J Med*, 313: 1111-1116.

Sellers, JR. 1991. Regulation of cytoplasmic and smooth muscle myosin. *Curr Opin Cell Biol*, 3: 98-104.

Shi, Q, King, RW. 2005. Chromosome nondisjunction yields tetraploid rather than aneuploid cells in human cell lines. *Nature*, 437: 1038-1042.

Shimizu, Y, Thumkeo, D, Keel, J, Ishizaki, T, Oshima, H, Oshima, M, Noda, Y, Matsumura, F, Taketo, MM, Narumiya, S. 2005. ROCK-I regulates closure of the eyelids and ventral body wall by inducing assembly of actomyosin bundles. *J Cell Biol*, 168: 941-953.

Shuster, CB, Burgess, DR. 2002. Targeted new membrane addition in the cleavage furrow is a late, separate event in cytokinesis. *Proc Natl Acad Sci U S A*, 99: 3633-3638.

Silverman-Gavrila, RV, Forer, A. 2001. Effects of anti-myosin drugs on anaphase chromosome movement and cytokinesis in crane-fly primary spermatocytes. *Cell Motil Cytoskeleton*, 50: 180-197.

Simmer, F, Moorman, C, van der Linden, AM, Kuijk, E, van den Berghe, PV, Kamath, RS, Fraser, AG, Ahringer, J, Plasterk, RH. 2003. Genome-wide RNAi of C. elegans using the hypersensitive rrf-3 strain reveals novel gene functions. *PLoS Biol*, 1: E12.

Sisson, JC, Field, C, Ventura, R, Royou, A, Sullivan, W. 2000. Lava lamp, a novel peripheral golgi protein, is required for Drosophila melanogaster cellularization. *J Cell Biol*, 151: 905-918.

Skop, AR, Liu, H, Yates, J, 3rd, Meyer, BJ, Heald, R. 2004. Dissection of the mammalian midbody proteome reveals conserved cytokinesis mechanisms. *Science*, 305: 61-66.

Skyldberg, B, Fujioka, K, Hellstrom, AC, Sylven, L, Moberger, B, Auer, G. 2001. Human papillomavirus infection, centrosome aberration, and genetic stability in cervical lesions. *Mod Pathol*, 14: 279-284.

Sluder, G, Nordberg, JJ. 2004. The good, the bad and the ugly: the practical consequences of centrosome amplification. *Curr Opin Cell Biol*, 16: 49-54.

Sluder, G, Thompson, EA, Miller, FJ, Hayes, J, Rieder, CL. 1997. The checkpoint control for anaphase onset does not monitor excess numbers of spindle poles or bipolar spindle symmetry. *J Cell Sci*, 110 ( Pt 4): 421-429.

Somers, WG, Saint, R. 2003. A RhoGEF and Rho family GTPase-activating protein complex links the contractile ring to cortical microtubules at the onset of cytokinesis. *Dev Cell*, 4: 29-39.

Somlyo, AP, Somlyo, AV. 2003. Ca2+ sensitivity of smooth muscle and nonmuscle myosin II: modulated by G proteins, kinases, and myosin phosphatase. *Physiol Rev*, 83: 1325-1358.

Somlyo, AV, Wang, H, Choudhury, N, Khromov, AS, Majesky, M, Owens, GK, Somlyo, AP. 2004. Myosin light chain kinase knockout. *J Muscle Res Cell Motil*, 25: 241-242.

Somma, MP, Fasulo, B, Cenci, G, Cundari, E, Gatti, M. 2002. Molecular dissection of cytokinesis by RNA interference in Drosophila cultured cells. *Mol Biol Cell*, 13: 2448-2460.

Soussi, T, Beroud, C. 2001. Assessing TP53 status in human tumours to evaluate clinical outcome. *Nat Rev Cancer*, 1: 233-240.

Soussi, T, Ishioka, C, Claustres, M, Beroud, C. 2006. Locus-specific mutation databases: pitfalls and good practice based on the p53 experience. *Nat Rev Cancer*, 6: 83-90.

Stewart, S, Fang, G. 2005. Destruction box-dependent degradation of aurora B is mediated by the anaphase-promoting complex/cyclosome and Cdh1. *Cancer Res*, 65: 8730-8735.

Stewenius, Y, Gorunova, L, Jonson, T, Larsson, N, Hoglund, M, Mandahl, N, Mertens, F, Mitelman, F, Gisselsson, D. 2005. Structural and numerical chromosome changes in colon cancer develop through telomere-mediated anaphase bridges, not through mitotic multipolarity. *Proc Natl Acad Sci U S A*, 102: 5541-5546.

Storchova, Z, Breneman, A, Cande, J, Dunn, J, Burbank, K, O'Toole, E, Pellman, D. 2006. Genome-wide genetic analysis of polyploidy in yeast. *Nature*, 443: 541-547.

Stossel, TP, Condeelis, J, Cooley, L, Hartwig, JH, Noegel, A, Schleicher, M, Shapiro, SS. 2001. Filamins as integrators of cell mechanics and signalling. *Nat Rev Mol Cell Biol*, 2: 138-145.

Straight, AF, Field, CM, Mitchison, TJ. 2005. Anillin binds nonmuscle myosin II and regulates the contractile ring. *Mol Biol Cell*, 16: 193-201.

Surks, HK, Mochizuki, N, Kasai, Y, Georgescu, SP, Tang, KM, Ito, M, Lincoln, TM, Mendelsohn, ME. 1999. Regulation of myosin phosphatase by a specific interaction with cGMP- dependent protein kinase Ialpha. *Science*, 286: 1583-1587.

Takahashi, T, Haruki, N, Nomoto, S, Masuda, A, Saji, S, Osada, H. 1999. Identification of frequent impairment of the mitotic checkpoint and molecular analysis of the mitotic checkpoint genes, hsMAD2 and p55CDC, in human lung cancers. *Oncogene*, 18: 4295-4300.

Takanishi, DM, Jr., Hart, J, Covarelli, P, Chappell, R, Michelassi, F. 1996. Ploidy as a prognostic feature in colonic adenocarcinoma. *Arch Surg*, 131: 587-592.

Takizawa, N, Schmidt, DJ, Mabuchi, K, Villa-Moruzzi, E, Tuft, RA, Ikebe, M. 2003. M20, the small subunit of PP1M, binds to microtubules. *Am J Physiol Cell Physiol*, 284: C250-262.

Tamguney, T, Stokoe, D. 2007. New insights into PTEN. *J Cell Sci*, 120: 4071-4079.

Tarapore, P, Fukasawa, K. 2002. Loss of p53 and centrosome hyperamplification. *Oncogene*, 21: 6234-6240.

Thompson, DA, Desai, MM, Murray, AW. 2006. Ploidy controls the success of mutators and nature of mutations during budding yeast evolution. *Curr Biol*, 16: 1581-1590.

Thompson, SL, Compton, DA. 2008. Examining the link between chromosomal instability and aneuploidy in human cells. *J Cell Biol*, 180: 665-672.

Thumkeo, D, Keel, J, Ishizaki, T, Hirose, M, Nonomura, K, Oshima, H, Oshima, M, Taketo, MM, Narumiya, S. 2003. Targeted disruption of the mouse rho-associated kinase 2 gene results in intrauterine growth retardation and fetal death. *Mol Cell Biol*, 23: 5043-5055.

Tlsty, TD, Coussens, LM. 2006. Tumor stroma and regulation of cancer development. *Annu Rev Pathol*, 1: 119-150.

Tohtong, R, Phattarasakul, K, Jiraviriyakul, A, Sutthiphongchai, T. 2003. Dependence of metastatic cancer cell invasion on MLCK-catalyzed phosphorylation of myosin regulatory light chain. *Prostate Cancer Prostatic Dis*, 6: 212-216.

Totsukawa, G, Yamakita, Y, Yamashiro, S, Hosoya, H, Hartshorne, DJ, Matsumura, F. 1999. Activation of myosin phosphatase targeting subunit by mitosis-specific phosphorylation. *J Cell Biol*, 144: 735-744.

Uetake, Y, Sluder, G. 2004. Cell cycle progression after cleavage failure: mammalian somatic cells do not possess a "tetraploidy checkpoint". *J Cell Biol*, 165: 609-615.

Vader, G, Kauw, JJ, Medema, RH, Lens, SM. 2006. Survivin mediates targeting of the chromosomal passenger complex to the centromere and midbody. *EMBO Rep*, 7: 85-92.

Vagnarelli, P, Hudson, DF, Ribeiro, SA, Trinkle-Mulcahy, L, Spence, JM, Lai, F, Farr, CJ, Lamond, AI, Earnshaw, WC. 2006. Condensin and Repo-Man-PP1 co-operate in the regulation of chromosome architecture during mitosis. *Nat Cell Biol*, 8: 1133-1142.

Van Eldik, LJ, Watterson, DM, Burgess, WH. 1984. Immunoreactive levels of myosin light-chain kinase in normal and virus-transformed chicken embryo fibroblasts. *Mol Cell Biol*, 4: 2224-2226.

VerPlank, L, Li, R. 2005. Cell cycle-regulated trafficking of Chs2 controls actomyosin ring stability during cytokinesis. *Mol Biol Cell*, 16: 2529-2543.

Wade, M, Wahl, GM. 2006. c-Myc, genome instability, and tumorigenesis: the devil is in the details. *Curr Top Microbiol Immunol*, 302: 169-203.

Wang, SI, Parsons, R, Ittmann, M. 1998. Homozygous deletion of the PTEN tumor suppressor gene in a subset of prostate adenocarcinomas. *Clin Cancer Res*, 4: 811-815.

Wang, X, Jin, DY, Ng, RW, Feng, H, Wong, YC, Cheung, AL, Tsao, SW. 2002. Significance of MAD2 expression to mitotic checkpoint control in ovarian cancer cells. *Cancer Res*, 62: 1662-1668.

Ward, Y, Yap, SF, Ravichandran, V, Matsumura, F, Ito, M, Spinelli, B, Kelly, K. 2002. The GTP binding proteins Gem and Rad are negative regulators of the Rho-Rho kinase pathway. *J Cell Biol*, 157: 291-302.

Warnke, S, Kemmler, S, Hames, RS, Tsai, HL, Hoffmann-Rohrer, U, Fry, AM, Hoffmann, I. 2004. Polo-like kinase-2 is required for centriole duplication in mammalian cells. *Curr Biol*, 14: 1200-1207.

Watanabe, N, Madaule, P, Reid, T, Ishizaki, T, Watanabe, G, Kakizuka, A, Saito, Y, Nakao, K, Jockusch, BM, Narumiya, S. 1997. p140mDia, a mammalian homolog of Drosophila diaphanous, is a target protein for Rho small GTPase and is a ligand for profilin. *Embo J*, 16: 3044-3056.

Word, RA, Casey, ML, Kamm, KE, Stull, JT. 1991. Effects of cGMP on [Ca2+]i, myosin light chain phosphorylation, and contraction in human myometrium. *Am J Physiol*, 260: C861-867.

Wu, Y, Muranyi, A, Erdodi, F, Hartshorne, DJ. 2005. Localization of myosin phosphatase target subunit and its mutants. *J Muscle Res Cell Motil*, 26: 123-134.

Wunderlich, V. 2002. Chromosomes and cancer: Theodor Boveri's predictions 100 years later. *J Mol Med*, 80: 545-548.

Xia, D, Stull, JT, Kamm, KE. 2005. Myosin phosphatase targeting subunit 1 affects cell migration by regulating myosin phosphorylation and actin assembly. *Exp Cell Res*, 304: 506-517.

Xu, W, Xie, Z, Chung, DW, Davie, EW. 1998. A novel human actin-binding protein homologue that binds to platelet glycoprotein Ibalpha. *Blood*, 92: 1268-1276.

Yamashiro, S, Totsukawa, G, Yamakita, Y, Sasaki, Y, Madaule, P, Ishizaki, T, Narumiya, S, Matsumura, F. 2003. Citron kinase, a Rho-dependent kinase, induces di-phosphorylation of regulatory light chain of myosin II. *Mol Biol Cell*, 14: 1745-1756.

Yamawaki, K, Ito, M, Machida, H, Moriki, N, Okamoto, R, Isaka, N, Shimpo, H, Kohda, A, Okumura, K, Hartshorne, DJ, Nakano, T. 2001. Identification of human CPI-17, an inhibitory phosphoprotein for myosin phosphatase. *Biochem Biophys Res Commun*, 285: 1040-1045.

Yang, D, Welm, A, Bishop, JM. 2004. Cell division and cell survival in the absence of survivin. *Proc Natl Acad Sci U S A*, 101: 15100-15105.

Yin, X, Grove, L, Rogulski, K, Prochownik, EV. 2002. Myc target in myeloid cells-1, a novel c-Myc target, recapitulates multiple c-Myc phenotypes. *J Biol Chem*, 277: 19998-20010.

Yin, XY, Grove, L, Datta, NS, Long, MW, Prochownik, EV. 1999. C-myc overexpression and p53 loss cooperate to promote genomic instability. *Oncogene*, 18: 1177-1184.

Yokoyama, T, Goto, H, Izawa, I, Mizutani, H, Inagaki, M. 2005. Aurora-B and Rho-kinase/ROCK, the two cleavage furrow kinases, independently regulate the progression of cytokinesis: possible existence of a novel cleavage furrow kinase phosphorylates ezrin/radixin/moesin (ERM). *Genes Cells*, 10: 127-137.

Yonemura, S, Hirao-Minakuchi, K, Nishimura, Y. 2004. Rho localization in cells and tissues. *Exp Cell Res*, 295: 300-314.

Yumura, S. 2001. Myosin II dynamics and cortical flow during contractile ring formation in Dictyostelium cells. *J Cell Biol*, 154: 137-146.

Zhang, D, Nicklas, RB. 1995. Chromosomes initiate spindle assembly upon experimental dissolution of the nuclear envelope in grasshopper spermatocytes. *J Cell Biol*, 131: 1125-1131.

Zhao, WM, Fang, G. 2005. Anillin is a substrate of anaphase-promoting complex/cyclosome (APC/C) that controls spatial contractility of myosin during late cytokinesis. *J Biol Chem*, 280: 33516-33524.

Zigmond, SH. 2004. Beginning and ending an actin filament: control at the barbed end. *Curr Top Dev Biol*, 63: 145-188.